LAND-USE CHANGE AND GREENHOUSE GAS EMISSIONS IN THE TROPICS

Forest degradation on peat soils

Jeffrey van Lent

Propositions

1. Carbon input rather than output controls the carbon balance of degraded, undrained tropical peat swamp forests.
   (this thesis)

2. Accurate accounting of N_2O emissions from tropical forest conversions should always include the first decade after land-use change.
   (this thesis)

3. Replication of published scientific results is equally important to scientific integrity as peer-reviewing manuscripts.

4. Unless all ecosystem services are accounted for, the monetary value of tropical forests remains smaller than that of agricultural land.

5. Planting trees to offset man-made carbon emissions is a short-term solution that is counterproductive over the long term.

6. Cultural diversity is positively correlated to economic prosperity.

Propositions belonging to the thesis, entitled

"Land-use change and greenhouse gas emissions in the tropics - forest degradation on peat soils"

Jeffrey van Lent

Wageningen, 12 October 2020

Land-use change and greenhouse gas emissions in the tropics

Forest degradation on peat soils

Jeffrey van Lent

Thesis committee

Promotors

Prof. Dr O. Oenema
Special Professor Nutrient Management and Soil Fertility
Wageningen University & Research

Prof. Dr J.W. van Groenigen
Personal chair at the Soil Biology Group
Wageningen University & Research

Co-promotors

Dr K. Hergoualc'h, Center for International Forestry Research (CIFOR), Lima, Peru
Dr L.V. Verchot, International Center for Tropical Agriculture (CIAT), Calí, Colombia

Other members

Prof. Dr P.A. Zuidema, Wageningen University & Research
Dr J.H.M. Wösten, Wageningen University & Research
Prof. Dr P. Boeckx, Ghent University, Belgium
Dr S. Sjögersten, University of Nottingham, United Kingdom

This research was conducted under the auspices of the C.T. de Wit Graduate School for Production Ecology and Resource Conservation (PE&RC).

Land-use change and greenhouse gas emissions in the tropics

Forest degradation on peat soils

Jeffrey van Lent

Thesis

submitted in fulfilment of the requirements for the degree of doctor
at Wageningen University
by the authority of the Rector Magnificus,
Prof. Dr A.P.J. Mol,
in the presence of the
Thesis Committee appointed by the Academic Board
to be defended in public
on Monday 12 October 2020
at 11 a.m. in the Aula.

Jeffrey van Lent
Land-use change and greenhouse gas emissions in the tropics - Forest degradation on peat soils,
230 pages

PhD thesis, Wageningen University, Wageningen, the Netherlands (2020)
With references, with summary in English, Spanish and Dutch

ISBN: 978-94-6395-453-2
DOI: https://doi.org/10.18174/526264

Abstract

Forest conversion and degradation are important contributors to worldwide anthropogenic greenhouse gas (GHG) emissions. In the tropics, this contribution is disproportionally large and reducing forest conversion and degradation can substantially reduce GHG emissions. If such GHG reduction efforts are driven by some kind of performance-based payment scheme (e.g. REDD+, The Green Climate Fund), an exact quantification of emissions is crucial in order to prevent over- or underestimation of such reduction efforts. However, for the tropics default IPCC Tier 1 emissions factors are generally based on few studies and on short-term measurements, sometimes from other climatic zones and/or different continents. Another source of low accuracy in GHG emission estimates occurs when emission factors for specific tropical land uses are missing and those emissions are not included in national GHG emission budgets. In this thesis I focus on both of these problems by increasing the mechanistic understanding of the effects of forest conversions on GHG emissions in the tropics, and to contribute to the derivation of robust emission factors for land-use change in the tropics.

In a meta-analysis I show that tropical forest conversion to cropland significantly increased N_2O emissions, irrespective of the region or type of crops. Nitrogen inputs from fertilizers and animal manure are useful proxies for general IPCC Tier 1 approaches in the tropics, while more detailed IPCC Tier 2 and 3 approaches could be extended with soil cultivation-induced soil organic nitrogen mineralization effects during the first years after conversion, as well as soil moisture and nitrogen availability indices.

Subsequently, I focus on a land use not studied to date: forest degradation on tropical peat swamp forest in the Peruvian Amazon. Forest degradation on peat consists of the harvesting of female fruit-baring *Mauritia flexuosa* palms in natural stands. This type of forest degradation was observed throughout three regions that were studied in the Peruvian Amazon. However, the intensity of degradation was not significantly related to soil carbon stock variability between sites. I then conducted a four-year field study to further investigate the impact of

palm harvesting on the soil carbon balance. In sites with >80% of fruit-bearing palms harvested (heavy degradation), litter production and composition altered and resulted in less carbon input into the soil. Carbon output, on the other hand, increased in heavily degraded situations due to faster peat and/or litter decomposition. The combined effects of more carbon output and less carbon input turned the soil at the heavily degraded peat swamp forest into a net source of carbon to the atmosphere of -7.1 Mg CO_2-C ha^{-1} yr^{-1}, while it remained at -0.1 Mg CO_2-C ha^{-1} yr^{-1} in undisturbed sites.

In conclusion, I show that forest degradation in tropical peat swamps can cause significant soil carbon dioxide losses – even without drainage or fertilization practices – and I present a first emissions estimate for this specific land use practice that can be included in national GHG emission estimates, if combined with a quantification of the level of degradation and the area where it occurs.

Table of contents

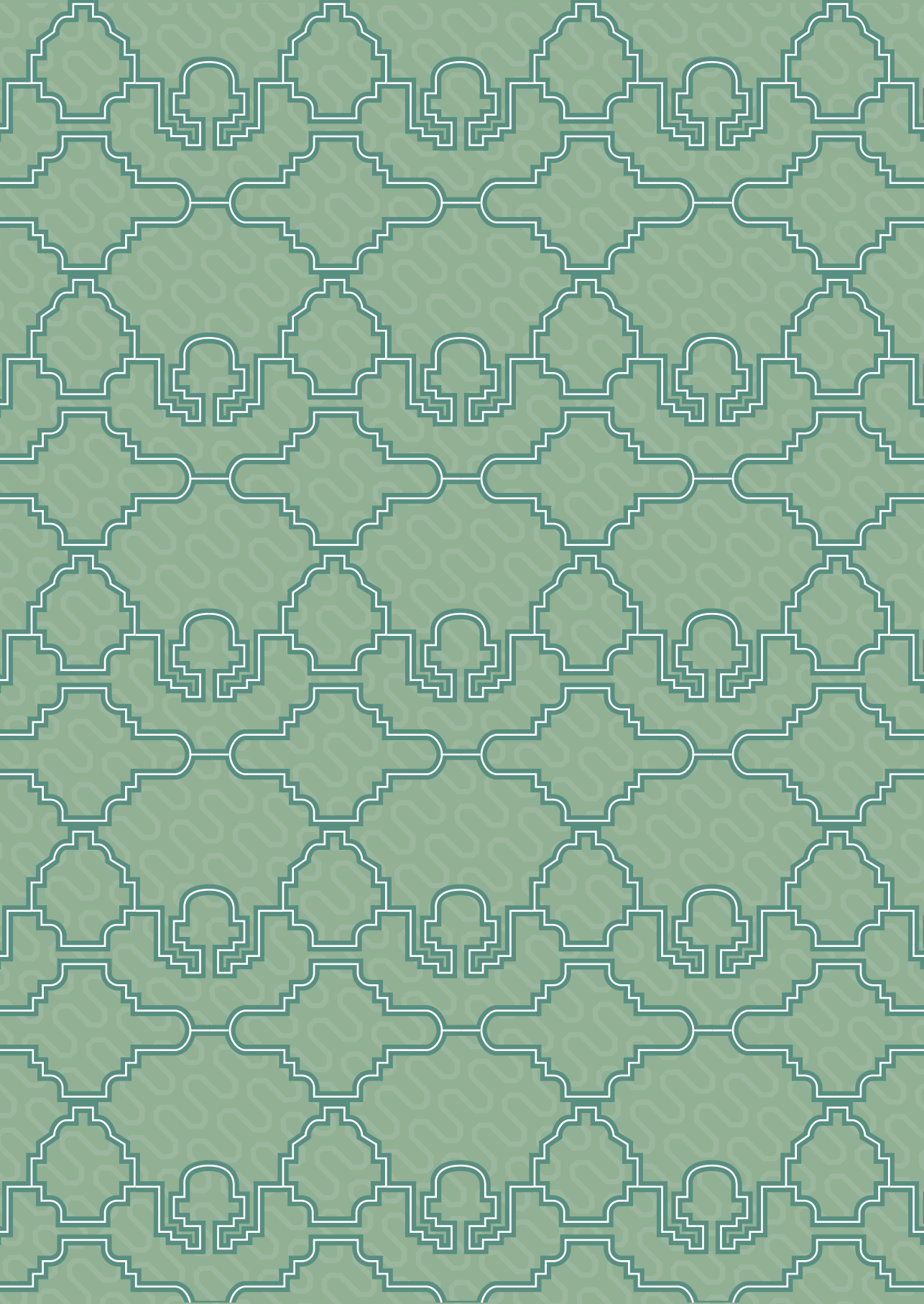

1

General introduction

1 General introduction

Anthropogenic emissions of greenhouse gasses (GHGs) are the main cause for climate change and global warming. Carbon dioxide (CO_2), methane (CH_4) and nitrous oxide (N_2O) are the most important GHGs, and a significant fraction of the total GHG emissions that originates from human activities. In a natural system plants take up CO_2 from the atmosphere and N from the soil to produce above and belowground biomass. In turn, CO_2, CH_4 and N_2O are released back into the atmosphere through plant respiration and decomposition of dead plant tissue and soil organic matter. In most natural systems these processes are more-or-less in balance and emissions are generally low, but anthropogenic activities can affect these processes and substantially elevate GHG emissions.

The agriculture, forestry and other land uses sector (AFOLU) accounted for 24% of human-caused global GHG emissions in 2010 (IPCC, 2014). The AFOLU sector can both sequester (through afforestation and improved land management) or emit carbon (through deforestation, forest degradation, peat drainage). In the period 2000-2010, GHG emissions from agriculture ranged between 5.0-5.8 Gt CO_2eq yr^{-1}, while forestry and other land uses (FOLU) activities accounted for 3.2 Gt CO_2eq yr^{-1} (IPCC, 2014). The most important GHG sources in the AFOLU sector (in terms of global warming potential) are land use change and forestry (emitting or sequestering CO_2), followed by enteric fermentation (CH_4 production), peat drainage and fires (resulting in CO_2, N_2O, CH_4 emissions), and manure and fertilizer applications (causing N_2O emissions) (see Figure 1.1). For tropical countries the AFOLU sector in general has a large share in the total annual GHG emissions. For instance, forestry and other land uses (FOLU) accounted for 42% and agriculture for 15% of the total annual emissions in Peru in 2016; whereas in the EU this was -14% for FOLU and 12% for agriculture, leaving 93% for energy combustion related emissions in the same year (CAIT, 2019). Negative FOLU emissions are common for Annex I countries, and represent a net sequestration of CO_2-C due to, for example, net afforestation rates.

FOLU activities that induce GHG emissions are essentially emissions that arise from land use, land-use change and forestry. Land-use change is either a change the way land is used (e.g. clearing of forest for agricultural use) or it

has an effect on the amount of biomass (e.g. logging). Causes of land-use change are a complex and interacting combination of economic, social and political factors (Lambin et al., 2001, 2003). Population growth and agricultural export correlate well with forest conversion rates (DeFries et al., 2010), and commercial

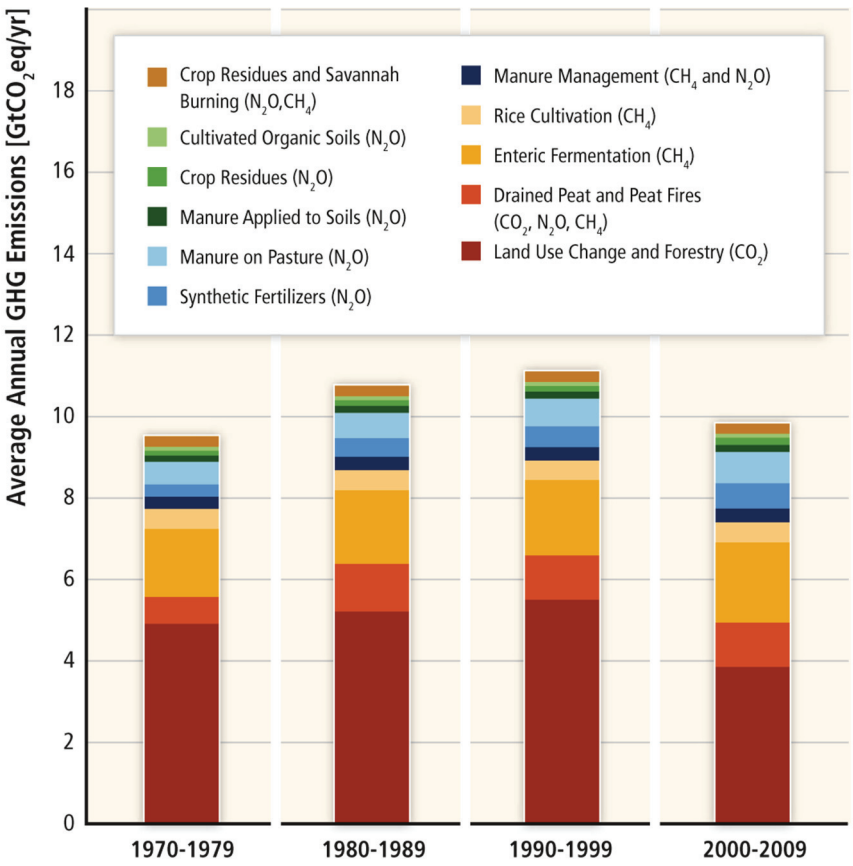

Figure 1.1 - AFOLU emissions during the last four decades. For the agricultural sub-sectors emissions are shown for separate categories, based on FAOSTAT, (2013). Emissions from crop residues, manure applied to soils, manure left on pasture, cultivated organic soils, and application of synthetic fertilizers are typically aggregated to the category 'agricultural soils' for IPCC reporting. For the Forestry and Other Land Use (FOLU) sub-sector data are from the Houghton bookkeeping model results (Houghton et al., 2012). Emissions from drained peat and peat fires are, for the 1970s and the 1980s, from JRC / PBL (2013), derived from Hooijer et al. (2010) and van der Werf et al. (2006) and for the 1990s and the 2000s, from FAOSTAT, 2013. (From IPCC, 2014).

and subsistence agriculture are the most prevalent deforestation driver in non-Annex I (i.e. low and middle income) countries (Hosonuma et al., 2012). Between 1980 and 2000, 83% of the new agricultural land within the tropical region was converted from intact or disturbed forest (Gibbs et al., 2010). The main commodity groups associated with emissions from deforestation are beef production (cattle meat) and production of oilseed products (i.e. palm oil and soybeans). For 2010-2014, a fifth of these emissions were estimated to be related to peatland drainage (Pendril et al., 2019).

Efforts to reduce human-induced GHG emissions requires knowledge and a mechanistic understanding of GHG emissions from land use (LU) and land-use change (LUC) in the AFOLU sector. If such reduction efforts are driven by some kind of performance-based payment scheme (e.g. REDD+, The Green Climate Fund), an exact quantification of these emissions is crucial in order to prevent over- or underestimation of GHG emission reduction efforts. Estimating emissions from the AFOLU sector is commonly based on IPCC Tier 1 values. However, the accuracy of GHG emission estimates is low whenever country-specific GHG emission factors (derived following detailed and precise IPCC Tier 2 or Tier 3 approaches) are missing, and annual emissions are estimated using default IPCC Tier 1 values. For the tropics such default emission factors are generally based on few studies and on short-term measurements, sometimes from other climatic zones and/or different continents. A second possible source of low accuracy in GHG emission predictions is when emission factors for specific land use practices are missing. The effects of both sources of uncertainties are of great importance for the AFOLU sector in tropical countries, because of its large surface area and relatively large contribution to annual GHG budgets.

In this thesis I focus on both of these problems by increasing the mechanistic understanding of the effects of forest conversions on GHG emissions in the tropics, and to contribute to the derivation of robust emission factors for land-use change in the tropics.

1.1 Improving emission factors for land use and land-use change in the tropics: N_2O emissions from land use and land-use change

Emission factors for N_2O emissions have high uncertainties in the 2006 IPCC Guidelines for national GHG inventories. The N_2O emission factor for land following conversions of tropical forests to agriculture was based on few studies and mostly from the temperate zone and non-tropical countries. Several studies have reported high N_2O emissions following land-use change (e.g. Ishizuka et al., 2005; Keller et al., 2005; Takakai et al., 2006; Verchot et al., 2006; Yashiro et al., 2008) and NO (e.g. Verchot et al., 1999; Erickson et al., 2002; Pérez et al., 2007; Davidson et al., 2008).

Although the absolute mass of N_2O emissions might be small, the global warming potential for N_2O over a 100-year time horizon is 298 times greater than that of CO_2 (Myhre et al., 2013). While NO is in fact an indirect GHG, it is relevant to study its dynamics in combination with that of N_2O as they share the same processes of production (nitrification and denitrification) in the soil and are hypothesized to be predicted by nitrogen availability and soil aeration indices (Firestone and Davidson, 1989; Davidson et al., 2000).

High uncertainties in the 2006 IPCC Guidelines can be explained by spatiotemporal variations, such as diurnal and seasonal variations in weather conditions and variations in soil properties (see e.g. Meixner et al., 1997; Chen and Huang, 2009; Lin et al., 2010; Dalal and Allen, 2008). However, uncertainties in emissions from land following conversions of tropical forests to agriculture can also be related to a general lack of experimental studies that reliably estimate seasonal and annual variations in N_2O emissions. An up-to-date overview would aid to assess spatiotemporal variation in N_2O and NO emissions for land use and land-use change, pinpoint gaps and directions for future investigations, and also to evaluate proxies and relationships between N-oxide emissions and environmental parameters.

1.2 Estimating GHG emissions from a region-specific land use not studied to date: forest degradation in tropical peatlands of the Amazon

Tropical peatlands are among the most efficient terrestrial ecosystems for carbon sequestration (Dommain et al. 2011; Page et al. 2004). Tropical peat builds up due to a continuous input of organic material from tropical evergreen vegetation, combined with anaerobic soil conditions (Jauhiainen et al. 2012). In natural conditions, the portion of peat that is decomposed and emitted as CO_2 or CH_4 is usually outweighed by the continuous input of fresh litter and roots (Jauhiainen et al. 2005; Hergoualc'h and Verchot, 2011; Hoyos-Santillan et al. 2015), and results in a net sequestration of CO_2-C in belowground peat deposits. This positive balance of C input > C output can be disturbed by LUC. It is well-known that peatlands in Southeast Asia are under great pressure from agricultural expansion, artificial drainage, and fires, which result in considerable GHG emissions to the atmosphere (Gaveau et al. 2015; Hergoualc'h and Verchot, 2014). Most studies dealing with LUC in tropical peat swamp forests (PSFs) consider the effects of drainage and conversions (e.g. to palm oil plantations). Drainage enhances peat decomposition and shifts the C input-output balance of peatlands towards a net source of CO_2-C to the atmosphere. However, if the peat is not drained, a lack of input of organic material from the vegetation potentially result in a similar situation and a negative C balance (C input < C output).

The case of forest degradation on peat in the Peruvian Amazon provides a unique opportunity for studying effects of reduced fresh litter inputs on the peat C balance. Contrary to Asia, anthropogenic forest degradation of peatland in the Peruvian Amazon is mostly related to recurrent harvesting of *Mauritia flexuosa* palms from natural stands without drainage or fire (Figure 1.2). The fruits from *M. flexuosa* palms (locally referred to as Aguaje) and palm weevils (*Rhynchophorus palmarum*) that grow inside dead palms are highly demanded food products in the regional market (Virapongse et al., 2017), and are important sources of vitamins and proteins for rural communities (Pacheco Santos, 2005). Even though more sustainable (climbing) techniques exist (Horn et al., 2012), fruit harvesting

Figure 1.2 – Harvesting of fruit from *M. flexuosa* palms occurs in natural populations throughout the Peruvian Amazon. Fruits are transported to major ports, such as Iquitos, and sold on the market (photos by Rupesh Bhomia).

continues to involve cutting down entire palms and occurs throughout the Amazon (Horn et al., 2018). Although the practice of palm-harvesting is not new, and already described in the 1980s (Padoch, 1988), effects of these practices on long-term peat accumulation remain unstudied.

Interest in the carbon pools of the Peruvian Amazon peatlands has increased in recent years. Since Lähteenoja et al. (2009b) explored their extent, research further expanded into other fields such as palaeoecology (Roucoux et al. 2013), C stocks estimates (Draper et al. 2014), and *M. flexuosa* management (Virapongse et al. 2017). The Amazon is estimated to harbour one of the largest extents of tropical

peatlands in the world (Gumbricht et al. 2017), and the Pastaza-Marañón basin in Peru is a hotspot with estimated C stocks ranging between 2 and 20 Pg C (Lähteenoja et al. 2012; Draper et al. 2014). In comparison, total aboveground biomass C in the entire Peru is estimated to contain 6.9 Pg C (Asner et al. 2014).

An assessment of C stocks variability and effects of selective harvesting of *M. flexuosa* palms is absent in current literature. It remains to be determined whether forest degradation on peat affects peat accumulation rates, to the extent that the peat switches from a C sink to a C source. Since the land use does not involve active drainage or fertilization practices, other proxies are needed to quantify and upscale these effects to the regional scale. If this land use leads to significant C losses, and the land use represents a wide-applied activity, its emissions should be accurately monitored and reported in national GHG inventories.

1.3 Research objectives

The overall goal of my thesis was to increase the mechanistic understanding of the effects of forest conversions on GHG emissions in the tropics. I aimed to systematically review all studies on N_2O and NO emissions from land use and land-use change in the tropics; in order to improve current emission factors for land use and land-use change in the tropics. Further, I aimed to examine CO_2, N_2O and CH_4 emissions from a region-specific land use not studied to date: forest degradation in tropical peatlands of the Amazon. My specific research objectives were as follows:

1. Synthesize the current knowledge of the effects of forest conversion to agricultural land on N_2O (and NO) emissions and their proxies in the global tropics.
2. Estimate C stocks of *M. flexuosa*-dominated peat swamp forest in three regions of the Peruvian Amazon and relate it to *M. flexuosa* harvesting.
3. Test proxies of *M. flexuosa* harvesting that can affect soil GHG emissions of palm-dominated peat swamp forests.
4. Quantify the effects of different levels of *M. flexuosa* harvesting on the peat carbon balance in the Peruvian Amazon.

1.4 Experimental setup

To address these objectives, I used a combination of methods: a meta-analysis, two field experiments, and a soil incubation study. For the first objective I performed a meta-analysis with all available studies measuring N_2O and NO emissions from land-use change in the tropics up to and including 2013. A meta-analysis allows for a comparison between independent studies, and weights studies according to their uncertainty (Hedges and Olkin, 1985). The result of the meta-analysis was an average effect size per land-use change category, indicating if emissions would significantly increase or decrease after land-use change. I further investigated correlations between these effect sizes and potential proxies for N_2O and NO emissions.

For objective 2 and 4 I performed two different field studies. The first field experiment was an explorative study to assess C-stocks and forest degradation status throughout the Peruvian Amazon. For this, three different regions were sampled: one in near the Tigre river that had high probabilities of forest degradation following the pilot study by Hergoualc'h, Gutiérrez-Vélez, et al. (2017); another along the Samiria river that is inside the national Pacaya-Samiria wetland reserve, and a last near the Itaya river that is close to Iquitos, the largest city in the Peruvian Amazon (Figure 1.3). Within these three regions, twelve sites were sampled for determination of total C stocks by measuring aboveground and belowground vegetation C stocks, downed woody debris and litter C stocks, and C stored in underlying soils. Evaluation of relationships between forest degradation status and C stocks were carried out to understand the role of anthropogenic factors such as palm harvesting on ecosystem C stocks. The role of regional landscape factors such as riverine sediment inputs on peat accumulation processes at a broader scale were also evaluated.

The second field experiment was to measure the peat C balance in the Itaya region on a monthly basis during four consecutive years (2014-2018). The three sites were degraded at varying intensities and consisted of an intact (Quistococha), a moderately (Las Brisas) and a heavily degraded site (San Julian). The experimental setup accounted for variations in the microtopography, and consisted of measurements at higher parts (hummocks) and lower parts (hollows). Heterotrophic soil respiration was separated from total soil respiration

by trenching plots, such that root growth was excluded (Subke et al., 2006). Further, I measured leaf- and woodfall rates, along with environmental factors such as water table, water-filled pore space and soil temperature.

Lastly, for objective 3, an *in vitro* incubation study was performed to test proxies of GHG production. I incubated soils from the three Itaya sites at varying moisture levels, measured the GHG production and built statistical relationships between the two. These relationships were later verified in the field study (objective 4).

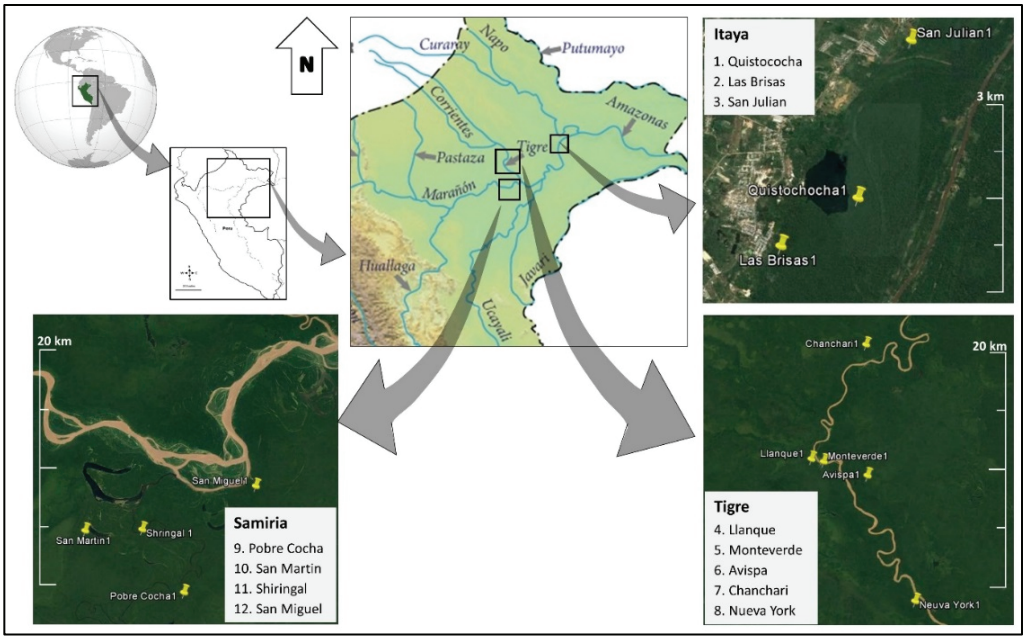

Figure 1.3 – Location of field study sites. C-stocks are measured in all 12 sites, four-year monitoring of the C balance was performed in the three sites at the Itaya region (from Chapter 3).

1.5 Outline

I formulated the following hypotheses that were tested in the previously mentioned experiments:

1. Forest conversion to agriculture causes an increase in N_2O emissions, and annually-averaged nitrogen availability and water-filled pore space provide useful proxies for N_2O (and NO) emissions. (Chapter 2)
2. Natural disturbances and palm harvesting practices both affect soil C stocks and peat accumulation rates of *M. flexuosa*-dominated peat swamp forests in the Peruvian Amazon. (Chapter 3)
3. Soil moisture indices, presence of aerating roots, litter quality, and microtopography were hypothesized to be affected by *M. flexuosa* harvesting and in turn affect GHG production and emissions in degraded peat swamp forests as compared to intact sites. (Chapter 4)
4. Severe forest degradation in peat swamp forests causes the peat soil to switch from being carbon neutral to being a net carbon source to the atmosphere (Chapter 5)

Each of the chapters addresses one of the objectives and matching hypotheses. In chapter 6, I present a general discussion of the four chapters and present some conclusions, outlook and directions for future research.


2

2

Soil N_2O and NO emissions from land use and land-use change in the tropics and subtropics: a meta-analysis

This Chapter is published as:
Van Lent, J.[1], Hergoualc'h, K.[2], & Verchot, L. V.[3] (2015).
Soil N_2O and NO emissions from land use and land-use change in the tropics and subtropics: a meta-analysis. *Biogeosciences*, 12, 7299-7313.

[1] Center for International Forestry Research (CIFOR), Jl. CIFOR, Situ Gede, Bogor 16115, Indonesia
[2] Department of Soil Quality, Wageningen University, Wageningen, The Netherlands
[3] Earth Institute Center for Environmental Sustainability, Columbia University, New York, 270 USA

2 Soil N_2O and NO emissions from land use and land-use change in the tropics and subtropics: a meta-analysis

Abstract

Deforestation and forest degradation in the tropics may substantially alter soil N-oxide emissions. It is particularly relevant to accurately quantify those changes to properly account for them in a REDD+ climate change mitigation scheme that provides financial incentives to reduce the emissions. With this study we provide updated land use (LU)-based emission rates (104 studies, 392 N_2O and 111 NO case studies), we determine the trend and magnitude of flux changes with land-use change (LUC) using a meta-analysis approach (44 studies, 135 N_2O and 37 NO cases) and evaluate biophysical drivers of N_2O and NO emissions and emission changes for the tropics.

The average N_2O and NO emissions in intact upland tropical forest amounted to 2.0 ± 0.2 (n = 90) and 1.7 ± 0.5 (n = 36) kg N ha^{-1} yr^{-1}, respectively. In agricultural soils annual N_2O emissions were exponentially related to N fertilization rates and average water-filled pore space (WFPS) whereas in non-agricultural sites a Gaussian response to WFPS fit better the observed NO and N_2O emissions. The sum of soil N_2O and NO fluxes and the ratio of N_2O to NO increased exponentially and significantly with increasing nitrogen availability (expressed as $NO_3^-/[NO_3^- + NH_4^+]$) and WFPS, respectively; following the conceptual Hole-In-the-Pipe model. Nitrous and nitric oxide fluxes did not overall increase significantly as a result of LUC (Hedges's d of 0.11 ± 0.11 and 0.16 ± 0.19, respectively), however individual LUC trajectories or practices did. Nitrous oxide fluxes increased significantly after intact upland forest conversion to croplands (Hedges's d = 0.78 ± 0.24) and NO increased significantly following the conversion of low forest cover (secondary forest younger than 30 years, woodlands, shrublands) (Hedges's d of 0.44 ± 0.13). Forest conversion to fertilized systems significantly and highly raised both N_2O and NO emission rates (Hedges's d of 1.03 ± 0.23 and 0.52 ± 0.09, respectively).

Changes in nitrogen availability and WFPS were the main factors explaining changes in N_2O emissions following LUC, therefore it is important that experimental designs monitor their spatio-temporal variation. Gaps in the

literature on N oxide fluxes included geographical gaps (Africa, Oceania) and LU gaps (degraded forest, wetland (notably peat) forest, oil palm plantation and soy cultivation).

2.1 Introduction

Land use (LU) and land-use change (LUC) are important contributors to global greenhouse gas (GHG) emissions. The current contribution of LUC to total anthropogenic GHG emissions is estimated between 7 and 18% (Houghton, 2003; Baumert et al., 2005; Baccini et al., 2012; Harris et al., 2012). This estimation heavily depends on biomass values and deforestation rates and is associated with high uncertainties, especially in the tropics (Houghton 2005). Causes of LUC are a complex and interacting combination of economic, social and political factors (Lambin et al., 2001, 2003). However, population growth and agricultural export correlate well with forest conversion rates (DeFries et al., 2010). A recent comparative study showed commercial and subsistence agriculture to be the most prevalent deforestation driver in non-Annex I (i.e. developing) countries (Hosonuma et al., 2012). Between 1980 and 2000, 83% of the new agricultural land within the tropical region were converted from intact or disturbed forest (Gibbs et al., 2010). As the world population and food demand are expected to grow (respectively 34% and 70% by 2050, FAO [2009]), further deforestation is likely in the near future.

By avoiding deforestation and forest degradation and through enhancing carbon (C) stocks in forests, reducing worldwide GHG emissions could be achieved with a reasonable level of cost-efficiency (Stern, 2008; Streck & Parker, 2012). However, for climate change mitigation schemes such as reducing emissions from deforestation and forest degradation (REDD+), where payments are based on performance, it is crucial to know how much emissions can be mitigated by preventing deforestation and reforesting. In addition to carbon dioxide (CO_2), several studies on LUC in the tropics reported high non-CO_2 GHG emissions, such as nitrous oxide (N_2O) (e.g. Ishizuka et al., 2005; Keller et al., 2005; Takakai et al., 2006; Verchot et al., 2006; Yashiro et al., 2008) and nitric oxide (NO) (e.g. Verchot et al., 1999; Erickson et al., 2002; Perez et al., 2007; Davidson et al., 2008). Although the absolute mass of N_2O emissions might be small, the global

warming potential for N_2O over a 100 year time horizon is 298 times greater than that of CO_2 (Forster et al., 2007). In addition this trace gas also contributes to ozone depletion in the stratosphere (Crutzen, 1970). Nitric oxide, on the other hand, is a free radical that enhances ozone production in the troposphere (lower atmosphere) (Chameides et al., 1992); ozone in the troposphere is a GHG (Myhre et al., 2013). Although NO is in fact an indirect GHG, it is relevant to study its dynamic in combination with that of N_2O as they share the same processes of production (nitrification and denitrification) in the soil and are hypothesized to be interlinked (Firestone & Davidson, 1989).

Emissions factors in the IPPC guidelines for national GHG inventories (2006) have high uncertainties although some of these were slightly reduced in the 2013 wetlands supplement (Drösler et al., 2014). On the one hand, this high uncertainty can be explained by the high temporal and spatial variability of N_2O and NO emissions which are known to vary diurnally, seasonally (see e.g. Meixner et al., 1997; Chen & Huang 2009; Lin et al., 2010), and locally due to micro site-specific soil variability (Dalal & Allen, 2008). On the other hand, the high uncertainty is partly due to the paucity of reliable estimates available in the peer-reviewed literature.

Sources of biogenic N_2O and NO fluxes from the soil can be a wide variety of microorganisms and processes (Anderson & Poth, 1989), but nitrification and denitrification are the main mechanisms (Davidson et al., 2000; Baggs & Philippot, 2010). Therefore, the magnitude of N_2O and NO fluxes depends on variables that enhance or inhibit nitrification and denitrification such as nitrogen (substrate) availability, soil water content (aeration status), soil temperature and pH (Skiba & Smith, 2000; Heinen, 2006; Dalal & Allen, 2008). Substrates for nitrification and denitrification are ammonium and nitrate, respectively. Ammonium (NH_4^+) is the result of microbial decomposition of soil organic matter and is converted to nitrate (NO_3^-) by the nitrifying bacteria under aerobic conditions. In this process, N_2O and NO are produced and partly emitted to the atmosphere. NO_3^- in return is used under anaerobic conditions as a terminal electron acceptor for denitrifying bacteria that reduce NO_3^- to N_2. Along this reduction gradient N_2O and NO are also produced and partly emitted to the atmosphere (Anderson & Poth, 1989; Baggs & Philippot, 2010).

Both nitrification and denitrification produce N_2O and NO but are influenced differently by the same soil variables. Therefore, models predicting N_2O and NO fluxes need to consider both processes. Firestone & Davidson (1989) proposed a conceptual model – dubbed the 'Hole-In-the-Pipe' (HIP) model – that uses two levels of control for N_2O and NO emissions in soils. The first level of control is nitrogen availability, symbolized as the amount of N flowing through the pipes. The second level of control is generally represented by the soil aeration status, explained as the size of the holes in the pipe through which N_2O and NO "leak" into the atmosphere. The HIP-model and its underlying assumptions were tested under distinct conditions, which showed that soil nitrogen availability could be expressed in different ways. Davidson et al. (2000) tested several indicators and found that the C:N ratio of litterfall and the ratio of NO_3^- to the sum of NO_3^- and NH_4^+ were promising proxies of N cycling. Underlining the importance of rapid cycling N in N-oxide production, Purbopuspito et al. (2006) showed a good correlation between $\delta^{15}N$ signatures of litter and soil and emissions of N_2O in Indonesia. Veldkamp et al. (1998) suggested that, in N fertilized systems of Costa Rica, the major factor controlling N_2O emissions was the soil aeration status (second level of control), as N availability exceeded demand. The soil aeration status is commonly expressed by the water-filled pore space (WFPS) (Linn & Doran, 1984); with a high WFPS meaning a low aeration (Heinen, 2006). Nitric oxide is mainly produced when the WFPS is below field capacity, whereas N_2O is produced at higher WFPS, exceeding field capacity (Davidson et al., 1991, 1993; Dobbie et al., 1999; Davidson & Verchot, 2000; Bateman & Baggs, 2005). Depending on soil texture, the field capacity is at a WFPS of around 60%; whenever the WFPS exceeds 80%, most of the N is expected to be denitrified into N_2.

The goal of this study was to review how the emissions of N_2O and NO in the tropics were affected by LU and LUC and to examine their variation in relation to biophysical parameters. We used all studies published in the peer-reviewed literature up to 2013 to calculate emissions per LU type and evaluated relationships with environmental parameters. Next, the effect of LUC was assessed by using a quantitative meta-analysis statistical approach that allows for a comparison between independent studies, and weights studies according to their uncertainty (Hedges & Olkin, 1985). We used the Hedges' d (Koricheva et al.,

2013) metric to evaluate LUC effects. This is a standardized mean difference similar to the Hedges' g but adjusted for small sample sizes. Finally we ran a meta-analysis regression to express the changes in emission rates following LUC as a function of environmental and soil variables changes.

2.2 Material and methods

We followed three main steps to assess how soil N_2O and NO emissions were affected by LU and LUC in the tropics and subtropics: (i) compiling a database of all studies on soil N_2O and NO fluxes, selecting those integrating seasonal variation in their experimental design and categorizing LU types; (ii) estimating average emission rate per LU category and exploring biophysical factors affecting them; and (iii) characterizing the magnitude of emission change due to LUC using a meta-analysis approach and evaluating how this change could be expressed as a function of the change in biophysical factors through a meta-analysis regression.

2.2.1 Data collection and calculation

The database of Stehfest & Bouwman (2006) (available at: www.mnp.nl/en/publications/2006) was used as a basis for our research. From this dataset, we extracted the 102 studies located in the tropics and subtropics (hereafter collectively referred to as 'tropics'), defined as climate types 3-6, using the climate classification defined by De Pauw et al. (1996). We then extended the database by including 279 additional peer-reviewed studies published between 1990 and 2013 on soil emissions of NO and/or N_2O in the tropics. A combination of the following keywords were used in the ISI Web of Science and ScienceDirect search engines: N_2O, nitrous oxide, NO, nitric oxide, emissions, fertilizers, forest, arable, grasslands, flux, nitrification, denitrification, land use, NOx, nitrogen-oxide, tropics, subtropics. As N_2O and NO fluxes are known to vary seasonally (e.g. Meixner et al., 1997; Chen & Huang, 2009), we manually selected the studies that measured the fluxes during both dry and wet seasons. The 103 studies selected (S1, Supplement available at: http://dx.doi.org/10.5194/bg-12-7299-2015-supplement), representing 392 N_2O and 111 NO LU case studies, were used to estimate annual mean N-oxides emission rates per LU category and to analyse

their relationship with environmental proxies. Out of the 104 papers 44 measured N_2O and/or NO emissions synchronically in at least two different LUs, one of which was a forest. These 44 papers represented 135 N_2O and 37 NO LUC case studies which were analysed using a meta-analysis statistical approach (S2, Supplement available at: http://dx.doi.org/10.5194/bg-12-7299-2015-supplement). We summarized the number of studies and assessed the representation of LU per continent categorizing them in five geographical areas: North-Central America, South America, Africa, South Asia and Oceania. Average annual emission rates were expressed in kg NO-N or N_2O-N ha^{-1} yr^{-1} using the estimates provided by the papers. Whenever annual fluxes were not provided by the authors, we calculated them. For studies covering year-round measurements, the annual flux was calculated by scaling up the units from hours or days to a year and cm^2 or m^2 to ha. Where possible reported fluxes were weighed according to their time interval. For instance, for studies covering measurements made during the dry and wet seasons, the annual flux was calculated as the sum of each seasonal flux weighted by the number of days per year corresponding to each season. The biophysical variables associated with N_2O and NO emissions from the publications were also expressed as annual averages. Soil variables (temperature, WFPS, bulk density, pH, C content, N content, NH_4^+ and NO_3^-) are from the soil top layer (0-10cm). Nitrogen fertilization and litterfall are given as a mass of nitrogen per hectare per year. In some cases the water-filled pore space (WFPS, %) was manually calculated as a function of the gravimetric water content (m, g g^{-1} d.w.), bulk density (y_d, g cm^{-3}) and particle density (y_s, g cm^{-3}) as WFPS = $100*(m*y_d)/(1-(y_d/y_s))$ (Linn & Doran 1984). A y_s default value of 2.65 g cm^{-3} was used for mineral soils (Hillel, 1980), whenever not provided by the studies. Nitrogen fixation was considered by using a dichotomous variable indicating the presence or absence of N_2 fixing species in the LU. Nitrogen fixation rates were barely reported and could not be included. For studies measuring N_2O and NO simultaneously, we calculated

Table 2.1 – Average of annual N_2O and NO emissions in the Tropics and associated environmental parameter values. Land uses are F: forest, WF: wetland forest, LFC: low forest cover, DegF: degraded forest, AGF: agroforestry, Pl: plantation, Pa: pasture, R: rice and Crop: cropland. NA: not available, no nitric oxide cases were available for WF. Standard error and sample size are indicated in brackets, # indicates no statistics were possible. Letters in superscript indicate significant differences among land uses, whenever differences were not significant no letter was indicated.

Land use	Flux (kg N ha^{-1} yr^{-1})	Annual precipitation (mm)	Annual temperature (°C)	Soil temperature (°C)	WFPS (%)	Bulk density (g d.w. cm^{-3})	pH	NH_4^+ (µg N g^{-1} d.w.)	NO_3^- (µg N g^{-1} d.w.)	C (%)	N (%)	Fertilization (kg N ha^{-1} yr^{-1})	Litterfall (kg N ha^{-1} yr^{-1})
						Nitrous oxide							
F	2.0[a]	2226	22.8	23.7[a,b]	56.1	.9[a]	4.9[a,b,c]	20.5[a]	10.8[a]	4.8[a]	0.4[a]	0[a]	100
	(0.2, 90)	(81, 90)	(0.4, 80)	(0.5, 29)	(3.4, 45)	(0.0, 58)	(0.1, 55)	(2.8, 47)	(1.5, 45)	(0.5, 45)	(0.0, 45)	(0, 87)	(17, 14)
WF	2.7[a,b]	2485	26.1	26.8[a,b]	44.5	0.1[b]	3.8[a]	412.0[b]	70.9[b]	49.7[b 1]	1.6[b]	0[a,b,d]	n.a.
	(1.9, 7)	(167, 6)	(0.4, 6)	(0.5, 4)	(7.7, 3)	(0.0, 4)	(0.2, 7)	(119.9, 4)	(12.2, 5)	(3.2, 7)	(0.1, 7)	(0, 7)	
LFC	0.5[a,b]	1546	23.9	28.8[a,b]	47.7	1.1[a,c]	5.0[a,b,c,d]	5.1[a]	3.1[a]	4.0[a]	0.3[a]	0[a,b,d]	n.a.
	(0.1, 11)	(390, 11)	(1.6, 9)	(1.2, 3)	(10.6, 8)	(0.1, 10)	(0.3, 11)	(1.1, 8)	(1, 8)	(0.9, 8)	(0.1, 8)	(0, 10)	
DegF	1.9[a,b]	2220	25.1	27.6[a]	48.4	0.9[a]	4.4[a,b]	44.4[a]	11.6[a]	30.0[c 1]	0.9[c]	0[a,b]	122
	(0.5, 30)	(123, 30)	(0.4, 28)	(0.6, 14)	(5, 19)	(0.1, 24)	(0.2, 23)	(17.4, 20)	(4.1, 20)	(6.2, 20)	(0.1, 20)	(0, 26)	(54, 3)
AGF	3.4[a,b]	2297	25.2	22.1[a,b]	77.1	1.2[a,c]	5.6[b,c,d]	10.7[a]	7.8[a,b]	2.8[a]	0.3[a,c]	39[a,b,c]	218
	(1.6, 8)	(112, 8)	(0.8, 6)	(2.3, 2)	(17.2, 3)	(0.1, 8)	(0.3, 7)	(4.6, 7)	(3.1, 7)	(0.5, 3)	(0.1, 3)	(31, 8)	(#, 1)
Pl	1.5[a,b]	2120	24.3	25.5[a,b]	59.0	1.0[a,c]	4.8[a,b,c]	11.9[a]	17.8[a,b]	6.7[a]	0.4[a]	53[a,b]	304
	(0.3, 40)	(137, 40)	(0.6, 38)	(0.6, 22)	(3.4, 26)	(0.1, 27)	(0.1, 37)	(2.3, 30)	(8.2, 27)	(2.2, 30)	(0.1, 31)	(25, 35)	(153, 5)
Pa	5.2[a,b]	1913	23.4	26.3[a,b]	64.2	1.2[c]	5.4[c,d]	26.1[a]	26.9[a,b]	5.1[a]	0.3[a]	90[b,d]	n.a.
	(1.3, 97)	(89, 90)	(0.5, 54)	(1.9, 8)	(4.6, 18)	(0, 54)	(0.1, 49)	(4.2, 29)	(13.7, 29)	(1.8, 41)	(0, 39)	(17, 70)	
R	5.1[a,b]	1562	21.9	20.9[b]	73.0	1.2[a,c]	6.0[d]	788.01	29.4[a,b]	13.6[a]	0.5[a,c]	228[c]	n.a.
	(1.7, 17)	(234, 13)	(1.9, 13)	(2.4, 5)	(1.2, 3)	(0, 4)	(0.3, 17)	(#, 1)	(2.0, 2)	(5.2, 17)	(0.1, 17)	(61, 17)	
Crop	8.6[b]	1965	24.4	25.3[a,b]	58.1	1.1[a,c]	5.7[d,e]	21.3[a]	12.2[a]	7.5[a]	0.4[a]	155[c,d]	77
	(2.0, 92)	(123, 76)	(0.6, 60)	(1.1, 23)	(5.2, 28)	(0.1, 44)	(0.1, 78)	(10.9, 36)	(2.6, 36)	(1.6, 55)	(0, 55)	(25, 92)	(28, 2)

(continued)

	Nitric oxide												
F	1.7 (0.5, 36)	2342 (166, 35)	21.6 [a] (0.8, 30)	24.9 [a] (0.4, 13)	60.1 (4.5, 24)	0.75 [a] (0.07, 24)	5.3 (0.3, 25)	15.4 (2.5, 21)	12.2 [a] (2.0, 21)	5.1 [a] (0.7, 15)	0.4 (0.1, 19)	0 [ab] (0, 36)	79 (16, 10)
DegF	2.9 (1.9, 20)	2119 (281, 19)	25.4 [bc] (0.9, 12)	26.4 [ab] (0.8, 9)	53.7 (7.8, 11)	1.08 [b] (0.09, 17)	5.6 (0.3, 17)	15.1 (3.1, 13)	5.6 [ab] (1.5, 13)	3.1 [ab] (0.8, 13)	0.3 (0.1, 10)	0 [b] (0, 20)	68 (6, 2)
AGF	2.3 (0.8, 5)	2219 (147, 5)	26.0 [acd] (0.0, 4)	24.4 [#] (#, 1)	56.0 (#, 1)	1.32 [b] (0.03, 5)	5.9 (0.2, 5)	9.5 (4.6, 4)	4.9 [ab] (3.1, 4)	2.5 (#, 1)	0.2 (#, 1)	12 [bdef] (12, 5)	n.a.
Pl	5.4 (5.3, 2)	2124 (1839, 2)	21.4 [acd] (4.4, 2)	n.a.	70.0 (#, 1)	1.23 [ab] (0.43, 2)	7.6 (#, 1)	n.a.	n.a.	n.a.	n.a.	180 [cf] (180, 2)	n.a.
Pa	2.6 (0.7, 28)	2279 (252, 26)	25.5 [bd] (0.1, 13)	27.8 [b] (0.7, 8)	66.8 (6.0, 14)	1.22 [b] (0.07, 16)	5.8 (0.3, 17)	27.0 (5.9, 17)	5.4 [b] (1.1, 17)	1.2 [b] (0.4, 13)	0.2 (0.1, 6)	91 [ce] (26, 26)	n.a.
Crop	3.1 (0.8, 20)	1686 (268, 14)	24.7 [acd] (1.1, 3)	27.8 [b] (0.4, 11)	43.0 (12.3, 6)	1.31 [b] (0.09, 13)	5.7 (0.2, 20)	28.2 (14.5, 12)	12.1 [ab] (2.3, 12)	2.5 [ab] (1.0, 9)	0.3 (0.1, 4)	88 [cd] (17, 20)	n.a.

[1] including 10 degraded peat forests, soil carbon content for non-peat soils was 3.8.

the ratio and sum of the two and tested their correlation with WFPS and soil N availability. The latter is expressed as the relative fraction of NO_3^- to total inorganic N ($NO_3^-/[NO_3^-+NH_4^+]$).

Three LU case studies from Takakai et al. (2006) and the celery plot in Xiong et al (2006) were excluded from the analysis because the very high fertilizations rates were about three times higher than the International Fertilizer industry Association (IFA) recommended dose for the studied crops.

2.2.2 Land use and land-use change characterization

The LU were classified into nine main categories: 1) forest (primary forest and secondary forest older than 30 years), 2) wetland forest (swamp on peat, swamp on mineral soil and riparian forest), 3) low forest cover (low canopy closure: woodlands and shrublands, secondary forest younger than 30 years), 4) degraded forest (human-induced low forest cover after logging and burning or fallows), 5) agroforestry systems, 6) plantations (mono-specific plantations, e.g. *Acacia*, rubber, oil palm, cinnamon), 7) pastures (pastures and grasslands), 8) rice fields, and 9) croplands (annual and perennial crops). For agroforestry, plantation, pasture, rice and cropland both fertilized and unfertilized cases were combined and the effect of fertilization was tested separately. Only a few studies included age after conversion in a chronosequential sampling design; therefore we pulled together LU cases from different studies to evaluate the change in emission rates as a function of time since conversion.

The studies either focused on a specific LUC type (e.g. forest conversion to pasture), or considered several LUC types which were representative for the study region. In the latter case, when only one control (forest) site was available, we used the same control for all converted sites. Whenever several control sites were available in a study we averaged the fluxes from all control sites. When a study measured emissions for several years, each year was considered a separate case. The following LUC were analysed: forest to degraded forest, agroforestry, plantation, pasture and cropland; wetland forest to degraded forest, plantation, pasture and rice; degraded forest to agroforestry; low forest cover to plantation, pasture and cropland. The effect of primary forest conversion to secondary forest is not included in this study as secondary forest (>30 years old) and primary forest

were merged into a single category. The same holds for logging impacts in degraded forests.

2.2.3 Statistics

Statistical analysis was performed using the software IBM SPSS Statistics for Windows 21.0 (IBM Corp. 2012) and statistical significance was set at a maximum probability level of 5%. The normality of the flux distribution was tested using the test of Shapiro-Wilks. Neither NO and N_2O nor their log-transformed values were normally distributed hence a generalized linear model with a post-hoc pair-wise comparison was performed for comparing the fluxes between LU. Throughout the text averages are followed by standard errors (± S.E.).

Stepwise multiple linear regression was performed to identify the environmental variables that were significantly related to soil fluxes of N_2O and NO. Variables available in <10% of all study cases were excluded to obtain a sufficient sample size for the regression. In order to maximize the data availability we used pair-wise exclusion for dealing with missing values. We also excluded predictor variables that were collinear (multicollinearity test, VIF statistics) to other variables already included in the model. A non-linear Gaussian function was fit between N_2O, NO fluxes and WFPS using averages per 10% WFPS intervals.

Meta-analysis

A meta-analysis was used to quantify the effect of LUC on soil annual N_2O and NO fluxes. For this we used the software Comprehensive Meta-Analysis version 2.2.064 (Biostat Inc., New Jersey, USA) and MetaWin 2.0 (Sinauer Associates, Sunderland, Massachusetts). We defined N_2O or NO emissions after land-use change as being the treatment and N_2O or NO emissions before land-use change as being the control. Hedges'd (d) was used as metric to evaluate the effect size of LUC on N_2O and NO fluxes. This metric is defined as:

$$d = \frac{(\bar{X}_T - \bar{X}_C)}{S} \times J \quad (1)$$

$$S = \sqrt{\frac{(N_C-1)(SD_C)^2+(N_T-1)(SD_T)^2}{N_C+N_T-2}} \quad (2)$$

$$J = 1 - \frac{3}{4(N_C+N_T-2)-1} \quad (3)$$

Where, $\bar{X}_T$ and $\bar{X}_C$ are the average N_2O or NO flux (in kg N ha^{-1} yr^{-1}) of the treatment and control, respectively; S is the pooled standard deviation from the control and treatment flux standard deviations (SD_C and SD_T) and J is the correction factor calculated from the sample sizes (N_T and N_C). The effect size (d) for all LUC case studies combined, or that for a particular LUC type, was assessed using a random model which allows for a varying true effect size between studies (Gurevitch & Hedges, 1999; Borenstein et al., 2009). A d equal or smaller than 0.2 indicates a small effect size, a d around 0.5 a medium one and a d > 0.8 a large effect. Positive and negative d's respectively imply an increase and decrease in N_2O or NO emission after LUC, respectively.

Calculation of d requires knowledge of the standard deviation and sample size associated with the average N_2O or NO flux rate. Whenever these were not available in the publication we contacted the authors, calculated it ourselves using the methodological description of the experimental design or measured it from the figures of the papers using PlotDigitizer 2.5.1 (Joseph A. Huwaldt, 2011).

Publication bias for studies with significant and/or high effect sizes was assessed using a normal quantile plot (Wang & Bushman, 1998). Deviation from linearity of the observed distribution suggests publication bias while gaps in the plotted scatter plot indicate that certain effect sizes are missing in the published literature (Borenstein, 2009).

Heterogeneity of effect sizes was assessed with the Q and I^2 statistics. A significant $Q_{overall}$ means that the variance among LUC study cases is greater than that expected by sampling. In a heterogeneous dataset, the ($1-I^2$) statistic quantifies the variation within case studies and I^2 the variation that could be explained by other variables (or 'real variation'). I^2 of 25%, 50%, 75% are respectively considered as low, moderate and high (Borenstein, 2009). An $I^2 > 0$ shows that a proportion of the observed variation is real; thus, subgroup division

into LUC types and/or meta-analysis regression can be used (Gurevitch & Hedges, 1999). LUC effect sizes obtained from a low sample size are likely to be influenced by random deviations; hence their interpretation should be handled with caution. Finally, we performed a meta-analysis regression (or 'meta-regression') (Higgins & Green, 2011) to assess how the changes in environmental factors affected changes in soil N_2O or NO emission as a result of LUC. We looked at how the standardized mean difference of an environmental parameter was affecting that of soil N_2O or NO emissions. A meta-analysis regression is considered robust when it includes ten cases studies at least (Borentstein, 2009; Higgins & Green, 2011).

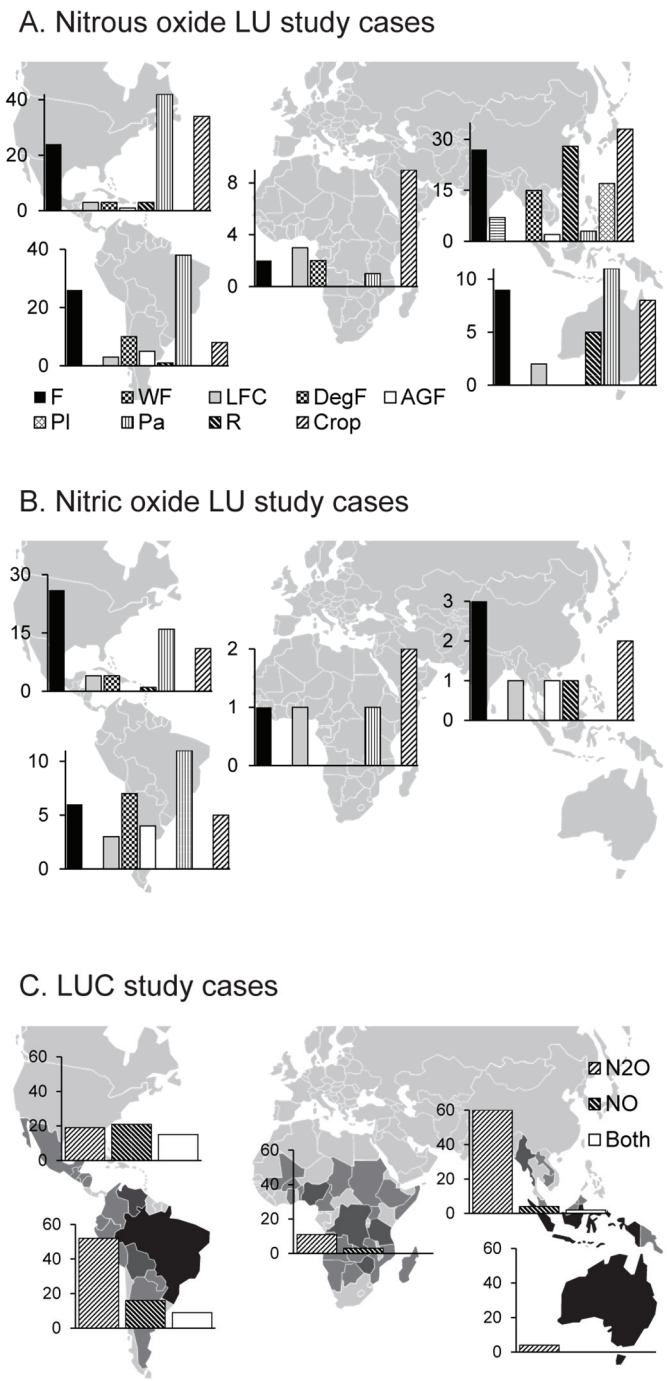

Figure 2.1 – Spatial distribution of land use case studies on soil fluxes of (a) N_2O and (b) NO per land use category in the tropics. Land uses are abbreviated as F: forest, WF: wetland forest, LFC: low forest cover, DegF: degraded forest, AGF: agroforestry, Pl: plantation, Pa: pasture, R: rice and Crop: cropland. Y-axes of the diagrams represent number of case studies per land use. Land use case studies from Europe are omitted (n = 2). (c) Spatial distribution of land-use change case studies on soil N_2O and NO fluxes, compared to a map of annual loss of forest area by country between 2005 and 2010. The four shades of grey, from black to light grey, respectively represent >500, 500-250, 250-50 and <50 net loss of area in 1,000 ha. Adapted from FAO (2010).

2.3 Results

2.3.1 Exploring the dataset

The publication rate of peer-reviewed papers on LU and soil emissions of N_2O and NO in the tropics has more than doubled over the past decade (less than 2 publications y^{-1} before 2000, more than 5 y^{-1} afterwards), but remains low. The Americas (combining North-Central and South America) and South Asia represented the majority of the dataset (n = 229 and n = 137), while Africa and Oceania were underrepresented (n = 21 and n = 35, respectively; Figure 2.1).

LU types studied varied substantially across continents (Figure 2.1). In South Asia 61% of the LUs studied were croplands, rice fields or plantations, while these were only 13% in South America. Some LUs were geographically well represented while others were clustered in one continent. For instance, agroforestry systems were spatially well represented, although few in numbers (n = 8), while rice paddies were mostly studied in Asia. Studies on wetland forest were underrepresented (n = 7) and restricted to South Asia (Figure 2.1a).

Ninety-four percent of the LU case studies on soil fluxes of NO were in North-Central and South America (respectively, n = 62 and n = 36). In Africa and South Asia, respectively, only five and eight LU case studies were found, while Oceania had no measurements at all.

2.3.2 Average land use emissions and environmental parameter values

Neither N_2O nor NO fluxes were normally distributed and about 90% of the observations were below 10 kg N_2O-N and 8 kg NO-N ha^{-1} yr^{-1}. Table 2.1 shows average annual N_2O and NO emissions per LU and environmental parameter associated. Croplands displayed the highest N_2O emission rate and also the highest average N fertilization rate. Both pastures and rice fields had relatively high N_2O emissions; however, these were characterized by a high variation. The average NO emission rates did not show any significant difference between LU.

Table 2.2 – Multiple regression between soil N_2O or NO emissions and associated environmental parameters; and meta-analysis regression between the standardized differences after and before land-use change of N_2O emissions (or Hedges' d, d_{N2O}) and of environmental factors ($d_{Navailable}$, d_{wfps}). The models are presented with slope and intercept ± SE; P values are indicated with * (p<0.05), ** (p<0.01) and *** (p<0.001). All regression models were significant (p≤0.01).

LU	R^2	df	Model
Linear regression LU study cases			
All	0.39	125	$Ln(N_2O+1.2)$ = 0.002*** ±0.0004 × $N_{fertilization}$ + 0.87** ±0.29 × $N_{available}$ + 0.014*** ±0.003 × $WFPS$ – 0.11^{ns} ±0.22
Agr[a]	0.83	40	$Ln(N_2O+1.2)$ = 0.008*** ±0.0007 × $N_{fertilization}$ + 0.017*** ±0.003 × $WFPS$ – 0.28^{ns} ±0.26
Non-Agr[b]	0.17	80	$Ln(N_2O+1.2)$ = 0.87** ±0.27 × $N_{available}$ + 0.008*** ±0.003 × $WFPS$ – 0.15^{ns} ±0.21
All	0.18	64	$Ln(NO)$ = 2.27** ±0.80 × $N_{available}$ + 0.0085* ±0.0039 × $N_{fertilization}$ – 1.42*** ±0.35
Agr[a]	0.31	44	$Ln(NO)$ = 0.0081*** ±0.0019 × $N_{fertilization}$ – 0.65* ±0.26
Non-Agr[b]	0.20	36	$Ln(NO)$ = 3.02** ±1.02 × $N_{available}$ – 1.67** ±0.47
Gaussian regression WFPS			
Non-Agr[b]	0.90	102	$N_2O = 2.3 \times exp(-0.5 \times ((WFPS^c - 61.8)/24.7)^2)$
Non-Agr[b]	0.89	36	$NO = 2.5 \times exp(-0.5 \times ((WFPS^c - 45.3)/16.5)^2)$
HIP model regression			
All	0.48	40	$Log(1+N_2O+NO) = 0.92^{***}$ ±0.15 × $N_{available} + 0.15^{*}$ ±0.06
All	0.39	42	$Log(1+N_2O/NO) = 0.0129^{***}$ ±0.003 × $WFPS - 0.32^{ns}$ ±0.18
Non-Agr[b]	0.40	29	$Log(1+N_2O/NO) = 0.0125^{***}$ ±0.003 × $WFPS - 0.27^{ns}$ ±0.20
Meta-analysis regression LUC study cases			
All	0.23	89	d_{N2O} = 0.65** ±0.14 × $d_{Navailable}$ –0.04 ±0.13
All	0.15	69	d_{N2O} = 0.55** ±0.22 × d_{wfps} +0.05 ±0.16

N_2O and NO are expressed in kg N_2O-N yr^{-1} or N-NO ha–1 yr^{-1}, $N_{available}$ is (NO_3^-/[NO_3^-+NH_4^+]) without units, NO_3^- and NH_4^+ in µg N g^{-1} d.w., $N_{fertilization}$ in kg N ha^{-1} yr^{-1} and WFPS in %.
[a]Agr includes cropland and pasture.
[b]Non-Agr includes forest, low forest cover, degraded forest, agroforestry and plantation.
[c]WFPS intervals of 10%.

The availability of environmental parameters in studies on N-oxides emissions was variable. For example, only 4% of the studies reported nitrogen input through litterfall, while precipitation was given in 91% of all cases. Although the comparison of values from different data sources may generate inconsistencies, some generalizations per LU category can be made. Overall, intact forest had a significantly lower bulk density compared to more compacted soils from pastures. Wetland forest soils had a significant lower bulk density compared to all other soils. Wetland forest soils were more acidic than other soils in general, while cropland soils were significantly less acid than forest soils. Mineral N content did not differ significantly between LU, except for high NH_4^+ and NO_3^- concentrations in wetland forest and rice paddy soils. Plantation soils were the only ones where NO_3^- concentrations exceeded those of NH_4^+, other LU showed the opposite trend. Carbon and nitrogen content in the soils of natural wetland forest were very high and significantly higher than that in all other LUs. Degraded forest soils showed a high carbon content which is due to the inclusion of eleven degraded peat forests out of the twenty cases. Excluding them resulted in a soil carbon content of 3.8 %.

The multiple linear regression analysis indicated that N fertilization, WFPS, and N availability (expressed as $[NO_3^-/ (NO_3^- + NH_4^+)]$) were the best proxies for estimating overall soil fluxes of N_2O (Table 2.2). For agricultural sites (i.e. crop and pasture) N fertilization rate explained part of the variation (R^2=0.31, df=160, p<0.01); but (pair-wise) including the WFPS more than doubled the R squared. Proxies for overall soil NO fluxes were N availability and N fertilization. For agricultural sites N fertilization explained 31% of the variation in NO fluxes, and the inclusion of the WFPS did not improve the relationship. In non-agricultural LUs a non-linear Gaussian function of the WFPS simulated with good fit N_2O and NO fluxes (Figure 2.2, Table 2.2). The relationship indicates that NO and N_2O fluxes peak at WFPS of 45% and 61%, respectively. The ratio of N_2O to NO displayed an exponential relationship with the WFPS (Figure 2.3, Table 2.2), which indicates N-oxide emissions predominantly in the form of N_2O (i.e. $N_2O/NO > 1$) above a WFPS of 48%. In non-agricultural sites the predominance of N_2O over NO happens at a slightly lower WFPS (46%). The sum of soil N_2O and NO emissions also increased exponentially with increasing N availability.

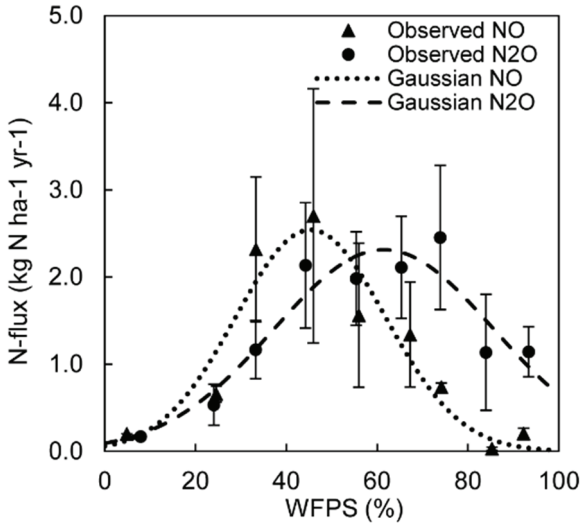

Figure 2.2 – Gaussian relationships (dashed lines) between the WFPS and N_2O and NO emissions in non-agricultural land uses. N_2O and NO fluxes are averaged in 10% WFPS intervals. Error bars are N flux standard errors in each WFPS interval.

Time since conversion was available in 26% of the LU cases only. Nitrous oxide fluxes from non-fertilized croplands appeared to be higher the first ten years after conversion and thereafter decrease, whereas fluxes from fertilized croplands remained high (Figure 2.4). For pastures the pattern was less apparent, the first years after conversion both high and low fluxes were observed.

2.3.3 Land-use change effects on N_2O and NO emissions and environmental parameters

Land-use change effects were evaluated by looking at differences in emissions after and before LUC. This was done for each LUC type and for all LUC combined. The effect sizes of LUC on N_2O emissions were not strictly normally distributed; however, all effect size ranges were present. Deviation from linearity occurred for high and low effect sizes indicating a potential bias for published studies measuring large effects following LUC. A normal quantile plot for NO emissions as affected by LUC indicated a normal distribution; however, some gaps were present in the observed values, possibly due to a biased representation of NO emission changes in the literature.

Nitrous oxide emissions were not overall affected by LUC (d = 0.11 ± 0.11); the slight increasing trend was not significant because of opposing effects in different LUC trajectories (Table 2.3). The LUC case studies overall did not share a common effect size (Q_{overal}= 221.3 P< 0.01) and the majority of the variation was within case studies (1-I^2, 59%). Similarly to N_2O emissions, and for the same reason, NO emissions were not overall affected by LUC; with a homogeneous effect size ($Q_{overall}$ = 31.7, P= 0.67) and 47% of the variation within LUC case studies (1-I^2).

Table 2.3 – Hedges' d ± SE (n) of N_2O (d_{N2O}) and NO (d_{NO}) emission change following land-use change (LUC). Hedges' d is the standardized mean difference of N_2O (or NO) flux rates after and before LUC. A d < 0 indicates a reduction in emission; a d > 0 an increase. Land uses are: F-forest, WF-wetland forest, LFC-low forest cover, DegF-degraded forest, AGF-agroforestry, Pl-plantation, Pa-pasture, R-Rice and Crop-cropland.

LUC	d_{N2O}	d_{NO}
F-DegF	0.09 ±0.29 (15)	0.08 ±0.34 (5)
F-AGF	0.34 ±0.29 (4)	- (1)[a]
F-Pl	0.06 ±0.37 (12)	-
F-Pa	-0.28 ±0.17 (36)	-0.56 ±0.67 (9)
F-Crop	0.78* ±0.24 (19)	- (2)[a]
Overall F	*0.11 ±0.14 (86)*	*-0.19 ±0.37 (17)*
WF-DegF	-0.17 ±0.31 (9)	-
WF-Pl	1.07 ±0.42 (3)	-
WF-Pa	2.37 ±1.80 (3)	-
WF-R	-0.06 ±0.62 (9)	-
Overall WF	*0.31 ±0.34 (24)*	-
DegF-AGF	0.27 ±0.19 (4)	0.72 ±0.28 (4)
LFC-Pl	- (2)[a]	-
LFC-Pa	0.47 ±0.37 (3)	-0.06 ±0.31 (5)
LFC-Crop	-0.29 ±0.40 (16)	0.57* ±0.09 (11)
Overall LFC[b]	*-0.07 ±0.25 (25)*	*0.44 * ±0.13 (20)*
Overall LUC	0.11 ±0.11 (135)	0.16 ±0.19 (37)
Fertilization[c]	1.03* ±0.31 (17)	0.52* ±0.23 (12)
N fixation[c]	-0.14 ±0.33 (13)	0.61 ±0.33 (8)

* p < 0.05; no statistics calculated for studies with n<3.

[a] no statistics possible.

[b] including 4 DegF-AGF LUC cases.

[c] Fertilization and N fixation indicate cases of forest conversion to fertilized LU and LU with N_2 fixing trees/crops.

Most studies focused on forest clearing for croplands ($n_{F\text{-}Crop}$+ $n_{WF\text{-}Crop}$+ $n_{DegF\text{-}Crop}$= 44) and pastures ($n_{F\text{-}Pa}$ + $n_{WF\text{-}Pa}$ + $n_{DegF\text{-}Pa}$ = 42). Transition from intact upland forest to croplands significantly increased N_2O emissions, while conversion to agroforestry showed a slight, but insignificant increasing trend. Intact forest conversion to pasture (F-Pa) tended to decrease N_2O emissions, whereas low forest cover conversion to pasture (LFC-Pa) showed the opposite trend. Further, conversion of low forest cover overall significantly increased NO emissions.

The Hedges' d effect size of forest conversion to fertilized LU amounted to 1.03 ± 0.31 and 0.52 ± 0.23 for N_2O and NO, respectively, indicating significant and high increased emissions after fertilization. Evidence for increased emission following conversion to LU with N fixing crops/trees was weak and fluxes of NO slightly raised but not significantly (d_{NO}=0.61 ±0.33 n = 8).

The results of the meta-regression, which was run pooling all LUC case studies together, are presented in Table 2.2. The change in N_2O fluxes as affected by LUC was positively related to changes in N availability and WFPS. No significant relationships were found for NO. The interactive effect of WFPS and N availability change on N_2O flux change is illustrated in Figure 2.5. Whenever N availability increased after LUC ($d_{Navailability}$>0) the increase in N_2O emissions (d_{N2O} > 0) was exacerbated if the WFPS also increased (d_{WFPS}>0), or diminished if the WFPS was decreased (d_{WFPS}<0). The slope of the regression between d_{N2O} and $d_{Navailibility}$ was raised by 143% for the d_{WFPS}>0 cases, reduced by 58% for d_{WFPS}<0 cases.

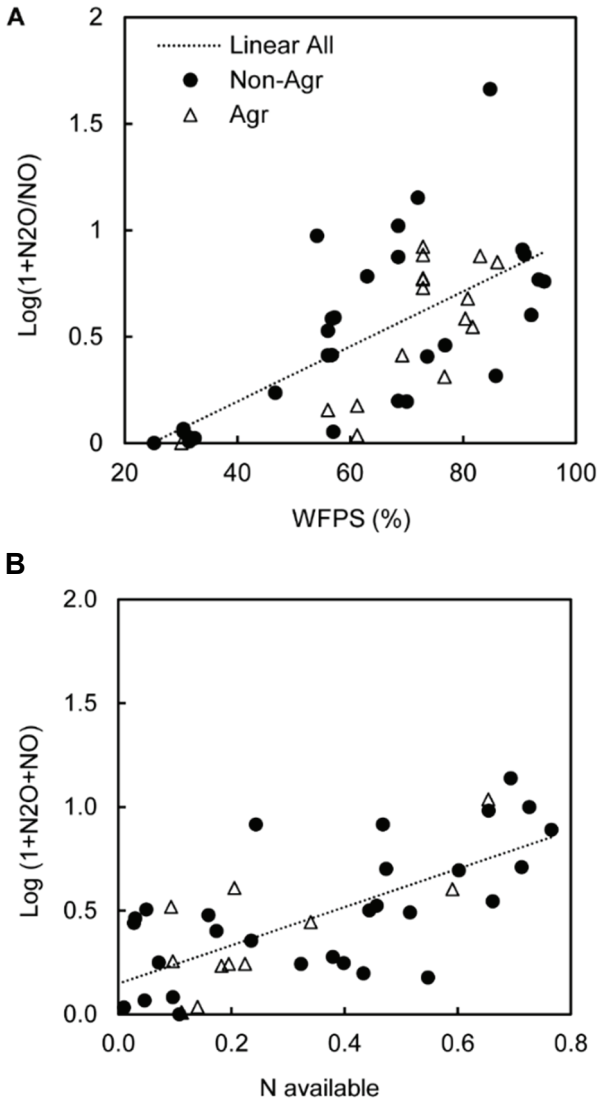

Figure 2.3 – Relationships between (a) the WFPS and the ratio of N_2O to NO; (b) $N_{available}$ ($NO_3^-/[NO_3^-+NH_4^+]$) and the sum of N_2O and NO. The domains of definition are (a) [0.02; 44.71] in N_2O to NO ratio and [30.4; 94.4] in WFPS; (b) [0.00;12.80] in N_2O + NO (kg N ha^{-1} yr^{-1}) and [0.01;0.77] in $N_{available}$.

2.4 Discussion

2.4.1 Dataset representativeness and average annual LU emissions

The body of research on LULUC and N_2O and NO emissions in the Tropics has increased during the past decade; however, Africa and Oceania remain strongly underrepresented. Most of Africa's LU case studies were from (converted) savannahs although Africa has a variety of forest types unaccounted for at present in the literature. Furthermore, a comparison between the spatial distribution of LUC case studies and global forest conversion for 2005-2010 (FAO 2010) shows that highest deforested areas overlapped well with studies on N emissions from LUC except for Oceania and Africa (Figure 2.1c). These regions need more research on soil N_2O and NO emissions, in representative LULUC categories. Sampling bias was not only geographical; some biofuel or food crops such as oil palm and soy were also underrepresented ($n_{oil\ palm}$ = 7 and n_{soy} = 4) although they are the most rapidly expanding perennial and annual crop in the tropics (Phalan et al., 2013). Land-use change categories were also not equally represented; there was a dominance of studies on forest conversion to croplands and pastures. Only a few cases (10-13%) assessed the effect of nitrogen fertilization or the use of N-fixing species after LUC. Those studies took place in Latin America (Matson et al., 1996; Veldkamp & Keller 1997; Veldkamp et al., 1998) and Asia (Verchot et al., 2006; Veldkamp et al., 2008). Some wetland forest conversion study cases showed high effect sizes for N_2O emissions (Hadi et al., 2005; Furukawa et al., 2005; Jauhiainen et al., 2012), but the overall tendency of wetland forest conversion to increase N_2O emissions was not significant (Table 2.3) as observed by Hergoualc'h & Verchot (2014). However, the sample size was small and none of the converted case studies were fertilized or intensively monitored following fertilization. Future research direction should consider conversion to fertilized land uses, using an experimental design adequate for capturing fertilization effects on N oxide emissions, and wetland forests in and outside of South Asia. Likewise, few papers studied forest degradation; a topic that needs more attention (Mertz et al., 2012).

The annual N_2O emission rate in intact upland forest (2.0 ± 0.2 kg N_2O-N ha^{-1} yr^{-1}, n = 88) is more than twice the value estimated by Stehfest & Bouwman (2006)

(0.85 kg N_2O-N ha^{-1} yr^{-1}, n = 77) for the tropics. We excluded the cases considered by Stehfest & Bouwman (2006) that did not cover seasonal variation, but ended up with a higher sample size by adding studies published after 2005. Our value is also larger than the model estimations of 1.4 kg N_2O-N ha^{-1} by Potter et al. (1996) and 1.2 kg N_2O-N ha^{-1} yr^{-1} by Werner et al. (2007). Dalal & Allen (2008) estimated average emissions in tropical forest of 3.0 ± 0.52 kg N_2O-N ha^{-1} yr^{-1} (n = 22) and Kim et al. (2013a, 2013b) of 1.91 kg N ±0.25 (n = 69). The annual NO emission rate in tropical forest amounts to 1.7 ±0.48 kg N-NO ha^{-1} yr^{-1} (n = 36), which is higher than previous estimates by Stehfest and Bouwman (2006) (0.39 kg NO-N ha^{-1} yr^{-1}, n = 33), Davidson and Kingerlee (1997) (0.8 kg NO-N ha^{-1} yr^{-1}, n = 15) and Potter et al. (1996) (1.2 kg NO-N ha^{-1} yr^{-1}).

Nitrous oxide emission in agricultural fields and pastures reported by Duxbury et al. (1982) were the largest in the entire dataset (average emissions of 65 kg N_2O-N ha^{-1} yr^{-1}). The study was conducted in Florida on drained organic soils under crops, grass or kept as fallows; that displayed high N mineralization rates (600-1,200 kg N ha^{-1} y^{-1}). Excluding them decreases the overall average N_2O emissions from 4.4 ± 0.6 (n = 387) to 3.5 ± 0.3 kg N_2O-N ha^{-1} yr^{-1} (n = 381), and croplands emissions from 8.6 ± 2.0 (n = 93) to 5.8 ±0.9 kg N_2O-N ha^{-1} yr^{-1} (n = 88).

2.4.2 Land-use change effects on the emissions

According to the meta-analysis LUC overall increased N_2O and NO emissions, albeit not significantly. Land-use change types or practices that induced significant changes in emissions all pointed towards increased rather than decreased emissions. The meta-analysis confirmed that intact upland forest conversion to croplands and nitrogen fertilization after LUC significantly and highly increased soil emissions of N_2O. It also corroborated high increases in NO emissions after low forest cover conversion in general and when fertilizer is applied after LUC. For most LUC trajectories the effect of emission change was not significant even when the sample size was relatively large. For instance, the analysis indicated a trend of decreased N_2O emissions following intact upland forest conversion to pasture, which was not significant since the LUC studies not all agreed on the direction of change. Several publications reported decreased emissions after conversion to pasture (e.g. Verchot et al., 1999; Erickson et al.,

2001; Garcia-Montiel et al., 2001), others reported the opposite (e.g. Melillo et al., 2001; Takakai et al., 2006) and one showed no effect (Neill et al., 2005). These apparent contradicting results have been explained by differences or absence of differences in time after conversion of the studied pastures (Keller et al., 1993, Veldkamp et al., 1999, Verchot et al., 1999, Neill et al., 2005, Wick et al., 2005) or the practiced or not slash and burn technique to clear the forest, both affecting N cycling (Luizao et al., 1989; Matson et al., 1990; Steudler et al., 1991; Keller & Reiners, 1994; Neill et al., 1995; Melillo et al., 2001; Garcia-Montiel et al., 2001). Biomass burning produces N_2O during fires and may enhance soil N_2O afterwards by stimulating N mineralisation (Skiba & Smith, 2000). The paucity of field observations together with the lack of land-use history description did not allow to evaluate clearing practices effects or temporal trends in soil emission dynamics with LUC thoroughly. For non-fertilized croplands and pastures, the fluxes of N_2O tended to increase during the first five to ten years after conversion and thereafter tended to decrease to average upland forest or low canopy forest levels (Figure 2.4). In fertilized croplands, however, flux rates remained at a high level even beyond this period. Soil physical disturbance following land clearing, high N inputs associated with clear-felling and soil preparation (e.g. compaction, drainage in wetland) all combined may be at the origin of the five to ten year emission peak. In fertilized croplands on the other hand, the sustained emission increase seems to be driven by high mineral N inputs. This temporal variability in emission change indicates that the first ten years following LUC are crucial for GHG budget calculations.

We used a meta-analysis statistical approach to assess the trend and magnitude of forest conversion on soil emissions of N oxides. Meta-analysis consists in comparing site specific (pair-wise) effects weighted according to their robustness, therefore it provides a direction and a magnitude of emission change more reliable and precise than those obtained by comparing average emission rates per LU category from individual papers. For example, the meta-analysis effect on N_2O emissions of intact upland forest conversion to croplands (0.78) was

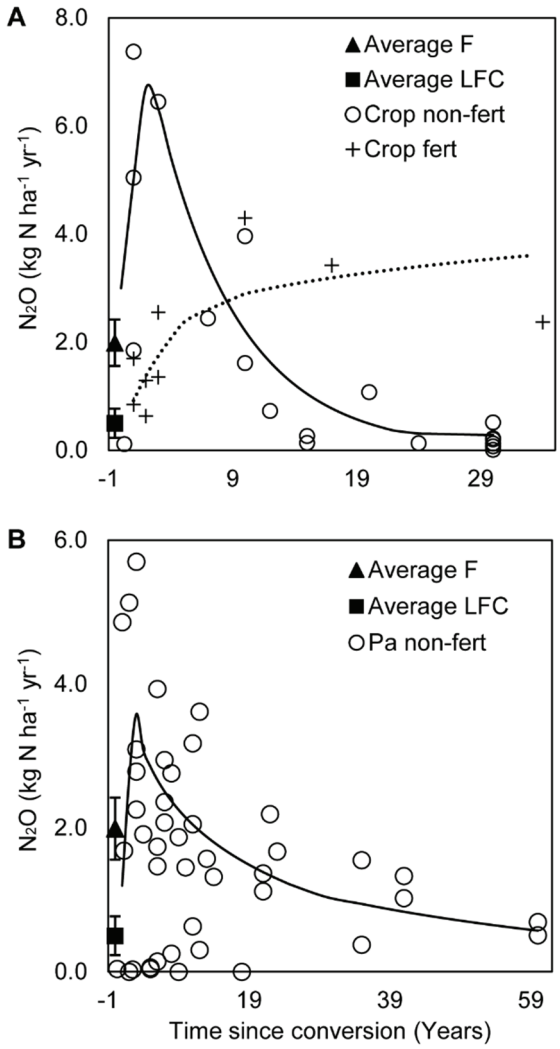

Figure 2.4 – Effect of time since conversion on N_2O fluxes in (a) croplands and (b) pastures. Average N_2O flux and 95% confidence intervals are given for upland forests (F, triangle) and low canopy forests (LFC, square). The solid and dashed lines represent a conceptual trend for non-fertilized and fertilized cases, respectively.

much higher than the effect calculated (0.48) using average values from Table 2.1 and Eq. (1). The effect calculated from average emission rate derived from individual studies can also lead to misleading conclusions such as in the case of intact upland forest conversion to pasture. The effect calculated from average emissions (0.34) was positive indicating increased emissions as opposed to the meta-analysis conclusion (-0.28). Simple assessments based on average values, in general, encompass more studies than meta-analysis but are biased due to the exclusion of pair-wise evaluations. In order to improve the understanding of LUC on trace gas emissions in general, more studies monitoring the fluxes simultaneously in control (forest) and converted sites are necessary. Whenever the conversion includes intermediary stages such as short fallows with the practice of slash-and-burn, the corresponding emission rates should be evaluated as well. When focusing on a specific crop/tree a chronosequential approach including different ages since planting should be considered, especially if fertilization rates evolve with time. The first few years after conversion are likely to be hotspots for N oxide emissions and time since conversion is an important factor to be included.

2.4.3 Biophysical drivers of NO and N_2O emission and emission change

An IPPC Tier 1 approach is generally used by countries in the Tropics to estimate their annual emissions of GHG. Average LU-based emission rates as provided in this paper or the contribution of N applied released as N_2O from agricultural soils (IPCC, 2006) illustrate the type of emission factors applied to activity data at a Tier 1 level. This approach is useful to compare anthropogenic emissions from different countries but does not capture the variations across climate regions for instance (Skiba et al., 2012). Soil fluxes of N_2O and NO are known to be controlled by climate (rainfall, temperature), soil conditions (drainage, aeration, texture, pH, etc.) and management (land cover, fertilization rate and type, etc.) (Skiba & Smith, 2000; Ludwig et al., 2001; Butterbach-Bahl et al., 2013). Country- or regional LU-specific emission factors that better account for local climate, soil management and properties are defined as Tier 2 level whereas Tiers 3 methods usually involves process-based models (Del Grosso et al., 2006). The multiple regression analysis of the dataset indicated that tropical N_2O and NO

fluxes could be expressed as a combination of nitrogen availability and/or application and WFPS; even though the predictive power for simulating overall N_2O emissions was low (R^2 = 0.39). However, the predictive power of the regressions increases when the database is split up in agriculture and non-agriculture cases (Table 2.2). The establishment of an emission factor for agricultural soils that includes the WFPS in addition to N fertilization rate is likely to improve estimates of direct agricultural N_2O emissions, one of the largest source of N_2O in most countries. For non-agricultural sites a more mechanistic approach appeared to fit better the observed data. The fluxes of both NO and N_2O followed a Gaussian type relationship with the WFPS – a key determinant for soil anaerobiosis. This type of relationship was hypothesized by Davidson (1991), demonstrated in case studies (Davidson et al., 2000; Davidson and Verchot, 2000; Veldkamp et al., 1998) and used in modelling (Parton et al., 2001; Parton et al., 1996; Potter et al., 1996). Its application in the context of the current tropical database confirms a maximum of N_2O emissions around a WFPS of 60% and indicates maximum NO emissions at a lower WFPS (45%) than that reported by Davidson et al. (2000) (55%). It also points out that N_2O emissions remain high at an 80% WFPS and diminish towards 100% WFPS. Neither air nor soil temperature were found to affect soil N-oxide fluxes across LUs, although the LU annual average span was wide (12-34 °C and 14-31 °C for air and soil temperatures). In the temperate zone exponential increases in N_2O emissions with increasing temperature have been reported, whereas in the tropics the evidence is mixed (Skiba and Smith, 2000). Substrate (e.g. N, P) and moisture constraints of microbial processes influencing N-oxide fluxes may reduce the temperature effect. Werner et al. (2006), for instance, demonstrated that variations in N_2O emissions from tropical rainforest soils were mainly affected by soil moisture changes and that temperature changes were of minor importance.

The data confirmed the concepts formulated in the HIP model (Davidson et al., 2000) with the availability of mineral N in the system (first level of control) controlling in an exponential fashion the (NO + N_2O) flux rate and the WFPS (second level of control) controlling also in an exponential fashion the ratio of N_2O to NO. Although our exponential models are similar to those obtained by Davidson and Verchot (2000) using the TRAGNET database and by Davidson et al. (2000)

using fluxes from forest to pasture conversions in the American Tropics, the magnitude of the coefficient is different. For a WFPS between 30 and 60% the N_2O to NO ratio obtained using the relationship of Davidson and Verchot (2000) is five to nine times lower than the one obtained with the relationship developed here. Above a $NO_3^-/[NH_4^+ + NO_3^-]$ ratio of 0.5 the relationship of Davidson et al. (2000) departs from the one we developed. For instance, at a 0.75 $NO_3^-/[NH_4^+ + NO_3^-]$ value, we estimate annual NO + N_2O emissions of about 6 kg N ha^{-1} y^{-1} whereas the model of Davidson et al. indicates 10 kg N ha^{-1} y^{-1}. The probable reason explaining the discrepancy is the temporal scale of the data, we used annual emission rates whereas Davidson et al. used hourly fluxes and thus took into account punctual high emission peaks less apparent in annual budgets. Also, given the nonlinear nature of the functions, an annual budget estimated by summing up fluxes simulated from e.g. hourly WFPS and inorganic N ratio values would lead to a different result than the one simulated from annual WFPS and inorganic N ratio values, as we did. This demonstrates that relationships used in modelling exercises should be developed according to the time step of the model.

Land-use change involves major transformations of the soil-plant-atmosphere continuum. As a result of land-clearing fires, mechanical ploughing and compaction, vegetation change, fertilization, etc., the soil system is highly altered from its previous state. Soil properties such as bulk density, porosity, moisture, WFPS, temperature, mineral N content and pH are often affected by LUC (Farquharson & Baldock, 2008; Dobbie et al., 1999; Verchot et al., 1999). Fertilization N input after land-use change increases highly and significantly both N_2O and NO fluxes, as reported by many studies, e.g. Stehfest & Bouwman (2006). However, increased emissions after LUC were not exclusively due to fertilization, changes in endogenous levels of soil nitrogen availability or WFPS were also key factors impacting the changes in N_2O fluxes. These variables should therefore systematically be measured and reported. Land-use change generally impacts more than one variable at a time, therefore changes in emissions will most likely result from an interaction of factors. This was illustrated by the interactive effect of the changes in N availability and WFPS on N_2O emission changes (Figure 2.5).

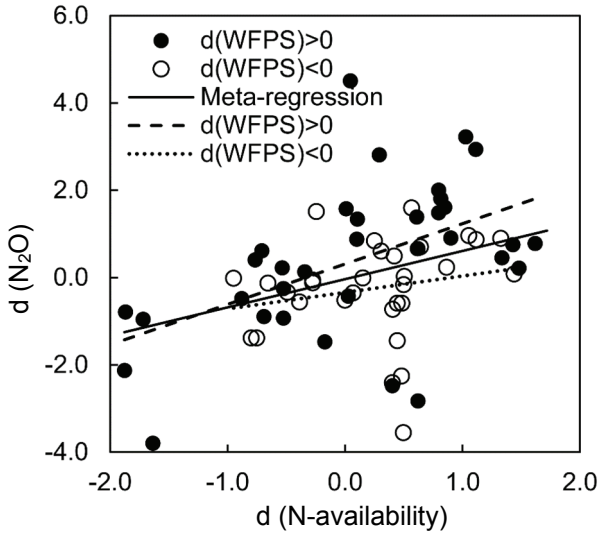

Figure 2.5 – N_2O Hedges'd as affected by the interactive changes in $N_{availability}$ and WFPS. The meta-analysis regression between d_{N2O} and $d_{Navailability}$ was performed for all cases (solid line) and for cases when $d_{WFPS}>0$ or $d_{WFPS}<0$ (dashed lines).Closed and open circles represent increased and decreased WFPS, respectively.

2.5 Conclusions

We estimate natural tropical forests to emit 2.0 kg N_2O-N ha^{-1} yr^{-1} on average and emission rates to be significantly increased after conversion to cropland, and to a smaller degree to agroforestry. Low forest cover also see their NO emissions raise significantly after being converted. These LUC trajectories can hence contribute substantially to non-CO_2 GHG emission increases whenever they represent a substantial area for a given country. Default Tier 1 N_2O and NO emission factors currently proposed by the IPCC for the tropical region are based on a limited number of studies and rely essentially on N inputs. However, mechanisms of N-oxide production are the result of microbial processes controlled by a combination of factors; thus the IPCC Tier 1 approach is somewhat flawed. Here we established a set of predictive relationships linking annual soil N_2O and NO emissions to biophysical parameters and emission changes to biophysical parameter changes. The analysis established that N availability or N inputs as well as the soil WFPS were the key explanatory factors of emissions or emission

changes. In particular, we developed a statistical model for tropical countries allowing the calculation of N_2O emissions from agriculture as a function of both N fertilization rate and WFPS. Improving the scientific understanding of N_2O and NO fluxes and how they relate to environmental parameters requires the design of experiments considering the high spatio-temporal variation of the fluxes and associated parameters and the use of standardized measurement methods. Also, studies considering a LUC transition pathway should include in their design all intermediate land use stages (e.g. degraded forest) susceptible to modify N cycling. Finally, even though the body of research on LUC and N_2O and NO emissions has steadily increased over the past decades, knowledge gaps are still important especially in Africa and Oceania, and for wetland forest (notably on peat), degraded forest and important world crops such as oil palm plantations and soy fields.

2.6 Acknowledgements

This research was generously supported by the contributions of the governments of Australia (Grant Agreement # 46167) and Norway (Grant agreement # QZA-10/0468) and the European Community's Seventh Framework Programme [FP7/2007-2013] (Grant Agreement # 226310) to the Center for International Forestry Research. This work was carried out as part of the Consultative Group on International Agricultural Research programs on Climate Change and Food Security (CCAFS). We gratefully thank Luluk Suhada for her work on the bibliography for this study and also all scientists that have measured and published the data that we used.

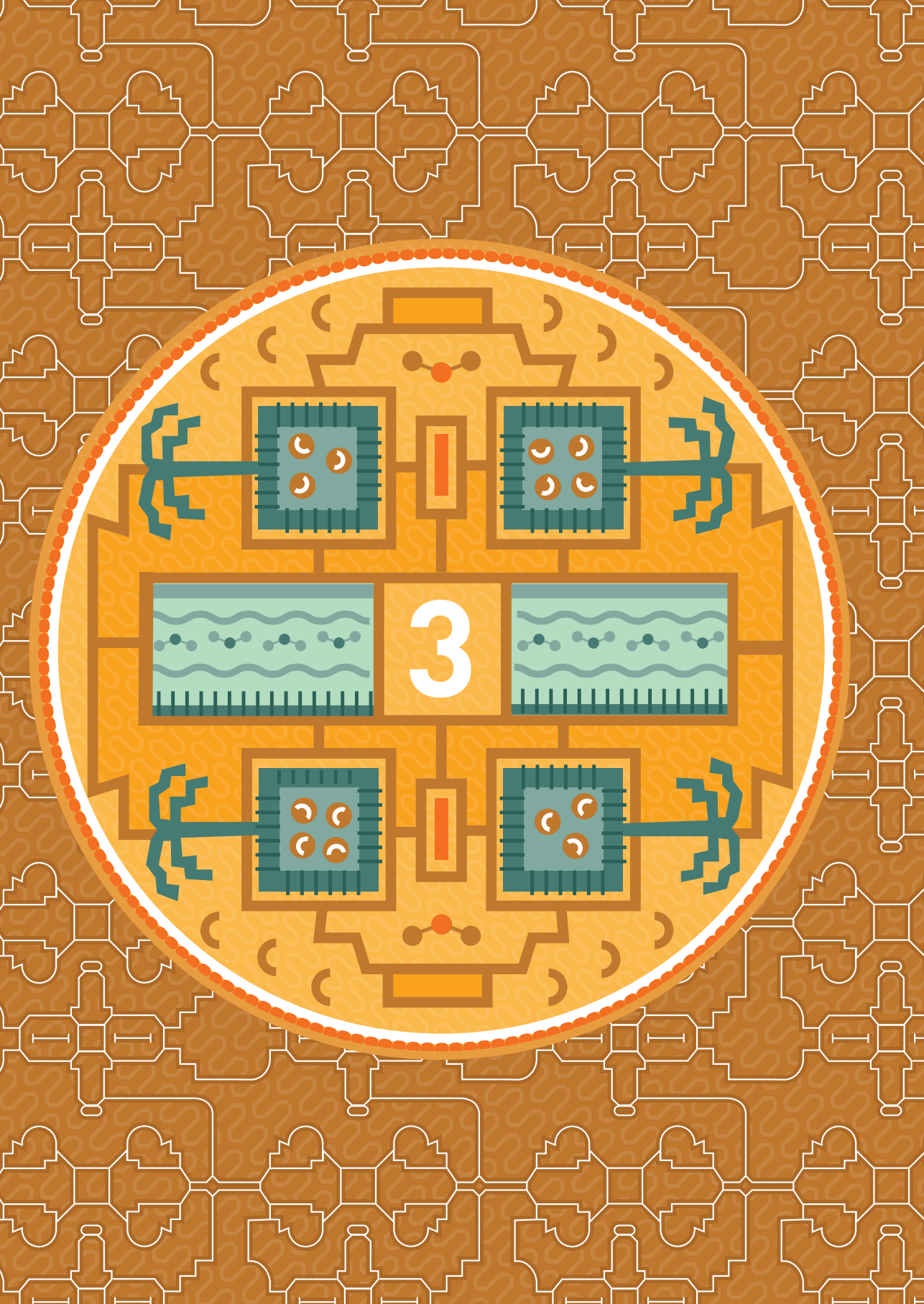
3

3

Impacts of *Mauritia flexuosa* degradation on the carbon stocks of freshwater peatlands in the Pastaza-Marañón river basin of the Peruvian Amazon

This Chapter is published as:
Bhomia, R. K.[1], van Lent, J.[2,3], Rios, J. M. G.[4], Hergoualc'h, K.[2], Coronado, E. N. H.[4], & Murdiyarso, D.[2] (2019). Impacts of *Mauritia flexuosa* degradation on the carbon stocks of freshwater peatlands in the Pastaza-Marañón river basin of the Peruvian Amazon. Mitigation and Adaptation Strategies for Global Change, 24(4), 645-668.

[1] Wetland Biogeochemistry Laboratory, Soil and Water Sciences Department, University of Florida, Gainesville, FL, USA
[2] Center for International Forestry Research (CIFOR), Jl. CIFOR, Situ Gede, Bogor 16115, Indonesia
[3] Department of Soil Quality, Wageningen University, Wageningen, The Netherlands
[4] Instituto de Investigaciones de la Amazonía Peruana (IIAP), Av. José A. Quiñones, Iquitos, Peru

3 Impacts of *Mauritia flexuosa* degradation on the carbon stocks of freshwater peatlands in the Pastaza-Marañón river basin of the Peruvian amazon

Abstract

Tropical peat swamp forests (PSF) are characterized by high quantities of carbon (C) stored as organic soil deposits due to waterlogged conditions which slows down decomposition. Globally, Peru has one of the largest expanse of tropical peatlands, located primarily within the Pastaza-Marañón river basin in the Northwestern Peru. Peatland forests in Peru are dominated by a palm species - *Mauritia flexuosa*, and *M. flexuosa*-dominated forests cover ~80% of total peatland area and store ~ 2.3 Pg C. However, hydrologic alterations, land cover change and anthropogenic disturbances could lead to PSF's degradation and loss of valuable ecosystem services. Therefore, evaluation of degradation impacts on PSF's structure, biomass, and overall C stocks could provide an estimate of potential C losses into the atmosphere as greenhouse gases (GHG) emissions.

This study was carried out at select locations within Pastaza-Marañón river basin to quantify PSF's floristic composition and degradation status and total ecosystem C stocks. There was a tremendous range in C stocks (Mg C ha^{-1}) in various ecosystem pools – vegetation (45.6 - 122.5), down woody debris (2.1 – 23.1), litter (2.3 – 7.8) and soil (top 1 m; 109 - 594). Mean ecosystem C stocks accounting for the top 1m soil were 400, 570 and 330 Mg C ha^{-1} in Itaya, Tigre and Samiria river basins, respectively. Considering the entire soil depth, mean ecosystem C stocks were 670, 1160 and 330 Mg C ha^{-1} in Itaya, Tigre and Samiria river basins, respectively. Floristic composition and Ca:Mg ratio of soil profile offered evidence of a site transitioning from minerotrophic to ombrotrophic system and undergoing vegetational succession. Degradation ranged from low to high levels of disturbance with no significant difference between regions. Increased degradation tended to decrease vegetation and forest floor C stocks and was significantly correlated to reduced *M. flexuosa* biomass C stocks. Long-term studies are needed to understand the linkages between *M. flexuosa* harvest and palm swamp forest C stocks, however river dynamics are important natural drivers influencing forest succession and transition in this landscape.

3.1 Introduction

Tropical forests that experience waterlogged conditions tend to accumulate partially decomposed organic matter, and a sustained accrual of this material on forest floor results in peat formation (Limpens et al., 2008; Rieley et al., 2008; Lähteenoja et al., 2009a). A unique class of tropical forests, referred to as peat swamp forests, are characterized by the presence of high below ground carbon (C) and organic matter at various stages of decomposition. Peatlands occurs wherever rainfall and topography are conducive to poor drainage, causing permanent waterlogging and substrate acidification (Bailey, 1951; Bradshaw et al., 2008). Peat swamp forests located at low altitudes occur in river valley basins, watersheds, and subcoastal areas of Southeast Asia, Africa, Caribbean, Central and South America (Hooijer et al., 2010; Posa et al., 2011).

Growing interest in tropical peatlands is mainly due to their increasingly recognized role in the global C cycle (Jauhiainen et al., 2005), greenhouse gas exchange (Kurnianto et al., 2015), paleoecology (Kelly et al., 2014; Lawson et al., 2015), maintenance of biological diversity (Posa et al., 2011), and provision of direct economic gains when peat swamp forests are logged, converted into agricultural farms and oil palm plantations (Roucoux et al., 2013). There is a considerable uncertainty in global distribution of tropical peatlands. A best estimate from available global data is 441,025 km^2 (Page et al., 2011), combined with discoveries in the Amazon (35,600 km^2; (Draper et al., 2014)) and the central Congo Basin (145,500 km^2; (Dargie et al., 2017)). Several studies indicate Peru has one of the largest extent of peatlands in the tropics (Gumbricht et al., 2017) and the known extent might increase as more explorations are conducted and data becomes available. Therefore, tropical peatlands play an important role in the global C cycle. Other than C storage and sequestration, tropical peatlands also play an important role in water regulation, habitat provision for biodiversity and livelihoods for local communities (Posa et al., 2011; Murdiyarso et al., 2013). However, hydrologic alterations and land cover change by anthropogenic or by natural causes could lead to peat swamp forests degradation, and loss of stored C to the atmosphere as greenhouse gases (GHG) emissions (Hergoualc'h and Verchot, 2011; Hergoualc'h and Verchot, 2014).

South America is estimated to harbor one of the largest area of tropical peatlands worldwide (Gumbricht et al., 2017), of which majority are located in the Amazon basin. In Peru, the majority of peatlands are located within Pastaza-Marañón foreland basin (PMFB) in Northwestern region of the Peruvian Amazon, forming an extensive continuous wetland characterized by the largest tropical system of fluvial aggradation (Räsänen et al., 1990; Räsänen et al., 1992). The PMFB region has extensive and deep accumulations of peat with depths up to 7.5 m and below-ground C stocks ranging from 2 – 20 Pg C (Lähteenoja et al., 2012; Draper et al., 2014). These peat C stocks are significant in the context of national and regional C budgets, because the total aboveground biomass C in the entire Peru are estimated to be 6.9 Pg C (Asner et al., 2014).

Previous studies have suggested that peatlands in this region of Peru supports different vegetation assemblages - palm swamp forest, 'pole' forests (low stature forest with many thin-stemmed trees), and herbaceous 'open' communities (Lähteenoja and Page, 2011; Lawson et al., 2015). Palms (family *Arecaceae*) are single most abundant arborescent plant family in Amazonian forests, especially in forests with frequent inundation (Kahn and Mejia, 1990; Terborgh and Andresen, 1998) and poor soil conditions, such as shallow rooting depth (Emilio et al., 2014). Some species, such as *Mauritia flexuosa,* are able to thrive in such conditions and establish nearly mono-dominant stands, which are locally known as *aguajales* (Kahn et al., 1988). These *Mauritia (*palm) forests are an important feature of this landscape - both economically and ecologically (Virapongse et al., 2017). A recent study determined actual peatland extent within PMFB to be ~35,000 km^2 with majority of it covered by palm swamps (Draper et al., 2014). The importance of *Mauritia* forests among Peruvian peatlands is evident from the fact that they cover ~80% of total peatland area and store ~ 2.3 Pg C (Draper et al., 2014).

Over the past few decades growing local and regional demands for *M. flexuosa* fruits (Endress et al., 2013) has resulted into increased harvesting pressure on *M. flexuosa* forests. It is one of the most heavily used plant species for non-timber forest products (NTFPs) with multiple applications in indigenous and rural activities, mostly associated with food, fibers, animal fodder, and construction (Zambrana et al., 2007; Goodman et al., 2013). *M. flexuosa* fruits are an important source of vitamins and proteins for rural communities (Maria Pacheco, 2005) and

other products (leaves, oil, wood) derived from *M. flexuosa* are also economically valuable (Virapongse et al., 2017). The most common practice of harvesting *Mauritia* fruit involves cutting down fruit bearing female trees causing localized reduction in the abundance of mature trees (Parodi and Freitas, 1990; Delgado et al., 2007; Manzi and Coomes, 2009). This selective removal of fruiting trees reduces viable seed source in a given forest stand, and unavailability of seeds hinders natural regeneration and recruitment of new *Mauritia* palms (Horn et al., 2012). Over time, such practices alter the structure and composition of *M. flexuosa* forests (Hergoualc'h, Gutiérrez-Vélez, et al., 2017), severely diminishing ecological integrity and loss of ecosystem services derived from these forests. Degradation of *Mauritia* forests could potentially result in destabilization of peat deposits and reduce its ability to sequester and store C (van Lent et al., 2018). Loss of habitat and food resources also have negative impacts on wildlife including fishes, birds (particularly macaw), large ungulates (such as lowland tapir, peccaries, deer) and primates.

These anthropogenic pressures, combined with enhanced seasonality in annual precipitation due to climate change pose an unprecedented threat to the peatland forests of the Peruvian Amazon. Our study was intended to determine the condition (status) of Peruvian peat swamp forests that are dominated by *M. flexuosa.* We estimated total C stocks in these ecosystems by measuring aboveground and belowground vegetation (C in live biomass), downed woody debris and litter (C on forest floor) and C stored in underlying soils. Evaluation of relationships between forest degradation status and C stocks were carried out to understand the role of anthropogenic factors such as palm harvesting on ecosystem C stocks. Role of regional landscape factors such as riverine sediment inputs on peat accumulation processes at a broader scale were also evaluated. In addition, we attempted to provide estimates that will help reduce uncertainties relating to the importance of peat C storage in these forests. An estimate of C stocks in these palm swamp forests will support refining determination of their role as a global sink/source of greenhouse gases (GHGs) and providing additional information for validation of peat distribution models in this region.

3.2 Material and Methods

3.2.1 Swamp Forests in Peru

The Peruvian Amazon basin covers an area of 77,535,384 ha (~60 % of Peru's territory) and is the largest physiographical region in the country (Rodríguez, 1990). The climate is warm and humid with mean annual temperature ~ 27 °C, with average daily minima around 20-22 °C and maxima around 29-31 °C (Marengo, 1998). Rainfall occurs throughout the year with an average annual precipitation of 3,087 mm and a weak dry season between June and September (Marengo, 1998).

Peru's wetlands, totaling 65,820 km^2 of land cover, can be subdivided into four ecosystem types: 1) peat swamp forests, 2) mangroves, 3) Andean wetlands (bofedales), and 4) coastal marshes and lagoons. Peat swamps with an area of 60,630 km^2 account for the greatest proportion of Peru's wetlands (MINAM, 2010; Queiroz et al., 2014). The majority of *Mauritia* palm swamps (*aguajales*), pole forests and open peatlands (~27,730 km^2) is found within Pastaza-Marañón foreland basin (PMFB) in the Loreto Department, with smaller patches in the departments of Ucayali and Madre de Dios (MINAM, 2010; Draper et al., 2014). The PMFB belongs to the western part of the Amazon basin and is characterized by a broad belt of subsiding basins formed during the Cenozoic uplift of the Andes (Räsänen et al., 1990; Räsänen et al., 1992). Since the Cretaceous period, rivers originating from the Andes have led to the accumulation of several kilometer thick minerogenic deposits in these subsiding forested basins (Lähteenoja et al., 2012). Consequently, the accumulation of organic matter and peat formation in this slowly subsiding basin is a dynamic process, influenced by lateral movements of river channels, e.g. meandering up to > 100 m in a year (Smith et al., 1989) and avulsions (abrupt changes in the location of river stretches) which can cause both burial and erosion of peat deposits (Kalliola et al., 1992; Neller et al., 1992). These hydromorphic processes control the quantity (depth) and location of peat deposits at local and regional scales, leading to spatial variability in below ground C stocks.

3.2.2 Study Area and Sampled Locations

The ecosystem C stocks were measured at twelve peatland swamp forest sites within Amazon basin in the Loreto region of north eastern Peru. At a regional scale, these sites fall into three different river basins/watersheds. Three sites were sampled near Iquitos town close to Itaya River, five sites along the northern reaches of Tigre River and four sites were sampled inside and in proximity to the Pacaya Samiria National Reserve within the Samiria River basin (Figure 3.1 and Table 3.1). The sampling sites in these three locations were subsequently grouped as Itaya, Tigre and Samira, respectively. The primary characteristics of all sampled forest sites was the presence of a palm species - *Mauritia flexuosa* (local name *aguaje*) and below ground peat. All sampled locations had individuals of *M. flexuosa* even though this species was not always the most abundant, as a result of degradation or natural variation. Sampled sites represented areas with variable degree of degradation - low to high.

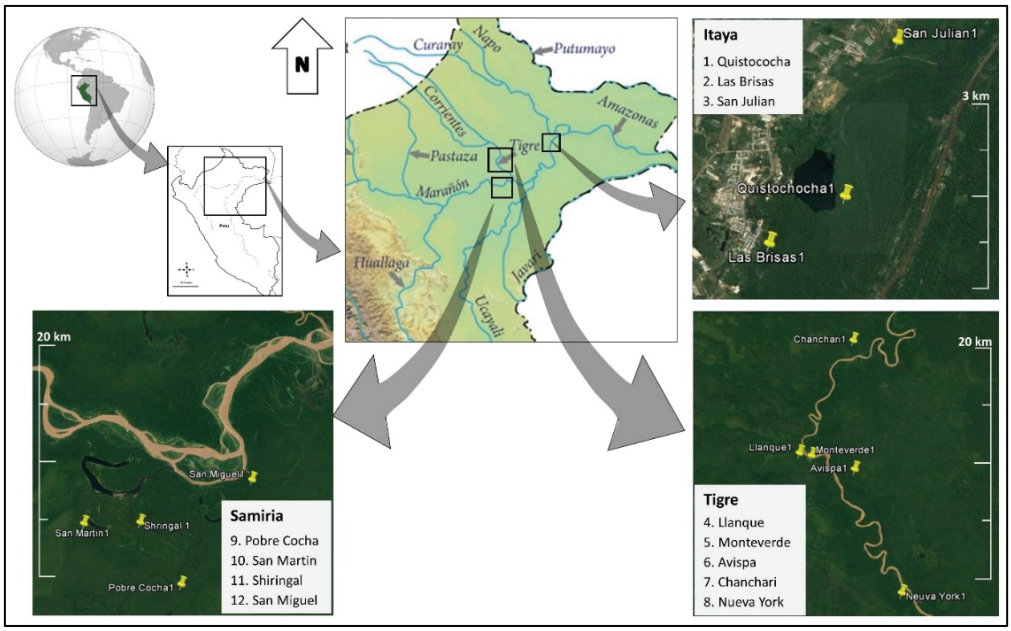

Figure 3.1 – Twelve peatland swamp forest sampling sites within Amazon basin. Sampling sites were grouped in three locations based on sub-watershed – Itaya, Tigre and Samiria.

Table 3.1 – Palm swamp forest location and characteristics where sampling was conducted. Organic soils were sampled with variable C content across a broad landscape.

Region	Site Name	Latitude/ Longitude	Degra-dation class[#]	Water pH	Soil depth* (m)	Peat depth (m)	Bulk density[§] (g/cm^3)	Peat C content[§] (%)	Peat C density[§] (g C/cm^3)
Itaya	Quistococha	S 03°49.886' W73°18.797'	0	5.9	2.20	1.92	0.10 ± 0.02	51.9 ± 1.2	3.2 ± 0.2
	Las Brisas	S 03°50.430' W73°19.549'	3	5.9	>2.65	1.90	0.12 ± 0.04	49.4 ± 1.3	3.2 ± 0.2
	San Julian	S 03°48.542' W73°18.349'	3	6.6	0.85	0.28	0.57 ± 0.09	16.5 ± 4.1	2.0 ± 0.3
	Llanque	S 04°09.800' W74°26.278'	3	4.9	>2.65	1.18	0.13 ± 0.01	40 ± 2.1	4.8 ± 0.3
Tigre	Monteverde	S 04°10.075' W74°25.182'	0	6.2	>2.65	1.88	0.16 ± 0.02	26.6 ± 2.7	3.7 ± 0.2
	Avispa	S 04°11.184' W74°21.645'	2	5.4	>2.65	2.25	0.13 ± 0.02	39.6 ± 2.2	4.3 ± 0.4
	Chanchari	S 04°00.353' W74°22.138'	1	4.2	>5.30	2.80	0.11 ± 0.01	52.7 ± 1.2	6.5 ± 0.5
	Nueva York	S 04°21.130' W74°17.598'	3	5.7	4.00	2.40	0.11 ± 0.00	44.4 ± 1.3	3.9 ± 0.4
Samiria	Pobre Cocha	S 04°50.399' W74°17.085'	3	6.4	1.31	0.55	0.22 ± 0.03	33.5 ± 6.6	3.7 ± 0.3
	San Martin	S 04°45.462' W74°25.301'	2	6.5	0.85	0.39	0.27 ± 0.03	22.5 ± 7.1	2.9 ± 0.5
	Shiringal	S 04°45.282' W74°20.756'	3	7	0.76	0.34	0.31 ± 0.04	27.5 ± 5.3	3.1 ± 0.8
	San Miguel	S 04°41.850' W74°11.483'	2	7.1	0.71	0.35	0.23 ± 0.04	19.5 ± 5.6	3.4 ± 0.2

[#] Level of degradation ranging from 0 (low) to 3 (high.) (See methods section for degradation class attribution).

* Soil depth was recorded by inserting a long probe into the ground. At Chanchari and Nueva York sites probe length (~5.3 m) and all other sites probe length (~2.65 m)

§ Bulk density, carbon content and carbon density in top 1m soil profile (mean ± Std. Error).

Table 3.2 – Allometric models for different vegetation to estimate aboveground biomass (AGB; kg dry mass) and belowground biomass (BGB; kg dry mass) from stem height (H stem; m) and diameter of trunk at the breast height (*dbh* or D; cm).

Genera	Aboveground biomass (AGB)	Reference
Arecaceae (palm) family		
Mauritia	$Ln(AGB) = 2.4647 + 1.37777 * ln\,(H\ stem)$	(Goodman et al., 2013)
Mauritiella	$AGB = 2.8662 * (H\ stem)$	
Astrocaryum	$AGB = 21.302 * (H\ stem)$	
Attalea	$Ln\,(AGB) = 3.2579 + 1.1249 * ln\,(H\ stem + 1)$	
Euterpe *(≥ 10m H stem)*	$AGB = -108.81 + 13.589 * (H\ stem)$	
Euterpe *(< 10m H stem)*	$Ln\,(AGB) = -3.3488 + 2.7483 * ln(D)$	
Oenocarpus	$Ln(AGB) = 4.5496 + 0.1387 * (H\ stem)$	
Socratea	$Ln(AGB) = -3.7965 + 1.0029 * (ln(D^2 * H\ stem))$	
Dicot trees (all families)		
All genera	$ln\,(AGB) = -2.286 + 2.471\ ln\,(D)$	(Sierra et al., 2007)
Belowground biomass (BGB)		
Mauritia	$Ln(BGB) = -3.3488 + 2.0106 * ln\,(H\ stem)$	(Goodman et al., 2013)
Mauritiella and all other palms	$Ln(BGB) = 1.0945 + 0.11086 * (H\ stem)$	
Dicot trees (all families)		
All genera	$Ln\,(BGB) = -4.394 + 2.693\ ln\,(D)$	(Sierra et al., 2007)

3.2.3 Sample collection

Information necessary to calculate total ecosystem C stocks including standing tree biomass, downed woody debris (dead wood on forest floor), belowground plant biomass, litter biomass on forest floor and soil C stocks was collected. CIFOR – USFS freshwater peatland forest sampling protocol was used to develop an estimate of total ecosystem C stocks (Kauffman et al. 2016). Aboveground forest structure, composition, and ecosystem C pools was determined at every site by establishing six subplots 50 m apart along a 250 m transect (Figure 3.2). Sub-plot location was determined on the basis of *M. flexuosa* presence (alive) or past presence (dead), usually 1-2 km inland from the main river channel. Once the first sub-plot was identified a 250 m long straight transect was laid in a random direction. If a deep/unpassable stream/ open water area was encountered, then the transect direction was altered so that all six subplots were representative of the forest ecosystem. Vegetation was identified and recorded for species inventory and calculation of above-ground and belowground biomass in live vegetation. Standing dead trees and downed woody debris (DWDs) were measured and counted to determine the quantity of C present in dead and

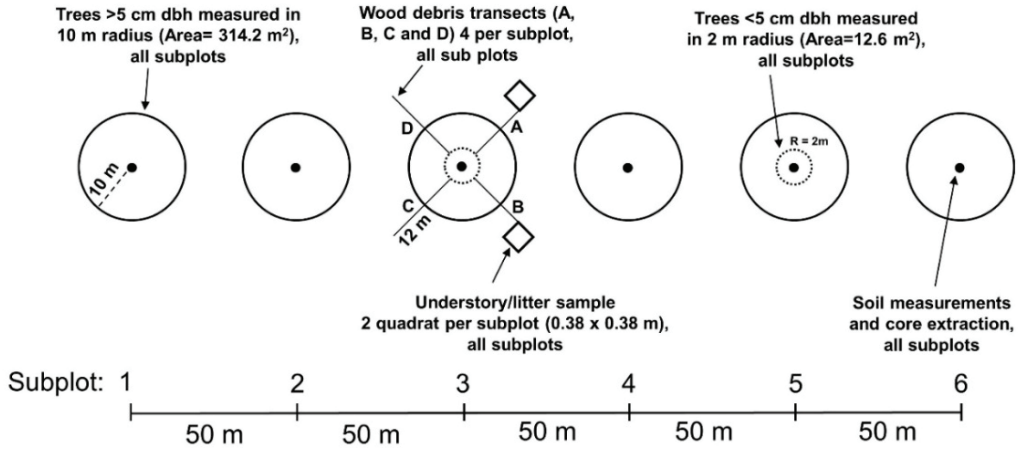

Figure 3.2 – Sampling design used for measuring aboveground forest structure, composition, and ecosystem C stocks. dbh = stem diameter measured at 1.3 m height from the ground. Total length of transect was 250 m.

downed woody components of the ecosystem. Vegetation litter on the forest floor was collected and bagged. And lastly, soil samples were obtained (up to 3 m depth) to determine carbon (C) and nitrogen (N) content within the soil profile.

3.2.4 Vegetation

Trees ≥ 5 cm dbh (dbh = stem diameter at 1.3 m above the ground) were measured inside each of the six circular subplots of 10 m radius (area = 314.2 m^2), while saplings (vegetation with dbh < 5 cm) were measured only inside a 2 m radius circle (area = 12.6 m^2) nested within the larger subplot. All individuals were identified in the field and at least one individual per species was collected. The herbarium vouchers were deposited at the Herbarium Herrerense in Iquitos for future reference. Relative importance value index of species was determined on the basis on their relative abundance, frequency and dominance in the plots using all trees ≥ 10 cm dbh (Curtis and McIntosh, 1951).

The stem height of all palms was measured using a clinometer (Suunto PM-5/360 PC). For palms with slanting trunks, the height of the crown from the ground and slope of the trunk was measured to calculate the length of palm tree trunk. Clinometer was also used to determine the angle of inclination of palm trunk and to determine the angle of elevation of the palm crown with respect to the horizontal ground surface. The length of palm trunks (m) were calculated by using general mathematical principles of trigonometry.

Dead tree measurements were categorized into three classes (I, II and III) depending on the existing branches and twigs attached to the dead tree at the time of sampling. Class I represented a dead tree with the majority of primary and secondary branches attached to the tree, while class III dead tree had no branches attached to the main trunk. Class II category was assigned to a dead tree which possessed primary branches but secondary branches were lost. Aboveground tree biomass (AGB; kg) and belowground tree biomass (BGB; kg) was determined using species-specific allometric equations with stem height (trunk length) as an independent variable in palms (Table 3.2). Vegetation biomass for dicot trees was determined using generic allometric equations with dbh as an independent variable. Biomass in standing dead trees was calculated based upon

their classes. Biomass of class I dead trees was estimated to be 97.5% of a live tree, class II was estimated to be 80% of a live tree, and class III trees were estimated to represent 50% of a live tree (Kauffman and Donato, 2012). Vegetation biomass (kg) was converted into Mg/ha before converting into carbon mass/ha. Biomass of trees (both above and below ground) was converted to C mass using specific conversion ratios. A conversion factor of 0.47 was used for aboveground C and 0.39 for belowground C (Kauffman and Donato, 2012).

3.2.5 Downed woody debris and litter

Downed woody debris were measured using the planar intercept technique (Brown, 1974; Harmon and Sexton, 1996). A survey tape was run 12 m from the plot center in 4 mutually perpendicular directions, oriented at 45° angle from the azimuth of main transect (Figure 3.2). Woody debris intersecting the survey tape were recorded at each of the 6 subplots. Downed wood ≥ 7.5 cm in diameter at the point of intersection with tape was classified as 'large' and measured along the entire length of 12 m long tape. Large wood (pieces ≥7.5 cm in diameter) were separated in two decay categories: sound and rotten. Woody debris that were ≥ 2.5 cm but < 7.5 cm in diameter at the point of intersection were called 'medium' and were measured along the last 5 m of each of the four DWD transects. To determine wood densities of DWDs, a one-time collection of ~20–25 pieces of each woody debris class was made. Each piece was measured for volume using the water mass displacement method and dried in oven to obtain dry mass. These values were used to compute wood density and obtain quadratic mean diameter (QMD) for medium woody debris size class (= 3.98 cm). Wood density (g cm^{-3}) was 0.25 and 0.59 for large rotten and large solid woody debris respectively, and 0.44 g/cm^3 for medium debris size class. A conversion factor of 0.47 was used to convert DWD mass into C mass.

Carbon mass in the litter component of sampled areas was determined by quantifying accumulated vegetation litter on the forest floor. A quadrat with fixed dimensions (0.38 m x 0.38 m) was used to collect litter at the far end of two DWD transects at each of the six subplots. This resulted in 12 samples from each sampled site and provided a good representation of litter deposition at a site.

Vegetation litter was brought to the lab, weighed and ~ 100 g subsample was dried in an oven at 40^0C. The dried subsample was weighed to determine moisture content (as loss in the weight), and was subsequently homogenized by using a combination of mechanical grinder and a mortar-pestle. Dried and finely ground litter samples from both quadrats at each subplot were mixed together and analyzed for N and C content. Carbon content in homogenized litter sample was used to determine overall C mass in forest litter on areal basis (C ha^{-1}). Total vegetation C (C ha^{-1}) at each location was derived by adding C in above and below ground vegetation, DWDs and litter.

3.2.6 Soils

Intact soil cores were obtained at each subplot up to a depth of 3 m and soil samples at specified depth intervals within soil profile were collected. For majority of sites, Russian peat auger (Eijkelkamp Peat Auger) was used; however, an open face auger was used at few subplots at Itaya sites. The auger consists of a semi-cylindrical chamber (radius = 2.87 cm for open face auger and 2.07 cm for Russian peat auger) and a detachable handle to extend its length and enable soil cores extraction up to 3 m depth. The soil core was divided into depth intervals of 0-15 cm, 15-30 cm, 30-50 cm, 50-100 cm, 100-150 cm, 150-200 cm, 200-250 cm, and 250-300 cm. A 5 cm section of soil from these depth intervals was obtained for laboratory determination of C. If there were interbedded mineral and organic soil layers within these zones, 5 cm section was collected from an area including both mineral and organic layer proportionally such that it was representative of that depth interval. Soil depth to point of refusal (minerogenic sediment) was measured at three locations around each plot center by inserting a graduated aluminum pole. Two probes were used with inference capacity of either 2.65 m or 5.3 m (longer probe was available only during half of the sampling). The pH of stagnant undisturbed water at each location was measured by a portable handheld pH measuring device (Oakton EcoTestr pH2 waterproof tester) (Table 3.1).

Forest soil, litter and downed woody samples were transported to the laboratory at Instituto de investigaciones de la Amazonía Peruana (IIAP), Iquitos for weighing, drying and grinding. Carbon and N concentrations in dry homogenized samples were determined by the induction furnace method in a Costech EA C-N analyzer at the analytical laboratory, University of Hawaii-Hilo. A smaller sub-set of total soil samples (count = 87) was tested for calcium (Ca) and magnesium (Mg) content by using ammonium acetate to extract the cations (Simard, 1993), followed by analysis of the solution on a Varian Vista CCD ICP-OES. Total Ca and Mg content is helpful in identifying the influence of riverine transport and external inputs of minerals and nutrients at a given location and is helpful in determination of nutrient status of a site. If Ca:Mg ratio of a peat soil is above 6 (avg. ratio in the rainwater), it indicates influence or inputs of river water, and would render a site minerotrophic, whereas lower Ca:Mg ratios are indicative of low nutrient status or ombrotrophic systems (Lähteenoja et al., 2009a). The selected samples for Ca and Mg analysis included soils from different depth in soil profile to allow determination of changes in the nutrient status of a site as preserved in its stratigraphy.

Soil C pools were obtained as the product of soil C concentration, bulk density, and plot specific soil depth measurements. Carbon masses from each soil section representing different depth horizons were added to derive total soil C stocks at a site. Soil C stocks are reported for two depth boundaries – 1) up to 1 m soil depth and 2) for the entire soil profile. Top 1 m soil profile C allows for an easy comparison among sites but C stocks in the entire soil depth reflect the variability in the soil profile encountered at different sites. Total ecosystem C stocks at each site were determined by adding C stocks in aboveground and belowground vegetation, DWDs, litter and soil profile.

3.2.7 Degradation criteria

Each site was assigned a degradation class to assess the effect of forest degradation on ecosystem C pools. These classes were based on the sum of three criteria : Quantity of DWD, *M. flexuosa* height distribution and presence of *M. flexuosa* seedlings at a site. Each site was scored with 1 if a degradation criterion was present or 0 if the criterion was absent, respectively.

The criteria for DWD were based on the count of DWD (diameter >20 cm) at a site relative to the total DWD (diameter >20 cm) counted at all sites. The presence of large quantity of DWD on the forest floor could be an indicator of disturbances (natural or anthropogenic)(Palace et al., 2012). A score of 1 was assigned if the count within one site was above the overall median, or 0 if this condition was not met. The relationship between *M. flexuosa* height distribution and degradation was based upon the study by Hergoualc'h, Gutiérrez-Vélez, et al. (2017). The height distribution of standing palms was split in 5 ranges (1-7 m, 7-13 m, 13-19 m, 19-25 m and 25-31 m). A site was categorized as degraded when the height distribution was skewed towards small or tall individuals, as found by Hergoualc'h, Gutiérrez-Vélez, et al. (2017). A score of 1 was assigned when the height ranges < 13 m represented < 25% of the standing *M. flexuosa* palms, or when the height ranges > 19m represented less than 28% of the standing *M. flexuosa* palms. In addition, an absence of seedling recruitment could indicate recurrent seed removal following fruit collection. Sites where no young palms (class 1-7 m) were present were scored 1. The degradation class for each site was calculated by summation of the scores assigned for these above mentioned 3 criteria. The maximum score or class of 3 suggests high degradation, the minimum score or class of 0 suggests low degradation.

3.2.8 Data analysis

All carbon parameters were tested for normality using skewness and kurtosis, with limits at ±1. If parameters did not conform to the assumptions of parametric statistics non-parametric methods were employed and Kruskal-Wallis tests were used to compare mean C estimates between locations and sites. In other cases, ANOVA's and Bonferroni post-hoc tests were used. All statistical operations were performed with the software IBM SPSS Statistics for Windows 21.0 (IBM Corp. 2012).

Table 3.3 – List of the seven most important species at the sites. Species are ordered by their importance value index in parenthesis (IVI value in % out of a total 300% per site) indicating at the top the most abundant, frequent and dominant. All individuals with dbh ≥ 10 cm were included in these calculations.

	Sites (total number of species)				
Itaya	**Quistococha (28)**	**Las Brisas (29)**	**San Julian (29)**		
	Mauritia flexuosa (29)*	*Mauritia flexuosa* (95)	*Cecropia membranacea* (43)		
	Tabebuia insignis (22)	*Vatairea sp.* (18)	*Hura crepitans* (36)		
	Hevea nitida (20)	*Mauritiella armata* (18)	*Ficus* sp. (29)		
	Mauritiella armata (20)	*Symphonia globulifera* (16)	*Virola pavonis* (23)		
	Fabaceae sp. (14)	*Himatanthus sucuuba* (15)	*Guatteria* sp. (18)		
	Clusiaceae sp. (13	*Lacmellea* sp. (13)	*Mauritia flexuosa* (17)		
	Parahancornia peruviana (9)	*Alchornea triplinervia* (11)	*Vismia angustifolia* (14)		
Tigre	**Llanque (31)**	**Monteverde (33)**	**Avispa (19)**	**Chanchari (30)**	**Nueva York (22)**
	Mauritia flexuosa (52)	*Mauritia flexuosa* (78)	*Mauritia flexuosa* (49)	*Virola duckei* (44)	*Mauritia flexuosa* (66)
	Iryanthera paradoxa (42)	*Vatairea guianensis* (32)	*Pachira brevipes* (49)	*Mauritia flexuosa* (33)	*Eschweilera* sp. (38)
	Cariniana multiflora (24)	*Attalea* sp. (29)	*Qualea acuminata* (40)	*Ilex laureola* (25)	*Euphorbiaceae* sp. (35)
	Oxandra leucodermis (22)	*Mauritiella armata* (26)	*Hevea guianensis* (30)	*Pachira brevipes* (24)	*Oxandra leucodermis* (16)
	Mauritiella armata (22)	*Symphonia globulifera* (23)	*Oxandra mediocris* (22)	*Alchornea triplinervia* (19)	*Guatteria* sp. (14)
	Hevea guianensis (17)	*Guatteria* sp. (8)	*Nealchornea yapurensis* (22)	*Parahancornia peruviana* (15)	*Malouetia tamaquarina* (13)
	Euterpe precatoria (14)	*Virola pavonis* (7)	*Apeiba membranacea* (21)	*Platycarpum loretensis* (13)	*Pseudoxandra lucida* (12)
Samiria	**Pobre Cocha (21)**	**San Martín (18)**	**Shiringal (21)**	**San Miguel (29)**	
	Euterpe precatoria (63)	*Mauritia flexuosa* (94)	*Hura crepitans* (57)	*Mauritia flexuosa* (64)	
	Mauritia flexuosa (27)	*Mauritiella armata* (35)	*Mauritia flexuosa* (39)	*Hura crepitans* (32)	
	Socratea exorrhiza (22)	*Pachira aquatica* (31)	*Ceiba samauma* (36)	*Fabacaeae* sp. (28)	
	Symphonia globulifera (20)	*Vatairea guianensis* (22)	*Euterpe precatoria* (27)	*Virola pavonis* (21)	
	Apeiba membranacea (19)	*Virola pavonis* (22)	*Symphonia globulifera* (19)	*Attalea* sp. (14)	
	Lacistema aggregatum (18)	*Macrolobium multijugum* (15)	*Oenocarpus mapora* (15)	*Macrolobium multijugum* (11)	
	Oenocarpus mapora (17)	*Euterpe precatoria* (11)	*Socratea exorrhiza* (13)	*Zygia* sp. (10)	

*IVI values for Quistococha where dbh of palms was not measured were computed without considering relative dominance

3.3 Results

3.3.1 Structure and composition of Palm Swamp Forests (PSF)

In total 2,338 individual living trees were counted and measured across the 12 sampled sites (Appendix - Table 1), corresponding to 58 families and 214 species. Approximately 16 -28 families of trees with dbh ≥ 5 cm were encountered at each sampled location, with a slightly lower number in Samiria region. Number of species varied among different locations (27-52 species), with highest number of species at Las Brisas (46), Llanque (52) and Monteverde (52) sites (Appendix Table 1). *Mauritia flexuosa* was present in all sites and it was the top most abundant, frequent and dominant species in most sites based on individuals with dbh ≥ 10 cm (Table 3.3). Other important trees and palms (dbh ≥ 10 cm) from these sites represent diversity of vegetation encountered in the sampled locations (Table 3.3). Species found to be abundant in peatland pole forest such as *Pachira brevipes* (Malvaceae), *Oxandra mediocris* (Annonaceae) and *Platycarpum loretensis* (Rubiaceae) (Draper et al., 2018) were present in the sites in Tigre region, except for Monteverde.

Two attributes of vegetation characteristics – basal area (m^2 ha^{-1}) and tree density (trees ha^{-1}) provide an indication of the forest structure at a location. Basal area ranged from 7-24 m^2 ha^{-1} for dicots, 0.2 to 5.5 m^2 ha^{-1} for other palms and 1.3 to 11.7 m^2 ha^{-1} for *M. flexuosa* among all sampled sites (Table 3.4). Highest basal area for dicot trees was observed at Avispa site while lowest was observed at San Martin. Among the eleven sites where dbh of palms was measured, highest basal area for *M. flexuosa* was observed at Monteverde site while lowest was observed at San Julian. Only four sites (San Julian, Avispa, Chanchari and Shiringal) had a basal area represented by all palms amounting to less than 40 % of total dicot tree basal area, which indicated that Arecaceae family was less prevalent in these forests.

Tree density ranged from 292 – 1517 ha^{-1} for dicots, 11 – 435 ha^{-1} for other palms and 16 – 170 ha^{-1} for *M. flexuosa* among sampled sites. Highest tree density for dicot trees was observed at Avispa, while lowest was observed at Shiringal. Highest *M. flexuosa* palm density was observed at Quistococha, while lowest was

at San Julian site. Two sites in Tigre (Chanchari and Monteverde) and three sites in Samiria (Pobre Cocha, San Martin and Shiringal) had a total palm density amounting to more than 40 % of dicot trees density.

3.3.2 Above and belowground biomass and soil C stocks

The highest and lowest aboveground vegetation C stock were found in Itaya region (Quistococha - 97.7 ± 15 Mg C ha^{-1} and San Julian - 36.8 ± 10.5 Mg C ha^{-1}; Appendix - Table 3). There was no difference in the mean aboveground vegetation

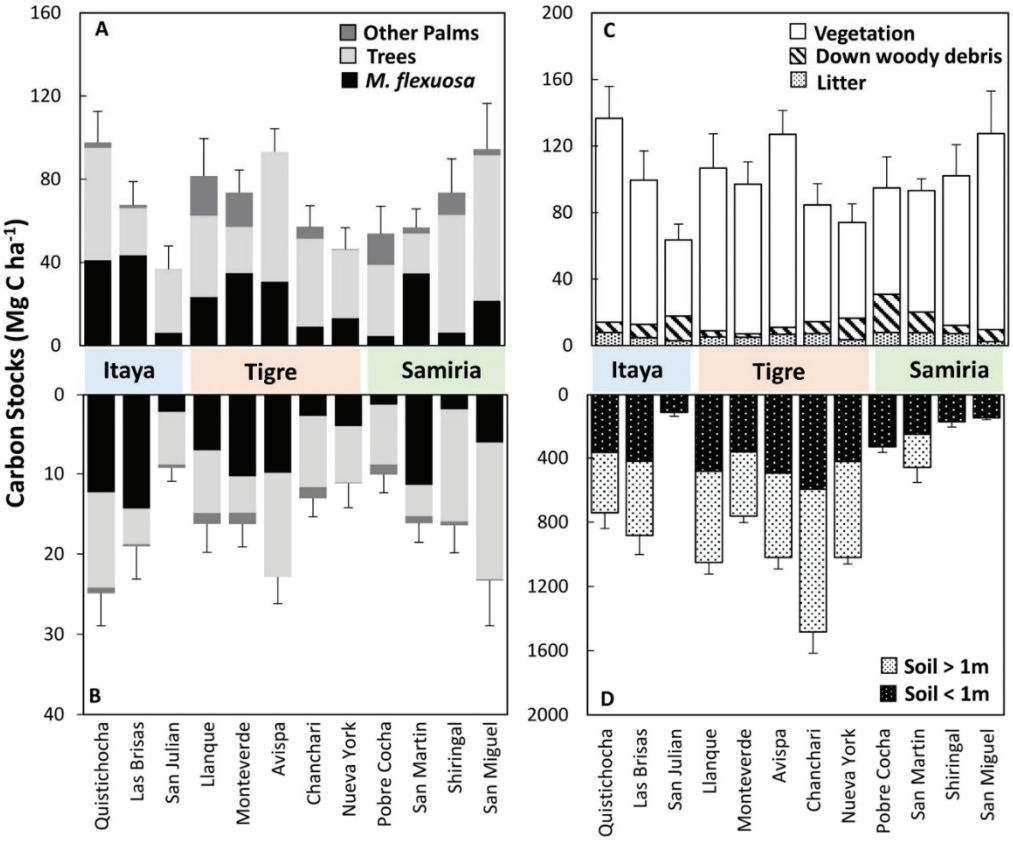

Figure 3.3 – Aboveground (A) and belowground (B) C stocks for *M. flexuosa* (MF), dicot trees (Trees) and other palms; (C) total vegetation, downed woody debris (DWD) and litter C stocks; (D) soil C stocks for soil layer <1m and >1m. Error bars represent one standard error for the entire stacked bar. Note the scales of y-axes differ.

C stocks among three regions, nor did individual sites differ significantly (Figure 3.3A). Mean belowground vegetation C stocks displayed similar variation across the sites, with highest and lowest belowground vegetation C stocks also in Itaya region (Quistococha - 24.9 ± 4.1 Mg C ha^{-1} and San Julian - 8.8 ± 2.5 Mg C ha^{-1}; Figure 3.3B). In addition, there was no difference in the total vegetation C stocks among different sites across regions (Figure 3.3C).

Within the sites sampled in Itaya region, Quistococha and Las Brisas had vegetation C stocks of 122.5 ± 19 and 86.7 ± 15.2 Mg C ha^{-1}, respectively; however, the third site – San Julian had only 45.6 ± 12.9 Mg C ha^{-1}. In Tigre region, highest vegetation C stocks were found at the Avispa (116.1 ± 14.2 Mg C ha^{-1}) and lowest at the Nueva York sites (57.6 ± 13.3 Mg C ha^{-1}). Within sites in the Samiria region, largest vegetation C stocks were present in San Miguel (117.8 ± 27.6 Mg C ha^{-1}) whereas lowest vegetation C stocks were found at Pobre Cocha (63.9 ± 15.2 Mg C ha^{-1}). Fraction of total aboveground vegetation C stocks contributed by palms ranged from 26-70 % within three regions, with no one region having high or low C stocks in palms (Table 3.5 and Appendix - Table 3).

Downed woody debris C ranged from 2.1 ± 0.7 Mg C ha^{-1} to 23.1 ± 14.9 Mg C ha^{-1} among different sites (Figure 3.3C, Table 3.5). Carbon in DWD was relatively small except for three sites (San Julian, Nueva York and Pobre Cocha) where it amounted to approximately 22 – 36 % of the total vegetation C stocks (Table 3.5). On the other hand, litter C was generally uniform among the sites representing ~ 6.9 % of total vegetation C. Lowest litter C was observed at San Miguel (2.3 ± 0.2 Mg C ha^{-1}) and highest at Quistococha (7.8 ± 1.3 Mg C ha^{-1}) and Pobre Cocha (7.8 ± 0.6 Mg C ha^{-1}).

The major repository of C in these forested ecosystems are the soils. Variability in soil C storages along the soil depth profile and among the six sub-plots at sampled sites reveals similarity within sampled regions, but wide variation exists between different regions (Figure 3.3D; Appendix - Table 4, 5, 6 and 7). Mean soil C stocks in top 1 m of soil profile for Itaya, Tigre and Samiria regions were 298 ± 96, 471 ± 39 and 225 ± 42 Mg C ha^{-1}, respectively. When the entire soil depth was included, the mean soil C stocks were 577 ± 238, 1067 ± 116 and 234 ± 44 Mg C ha^{-1} for these three regions, respectively.

Table 3.4 – Vegetation (dbh ≥ 10 cm) basal area and density attributes in sampled areas (Mean ± std. error).

Location	Basal area ($m^2 ha^{-1}$)			Density (trees ha^{-1})		
Site name	**Trees**	**Other Palms**	***M. fleuxosa***	**Trees**	**Other Palms**	***M. fleuxosa***
Itaya						
Quistococha*	19.4 ± 2.8	n. a.	n. a.	1496 ± 198	180 ± 83	170 ± 54
Las Brisas	9.8 ± 1.3	1.0 ± 0.4	10.9 ± 3.4	700 ± 104	90 ± 32	164 ± 67
San Julian	10.8 ± 3.4	0.2 ± 0.2	1.3 ± 0.8	679 ± 237	11 ± 11	16 ± 11
Tigre						
Llanque	16 ± 3.3	2.6 ± 1.1	6.9 ± 2.3	1332 ± 119	276 ± 102	90 ± 28
Monteverde	8.8 ± 1.4	5.5 ± 1.2	11.7 ± 3.1	801 ± 98	244 ± 119	149 ± 48
Avispa	23.9 ± 3.8	--	7.7 ± 2.5	1517 ± 165	--	106 ± 31
Chanchari	15.6 ± 2.4	1.9 ± 0.3	3.2 ± 1.5	833 ± 66	435 ± 82	48 ± 20
Nueva York	11.6 ± 1.7	0.5 ± 0.4	5.7 ± 1.8	727 ± 113	32 ± 20	80 ± 27
Samiria						
Pobre Cocha	11.7 ± 2.4	4.7 ± 1.1	2.0 ± 0.8	403 ± 59	286 ± 74	21 ± 7
San Martin	7.4 ± 2.5	2.6 ± 1.7	10.1 ± 2.2	509 ± 134	202 ± 154	117 ± 24
Shiringal	14.1 ± 3.3	1.4 ± 0.5	2.6 ± 0.6	292 ± 45	117 ± 46	27 ± 5
San Miguel	19.1 ± 5.3	1.4 ± 0.5	7.6 ± 1.2	499 ± 59	37 ± 15	101 ± 15

* Palm dbh was not measured at this location.

Table 3.5 – Carbon stocks (Mean ± std. error) in downed woody debris (DWD), litter on forest floor and vegetation (aboveground (AG) and belowground (BG) combined). Site mean obtained from six sub-plot measurements.

Region	Site name	Downed woody debris C	Litter C	Vegetation C (AG + BG)	Percent relative to vegetation C	
		(Mg C ha^{-1})			DWD (%)	Litter (%)
Itaya	Quistococha	6.3 ± 1.7	7.8 ± 1.3	122.5 ± 19	5.1	6.4
	Las Brisas	8 ± 2.9	4.7 ± 0.6	86.7 ± 15.2	9.3	5.4
	San Julian	14.9 ± 12.2	2.9 ± 0.6	45.6 ± 12.9	32.7	6.3
	Mean	9.8 ± 2.6	5.1 ± 1.4	84.9 ± 22.2	11.5	6.0
Tigre	Llanque	3.8 ± 1.1	5.1 ± 0.2	97.8 ± 20.8	3.9	5.2
	Monteverde	2.1 ± 0.7	5 ± 0.9	89.9 ± 13.5	2.3	5.6
	Avispa	4.2 ± 1.2	6.7 ± 0.7	116.1 ± 14.2	3.6	5.8
	Chanchari	7.1 ± 4.1	7.2 ± 1.1	70.2 ± 12.4	10.2	10.3
	Nueva York	12.8 ± 3.6	3.5 ± 0.2	57.6 ± 13.3	22.3	6.2
	Mean	6 ± 1.9	5.5 ± 0.7	86.3 ± 10.3	7.0	6.4
Samiria	Pobre Cocha	23.1 ± 14.9	7.8 ± 0.6	63.9 ± 15.2	36.2	12.1
	San Martin	12.4 ± 5.1	7.7 ± 0.8	73 ± 11.2	17.1	10.6
	Shiringal	4.9 ± 2.1	7.2 ± 0.8	90 ± 19.3	5.4	8.0
	San Miguel	7.4 ± 2.4	2.3 ± 0.2	117.8 ± 27.6	6.2	2.0
	Mean	12 ± 4	6.2 ± 1.3	86.3 ± 11.9	13.8	7.2

3.3.3 Soil physico-chemical properties

There was a considerable variation in soil depths across the three regions ($p < 0.01$), and among the sampled sites ($p < 0.01$) (Table 3.1). The majority of sites had a surface layer of organic peat, followed by peaty clay, and then a dense gleyed clay horizon. Bulk density (g cm^{-3}) was typically low within the surface soils (1 m soil profile) suggesting a prevalence of organic matter, except in sections where underlying clay deposits were encountered (Appendix - Table 4, 5 and 6). For instance, within the Itaya region, Las Brisas and Quistococha had deep organic soils; however, San Julian soils were shallow and had higher bulk density (Table 3.1). In Tigre region, bulk density was low (< 0.3 g cm^{-3}) in the surface soils (top 1 m soil) at all sampled sites. Soils in Samiria region were shallower and thick-textured with higher bulk density than the other two regions ($p < 0.01$). Carbon concentration in surface 1-m soil profile in Itaya region ranged from 50 - 53 % in Quistococha and Las Brisas and considerably lower at San Julian (17 %; Appendix - Table 4). Low C content and high bulk density in San Julian soils reflects mineral nature of sampled soils instead of peat observed at other sites, which was specifically visible in subplots 4, 5 and 6 at this site (Appendix – Table 4)As a consequence peat C density at San Julian was low in comparison to peat density in the other two sites in Itaya region ($p < 0.01$) (Table 3.1). In Tigre region, C content in top 1 m soil ranged from 26 - 53 % with Chanchari having highest (>52%) and Monteverde lowest (<30%) C concentration. In Samiria region, C content in top 1 m soil ranged from 20 - 34 % among sites (Table 3.1). Carbon density was on average higher in Tigre region (4.6 g C cm^{-3}) in comparison to Itaya (3.2 g C cm^{-3}) and Samiria (3.1 g C cm^{-3}) regions ($p < 0.01$).

The Ca:Mg ratio profiles from the sampling locations yielded information about the prevailing conditions during soil/peat formation at these palm swamp forests. All sampled sites in Samiria showed Ca:Mg > 6 (Figure 3.4A and 4B), suggesting presence of riverine inputs in this region. In Itaya region, Ca:Mg ratio at San Julian was < 6 indicating minimal influence of riverine inputs over short time horizons. Only one site in Tigre region (Chanchari) had a Ca:Mg ratio > 6 while other four sites had low Ca:Mg ratio where periodic river inputs may have been minimal. The depth profile of Ca:Mg ratio at Chanchari showed an interesting pattern, with a low Ca:Mg ratio (< 6) at the surface and high Ca:Mg ratio (~13) at about 125 cm, and

then again low ratio at 175 cm depth followed by high Ca:Mg ratio again at deeper depths. This may be indicative of flooding events that took place at various times in the history, and its signature (in the form of high Ca:Mg ratio) got embedded within the peat layer.

Among the sampled sites, strong relationships between soil nutrients and bulk density were observed within the top 1 m of soils (Figure 3.5A and B). Soil N content increased linearly with increasing C content while bulk density decreased logarithmically with increasing C content. Within the top 1 m of soil profile, >70% of samples had a bulk density < 0.2 g cm^{-3} and a C content > 20%. Surface soil (0-30 cm) contained majority of C stored in these soils and soil C content declined dramatically with increasing soil depth (Figure 3.5B).

3.3.4 Total ecosystem carbon stocks and effect of palm swamp forests degradation

Total ecosystem C stocks in PSF of Peruvian Amazon ranged from 200 – 1000 Mg C ha^{-1} in Itaya, 900 – 1600 Mg C ha^{-1} in Tigre and from 300 – 400 Mg C ha^{-1} in Samiria region (See Appendix Table 7 for complete dataset). Mean ecosystem C stocks in Samiria (337.9 ± 38.1 Mg C ha^{-1}) were lowest in comparison to mean ecosystem C in Itaya (677 ± 254.1 Mg C ha^{-1}) and Tigre (1164.7 ± 114.1 Mg C ha^{-1}; $p < 0.01$). Carbon stocks in Itaya region were significantly lower than carbon stocks in Tigre region ($p < 0.01$). The largest contribution to total ecosystem C stocks was by forest soils for all sites; however, C stocks in vegetation were important fractions in these systems (Table 3.6). Sampled sites in Samiria region had relatively higher fraction of C stock in vegetation biomass ~ 25% of total ecosystem C stocks (when both above and below ground fractions were combined). Soils C typically represented 70-90% of total ecosystem C stocks. Carbon stocks in downed woody debris and litter were sizeable (~ 10 – 15 Mg C ha^{-1}); however, in comparison to vegetation and soil C compartments, these together constituted < 5 % of the total ecosystem C stocks (Table 3.6).

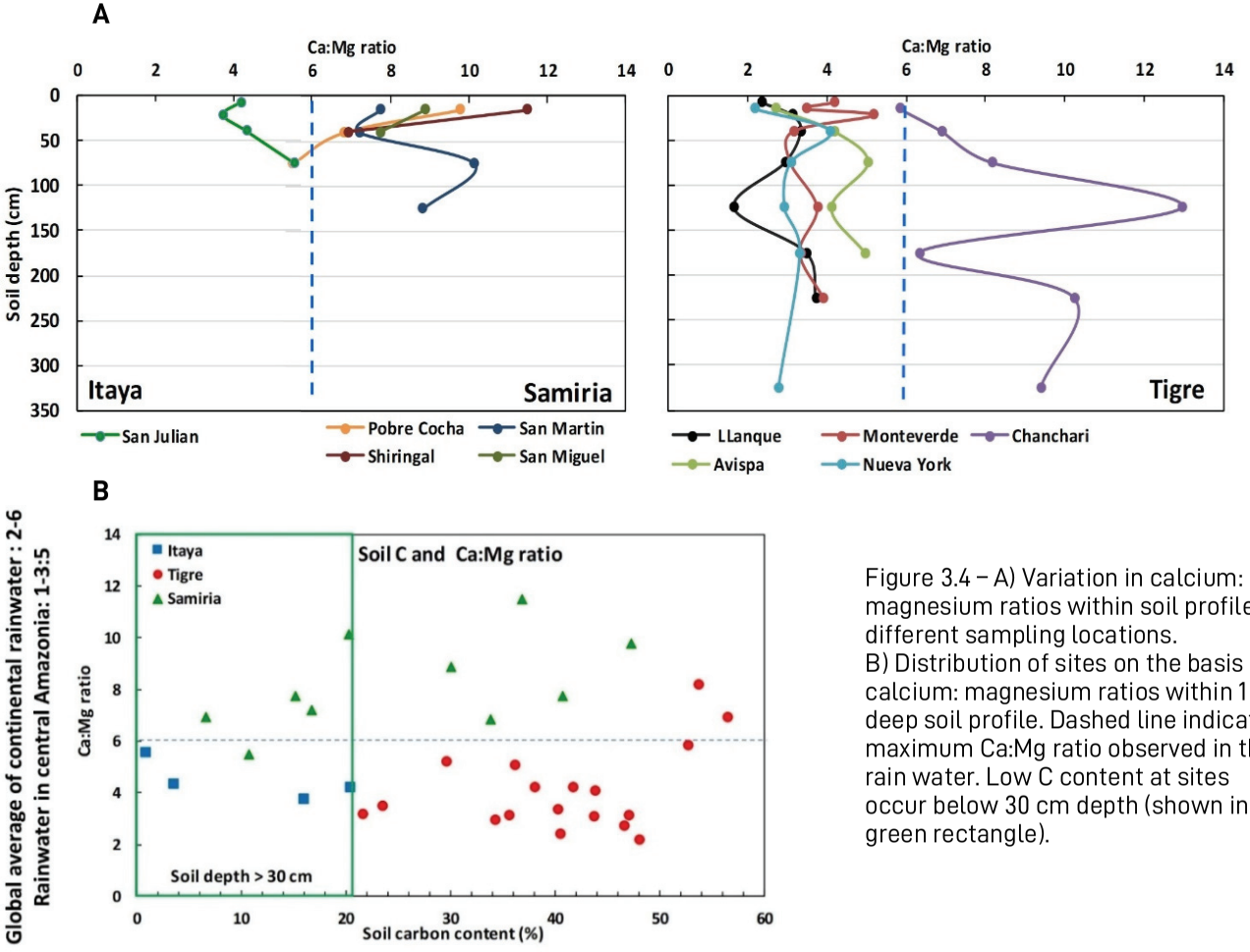

Figure 3.4 – A) Variation in calcium: magnesium ratios within soil profile at different sampling locations.
B) Distribution of sites on the basis of calcium: magnesium ratios within 1 m deep soil profile. Dashed line indicates maximum Ca:Mg ratio observed in the rain water. Low C content at sites occur below 30 cm depth (shown in green rectangle).

The average degradation scores for Itaya, Tigre and Samiria regions were 1.3, 1.4 and 2.3, respectively. There were no differences between regions ($p = 0.42$); degradation classes ranged from low disturbance to higher levels of disturbance within each region (Table 3.1). Degradation did not correlate with soil C up to 1m depth, nor the entire soil profile. However, increased levels of degradation showed a trend for lower total vegetation C and forest floor C (DWD + litter) (Figure 3.6A). Moreover, the C stock in above and belowground *M. flexuosa* vegetation showed a clear and significant reduction with increased degradation ($r^2 = 0.60$, $p < 0.01$) (Figure 3.6B). The C stock in trees, other palms and the forest floor was not significantly correlated to degradation class.

Table 3.6 – Carbon stocks as fraction of total ecosystem carbon in measured locations.

Location	**Sites**	**Carbon in top 1 m soil**				**Carbon in entire soil depth**			
		Litter	DWD	Vege-tation	Soil	Litter	DWD	Vege-tation	Soil
Itaya	Quistochocha	1.6	1.3	24.4	72.8	0.9	0.7	14.0	84.4
	Las Brisas	0.9	1.5	16.7	80.9	0.5	0.8	8.8	89.9
	San Julian	1.7	8.7	26.5	63.2	1.7	8.7	26.5	63.2
	Mean	*1.3*	*2.4*	*21.3*	*74.9*	*0.8*	*1.4*	*12.5*	*85.3*
Tigre	Llanque	0.9	0.6	16.6	81.9	0.4	0.3	8.5	90.8
	Monteverde	1.1	0.5	19.6	78.8	0.6	0.2	10.5	88.7
	Avispa	1.1	0.7	18.7	79.5	0.6	0.4	10.1	88.9
	Chanchari	1.1	1.1	10.3	87.5	0.5	0.5	4.5	94.6
	Nueva York	0.7	2.6	11.6	85.1	0.3	1.2	5.3	93.2
	Mean	*1.0*	*1.1*	*15.2*	*82.8*	*0.5*	*0.5*	*7.4*	*91.6*
Samiria	Pobre Cocha	1.8	5.5	15.1	77.6	--	--	--	--
	San Martin*	2.2	3.6	21.1	73.1	2.0	3.3	19.2	75.5
	Shiringal	2.6	1.8	32.6	63.0	--	--	--	--
	San Miguel	0.9	2.7	43.4	53.0	--	--	--	--
	Mean	*1.9*	*3.6*	*26.2*	*68.3*	*--*	*--*	*--*	*--*

***** Only one site (San Martin) had soil profile deeper than 1m in Samiria region.

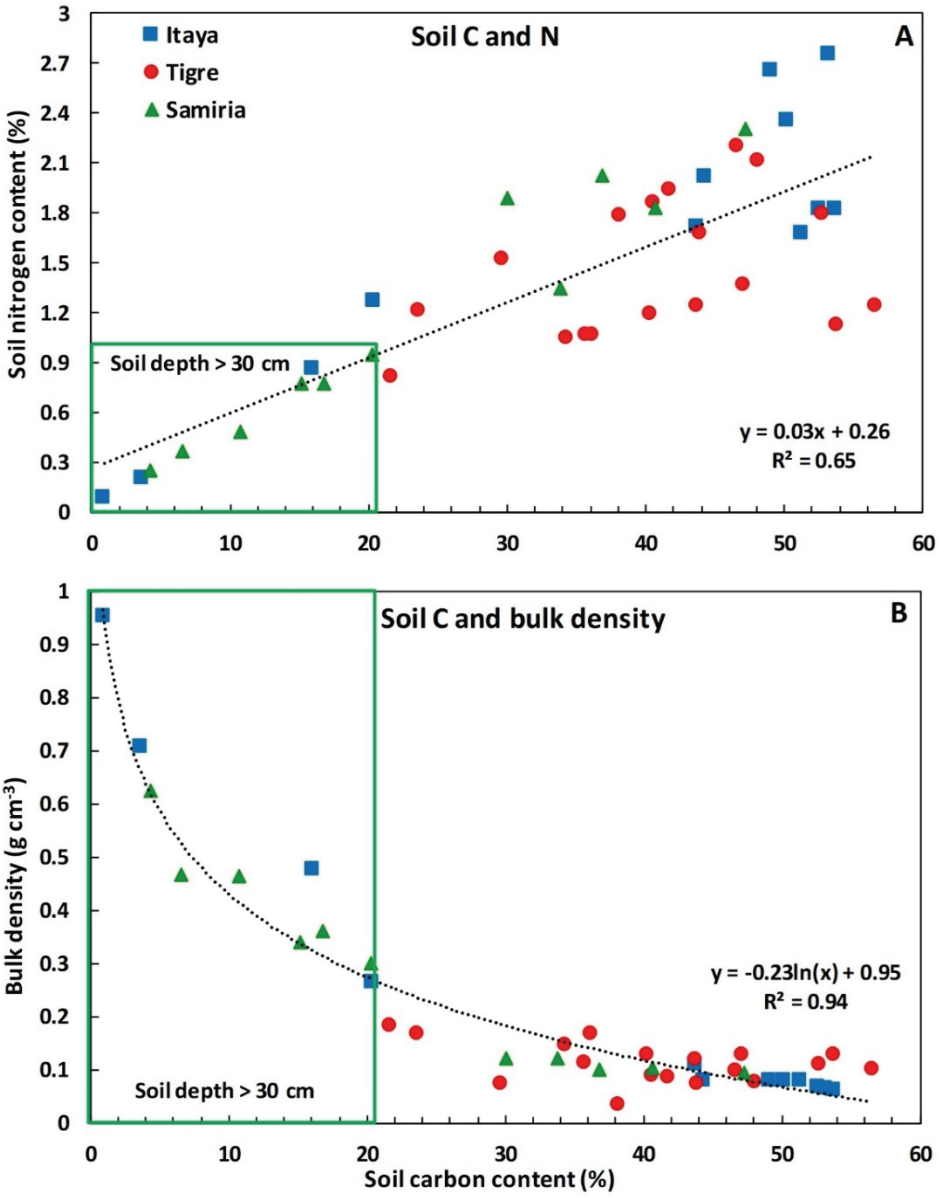

Figure 3.5 – Relationships between soil carbon content and soil nitrogen content (A) and bulk density (B) within the top 1m soil depth (n = 41). In (A) and (B) soil samples with a C content < 20% are from below 30 cm of soil depth in the Itaya and Samiria regions.

3.4 Discussion

Palm swamp forests account for most of Peru's wetlands and the majority of this wetland type is found within the Pastaza-Marañón foreland basin in the western Amazon. Our study was aimed at quantitative assessment of C stocks in these swamp forests, evaluation of C stocks variability across the Pastaza-Marañón region and appraisal of potentials of overharvesting of *M. flexuosa* on disruption of forest structure and loss of ecosystem functions leading to soil C losses.

3.4.1 Carbon dynamics on a regional scale

Total ecosystem C stocks determined in this study (200 -1600 Mg C ha^{-1}) were within the range reported by Lähteenoja et al. (2009b); Lähteenoja et al. (2012) and Draper et al. (2014) from the north eastern region of Peru. Soil C typically represented 70-90% of total ecosystem C, followed by vegetation C as second largest component, followed by DWD and litter. The C stocks in primary (384 Mg C ha^{-1}) and secondary (230 Mg C ha^{-1}) forests of Colombia (Sierra et al., 2007) were much smaller in comparison to the Peruvian palm swamp forests C stocks because of the absence of C rich peat layer. Although litter may represent only a small fraction, a significant amount of soil C originates from residual refractory C that accumulates on the forest floor as litter and does not decompose due to prevailing anoxic conditions of swamp forests.

All sampled locations in Itaya and Tigre regions had high C stocks when the complete soil profile was accounted (except for San Julian and sites in Samiria region) where peat depths were shallow (< 1 m). This represents an interesting finding since the standing vegetation (both aboveground and belowground) C in the three sampled regions were similar; although soil C and peat depth varied between site-to-site. This suggests that landscape level factors (sediment inputs and hydro-dynamic processes controlled by annual river flooding) could play an important role in organic matter accumulation, peat formation and stabilization or erosion in this region. Since the Cretaceous period, rivers originating from the Andes have led to the accumulation of several kilometer thick minerogenic deposits in these subsiding basins (Lähteenoja et al., 2012). Consequently, the accumulation of peat in this slowly subsiding basin is a dynamic process, influenced by lateral movements of river channels, e.g. meandering up to > 100 m

in a year (Smith et al., 1989) and avulsions (abrupt changes in the location of river stretches) which can cause both burial and erosion of peat deposits (Kalliola et al., 1992; Neller et al., 1992). Moving rivers may be responsible both for burial and erosion of peat located in their path (Morozova and Smith, 2003).

The complex stratigraphy observed in many of the sites demonstrate that peat burial and mixing with minerogenic sediments is common in areas influenced by river flooding and sediment inputs. The peat layer within Tigre region was relatively thick and the upper soil layers did not contain minerogenic deposits (Figure 3.4) however sites from Samiria region had shallow peat layer with overlying clay deposits. Carbon content in Tigre region was highest but N % was relatively low (Figure 3.5A). This could be indicative of the humification process where recalcitrant C accumulates while N is reduced along the soil profile. In Itaya and Samiria regions, high soil bulk density was observed underneath 30 cm depth horizon (Figure 3.5B), whereas bulk densities of surficial layers were relatively low. This may indicate a past incident of flooding or river migration when clayey sediments were deposited. Subsequent accumulation of vegetation litter and organic matter over clayey sediment resulted in forming a high C content surficial layer, which overtime forms the peaty layer we encountered.

At Tigre sites however, bulk density remained generally low throughout the deeper soil horizons. Lack of clayey riverine sediment deposits in Tigre region is also indicative of lower hydrodynamic energy of the system, which enhances accumulation and accrual of organic matter and is conducive of peat formation (Bailey, 1951). Sites in Tigre basin seem to be stable over a historic period of time and do not seem to be affected by landscape shaping characteristics of the main river (Draper et al., 2014). Interestingly, soil bulk density and C content at Chanchari did not show differences with other sampled locations in Tigre region but the Ca:Mg ratio at this site changed dramatically with soil depth, and was very dissimilar to other sites (Figure 3.4). While it is reasonable to assume that river mediated inputs of sediments have been relatively low or absent for sites situated ~12-15 km downstream of Chanchari, it is possible that the river dynamics affecting and shaping the palm forests of Chanchari were different than other sites in the Tigre basin. On the other hand in Samiria region, relatively shallow depth of organic layer, fine clay deposits and high Ca:Mg ratio suggests that

sampled sites were directly affected by the river dynamics (Figure 3.4 and Figure 3.5).

Using low Ca:Mg ratios as an indicator of ombrotrophic conditions and limited riverine influences, it can be surmised that majority of C stored in the top 1 m soil surface in Itaya and Tigre regions is autochthonous. On the other hand, high Ca:Mg ratio in Samiria region suggested riverine influence and therefore soil C at these sites may be associated with the mineral and fine clay particles brought by the river/flood waters. This observation is also supported by elevated soil bulk density in Samiria sites (Figure 3.5) and provides another evidence of river flooding in depositing mineral sediments and shaping soil characteristics at a site. A steady decline in Ca:Mg ratio from high (~13) at 130 cm to low (~5.8) at the surface at Chanchari (Figure 3.4A) shows an interesting dynamic process in action. It represents late successional stage of minerotrophic mire and its transition into an ombrotrophic system (Lähteenoja et al., 2009a), possibly facilitated by lower hydrodynamic energy of the system (reduced flooding) and vegetation change.

In Peru, peatlands are found at both low (Lähteenoja et al., 2009b; Householder et al., 2012; Lähteenoja et al., 2013; Draper et al., 2014) and high altitudes (Hribljan et al., 2016; Hribljan et al., 2017) and can be ombrotrophic or minerotrophic (Lähteenoja et al., 2009a) which support the growth of different vegetation types (Roucoux et al., 2013; Draper et al., 2018). No difference in total ecosystem C stocks was observed between ombrotrophic or minerotrophic sites, even though areas that are less influenced by river systems may continue to accumulate organic matter and transform into elevated ombrotrophic bogs (Lähteenoja et al., 2009a; Lawson et al., 2014). It is also likely that vegetation composition (species diversity) may vary between ombrotrophic and minerotrophic sites (Roucoux et al., 2013; Kelly et al., 2017). At Chanchari site where we observed declining Ca:Mg ratios (site transitioning from minerotrophic to Ombrotrophic status) most important vegetation species was *Virola duckei* (Table 3.3) instead of *M. flexuosa*. *M. flexuosa* density can range from 130-250 individuals per ha in extensive stands of palm swamp forests in Peru (Kahn, 1991), however at Chanchari we found lowest *M. flexuosa* density (48 palms ha^{-1}) among the five sampled sites in Tigre basin. The reduction in *M. flexuosa* density could be due to anthropogenic impacts (*M. flexuosa* fruit harvesting) or due to natural forest succession. However, this site

has maintained itself as a peatland and has the highest overall C stocks in the region (Figure 3.3, Appendix Table 7). Based on the floristic composition, some of the sites sampled in Tigre region contained species that are found in ombrotrophic pole forests. For example, species such as *Pachira brevipes, Oxandra mediocris* and *Platycarpum loretensis* found in Avispa and Chanchari, respectively may be indicative of succession of palm swamp forests to the pole forests (Draper et al., 2018). Therefore, the potential stability of peatlands in this region may also relate to natural succession of the vegetation, and some sites may be undergoing a transition to a pole forest as suggested by floristic composition (e.g. evidence of pollen record at San Jorge in Rio Amazonas; (Kelly et al., 2017)). On the other hand, dominance of a pioneer species, *Cecropia membranacea* in San Julian in Itaya region indicates heavy loss of canopy cover which can be attributed to the degradation caused by anthropogenic impacts. As a result, the degradation score was 3 and vegetation C stocks at San Julian were only 45.6 ± 12.9 Mg C ha^{-1}, lowest of all 12 sampled sites.

3.4.2 Vegetation characteristics, degradation and ecosystem carbon stocks

The aboveground vegetation C stock in our sites averaged at 69.9 Mg C ha^{-1}, which was similar to values presented in a review from Southeast Asian peatlands (Hergoualc'h and Verchot, 2011) and from palm swamp peatlands of Peru at different levels of degradation (Hergoualc'h, Gutiérrez-Vélez, et al., 2017). Comparing to Southeast Asian peatlands, our values were closer to the average aboveground C stocks of logged peat swamp forests (85.1 Mg C ha^{-1}), than to virgin peat swamp forests (181.9 Mg C ha^{-1}) (Hergoualc'h and Verchot, 2011). Utilizing established metric of classifying forest degradation (Thompson et al., 2013) based on tree density and magnitude of DWDs, sampled sites were categorized into different degradation classes. The impact of anthropogenic forest degradation in this sense is relatively recent in some sites (e.g. Las Brisas, Shiringal) and is not reflected in the observed variation of soil C. We observed that our score of degradation is reflected in the vegetation C; recurrent harvesting of M. *flexuosa* likely resulted in lower vegetation C. Since swamp forests soil C typically represented 70-90% of total ecosystem C (Table 3.6), we did not observe any relationship between soil C stocks and our assigned degradation classes.

Although the effect of degradation in our sites was not clearly evident on the total ecosystem C stocks, contribution to belowground C by forest vegetation in the form of litter (Melillo et al., 1989; Yule and Gomez, 2009) and root biomass might be lower at a degraded site, and it could negatively impact overall C accumulation rates at that site.

Vegetation C fraction was the second largest component and showed large variation both within and between regions, but only showed a trend of reduced C with increased level of degradation (Figure 3.6A). However, the observed C stocks in *M. flexuosa* palms did uniformly decrease in all sites and regions with increased level of degradation (Figure 3.6B). The overall variation observed in *M. flexuosa* C stocks within one degradation class was substantial, e.g. for category 1 this ranged from 12 to 58 Mg C ha^{-1}. This indicates an additional source of variation related to, for example, natural disturbances or succession and less so to anthropogenic disturbances. It is possible that natural succession (transition of PSF into pole forests) may contribute to a 'higher' score on degradation scale in our protocol, however separating natural disturbances and succession from anthropogenic disturbances is quite challenging in lack of a long-term study. The degradation scores based on DWD captures impacts within a short time scale (0-5 years), after which the palm trunks gradually disintegrate and disappear from forest floor. The palm height distribution and seedling absence are typically visible for longer time periods after selective harvesting and are used to capture disturbance, but these effects could also be due to natural disturbances or vegetation succession. The only way to truly distinguish between natural and anthropogenic disturbances is by monitoring sites for long time periods and by conducting interviews with local villagers about local practices and land use history, or by monitoring origin of fruits at local markets. Other researchers have recognized this lack of understanding between *M. flexuosa* harvest and palm swamp forest dynamics (Endress et al., 2013; Virapongse et al., 2017). Evidence of natural succession is evident in Pobre Cocha and Shiringal in Samiria region where *Mauritia flexuosa* density was low and species representative of seasonally flooded forest were dominant (e.g. *Euterpe precatoria* and *Hura crepitans*) suggesting the sites corresponded to more recently developed palm swamps. Palaeo-environmental records from two peatland sites from the studied region

(San Jorge and Quistococha) showed that the vegetation changes during early phases of peat initiation were a result of autogenic succession and fluvial influence (Roucoux et al., 2013; Kelly et al., 2017). Pollen data and sedimentary evidence from these two sites confirmed the dominant role of flooding in vegetation transition and succession. Stratigraphic record also indicated multiple

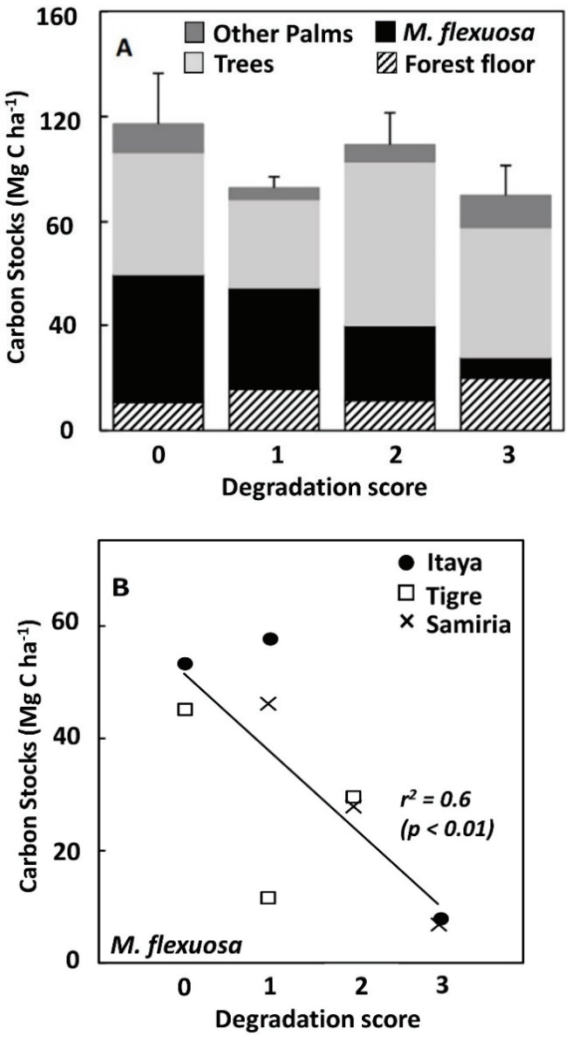

Figure 3.6 – Average carbon stocks in standing (MF: *Mauritia flexuosa*, Trees: dicot trees and Forest floor: dead vegetation) for the different degradation classes (A). Correlation between degradation classes and *M. flexuosa* C stock (B).

abrupt transitions, repetitions and existing complexity in the processes that shaped the current landscape. Existing palm swamp forests and its peat deposits are an outcome of several dynamic and unpredictable processes that has been active for past 1000s of years, and anthropogenic disturbances need to be minimized to maintain that process.

3.4.3 Conclusions

The results of this study on quantification of C stocks in PSFs in Peruvian Amazonia are meant to highlight the importance of these ecosystems as C repositories. Our investigation was an attempt to quantify existing C stocks in these areas and emphasize the potential role in C storage and global climate change that these ecosystems could play. We utilized a quantitative metric to differentiate peat swamp forests on the basis of existing disturbances and assigned different degradation scores to the studied sites. There was a large amount of variation caused by many factors in our dataset, and the degradation score was only able to explain a small portion of variation in the ecosystem C stocks. Clayey sediments embedded in the peat deposits, Ca/Mg ratios and discontinuous elevated bulk-densities in the soil profiles indicated the influence of river flooding in shaping this landscape. Forest transition and loss of *M. flexuosa* can be caused by natural succession or by anthropogenic extraction of *M. flexuosa* fruits, however the only way to truly distinguish between natural and anthropogenic disturbances is by monitoring sites for long time periods. Since our study protocol does not lend that ability, perhaps a diagnostic criterion can be added that distinguishes natural variation from degradation, and that captures characteristic of pole forests, or successional environments naturally succeeding away from palm swamps.

We found that the Tigre region has been less influenced by rivers during the formation of its peat and consist of large ombrotrophic peatlands with greater depths that have likely formed over longer time-scales. The stability and lower frequency of river avulsions in this region probably were caused due to isolation of Rio Tigre from the Rio Pastaza some 8000 years BP (Bernal et al., 2011). Northern parts of Rio Tigre basin therefore experienced build-up of peat over time and transitioned from high- to low-nutrient status (minerotrophic to ombrotrophic),

and may experience vegetation succession to pole forests (Draper et al., 2014). The area in Samiria basin is more influenced by river dynamics and likely underwent sediment deposition, erosion and burial of peat in not so distant past. Moreover, we see that largest C stocks is in the Tigre river outside of the currently protected Pacaya Samiria reserve. This might point towards a need for new conservation areas in this area highlighting the conservation of palm swamp and pole forests where the largest carbon stocks are stored (Draper et al., 2014). Long-term site-specific studies aimed towards investigating linkages of forest degradation with soil C stocks may provide useful information in this context. In the degraded palm swamps management plans or interventions to conserve fruit production and genetic resources are needed in order to have a greater potential to protect existing C stocks, while simultaneously preserving all the ecosystem services associated with it.

3.5 Acknowledgements

This study was made possible by a grant from the USDA, Forest Service, Washington Office, and USFS International Programs, implemented by Department of Environmental Sciences, Wageningen University, The Netherlands. The research was a collaborative effort with partners from Instituto de investigaciones de la Amazonía Peruana (IIAP). Authors would like to thank Prof. Martin Herold, Dennis Del Castillo, Monica Aleman and Gloria Arellano and a group of enthusiastic people who enabled data collection in the field. We acknowledge the effort of field crew members - Nicole M Riviera, Julio Irarica, Diego Martin, Jack Pacaya, Victor Ruiz, Cecilia B Falcón, Ricardo Z Young, Elvis J Paredes, Rique B Estrada, Jose Manuel R Huaymacari, Maria E R Pena, Jhon del A Pasquel, Carlos G Hidalzo Pizano and Luisa N Huaratapairo. The Analytical Lab, University of Hawaii, Honolulu, is also acknowledged for performing soil elemental analysis. We also thank the SERNANP for providing research permit (Nº 009-2015-SERNAP-RNPS-JEF) that enabled sampling in the Pacaya Samiria National Reserve. Finally, we thank two anonymous reviewers and associate editor for their insightful comments that greatly improved this manuscript.

3.6 Appendix – Supplementary tables

Table 1. Vegetation composition and variation among sampling sites. Number of vegetation families, species and individuals measured.

	Site Name	Diameter class	Individuals	Families	Species
Itaya	Quistococha	< 5 cm	N/A	N/A	N/A
		≥ 5 cm	324	21	38
	Las Brisas	< 5 cm	16	12	12
		≥ 5 cm	153	23	46
	San Julian	< 5 cm	5	5	5
		≥ 5 cm	122	23	37
Tigre	Llanque	< 5 cm	22	9	10
		≥ 5 cm	288	23	52
	Monteverde	< 5 cm	25	11	17
		≥ 5 cm	196	28	52
	Avispa Cocha	< 5 cm	31	12	17
		≥ 5 cm	255	18	30
	Chanchari	< 5 cm	17	12	12
		≥ 5 cm	221	19	34
	Nueva York	< 5 cm	18	12	13
		≥ 5 cm	135	19	33
Samiria	Pobre Cocha	< 5 cm	5	3	3
		≥ 5 cm	123	17	27
	San Martin	< 5 cm	10	7	8
		≥ 5 cm	130	16	27
	Shiringal	< 5 cm	45	2	2
		≥ 5 cm	80	20	33
	San Miguel	< 5 cm	5	2	2
		≥ 5 cm	112	19	34
TOTAL			2,338	58	214

Table 2. Variation in soil carbon storages at various depths among six sampled subplots.

	Site Name	Depth*	Soil carbon in sampled subplots (Mg ha^{-1})						Soil Carbon (Mg C ha^{-1})
		(cm)	1	2	3	4	5	6	(Mean ± SE)
Itaya	Quistococha	0-15	42.4	49.9	36.8	70.8	62.2	42.2	50.7 ± 5.4
		15-30	41.7	60.4	41.3	38.2	52.4	54.5	48.1 ± 3.6
		30-50	63.4	56.9	50.9	39.7	119.6	84.2	69.1 ± 11.8
		50-100	151.1	269.3	152.7	148.8	259.8	201.4	197.2 ± 22.8
	Las Brisas	0-15	43.9	55.7	50.9	74.2	52.2	56.8	55.6 ± 4.2
		15-30	58.5	33.4	37.9	66.6	67.9	81.7	57.7 ± 7.6
		30-50	76.8	58.5	78.5	74.6	59.8	67.3	69.3 ± 3.6
		50-100	128.8	153.8	190.5	307.3	217.7	427.4	237.6 ± 45.6
	San Julian	0-15	47.8	29.4	34.0	39.8	21.0	21.9	32.3 ± 4.3
		15-30	37.5	34.8	37.5	30.8	6.2	6.8	25.6 ± 6.1
		30-50	36.9	20.9	64.2	23.0	22.5	7.0	29.1 ± 8
		50-100	50.5	26.6	53.8	--	--	--	43.7 ± 8.6
Tigre	Llanque	0-15	55.0	63.1	56.3	50.5	75.4	21.7	53.7 ± 7.3
		15-30	81.8	95.5	96.6	81.1	101.5	75.6	88.7 ± 4.3
		30-50	80.2	106.5	96.2	118.6	111.3	95.3	101.3 ± 5.6
		50-100	210.0	239.6	257.4	251.7	246.1	226.2	238.5 ± 7.2
	Monteverde	0-30	84.8	113.4	118.4	108.6	79.9	--	101 ± 7.8
		30-50	80.6	75.4	103.1	69.4	78.4	50.4	76.2 ± 7
		50-100	188.5	149.7	152.8	175.7	237.3	252.5	192.8 ± 17.6
	Avispa	0-30	108.0	147.2	93.4	138.8	214.6	99.6	133.6 ± 18.4
		30-50	88.1	63.8	69.6	48.8	89.1	52.2	68.6 ± 7
		50-100	325.1	223.5	250.9	255.9	348.1	345.3	291.5 ± 22.2
	Chanchari	0-30	--	236.6	167.4	184.0	104.2	176.6	173.8 ± 21.1
		30-50	79.0	113.2	125.5	135.1	97.6	125.5	112.7 ± 8.6
		50-100	382.5	375.7	373.4	388.8	242.1	255.5	336.3 ± 27.8
	Nueva York	0-30	85.7	109.7	105.4	134.9	126.6	94.8	109.5 ± 7.6
		30-50	62.1	49.9	71.2	65.2	72.1	55.8	62.7 ± 3.6
		50-100	193.3	304.3	281.7	284.7	252.5	185.6	250.3 ± 20.4
Samiria	Pobre Cocha	0-30	139.7	130.9	137.3	103.2	151.7	118.1	130.2 ± 7
		30-50	57.8	83.3	72.2	34.9	58.5	69.6	62.7 ± 6.8
		50-100	96.3	134.4	217.1	34.8	173.0	160.8	136.1 ± 26.1
	San Martin	0-30	112.3	72.0	106.0	176.8	128.5	124.8	120.1 ± 14
		30-50	37.9	27.3	92.0	16.0	84.7	97.3	59.2 ± 14.7
		50-100	--	--	--	--	149.4	293.2	221.3 ± 71.9
	Shiringal	0-30	113.7	116.7	100.7	74.3	105.8	137.7	108.1 ± 8.5
		30-50	65.1	70.5	65.7	--	21.0	38.9	52.2 ± 9.6
	San Miguel	0-30	130.7	114.6	102.2	92.7	--	75.9	86 ± 18.8
		30-50	--	91.8	49.2	86.7	95.4	24.7	69.6 ± 13.9

*For easy comparison only top 1 m of soil depth reported in this table.

Table 3. Mean aboveground (AG) and belowground (BG) vegetation C stocks in dicot trees and palms (including *M. Flexuosa)*.

	Location	AG trees C	BG trees C	AG palms C	BG palms C	Total AG C	Total BG C
	Site name	(Mean ± std. error; Mg C ha^{-1})					
Itaya	**Quistococha**	54 ± 11.9	11.9 ± 3	43.6 ± 8.8	13 ± 2.3	97.7 ± 15	24.9 ± 4.1
	Las Brisas	22.6 ± 3.9	4.5 ± 0.8	45 ± 11.3	14.6 ± 4.1	67.6 ± 11.2	19 ± 4.1
	San Julian	30.6 ± 11.2	6.7 ± 2.6	12.4 ± 4.2	4.3 ± 2.1	36.8 ± 10.5	8.8 ± 2.5
	Mean	*35.7 ± 9.4*	*7.7 ± 2.2*	*37.9 ± 10.6*	*11.9 ± 3.2*	*67.3 ± 17.6*	*17.6 ± 4.7*
Tigre	**Llanque**	39 ± 10.4	7.8 ± 2.3	42.5 ± 12	8.4 ± 1.5	81.5 ± 17.9	16.2 ± 3.6
	Monteverde	22.2 ± 3.7	4.5 ± 0.8	51.4 ± 10.6	11.7 ± 2.8	73.6 ± 10.8	16.3 ± 2.9
	Avispa	62.5 ± 12	13 ± 2.7	30.8 ± 10.1	9.9 ± 3.5	93.2 ± 11.1	22.9 ± 3.3
	Chanchari	42.3 ± 9.3	9 ± 2.1	14.8 ± 4.2	4 ± 1.1	57.2 ± 10.1	13 ± 2.3
	Nueva York	32.8 ± 5.3	7 ± 1.2	13.6 ± 6.4	4.1 ± 2.2	46.4 ± 10.3	11.2 ± 3
	Mean	*39.8 ± 6.6*	*8.3 ± 1.4*	*30.6 ± 7.5*	*7.6 ± 1.5*	*70.4 ± 8.4*	*15.9 ± 2*
Samiria	**Pobre Cocha**	34.2 ± 8.5	7.6 ± 2	19.7 ± 7.6	2.5 ± 0.6	53.8 ± 13.2	10.1 ± 2.3
	San Martin	19.1 ± 7	3.9 ± 1.5	37.7 ± 6.7	12.3 ± 2.1	56.8 ± 8.9	16.2 ± 2.4
	Shiringal	56.4 ± 13	14.1± 3.2	17.2 ± 8.4	2.3 ± 0.6	73.6 ± 16.2	16.4 ± 3.4
	San Miguel	69.9 ± 23	17.1 ± 6	24.6 ± 5.2	6.2 ± 1.6	94.5 ± 22	23.3 ± 5.6
	Mean	*44.9 ± 11.3*	*10.7 ± 3*	*24.8 ± 4.6*	*5.8 ± 2.3*	*69.7 ± 9.3*	*16.5 ± 2.7*

Table 4. Range and average values of soil bulk density (g cm^{-3}), carbon concentration (%) and carbon density (g C cm^{-3}) within soil profile at sites around Itaya region.

	Itaya	Bulk density		Carbon concentration		Carbon density
	Depth range	(g cm^{-3})		(%)		(g C cm^{-3})
	(cm)	(Min – Max)	(Mean ± SE)	(Min – Max)	(Mean ± SE)	(Mean ± SE)
Quistococha	0-15	0.05 - 0.08	0.06 ± 0.01	45 - 63.8	53.2 ± 3.2	3.4 ± 0.9
	15-30	0.04 - 0.07	0.06 ± 0.01	48 - 63.6	53.7 ± 2.2	3.2 ± 0.6
	30-50	0.04 - 0.11	0.07 ± 0.01	49.4 - 55.6	52.6 ± 0.9	3.5 ± 1.4
	50-100	0.06 - 0.11	0.08 ± 0.01	47.8 - 53.9	51.3 ± 1	3.9 ± 1.1
	100-130	0.09	0.09	47.5	47.5	4.3
	100-140	0.06 - 0.1	0.09 ± 0.01	49.5 - 59	55.7 ± 3.1	4.9 ± 1.2
	100-165	0.11	0.	52.8	52.8	5.6
	100-200	0.1	0.1	41.5	41.5	4.2
	140-180	0.15	0.15	35.3	35.3	5.2
	140-185	0.86	0.86	8	8	6.9
	165-215	0.12	0.12	38.8	38.8	4.7
Las Brisas	0-15	0.05 - 0.1	0.08 ± 0.01	39.9 - 55	49.1 ± 2.8	3.7 ± 0.7
	15-30	0.04 - 0.11	0.08 ± 0.01	40.8 - 64.8	50.2 ± 3.4	3.8 ± 1.2
	30-50	0.06 - 0.09	0.08 ± 0	35.3 - 52.1	44.3 ± 2.5	3.5 ± 0.4
	50-100	0.06 - 0.19	0.11 ± 0.02	41.1 - 46	43.7 ± 0.7	4.8 ± 2.2
	100-165	0.21	0.21	28.7	28.7	6.1
	100-200	0.09 - 0.11	0.09	27.2 - 46.5	41 ± 3.6	3.9 ± 0.9
	165-200	1.16	1.16	10.7	10.7	12.5
San Julian	0-15	0.07 - 0.74	0.26 ± 0.11	1.9 - 34.6	20.4 ± 6.2	2.2 ± 0.7
	15-30	0.08 - 1.01	0.47 ± 0.18	0.4 - 32.5	16 ± 6.6	1.7 ± 1
	30-50	0.26 - 1	0.71 ± 0.13	0.4 - 12.4	3.7 ± 1.9	1.5 ± 1
	50-100	0.89 - 1.05	0.95 ± 0.05	0.5 - 1.2	0.9 ± 0.2	0.9 ± 0.3

Table 5. Range and average values of soil bulk density (g cm^{-3}), carbon concentration (%) and carbon density (g C cm^{-3}) within soil profile at sites around Tigre region.

	Tigre	Bulk density		Carbon concentration		Carbon density
	Depth range (cm)	(g cm^{-3}) (Min – Max)	(Mean ± SE)	(%) (Min – Max)	(Mean ± SE)	(g C cm^{-3}) (Mean ± SE)
Llanque	0–15	0.04 - 0.11	0.09 ± 0.01	35.4 - 46	40.6 ± 1.7	3.6 ± 1.2
	15–30	0.11 - 0.14	0.13 ± 0.01	44.3 - 50.2	47.1 ± 0.9	5.9 ± 0.7
	30–50	0.11 - 0.16	0.13 ± 0.01	34.2 - 47	40.3 ± 2	5.1 ± 0.7
	50–100	0.11 - 0.2	0.14 ± 0.01	25.5 - 43	34.3 ± 2.3	4.8 ± 0.4
	100–150	0.13 - 0.26	0.19 ± 0.02	10 - 35.2	18.1 ± 4	3.2 ± 1
	150–200	0.09 - 0.17	0.13 ± 0.01	21.3 - 56.5	41.4 ± 6.1	5.3 ± 1.6
	200–250	0.1 - 0.13	0.11 ± 0.01	40.4 - 54.8	49.1 ± 3.3	5.6 ± 1.2
Monteverde	0–15	0.03	0.03	38.1	38.1	1.2
	0–30	0.1 - 0.32	0.17 ± 0.04	11.8 - 38.4	23.6 ± 4.5	3.4 ± 0.6
	15–30	0.07	0.07	29.7	29.7	2.1
	30–50	0.15 - 0.21	0.18 ± 0.01	11.8 - 25.3	21.7 ± 2.1	3.8 ± 0.9
	50–100	0.08 - 0.17	0.11 ± 0.01	29.8 - 44.8	35.7 ± 2.5	3.9 ± 0.9
	100–150	0.07 - 0.12	0.1 ± 0.01	25.5 - 49.4	40.4 ± 3.4	3.9 ± 0.9
	150–200	0.05 - 0.55	0.26 ± 0.09	2.9 - 49.5	23.1 ± 8.2	2.9 ± 1
	200–250	0.14 - 0.24	0.19 ± 0.05	11.2 - 34.8	23 ± 11.8	3.7 ± 1.4
Avispa	0–30	0.07 - 0.14	0.09 ± 0.01	41.4 - 49.6	46.6 ± 1.2	4.5 ± 1.5
	30–50	0.06 - 0.14	0.08 ± 0.01	30.7 - 48.1	41.8 ± 2.4	3.4 ± 0.9
	50–100	0.12 - 0.22	0.16 ± 0.02	29.4 - 41.1	36.2 ± 1.7	5.8 ± 1.1
	100–150	0.09 - 0.15	0.11 ± 0.01	35.8 - 48.4	43.6 ± 1.9	4.7 ± 0.9
	150–200	0.08 - 0.58	0.18 ± 0.08	4.4 - 55.9	42.8 ± 7.8	4.9 ± 1.6
	200–250	0.33	0.33	16.6	16.6	5.5
Chanchari	0–30	0.07 - 0.16	0.11 ± 0.01	48.2 - 56	52.7 ± 1.4	5.8 ± 1.6
	30–50	0.07 - 0.12	0.1 ± 0.01	53 - 60.1	56.5 ± 1.1	5.6 ± 1
	50–100	0.09 - 0.16	0.13 ± 0.01	47.8 - 56.5	53.8 ± 1.3	6.7 ± 1.4
	100–150	0.08 - 0.16	0.11 ± 0.01	52 - 56.9	55.2 ± 0.8	5.9 ± 1.7
	150–200	0.07 - 0.13	0.1 ± 0.01	53.4 - 58.6	56.2 ± 0.7	5.7 ± 1.4
	200–250	0.11	0.11	57.9	57.9	6.5

continued

Nueva York	0-30	0.06 - 0.09	0.08 ± 0	44.3 - 52.2	48.1 ± 1.1	3.7 ± 0.6
	30-50	0.06 - 0.09	0.07 ± 0	39.3 - 50.6	43.9 ± 1.6	3.1 ± 0.4
	50-100	0.07 - 0.14	0.12 ± 0.01	39.3 - 52.1	43.7 ± 1.8	5 ± 1
	100-150	0.08 - 0.14	0.1 ± 0.01	33.7 - 48.1	42.8 ± 2.1	4.4 ± 0.8
	150-200	0.08 - 0.16	0.12 ± 0.01	21.4 - 46.8	36 ± 4.1	4 ± 0.8
	300-350	0.1 - 0.23	0.17 ± 0.02	15.2 - 31	21.8 ± 2.9	3.5 ± 0.9

Table 6. Range and average values of soil bulk density (g cm^{-3}), carbon concentration (%) and carbon density (g C cm^{-3}) within soil profile at sites in Samiria region.

	Samiria	**Bulk Density**		**Carbon concentration**		**Carbon density**
	Depth range	(g cm^{-3})		(%)		(g C cm^{-3})
	(cm)	(Min – Max)	(Mean ± SE)	(Min – Max)	(Mean ± SE)	(Mean ± SE)
Pobre Cocha	0-30	0.07 - 0.11	0.09 ± 0.01	41.2 - 50.5	47.2 ± 1.5	4.3 ± 0.6
	30-50	0.04 - 0.25	0.12 ± 0.03	11.8 - 48.9	33.8 ± 6.6	3.1 ± 0.8
	50-100	0.11 - 0.85	0.46 ± 0.1	0.8 - 38.5	10.7 ± 5.6	2.7 ± 1.3
San Martin	0-30	0.06 - 0.17	0.1 ± 0.02	31.2 - 48.8	40.6 ± 3	4 ± 1.1
	30-50	0.12 - 0.68	0.36 ± 0.09	1.2 - 42.1	16.7 ± 7.2	3 ± 1.8
	50-100	0.17 - 0.42	0.3 ± 0.12	7 - 33.5	20.3 ± 13.2	4.4 ± 2
	100-150	0.56 - 0.56	0.56 ± 0	7.4 - 7.4	7.4 ± 0	4.1 ± 0
Shiringal	0-30	0.06 - 0.12	0.1 ± 0.01	31.7 - 40.6	36.8 ± 1.6	3.6 ± 0.7
	30-50	0.22 - 0.82	0.47 ± 0.09	1.3 - 14.4	6.6 ± 2.2	2.2 ± 1.4
	50-100	0.62 - 0.62	0.62 ± 0	4.3 - 4.3	4.3 ± 0	2.7 ± 0
San Miguel	0-30	0.09 - 0.15	0.12 ± 0.01	21.1 - 37.5	30.1 ± 3.1	2.9 ± 1.5
	30-50	0.17 - 0.76	0.34 ± 0.09	1.6 - 26.6	15.1 ± 4.5	2.9 ± 2

Table 7. Carbon stocks (Mg C ha^{-1}; mean ± SE) in the measured ecosystem compartments in the palm swamp forests of Peruvian Amazon.

Location Site Name	(Mean ± SE)	Downed woody debris (Mg C Ha^{-1})	Litter	Total Vegetation	Soil (up to 1m soil depth)	Soil C (complete depth)	Total Ecosystem (including 1 m soil)	Total Ecosystem (entire soil)
Itaya	Quistococha	6.3 ± 1.7	7.8 ± 1.3	122.5 ± 19	365.1 ± 35.6	740.3 ± 99	501.7 ± 36.8	876.9 ± 108.5
	Las Brisas	8 ± 2.9	4.7 ± 0.6	86.7 ± 15.2	420.1 ± 53.9	882.3 ± 118.7	519.5 ± 56.1	981.7 ± 126.1
	San Julian	14.9 ± 12.2	2.9 ± 0.6	45.6 ± 12.9	108.9 ± 25.6	108.9 ± 25.6	172.3 ± 29.3	172.3 ± 29.3
	Mean	*9.8 ± 2.6*	*5.1 ± 1.4*	*84.9 ± 22.2*	*298 ± 95.9*	*577.1 ± 237.7*	*397.8 ± 112.9*	*677 ± 254.1*
Tigre	Llanque	3.8 ± 1.1	5.1 ± 0.2	97.8 ± 20.8	482.2 ± 19.4	1050.2 ± 72.3	588.8 ± 30.8	1156.9 ± 82.7
	Monteverde	2.1 ± 0.7	5 ± 0.9	89.9 ± 13.5	361.5 ± 8.3	762.9 ± 39.5	458.5 ± 18.9	859.9 ± 35.5
	Avispa	4.2 ± 1.2	6.7 ± 0.7	116.1 ± 14.2	493.7 ± 35.7	1018.8 ± 72.2	620.7 ± 44.2	1145.9 ± 80.9
	Chanchari	7.1 ± 4.1	7.2 ± 1.1	70.2 ± 12.4	593.8 ± 50.6	1482.6 ± 133	678.4 ± 45.6	1567.2 ± 131.9
	Nueva York	12.8 ± 3.6	3.5 ± 0.2	57.6 ± 13.3	422.6 ± 26.9	1019.8 ± 40.5	496.6 ± 21.8	1093.8 ± 32.6
	Mean	*6 ± 1.9*	*5.5 ± 0.7*	*86.3 ± 10.3*	*470.7 ± 38.8*	*1066.9 ± 116.2*	*568.6 ± 40.3*	*1164.7 ± 114.1*
Samiria	Pobre Cocha	23.1 ± 14.9	7.8 ± 0.6	63.9 ± 15.2	329 ± 36	329 ± 36	423.8 ± 47.9	423.8 ± 47.9
	San Martin	12.4 ± 5.1	7.7 ± 0.8	73 ± 11.2	253 ± 63.7	287.3 ± 94	346.2 ± 67	380.5 ± 97.4
	Shiringal	4.9 ± 2.1	7.2 ± 0.8	90 ± 19.3	173.9 ± 33.6	173.9 ± 33.6	276 ± 30.1	276 ± 30.1
	San Miguel	7.4 ± 2.4	2.3 ± 0.2	117.8 ± 27.6	144 ± 17.9	144 ± 17.9	271.5 ± 28.7	271.5 ± 28.7
	Mean	*12 ± 4*	*6.2 ± 1.3*	*86.2 ± 11.9*	*225 ± 41.6*	*233.6 ± 44.3*	*329.4 ± 35.8*	*337.9 ± 38.1*


4

4

Greenhouse gas emissions along a peat swamp forest degradation gradient in the Peruvian Amazon: soil moisture and palm roots effects

This Chapter is published as:
van Lent, J.[1,2], Hergoualc'h, K.[1], Verchot, L.[3], Oenema, O.[2], & van Groenigen, J. W.[2] (2019). Greenhouse gas emissions along a peat swamp forest degradation gradient in the Peruvian Amazon: soil moisture and palm roots effects. Mitigation and Adaptation Strategies for Global Change, 24(4), 625-643.

[1] Center for International Forestry Research (CIFOR), Jl. CIFOR, Situ Gede, Bogor 16115, Indonesia
[2] Department of Soil Quality, Wageningen University, Wageningen, The Netherlands
[3] International Center for Tropical Agriculture (CIAT), Cali, Colombia

4 Greenhouse gas emissions along a peat swamp forest degradation gradient in the peruvian amazon: soil moisture and palm roots effects

Abstract

Tropical peatlands in the Peruvian Amazon exhibit high densities of *Mauritia flexuosa* palms, which are often cut instead of being climbed for collecting their fruits. This is an important type of forest degradation in the region that could lead to changes in the structure and composition of the forest, quality and quantity of inputs to the peat, soil properties and greenhouse gas (GHG) fluxes. We studied peat and litterfall characteristics along a forest degradation gradient that included an intact site, a moderately degraded site and a heavily degraded site. To understand underlying factors driving GHG emissions we examined the response of *in vitro* soil microbial GHG emissions to soil moisture variation, and we tested the potential of pneumatophores to conduct GHGs *in situ*. The soil phosphorus and carbon content and carbon-to-nitrogen ratio as well as the litterfall nitrogen content and carbon-to-nitrogen ratio were significantly affected by forest degradation. Soils from the degraded sites consistently produced more carbon dioxide (CO_2) than soils from the intact site during *in vitro* incubations. The response of CO_2 production to changes in water-filled pore space (WFPS) followed a cubic polynomial relationship with maxima at 60-70% at the three sites. Methane (CH_4) was produced in limited amounts and exclusively under water-saturated conditions. There was no significant response of nitrous oxide (N_2O) emissions to WFPS variation. Lastly, the density of pneumatophore decreased drastically as the result of forest degradation and was positively correlated to *in situ* CH_4 emissions. We conclude that recurrent *M. flexuosa* harvesting could result in a significant increase of *in situ* CO_2 fluxes and a simultaneous decrease in CH_4 emissions via pneumatophores. These changes might alter long-term carbon and GHG balances of the peat, and the role of these ecosystems for climate change mitigation, which stresses the need for their protection.

4.1 Introduction

Tropical peatlands are a globally important carbon stock of 87 – 350 GtC (Gumbricht et al. 2017; Page et al. 2011) and are crucial for mitigating climate change (Murdiyarso et al. 2013). In addition, tropical peatlands are among the most efficient terrestrial ecosystems for carbon sequestration (Dommain et al. 2011; Page et al. 2004), as continuous input of organic material from lowland tropical evergreen vegetation combined with anaerobic soil conditions lead to a build-up of soil organic matter (SOM) over time (Jauhiainen et al. 2012). In natural conditions, the portion of SOM that is decomposed and emitted as carbon dioxide (CO_2) or methane (CH_4) is usually outweighed by the continuous input of fresh litter and roots (Jauhiainen et al. 2005; Hergoualc'h and Verchot, 2011; Hoyos-Santillan et al. 2015). Models such as the Holocene Peat Model – HPM (Frolking et al., 2010; Kurnianto et al., 2015) use this balance to predict long-term peat accumulation via vegetation-specific characteristics such as decomposition speed and primary production.

Peru is estimated to harbor one of the largest extents of tropical peatlands in the world (Gumbricht et al. 2017; Draper et al., 2014; Page et al., 2011). *Mauritia flexuosa*-dominated palm swamp forests are the dominant peatland ecosystem type in the Peruvian Amazon (Draper et al., 2014). Interest in the carbon pools of the Peruvian Amazon peatlands has increased in recent years. Since Lahteenoja et al. (2009b) explored their extent, research further expanded into other fields such as palaeoecology (Roucoux et al. 2013), C stocks estimates (Draper et al. 2014), *M. flexuosa* management (Virapongse et al. 2017), the characterization of degradation (Hergoualc'h, Gutiérrez-Vélez, et al., 2017) and greenhouse gas (GHG) fluxes (Teh et al., 2017). The challenges that Peruvian peatlands face are substantially different from those in Southeast Asia. Therein Southeast Asia, peatlands are under great pressure from agricultural expansion, artificial drainage and fires, which result in considerable GHG emissions (Gaveau et al. 2014; Hergoualc'h and Verchot, 2014). In contrast, anthropogenic degradation of peatland in the Peruvian Amazon is mostly related to recurrent harvesting of *M. flexuosa* palms from natural stands without drainage or fire. The fruits from *M. flexuosa* palms (locally referred to as "*Aguaje*") and palm weevils (*Rhynchophorus palmarum*) that grow inside dead palms are highly demanded products in the

regional market and are important sources of vitamins and proteins for rural communities (Pacheco Santos, 2005). Even though more sustainable (climbing) techniques exist (Horn et al. 2012), fruit harvesting continues to involve cutting down entire palms. The effect of this practice substantially alters the composition and structure of the forest (Hergoualc'h, Gutiérrez-Vélez, et al., 2017); however, its impact on long-term peat accumulation remains unstudied.

Information about driving factors of GHG fluxes is crucial to accurately model and predict long-term changes in the soil carbon pool and exchanges of GHG with the atmosphere (Ryan and Law, 2005). Hereafter and throughout the text soil CO_2, CH_4 and nitrous oxide (N_2O) fluxes are collectively referred to as GHG fluxes. Factors that drive GHG flux dynamics include, among others, soil substrate quality, nutrient availability, and aeration. Soil water-filled pore space (WFPS) is commonly used as an indicator for soil aeration. For a wide range of soils, the WFPS has been reported to affect the emissions of CO_2 (e.g. Husen et al. 2014; Howard and Howard, 1993), CH_4 (e.g. Verchot et al. 2000; Del Grosso et al. 2000), and N_2O (e.g. van Lent et al, 2015; Davidson et al. 2000). Maximum respiration rates typically occur around 60% WFPS (Linn and Doran, 1984); below this level the microbial activity is limited by water, and above it, oxygen deficiency hampers microbial respiration (Moyano et al., 2013). N_2O emissions predominantly arise from nitrification and denitrification (Davidson et al., 2000), and maximum N_2O emission reported by Van Lent et al. (2015) was around 60% WFPS for a wide range of tropical mineral soils. Methanogenesis is the anaerobic microbial decomposition of organic material, which occurs in waterlogged soils or in anaerobic microaggregates, whereas methanotrophy takes place in parts of the soil where oxygen is available. Both processes concur in soils, and – among other factors – are modulated by soil structure and WFPS% (Smith et al., 2003; Teh et al., 2005). In waterlogged soils at 100% WFPS methanogenesis is likely the dominant process, whereas at WFPS <100% CH_4 is solely produced in anoxic microsites and part of the CH_4 is oxidized.

GHG production is also influenced by the quality and quantity of fresh roots and litter that enter the soil (Updegraff et al. 1995). For instance, in the DAYCENT model the carbon-to nitrogen-ratio (C/N ratio) of different plant parts is an input for SOM turnover rates, and consecutively influences C mineralization, which are

in turn controlled by factors such as soil moisture, temperature and texture (Parton et al., 1993, Del Grosso et al., 2001). In addition, Oktarita et al. (2017) found increased soil N_2O when soil C/N ratios decreased. We hypothesize that palm harvesting leads to changes in vegetation composition, and in turn to alteration of litter inputs by secondary regrowth and the C/N ratio of the soil substrate. We expect this change in substrate to result in increased decomposition in areas where palms are harvested as compared to undisturbed conditions; which would be reflected in higher GHG emissions in those disturbed sites.

In saturated conditions aerating roots potentially play an important role for soil GHG fluxes. Plants need to adapt themselves to cope with anoxic conditions (Bruhn et al. 2012). Such adaptations are generally aimed at increasing the influx of oxygen to the root zone through adventitious roots, lenticels and enlarged aerenchymous tissues (Haase and Rätsch 2010). This acquired oxygen is used for a variety of essential plant functions, such as root respiration (Colmer and Voesenek, 2009). A thickened exodermis around the aerenchyma acts like a barrier and only allows for oxygen to leak near and around the root tip (van Noordwijk et al., 1998). Granville (1969) described the presence of such tissues in the aerating pneumatophores of *M. flexuosa* palms. These pneumatophores may also conduct N_2O or CH_4 produced in the anoxic soil layers to the atmosphere, as has been shown for aerenchymous tissues in the stalks of rice (see e.g. Minoda & Kimura, 1994) as well as for tree stem lenticels in temperate and tropical forested wetlands (Gauci et al., 2010; Pangala et al. 2013). In this way, CH_4 is directly emitted from the soil, and avoids potential oxidation in upper aerobic soil layers. Similarly, dissolved N_2O and CH_4 can be taken up by roots and subsequently emitted during root or leaf respiration (Pihlatie et al, 2005; Gauci et al., 2010). The existence and the contribution of pneumatophores to total soil GHG emissions has not been reported for palm swamp forests in the Amazon.

Current practices of palm harvesting in the Peruvian Amazon may lead to changes in soil moisture, alteration of the quality of substrate inputs, and decreases in aerating pneumatophores. However, to date, there is no assessment on how these changes could affect GHG emissions. In this context, we set as a first objective for this study to test the response of GHG production to varying levels of WFPS, across a gradient of forest degradation involving substrate

alteration. Secondly, we aimed to evaluate the contribution of aerating pneumatophores to surface GHG fluxes in undisturbed and degraded palm swamp sites.

4.2 Method

We conducted two experiments. The first one was to determine the response of soil microbial GHG emissions to variations in soil moisture and was performed *in vitro* with samples without live roots. In the second experiment, we estimated the potential of root pneumatophores to conduct GHGs by relating pneumatophore densities to corresponding *in situ* soil GHG fluxes. The effect of degradation was assessed by including three sites differing in level of degradation. We acknowledge (and further discuss) the limits of our experimental design, which include no field-level replication for each degradation level.

4.2.1 Study site

The study was conducted southwest of the city of Iquitos, in the province of Loreto in the Peruvian Amazon. The area exhibits a tropical humid climate with an average annual precipitation of 3,087 mm and a weak dry season between June and September (Marengo, 1998). Mean annual temperature is 27°C, with average daily minima around 20-22°C and maxima around 29-31°C (Marengo, 1998). Humidity is at 80-90% year-round.

The palm swamp peatlands were located near Lake Quistococha (S 3°49.75000' W 73°19.11333'). Peat deposits up to a 5 m thick have been reported, with the 390-400 cm layer radiocarbon dated at 2335 ±15 cal. BP (Lahteenoja et al. 2009b). Permanently waterlogged palm swamp originated around 1000 years ago, while the *M. flexuosa*-dominated vegetation cover observed today was established around 600 years ago (Roucoux et al., 2013). The flooding regime plays an important role for the vegetation development during these time scales. There is currently no man-made drainage in the area and the water table rarely goes deeper than 20 cm below soil surface level (Kelly et al., 2014). The peatlands occasionally flood; Roucoux *et al.* (2013) mention flooding events in 1998 (30 cm)

and 2012 (100 cm). We observed another 100-cm flooding during the 2015 El Niño (van Lent, *unpublished data*). The area likely receives nutrients during these flooding events, as well as during the annual Amazon River flood pulses. In the region both minerotrophic (nutrient rich) and ombrotrophic (nutrient poor) peatlands have been reported (Lahteenoja and Page, 2011). Teh et al. (2017) characterized the *Quistococha* peatland in transition between minerotrophic and ombrotrophic conditions, while and Lahteenoja (2011) characterized it as minerotrophic.

The present study is part of a long-term experiment monitoring soil GHG fluxes along the previously mentioned gradient of forest degradation. The experimental design comprised an intact site ("I", S 03°49.949' W 073°18.851'), a moderately degraded site ("mD", S 03°50.364' W 073°19.501') and a heavily degraded site ("hD", S 03°48.539' W 073°18.428'). The sites are part of the same peatland complex and are 1.3-1.7 km distant to the Itaya River, one of the anastomosing channels of the Amazon river (Figure 4.1).

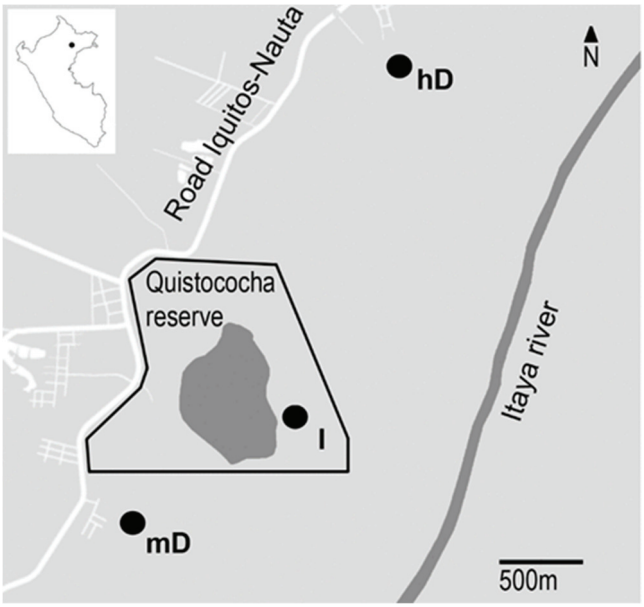

Figure 4.1 – Map of the study location near Iquitos, Peru. The locations along the Itaya River of the intact (I), moderately (mD) and highly (hd) degraded sites are indicated with black dots. Both degraded sites are close to settlements (white lines represent streets). The black line around the Quistococha lake (dark grey) delimits the border of the reserve.

The I site was located within the Quistococha regional reserve (369 ha.), an officially protected area since it was registered as a national touristic park in 1984 (Resolución Suprema No 223-84 ITI/tur). The other two sites were adjacent to the reserve and are utilized by local villagers for extraction of *M. flexuosa* fruits, collection of palm weevils (*R. palmarum*), and timber harvesting. The common, unsustainable practice is to cut down entire palms for fruit and weevil collection (Horn et al, 2012). Recurrent harvesting has resulted in a reduced canopy closure at the mD site, which is close to a village founded in 2010. The hD site is close to a village that expanded in 2014, according to satellite images, and has few standing palm trees left.

4.2.2 Soil and litterfall properties

Peat depth was measured with a soil probe at six locations per site (Bhomia et al., *unpublished*). Eighteen samples per site were collected from the top 5 cm using a metal ring (radius = 4.5 cm). Samples were dried until constant weight at 60°C and bulk density was determined from the dry mass per volume of the ring. Six samples per site (three from hollows and three from hummocks) were ground, homogenized, and sent for determination of total carbon (C) and nitrogen (N) by the induction furnace method (Costech EA C-N Analyzer); Calcium (Ca), Potassium (K), Magnesium (Mg), Sodium (Na) by the ammonium acetate method (Ross & Ketterings, 2011); and Copper (Cu), Manganese (Mn), Zinc (Zn) and Phosphorus (P) by the Mehlich 3 method (Ziadi & Tran, 2007). All analyses were conducted by the University of Hawaii-Hilo. The Ca and Mg content is useful for determining the nutrient status of the sites. A Ca/Mg ratio <6 classifies as a nutrient poor, rain-fed ombrotrophic peatland; while a ratio >6 is indicative of inputs from river water and classifies as a minerotrophic peatland (Lahteenoja et al., 2009b).

Vegetation litter was collected from 27 litter traps (total surface = 4.32 m^2) per site in September 2016. Although flowering and fruiting can be seasonal, litterfall rates are dominated by leaf litter and samples were representative for our sites. Aguila-Pasquel et al. (2014) reports litterfall rates near our study location and showed that leaf litter C represents ~70% ± 2% throughout the year, and 77% in September alone. The litter was weighed and a ~100 gram subsample was dried in

an oven at 40°C until constant weight. Litterfall C and N concentration was analyzed as described above.

4.2.3 *In vitro* incubation

The objective of this experiment was to evaluate the effect of WFPS on GHG flux rates along the gradient of forest degradation. For this purpose, two 500 g soil samples were excavated from the top 30 cm in three plots at ~150 m distance from each other within each site. Large roots were manually removed on-site and the remaining soil was air-dried at approximately 25-30°C for three to five days. Next, smaller roots and aggregates were removed by gently crushing and sieving the soil (mesh size 2 mm). Then the six samples were mixed to obtain one homogenous sample per site and stored at 7°C for a week until the start of the incubation.

A pilot incubation experiment was carried out to determine the appropriate incubation time and quantity of air-dried soil needed. The first objective of the pilot was to obtain a linear increase in CO_2 concentrations over time, while not exceeding the maximum CO_2 standard gas concentration used to calibrate the gas chromatograph (4990 ppm CO_2). The second objective was to evaluate the amount of water needed to bring the samples to WFPS values ranging from 20% to 100%.

In the final incubation experiment, triplicates of 15 g air-dried soil were placed in an Erlenmeyer flask (600 ml) and treated with 0, 10, 20, 30, 40, 50 and 70 ml of DI water. The 70-ml treatment intentionally surpassed the water holding capacity to mimic flooded field conditions. Soil and water were mixed with a mechanical shaker and left uncapped to settle for 48 hours, to allow the microbial community to stabilize following the drying and rewetting process. Afterwards, GHG flux measurements were performed on four consecutive days. At each day the flasks were closed and four air samples were taken from the headspace at 1-hour intervals. At the onset flasks were vented with ambient air for 10 seconds using a vacuum pump and then closed with a rubber stopper equipped with a sampling port. After closure, air samples (10 ml) were taken with a disposable syringe and stored in 10 ml evacuated glass vials with septa caps until further analysis by gas chromatography. Laboratory air temperature and pressure were recorded after the first headspace sample was taken.

Between sampling dates the flasks were left uncapped at room temperature (~21°C) and the wet soil slurry weight was kept constant through addition D.I. water. At the end of the experiment samples were oven-dried at 60°C until constant weight, followed by sample-specific bulk density determination. The WFPS was calculated following the formula by Linn and Doran et al. (1984), assuming a particle density of 1.4 g cm^{-3} (Driessen and Rochimah, 1976).

GHG fluxes from individual flasks at each sampling day were calculated by linear regression of GHG concentration against time, expressed per mass of oven-dried soil. C mineralization was calculated as the site-averaged CO_2 production rate per unit C in the soil. WFPS values were calculated for each water addition treatment (n=12) to test the response of GHG fluxes to WFPS per site.

4.2.4 Pneumatophore gaseous exchanges experiment

The objective of this experiment was to determine the potential of root pneumatophores to conduct CO_2, CH_4 or N_2O from the soil to the atmosphere. As part of a long-term GHG monitoring study, nine chambers per site were installed in July 2014 (I), September 2014 (hD) and April 2015 (hD) at > 1.5 m distance from a tree or a palm in order to avoid the elevated areas surrounding trunks (hummocks). The lower parts (hollows) are more often flooded, and highest density of pneumatophores are observed in hollows (Granville, 1969). These areas represent >80% of the total surface area in all three sites (*data not shown*). CO_2, CH_4 and N_2O fluxes were measured using the static closed chamber method, and measured monthly between August and October 2015. The chambers (25 cm height and 30 cm diameter) were pushed 3-5 cm in the soil. Their lids were equipped with a centre port for gas sampling and a vent to equalize pressure inside the chamber with that outside. At the start of each measurement, chambers were vented, closed and gas samples (30 ml) were taken from the enclosed headspace at t=0, 10, 20 and 30 minutes using a 50-ml disposable syringe. Twenty ml of this sample were injected in pre-evacuated glass vials (10 ml) to store the samples under over-pressurized conditions. The vials were sealed with silicon to prevent leakage during transportation by air from Iquitos to Lima. Air pressure, air and soil temperatures were monitored concomitantly with gas

flux measurements. Soil temperature was measured with a probe outside, but within 20 cm of the chamber to prevent soil disturbance.

The number of pneumatophores within each permanent chamber was counted in September 2015. The water table depth (WTD) and WFPS were measured simultaneously with GHG sampling. The WTD was obtained from PVC wells (10 cm diameter, 1.5 m height) installed within 50 cm of each GHG flux chamber. The WFPS was calculated from soil samples collected from the top 10 cm soil layer at each GHG flux chamber, using the same method as described for the *in vitro* incubation.

4.2.5 Gas analysis and flux calculation

Gas samples were analyzed at the CIFOR laboratory in Lima, Peru using a gas chromatograph (GC, Perkin Elmer, USA) within 1 week of sample collection on average. The GC was equipped with a ^{63}Ni electronic capture detector (ECD) for N_2O analysis and with a flame ionization detector (FID) with a methanizer for analysis of CH_4 and CO_2. The flux was computed by linear regression against time using the four sampling points. Samples were discarded following a visual quality check for leakage or departure from linearity. Leakage corresponded to a sample for which the concentration of the three GHGs was similar to atmospheric concentrations (except for the sample taken immediately after closure). Departure from linearity of the regression happens because the chamber creates an artefact by reducing the concentration gradient between the soil and the atmosphere (Collier et al., 2014). This usually happens for the last sample time-point.

4.2.6 Statistical analysis

Statistical analysis was performed using the software IBM SPSS Statistics for Windows 21.0 (IBM Corp. 2012) and statistical significance was set at an alpha level of 5%. Normality was tested using the Shapiro Wilk test, and visual interpretation of Q-Q plots. Comparisons between sampling dates and replicates was done with ANOVA's and post hoc Bonferroni tests for CO_2 in case of significant differences between groups. The *in vitro* CH_4, N_2O and the soil nutrients were compared with the Kruskal-Wallis test and pairwise comparisons. The

comparisons between sites should be used with care due to the low sample size. Regression models were constructed with the average WFPS and GHG flux per water addition treatment. The response of the fluxes to WFPS were modelled using cubic and quadratic polynomial functions that allow for a decrease in fluxes at high WFPS%. The r^2 values were used to estimate which model fit best the observations. The cumulative *in situ* CH_4 fluxes and pneumatophore densities were positively skewed and therefore log-transformed to improve normality. Pneumatophore density were correlated with cumulative CH_4 fluxes.

4.3 Results

4.3.1 Soil and litterfall properties

Soil and litterfall properties are presented in Table 4.1. The peat at the hD site was shallower than at the other sites. Bulk densities overall were low which is typical of peat soils. The Ca/Mg ratios were similar among sites and were >6, indicating minerotrophic conditions. Soil P, C and C/N ratio at the hD site exhibited lower values than the values at the other sites. Litterfall N and C/N, respectively, increased and decreased with increasing level of degradation. Differences between hummocks and hollows were non-significant, except for Mn, which showed higher concentrations in hummocks.

Table 4.1 – Soil (0-5 cm) and litterfall properties at the intact (I), moderately (mD) and heavily (hD) degraded sites. Averages are given with standard errors (n=6, bulk density n=18) and letters indicate significant differences between sites (n=1). Nutrients considered are: Carbon (C), Nitrogen (N), Calcium (Ca), Potassium (K), Magnesium (Mg), Sodium (Na), Copper (Cu), Manganese (Mn), Zinc (Zn) and Phosphorus (P). Bulk density is in g d.w. cm^{-3}.

Site	Peat depth (m)	Bulk density	Soil (mg/kg)					Soil (mg/kg)			
			Ca	K	Mg	Na	Ca/Mg	Cu	Mn	Zn	P
I	2.2[a]	0.09	4732.5	398.3	487.6	70.29	11.8	0.20	80.2	10.6	224.7[a]
	±0.1	±0.01	±761.3	±87.6	±74.8	±8.66	±3.0	±0.02	±27.2	±1.3	±33.3
mD	>2.65[#]	0.10	4557.7	475.5	375.6	85.12	12.5	0.16	145.3	13.3	247.3[a]
		±0.01	±681.3	±54.1	±44.4	±10.80	±1.5	±0.02	±53.4	±1.9	±38.8
hD	1.0[b]	0.11	7082.8	660.2	496.6	89.85	15.2	0.19	90.2	9.8	71.7[b]
	±0.2	±0.01	±280.8	±115.9	±50.6	±27.53	±2.0	±0.01	±4.3	±1.1	±14.6

4.3.2 Response of *in vitro* GHG fluxes from root-free soils to WFPS variation

Average CO_2 production across WFPS treatments was consistently lower (p = 0.01) in soils from the I site (1.67 ±0.18 µg C-CO_2 g^{-1} d.w. h^{-1}), compared to production in soils from the mD (2.34 ±0.16) and hD sites (2.45 ±0.16) (Table 4.2). The difference between sites was more pronounced when expressed as C mineralization: 3.9 ±0.4, 5.1 ±0.4 and 7.0 ±0.5 µg C g^{-1} C h^{-1} for the I, mD and hD sites, respectively. At all sites, the best model fitting the response of CO_2 to WFPS was cubic polynomial with maxima between 60 and 70% WFPS (Figure 4.2). The difference in CO_2 production between sites was largest at the maximum flux, where soils from the mD and hD site produced 134% and 139% of that produced by soils from the I site, respectively. Soil CO_2 production remained relatively stable during the incubation period. There were only a few cases where fluxes varied between sampling dates (Annex 1).

Fluxes of CH_4 from the hD site were significantly higher compared to fluxes from the I and mD sites, at all WFPS levels (p<0.01; Table 4.2). Soils from the I and mD sites were CH_4 sinks for all water addition treatments. The soil from the hD site was a net CH_4 sink below 70% WFPS (-0.15 ± 0.09 ng C-CH_4 g^{-1} d.w. h^{-1}), thereafter switching to a net source (6.5 ± 0.6 ng C-CH_4 g^{-1} d.w. h^{-1}). The response of CH_4 fluxes to varying WFPS was best described by a quadratic function. For the I and mD site the response was very weak, whereas for the hD site CH_4 fluxes showed a strong increase above 54% WFPS. Soils from the I and mD sites did not display significant differences in flux rate over time, whereas soil CH_4 production from the hD site increased over time (r^2 = 0.14, p < 0.01) (Annex 1).

continued

Soil (%)			Litterfall (%)		
N	C	C/N	N	C	C/N
2.6 ±0.1	44.1[a] ±1.5	17.1[a] ±0.5	1.4[a] ±0.0	46.4 ±0.0	33.9[a] ±0.2
2.6 ±0.1	44.4[a] ±0.8	16.9[a] ±0.6	1.5[ab] ±0.0	46.7 ±0.1	32.1[ab] ±0.1
2.5 ±0.1	35.3[b] ±1.4	14.2[b] ±0.3	1.8[b] ±0.2	45.0 ±0.9	25.6[b] ±3.3

[#]peat depth surpassed the length of the soil probe.
No letters are displayed in the absence of a significant difference

Averaged N_2O fluxes from the I site (36.68 ± 7.86 ng $N\text{-}N_2O$ g^{-1} d.w. h^{-1}) were significantly higher than fluxes from the mD (2.80 ± 0.65) and hD sites (0.08 ± 0.06) for WFPS >70% ($p < 0.01$), but not for WFPS <70% ($p = 0.6$). N_2O production in soils from the I site steeply increased above 70% WFPS and decreased in the flooded treatment. N_2O production in soils from the mD and hD site did not respond significantly to variation in WFPS. Production rates reduced over time for the >67% WFPS treatments of the I ($p < 0.01$) and mD sites ($p < 0.01$); soils displayed overall larger fluxes on the first day of incubation compared to other days.

Table 4.2 – Relationships between water-filled pore space (WFPS) and carbon dioxide (CO_2), methane (CH_4) and nitrous oxide (N_2O) production from *in vitro* incubations of soils from the intact (I), moderately (mD) and heavily (hD) degraded sites. Units are: µg $C\text{-}CO_2$, ng $C\text{-}CH_4$, and ng $N\text{-}N_2O$ g^{-1} d.w. h^{-1}. Letters indicate significant differences between sites.

Site	Equation	r^2	Average flux (min – max)
I	$CO_2 = 0.0420^{**} \times WFPS - 0.0002^{**} \times WFPS^2 - 8.24x10^{-7**} \times WFPS^3 + 0.4466^{**}$	0.31	1.67^a (0.31 – 3.36)
	$CH_4 = -0.03283^{*} \times WFPS + 0.0002558^{*} \times WFPS^2$	0.18	-0.64 (-3.51 – 1.87)
	$N_2O = -0.953^{*} \times WFPS + 0.0158^{*} \times WFPS^2$	0.78	36.68 (-1.4 – 290.42)
mD	$CO_2 = 0.1101^{**} \times WFPS - 0.0014^{**} \times WFPS^2 + 5.48x10^{-6**} \times WFPS^3 - 0.0179^{**}$	0.27	2.34^b (0.86 – 3.42)
	$CH_4 = -0.03879^{**} \times WFPS + 0.0003547^{*} \times WFPS^2$	0.12	-0.71 (-3.06 – 1.00)
	$N_2O = ^{NS}$		0.28 (-1.56 – 21.49)
hD	$CO_2 = 0.0770^{**} \times WFPS - 0.0008^{**} \times WFPS^2 + 2.41x10^{-6**} \times WFPS^3 + 0.6126^{**}$	0.27	2.45^b (0.72 – 3.69)
	$CH_4 = -0.1087^{ns} \times WFPS + 0.001798^{*} \times WFPS^2$	0.58	3.65 (-1.46 – 17.33)
	$N_2O = ^{NS}$		0.08 (-0.89 – 2.15)

* $p < 0.05$, ** $p < 0.01$, *** $p < 0.001$, ns = not significant
No letters are displayed in the absence of a significant difference

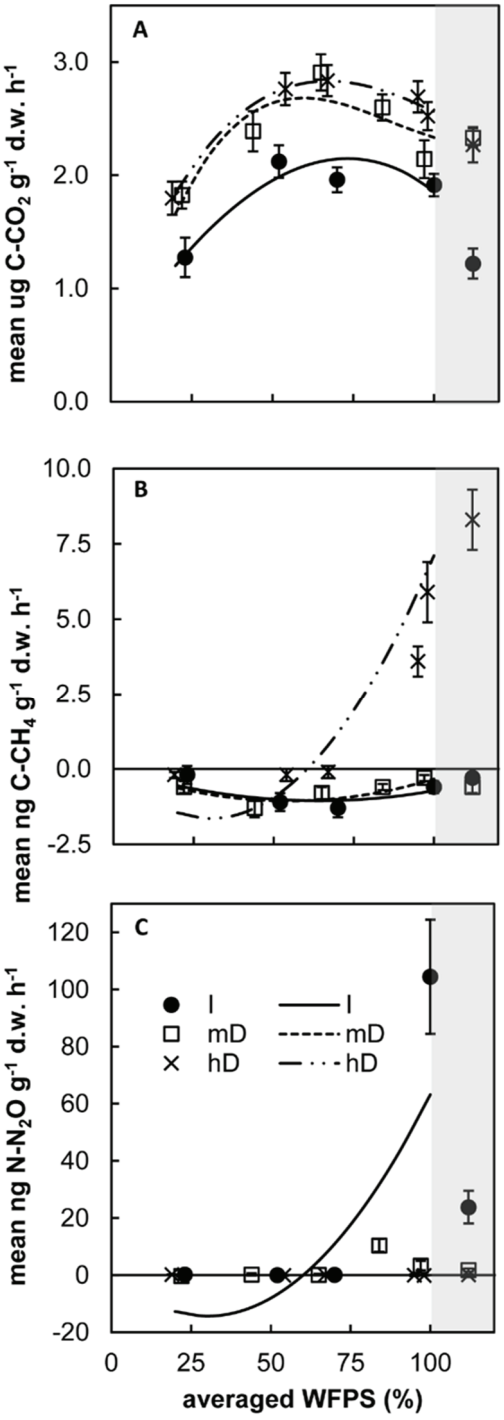

Figure 4.2 – In vitro response of soil carbon dioxide (CO_2) (A), methane (CH_4) (B) and nitrous oxide (N_2O) (C) fluxes to varying water-filled pore space (WFPS). Curves indicate statistical models for the intact (I), moderately (mD) and heavily (hD) degraded sites. Soils incubated under flooded conditions are indicated by shaded areas. Error bars present the standard error (n=12).

4.3.3 Contribution of aerating roots to *in situ* GHG fluxes

Pneumatophore density was higher at the I site (5.6 ± 1.2 pneumatophores dm^{-2}) compared to density at the mD (1.9 ± 0.6) and hD (0.3 ± 0.2) sites ($p<0.01$). At the I site, all chambers had at least 0.7 pneumatophore dm^{-2}, whereas at the mD and hD sites 22% and 67% of the chambers, respectively, did not have pneumatophores at all. CH_4 fluxes varied strongly within sites, and cumulative CH_4 fluxes were not significantly different between sites ($p = 0.45$). Among all GHG, only CH_4 fluxes were significantly correlated to pneumatophore density (Figure 4.3). The relationship was most robust for the I site ($r^2 = 0.5$, $p = 0.03$). Regression lines for pneumatophore densities and CO_2 or N_2O were insignificant and had nearly horizontal slopes. Water table depth (WTD) varied significantly between sites, in the order I < hD < mD with respective averages of -21.9 ±1.6, -6.5 ±1.4 and -2.0 ±1.2 cm below the soil surface, respectively. Average WFPS followed the same trend as the WTD, with I = hD < mD, and averages of 60 ±2, 69 ±4 and 94 ±2 %, respectively.

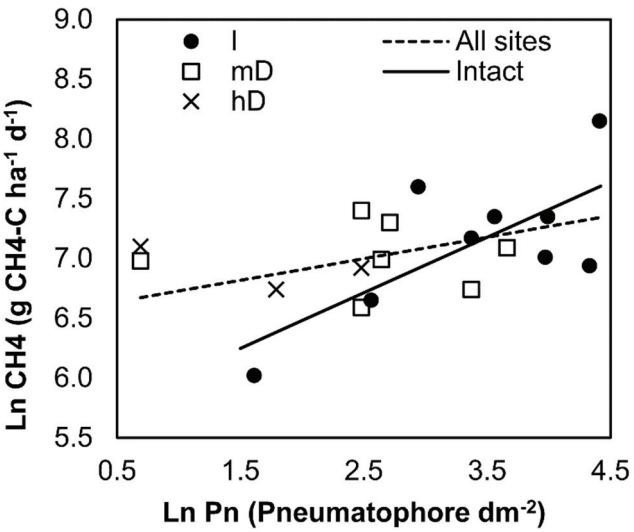

Figure 4.3 - Relationship between pneumatophore density (Pn) and methane (CH_4) fluxes in the intact (I), moderately degraded (mD) and heavily degraded (hD) sites. Greenhouse gas chambers with no pneumatophores were excluded (n = 9, 7 and 3, respectively). Equations for the regression lines are: $\ln(CH_4)_{all\ sites} = 0.2^{*} \pm 0.1 \times \ln(Pn) + 6.5^{**} \pm 0.3$ ($r^2 = 0.2$) and $\ln(CH_4)_{intact} = 0.5^{*} \pm 0.2 \times \ln(Pn) + 5.5^{**} \pm 0.6$ ($r^2 = 0.5$), * = $p < 0.05$, ** $p < 0.01$.

4.4 Discussion

The topsoil at all three sites displayed minerotrophic properties, in agreement with findings by Lahteenoja et al. (2009) at the Quistococha reserve. The sites exhibited similar levels of cations and a similar minerotrophic state. Accordingly, the lower soil C content and C/N ratio at the hD site compared to those at the other sites may indicate a higher degree of humification (Tfaily et al., 2014). The lower P content at the hD site than at the other sites may also suggest a more advanced decomposition status of the peat (Jordan et al., 2007; Könönen et al., 2015). Recurrent harvesting of *M. flexuosa* palms leads to shifts in forest structure and composition (Hergoualc'h, Gutiérrez-Vélez, et al., 2017). Bhomia et al. (*unpublished*) found that the I site harboured a higher density of dicot trees (~1500 ha^{-1}) than the degraded sites (~ 700 ha^{-1}). Furthermore, the density of palms overall and of *M. flexuosa* palms in particular, was much lower at the hD site (53 and 16 ha^{-1}, respectively) than at the I and mD sites (~ 300 and 170 ha^{-1}, respectively). The presence of a high number of individuals of *Cecropia spp.* – a pioneer species observed at the hD site is indicative of its degraded status. In addition, the gaps formed upon harvesting are colonized by small (<2 m) fast-growing herbaceous vegetation (*personal observation*). Such drastic differences in forest structure can be expected to lead to lower above and belowground litter inputs at the degraded sites as compared to inputs at the I site. Differences in forest composition may also induce significant changes in litter quality, as indicated by the difference in litterfall C/N ratio between sites (Table 4.1). Decreased C/N ratio of litterfall with increased degradation is in agreement with observations by Feldpausch et al. (2004) along a sequence of secondary forest regeneration in Central Amazonia. During early forest succession the biomass accumulates rapidly and consists mainly of easily-decomposable litter and less of wood (Gehring et al. 2005; Guariguata and Ostertag, 2001). More readily decomposable litter may on the long-term lead to reduced peat accumulation at the degraded sites (Frolking et al., 2001).

The changes in litter quality and the less-decomposed SOM pool as outlined above could explain the differences in C mineralization we found between sites. This is in line with Nilsson and Bohlin (1993), who found that more decomposed

peat soils produced more CO_2 than less decomposed, more fibrous peat soils in temperate climate. In contrast, incubation studies by Jauhiainen et al. (2016) and Swails et al. (2017) showed that soils from degraded peatlands with secondary regrowth or cultivated with oil palm produced less CO_2 than soils from intact peat swamp forests. However, the degraded peatlands of Indonesia were drained and burnt, while sites in our study were not. The effect of such drainage and fire practices generally accelerates the peat mineralization (Hergoualc'h and Verchot, 2011, 2014). An intact hydrology at our study area might prohibit the easily-decomposable litter in the degraded sites to decompose. During relative dry periods (60-70% WFPS) the *in situ* CO_2 fluxes in degraded peat swamp forests could show a stronger response to lower WFPS as compared to undisturbed peat swamp forests. Periods with less precipitation are therefore expected to result in increased CO_2 fluxes *in situ*.

The response of CO_2 production to changes in WFPS followed a cubic polynomial relationship, which is in agreement with results reported by Howard and Howard (1993) for a wide range of soils and by Husen et al. (2014) for peat soils under oil palm cultivation in Indonesia. The maximum CO_2 production at 60-70% WFPS for all three sites is in accordance with common values around 60% WFPS found in the literature (Davidson et al. 1998; Linn and Doran, 1984), but slightly higher than the 50% value reported by Husen et al. (2014).

In the incubation study, CH_4 was solely produced in soil from the heavily-degraded site at anoxic conditions (WFPS >100%), as has been reported by Smith et al. (2003) and similar to 88% WFPS reported by Melling et al. (2005) for tropical peat swamp forest. The soil samples from the I and mD site were likely not lacking in C substrate for the methanogens (Table 4.1), and the water addition treatment mimicking flooded conditions should have ensured anaerobic soil samples. Possibly, CH_4 production was inhibited due to high nitrate and other denitrification products, which inhibits methanogenesis in rice paddy soils (Klüber and Conrad, 1998a,b). The absence of N_2O production in the hD site could indicate a lack of nitrate or other denitrification product in these soils. In addition, the soils from the I and mD produced large amounts of N_2O at WFPS% >70%, which could indicate the inhibition of methanogenesis due to the presence of nitrate or other denitrification products. Most likely the time for recovery to conditions favoring

methanogenesis in the soil samples was inadequate. We did see an effect of increased CH_4 production towards the end of the incubation experiment (Annex 1), which confirms this lag in recovery.

N_2O was predominantly produced at WFPS greater than 70% for soils from the I and mD sites. Mathieu et al. (2006) used ^{15}N stable isotope tracers to demonstrate that in water-saturated soils denitrification accounted for 85-90% of emitted N_2O. Therefore, we expect that N_2O in our peat soils predominantly originated from denitrification instead of nitrification. In addition, we observed a reduced production with increased incubation time that could indicate a depletion of substrate for denitrification, or a further reduction to dinitrogen (N_2) (Annex 1). In contrast to the soils from the I and mD sites, the soils from the heavily-degraded site did not produce any significant amount of N_2O. The large CH_4 flux from the same hD soils indicates highly reducing conditions in the soil sample. Possibly denitrification in these soils predominantly resulted in N_2, which is the dominant product of denitrification in wet, anaerobic conditions (Davidson et al. 2000); while at the same it is non-toxic for methanogenesis (Roy and Conrad, 1999). The maximum N_2O production rate occurred at 100% and 84% WFPS for soils from the I and mD sites (Figure 4.2c), respectively, much above the 60% value presented by Van Lent et al. (2015) for a wide range of tropical mineral soils. This indicates that nitrification is lacking in these peat soils and N_2O predominantly originates from denitrification instead.

The absolute flux rates from the incubated soils are of limited use; however, as presented above, we were mainly interested in the relative flux rates that are useful for interpretation and modelling of field-based fluxes. Nevertheless, the average peat CO_2 and CH_4 flux rates measured *in vitro* were in the same order of magnitude as *in situ* rates from the literature. A hypothetical 30-cm peat profile with the overall average bulk density of 0.1 g cm^{-3} and the average maximum *in vitro* production rate of 2.7 µg $C\text{-}CO_2$ g^{-1} d.w. h^{-1} (Figure 4.2a, 60-70% WFPS) would result in CO_2 surface fluxes of 81 mg $C\text{-}CO_2$ m^{-2} h^{-1}. This compares well to the average value of 79 mg $C\text{-}CO_2$ m^{-2} h^{-1} reported by a review of soil surface CO_2 from tropical peat swamp forests in Southeast Asia (Hergoualc'h and Verchot, 2011). The 30-cm depth is expected to represent the soil surface flux since deep peat layers contribute little to total GHG efflux (Moore and Dalva, 1997; Jauhiainen et al. 2016).

The average maximum *in vitro* CH_4 production rate of the water-saturated soils (WFPS >95%) from the hD site was 5.9 ng C-CH_4 g^{-1} d.w. h^{-1} or 0.18 mg C-CH_4 m^{-2} h^{-1} which is similar to the rate of 0.33 mg C-CH_4 m^{-2} h^{-1} reported by Hergoualc'h and Verchot (2014), but an order of magnitude lower than the average of 1.50 mg C-CH_4 m^{-2} h^{-1} reported from similar *M. flexuosa* palm swamp forests (Teh et al., 2017). In contrast to CO_2 and CH_4, N_2O fluxes measured *in vitro* were much higher than rates measured *in situ*. The average maximum N_2O production rate from *in vitro* incubated soils from the I and mD site were 105 and 10 ng N-N_2O g^{-1} d.w. h^{-1} (respectively, 84 and 100% WFPS), or 3.2 and 0.3 mg N-N_2O m^{-2} h^{-1}, respectively. For the soils from the intact site this was an order of magnitude above the average of 0.74 mg N-N_2O m^{-2} h^{-1} reported by Van Lent et al. (2015) for tropical peat soils. Differences between fluxes measured *in situ* and *in vitro* may originate from soil disturbance during sampling or incubation preparation, differences in active peat layers producing or consuming N_2O and environmental conditions, or lack of a plant sink for mineralized N (Butterbach-Bahl et al., 2013). Lastly, an artefact could have been created due to an up-build of GHGs in the soil and water suspension between sampling days, which then diffused into the headspace after venting at the onset of the measurements. However, we took special care to minimize this effect by leaving the flasks open between sampling days.

Cumulative *in situ* CH_4 emissions were correlated with pneumatophore density (Figure 4.3), indicating a potential role for aerating roots to conduct CH_4 to the atmosphere in these peat swamp forests. Recently, vegetation-based CH_4 fluxes have been synthesized to represent 5-22% of the total global CH_4 budget, of which 58-78% is conducted by a variety of plant structures and 22-42% is thought to be produced by plants themselves (Carmichael et al. 2014; Schlesinger and Bernhardt, 2013). Pangala et al. (2013) roughly estimated that CH_4 emissions from woody tree stems alone represented 62-81% of the total ecosystem flux in an Indonesian peat swamp forest, while the contribution of pneumatophores was thought to be negligible (<2%). The specific contribution of roots to conduct CH_4 has been further studied in Indian (Purvaja et al. 2004) and Australian (Kreuzwieser et al. 2003) mangroves; however, to our knowledge this study is the first to do so for a tropical palm-dominated swamp forest. Our setup was unable to quantify the contribution of these roots to the total ecosystem flux, but it

highlights the need for additional research in order to elucidate the role of pneumatophores for CH_4 emissions in these ecosystems, and to investigate to what extent this observation holds with different vegetation compositions and soil types throughout the Amazon. Long-term GHG monitoring studies should therefore include aerating roots as potential sources in their experimental design.

The body of knowledge on tropical *M. flexuosa* dominated peatlands in the Peruvian Amazon steadily increased in recent years; even though research in this remote region has its practical limitations. This study should be seen as a first exploration of soil moisture and roots as controlling factors for GHG fluxes along a degradation gradient in this region. Despite no site replication, we were able to find enough variation of the underlying drivers of the processes of interest to detect significant relationship. To be able to make inferences about the effects of degradation on biogeochemical cycles and GHG emissions, we would need to undertake a more extensive and replicated experiment. However, this study does show the importance of various site-specific factors that drive the spatial and temporal variations of GHG emissions, and that recurrent harvesting of *M. flexuosa* could alter the GHG balance on the long-term. Sustainable management of the *M. flexuosa*-dominated peat swamp forests is needed and should aim at providing a continuous source of income for many families, while conserving the peat and its role for climate change mitigation at the same time.

4.5 Acknowledgements

This research was made possible through support to CIFOR by the United States Agency for International Development (Grant number: AID-BFS-G-11-00002) as part of the CGIAR research programs on Forests, Trees and Agroforestry and Climate Change, Agriculture and Food Security (CCAFS). We would like to thank Rupesh Bhomia for the peat depth data. Further, we are grateful to Nicole Mitidieri Rivera and Julio Miguel Grandez Rios for their help in the field and Marcella Dionisio for the GC analysis.


5

5

Palm-harvesting on peat leads to large carbon losses in western amazonia

Jeffrey van Lent[1,2], Jan Willem van Groenigen[2], Julio Grandez Rios[3], Mariela Lopez[1], Louis Verchot[4], Oene Oenema[2], Kristell Hergoualc'h[1]

[1] Center for International Forestry Research (CIFOR), Bogor, Indonesia

[2] Department for Soil Quality, Wageningen UR, Wageningen, The Netherlands

[3] Instituto de Investigaciones de la Amazonía Peruana (IIAP), Iquitos, Peru

[4] International Center for Tropical Agriculture (CIAT), Cali, Colombia

5 Palm-harvesting on peat leads to large carbon losses in western Amazonia.

Abstract

Tropical peat swamp forests (PSFs) are among the most carbon-dense ecosystems in the world and behave as a carbon (C) sink or source depending on human intervention and climatic variation. Unlike their Southeast Asian counterpart, PSFs in the Peruvian Amazon have not suffered extensive drainage and conversion. Instead, the prevailing *Mauritia flexuosa*-dominated PSFs have been severely degraded over decades. Degradation, which consists in recurrent cutting of palms for fruit harvesting, could severely alter C cycling. Between April 2014 and July 2018 soil respiration and leaf- and woodfall rates were measured monthly along a PSF degradation gradient comprising an intact site, a moderately degraded site, and a heavily degraded site. Microtopographical variations consisted of hummocks and hollows that were located around standing and cut palms. Hummocks displayed lower water table, lower water-filled pore space, more roots, and respired at higher rates than hollows. Lower palm and tree densities at the heavily degraded site resulted in lower leaf- and wood-fall rates (2.3 Mg C ha^{-1} yr^{-1}), than the intact and medium degraded sites (5.1 and 5.8 Mg C ha^{-1} yr^{-1}, respectively). Heterotrophic respiration showed an inversed trend, and was higher at the heavily degraded site (10.3 ± 1.0 Mg C ha^{-1} yr^{-1}) than the other sites (7.9 and 7.3 Mg C ha^{-1} yr^{-1}, respectively). Therefore, the peat at the heavily degraded site was a net C source (-7.1 ± 1.4 Mg C ha^{-1} yr^{-1}), while net fluxes at the intact and medium degraded sites were close to zero (-0.1 ± 1.5 and -0.2 ± 2.2 Mg C ha^{-1} yr^{-1}, respectively). Sustainable management of *M. flexuosa*-dominated PSFs would provide economic benefits for local populations and it would prevent significant CO_2 emissions.

5.1 Introduction

Tropical peat swamp forests (PSFs) are among the most carbon-dense ecosystems and have functioned as long-term carbon sinks over the past millennia (Page, Rieley, & Banks, 2011). Global estimates of peat volume remain scarce and are have large uncertainties, specifically for the tropics (Gumbricht et al., 2017; Xu, Morris, Liu, & Holden, 2018). While Southeast Asia was previously thought to hold 77% of the tropical peat volume (Page et al., 2011), large stretches of shallow peat previously unaccounted for in the Amazon region have recently been appraised (Gumbricht et al., 2017). In the northwest Peruvian Amazon, the Pastaza-Marañón river basin is a peat hotspot, with an estimated peat area of 35,600 km^2 and a total carbon stock of 3.14 Pg C (Draper et al., 2014) sequestered in vegetation and relatively deep deposits of more than 5 m (Bhomia et al., 2019; Lähteenoja, Ruokolainen, Schulman, & Oinonen, 2009).

Accumulation or loss of peat is determined by the balance of organic matter inputs from litterfall and root mortality, and outputs through organic matter mineralization and leaching from the soil (Drösler, Verchot, Freibauer, & Pan, 2013). These fluxes exhibit substantial spatial and temporal variability, particularly in PSFs. The forest floor in PSFs has irregular microtopography made up of hummocks supporting palms and hollows surrounding hummocks. These features display distinct hydrological characteristics and rooting densities, which affect respiration (Jauhiainen, Takahashi, Heikkinen, Martikainen, & Vasander, 2005). Hummocks respire more than hollows (e.g. Comeau et al., 2016; Swails, Hertanti, Hergoualc'h, Verchot, & Lawrence, 2019) as the result of higher root respiration and lower soil water-filled pore space (WFPS) (Hergoualc'h, Hendry, Murdiyarso, & Verchot, 2017; van Lent et al., 2019). Month-to-month variation results from seasonal changes in precipitation and temperatures, while inter-annual climatic variability can be caused by the El Niño/La Niña southern oscillation (ENSO), which affects rainfall patterns in Amazonia (Seneviratne et al., 2012). Rainfall variability affects water levels, soil respiration rates, and root and litter productivity. Temporal rainfall variation may affect hummocks and hollows differently, for example in an Indonesian PSF, hummocks were less impacted by water table fluctuations, than hollows (Swails et al., 2019).

PSFs are receiving a lot of attention because of their large C stocks and their potential role in climate change mitigation (Murdiyarso, Kauffman, & Verchot, 2013). Thus far, this mitigation potential is mostly studied in Southeast Asian peatlands, where PSFs are commonly drained and converted to plantation crops (e.g. Gaveau et al., 2015; Hergoualc'h & Verchot, 2014). However, PSFs in the Peruvian Amazon have not suffered extensive drainage and conversion, but the prevailing *Mauritia flexuosa*-dominated PSFs have been severely degraded over decades. The common local practice for harvesting *M. flexuosa* fruits involves cutting the palms and leaving the trunks on the ground where they are colonized by palm weevils *(Rhynchophorus palmarum*), which are later also harvested for food. Even though more sustainable harvesting (e.g. climbing) techniques exist (Horn, Gilmore, & Endress, 2012), fruit harvesting commonly continues to involve cutting entire palms (Virapongse, Endress, Gilmore, Horn, & Romulo, 2017). This practice results in degradation of *M. flexuosa* habitats with both economic and ecological consequences (Endress, Horn, & Gilmore, 2013).

Recurrent harvesting of *M. flexuosa* palms alters the composition, structure and microclimatic conditions of the forest (Bhomia et al., 2019; Hergoualc'h, Gutiérrez-Vélez, Menton, & Verchot, 2017; van Lent, Hergoualc'h, Verchot, Oenema, & van Groenigen, 2019). Densities of *M. flexuosa* decline with increasing degradation and when palms fail to regenerate gaps that are colonized by pioneer species, such as *Cecropia membranacea* (Bhomia et al., 2019). These alterations change the quality and quantity of organic material inputs to the peat, potentially inducing increased soil organic matter mineralization as suggested by results from peat incubations *in vitro* (van Lent et al., 2019).

The aim of this study was to understand the effects of vegetation degradation on the carbon cycling in *M. flexuosa*-PSFs of the Peruvian Amazon. Our approach was to substitute space for time and compare carbon fluxes in intact and degraded sites in a single peat formation. More specific objectives included (i) the characterization of the spatio-temporal variability of C fluxes and environmental variables in intact and degraded sites; (ii) the determination of environmental variables controlling the spatial and temporal variability of fluxes across sites; and (iii) the quantification of the effect of degradation on peat net C accumulation or loss rate. For this, we measured total (R_s) and heterotrophic (R_h) respiration,

leaf- and woodfall rates, water table, water-filled pore space, soil temperature at hummocks and hollows, along a degradation gradation gradient consisting of an intact, moderately and heavily degraded site. Measurements were done between 2014 and 2018, and included several *El Niño*/*La Niña* events.

We hypothesize that R_s and R_h vary according to soil microtopography, and that these are related to changes in soil temperature, water table depth, and WFPS. Secondly, we expect that *El Niño*/*La Niña* events induce variations in temperature, rainfall, water level, WFPS, and consequently alter respiration and litterfall rates. Thirdly, forest degradation causes a reduction in palm and tree densities (Bhomia et al., 2019), and we hypothesize that this results in reduced soil C inputs from litterfall, while C output from the soil increases due to an increased C mineralization rate (van Lent et al., 2019). Taken together, severe forest degradation on tropical peat is expected to turn these soils into a net source of C to the atmosphere.

5.2 Methods

5.2.1 Study site

Peruvian Amazon PSFs have been classified as pole forests, palm swamps and opened peatlands (Draper et al., 2014). Palm swamp forests are the dominant vegetation type (Draper et al., 2014), and can be dense palm swamps when they are dominated by *Mauritia flexuosa* palms or mixed palm swamps when they are formed by stands of *M. flexuosa* combined with other palms or trees (Freitas Alvarado et al., 2006; Hergoualc'h, Gutiérrez-Vélez, et al., 2017).

The study took place in and around the Quistococha reserve, located 10 km southwest of the city of Iquitos in the region of Loreto. Weather observations during 2007 - 2017 from the nearby Puerto Almendra station indicate an average annual temperature of 27°C and average annual precipitation of 2,833 mm. The area does not exhibit a strong dry season, but the period February - April is on average the rainiest quarter (Marengo, 1998). Palaeoecological records at the Quistococha reserve suggest that the current palm swamp developed around 400 cal. yr BP (Roucoux et al., 2013) and its deepest peat layers were dated at 2,335 ±15 cal. yr BP (Lähteenoja, Ruokolainen, Schulman, & Oinonen, 2009). There is no

evidence of man-made drainage in the reserve and surroundings, and the water table rarely goes deeper than 20 cm below the soil surface (Kelly et al., 2014). The swamp floods occasionally such as in 1998 (~30 cm) (Roucoux *et al.* 2013) and 2012 (~100 cm) (Kelly et al 2014). The peat in the area is classified as minerotrophic (Lähteenoja, Ruokolainen, Schulman, & Alvarez, 2009; van Lent et al., 2019).

Inside a palm swamp complex of about 500 ha, we selected three 2-ha sites that vary in the level of degradation: one intact area, one moderately degraded area and one highly degraded area (Figure 5.1; van Lent et al., 2019). The intact site ("I", S 03°49.949' W 073°18.851') was situated within the Quistococha reserve, which has been conserved since it was established as a national park in 1984 (Resolución Suprema No 223-84 ITI/tur). The moderately degraded site ("mD", S 03°50.364' W 073°19.501') was located less than 2 km southwest of the intact site, near a village founded in 2010. The heavily degraded site ("hD", S 03°48.539' W 073°18.428') was located less than 3 km northeast of the intact site, at the border of a village, which expanded substantially in 2014. Both degraded sites have undergone cutting of *M. flexuosa* palms for fruit collection and logging of trees for housing construction, with varying intensity. *M. flexuosa* was dominant in the I and mD sites, while forest degradation has led to a reduced canopy closure at the hD site, with few *M. flexuosa* palms and trees. This site was dominated by *Cecropia membranacea* (Bhomia et al., 2019). The density of *M. flexuosa* palms was 170, 164 and 16 stems ha^{-1} and the density of trees was 1496, 700 and 679 stems ha^{-1} at the I, mD and hD sites, respectively. The peat is shallower at hD site (1.0 ± 0.2 m) than the I and mD sites (respectively 2.2 ± 0.1 and > 2.65 m) (Bhomia et al., 2019).

5.2.2 Experimental setup

The experiment started in April 2014, July 2014, and February 2015 at the I, hD and mD sites, respectively and ended in July 2018. It was designed to capture micro-level spatial heterogeneity associated with soil microtopography (hollows vs. hummocks) and overstory species (palms vs. trees), and the effects of degradation (live vs. cut *M. flexuosa* palms). The influence of species was measured only at the intact site; the effect of degradation only at the degraded sites. Degradation impacts at the macro-level were inspected by comparing site-scale results (see section 2.6).

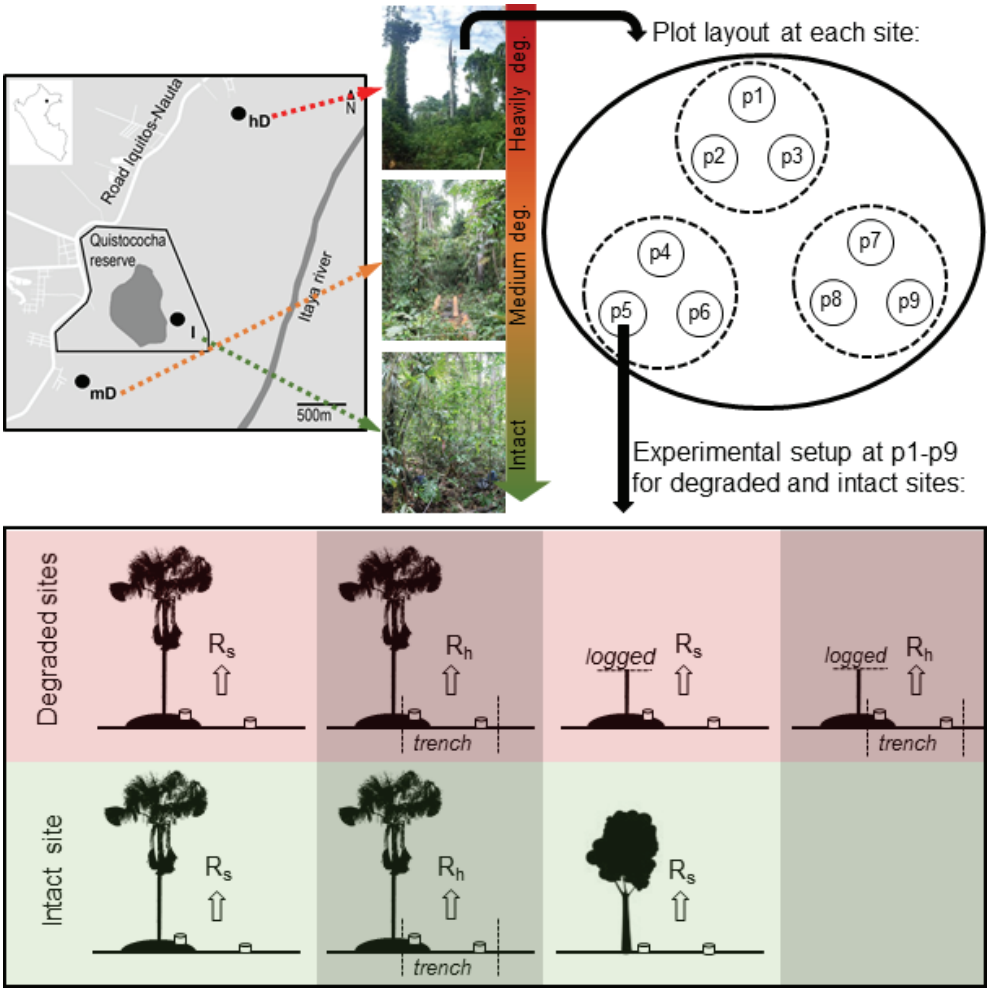

Figure 5.1 – Map of the study location near Iquitos, Peru (top left); layout of plots per at each sit (top right); and sketch of the experimental setup (bottom). The location of the intact (I), moderately (mD) and highly (hD) degraded sites is indicated with black dots. Both degraded sites are close to settlements (white lines represent streets). The black line around the *Quistococha* lake (dark grey area) delimits the border of the reserve. Photos from each site illustrate the degradation gradient. At each site nine plots were layout as illustrated (p1 till p9). The experimental setup per plot consisted of 4 subplots at the degraded sites (red shaded), and 3 subplots at the intact site (green shaded). Per subplot 2 collars for total soil respiration (R_s) or heterotrophic respiration (R_h) were installed, one on a hummock surrounding a palm and another in hollow parts at a ~1.5 meter from a palm. In addition, in degraded sites two subplots were included for harvested palms and at the intact site one subplot was included for trees.

We established three study areas (~0.2 ha), separated by 150m, at each site, and three plots (~0.02 ha) within each study area that were ~15 m from each other (Figure 5.1). At the intact site measurements we measured three 2.5 x 2.5 m subplots per plot, two of which included a live *M. flexuosa* palm, the third included a tree. At the degraded sites we measured four subplots per plot; two of which included a live *M. flexuosa* palm and the other two included a cut *M. flexuosa* palm. We measured the pairs of live and cut palms, one for total soil respiration (R_s) and the other for heterotrophic soil respiration (R_h). We did not make this distinction for trees at the intact site as there was no palm harvesting. In all subplots, measurements were spatially stratified, differentiating hummocks from hollows. Sampling in hummocks was performed close (<0.5 m) to a trunk in the main rooting zone, sampling in hollows was located further (>1.5 m) from the trunk outside the main rooting zone. Soil microtopography around trees was not as pronounced as it was around *M. flexuosa* palms. Soil respiration, water table level, soil moisture and air and soil temperatures were concomitantly measured monthly at each sampling point (see 2.4). Boardwalks were constructed at the onset of the experiment to access sampling points without creating disturbance.

5.2.3 Soil respiration

We measured soil respiration using the dynamic closed chamber method, by placing a non-transparent PVC chamber on onto permanently installed PVC collars (diameter 10 cm, height 10 cm) (SRC-1, PP systems, USA). The collars, installed 3-5 cm into the soil to ensure air-tightness. The covers were connected to a portable infrared gas analyzer (EGM-4, PP systems, USA) with Teflon tubing. Chambers were manually fanned before closing and the CO_2 concentration was recorded automatically every 4.8 seconds for about 2-3 minutes. The CO_2 flux was calculated from the linear increase of the concentration over time. To reduce humidity entering into the EGM-4 and ensure stable CO_2 measurements, the device was equipped with a filter filled with indicating drierite (≥ 98% $CaSO_4$ and ≤ 2% $CoCl_2$). Notwithstanding, the equipment failed on several occasions, resulting in missing data.

We used the trenched plot method to measure heterotrophic respiration (R_h). Other root exclusion methods such as girdling and clipping are not suitable for

palm-dominated vegetation (Subke, Inglima, & Cotrufo, 2006). Untrenched subplots including live or cut palms were used to measure R_s. We dug trenches 0.5 m wide and 1.5 m deep along a 2 x 2 m quadrant using a chainsaw and spades at the onset of the experiment. Soil coring revealed few roots beyond 1.5 m depth. To prevent roots from growing into the trenched suplots, the inner walls of trenches were covered with six layers of construction plastic and backfilled. Recruitment of new vegetation in the quadrant was prevented through monthly seedling removal. We double-checked the effectiveness of the trenching when we withdrew the plastic inserts August 2018 and found no roots inside the trenched quadrants.

5.2.4 Environmental variables

Daily precipitation rates were measured using a rain gauge with tipping bucket (0.2 mm resolution, Delta Ohm HD2013R, Italy). The device was installed 0.8, 1.2 and 2.9 km away from the I, mD and hD sites, respectively. All other environmental factors were recorded concurrently with soil respiration measurements at the side of each collar. The water table (WT) relative to the soil surface was measured in perforated PVC tubes (5 cm in diameter, 1.5 m in length) inserted permanently into the soil to 1 m depth at 50 cm distance from each collar. Water depth during flooding was measured with a pole. Soil moisture was determined by collecting one soil sample from the top 10 cm, near each collar, using a metallic cup (6 cm diameter). The water-filled pore space (WFPS) was calculated from the fresh mass, the oven-dried mass (~2 days at 60°C), and the site-microtopographic-specific mean bulk density, following the formula by Linn and Doran et al. (1984) and assuming a particle density of 1.4 g cm^{-3} (Driessen and Rochimah, 1976). Air temperature was measured using a portable thermometer and soil temperature at 10 cm depth using the EGM-4 temperature probe.

5.2.5 Litterfall

Measurement of tree leaf litter fall started two months after the onset of the respiration measurements until July 2018. Larger-size litter was measured between June 2016 and July 2018. Litterfall included tree leaves and larger-size litter consisting of *M. flexuosa* trunks and leaves and tree branches. Tree leaf

litterfall was measured in traps (0.09 m^2) installed randomly on trees (~1 m above soil) in triplicates per subplot; totalling 27 traps at the I site and 36 traps at each degraded site. Samples were oven-dried at 60°C to constant mass and weighed. Larger-size litter (dead wood) was measured in three 5 by 5 m quadrants per site. The quadrants were cleared of debris at the onset of the experiment and after each litter collection. All *M. flexuosa* trunks and leaves and tree branches were collected from the ground bi-monthly and weighed *in situ*. A representative subsample of each component was dried at 60°C to constant mass, and its dry-to-wet ratio used to calculate the dry mass of the samples. All samples were dried at the Quistococha research laboratory of the Instituto de Investigaciones de la Amazonía Peruana (IIAP). The C content of the tree leaf and branch, and *M. flexuosa* leaf was measured from triplicate samples per site by the induction furnace method (Costech EA C-N Analyzer), for *M. flexuosa* trunks the average C% of dicot branches was used.

5.2.6 Computations of annual and site-scale fluxes

Soil respiration rates in the first three months were not use because heterotrophic respiration during this period was stimulated by the decomposition of freshly excised roots inside the trenched quadrants (see Figure S1 in Supplementary Information). Thus, environmental variables and soil respiration fluxes were compared among sites for the years April 2015 – March 2016, April 2016 – March 2017, and April 2017 – March 2018; dubbed Year 1, Year 2, and Year 3.

Monthly average R_s and R_h rates were calculated from the nine replicate plots per site (I, mD, hD), palm status (standing live or cut palm), and stratified by microtopography (hummock and hollow). At the intact site, monthly average R_s of trees was also computed from nine replicated measurements close (~0.5 m) and far (~1.5 m) from trees. Annual respiration rates were obtaining by integration of monthly averages applying a linear interpolation between measurement dates. Site-scale annual respiration rates were computed by considering the heterogeneity in spatial topography (hummocks and hollows) and degradation (live and cut palms) at each site. For this, we inventoried the density of *M. flexuosa* palms and trees, and the surface areas of hummocks with standing live palms and with cut palms at each site (see detailed methods and calculations in SI2).

Degradation and spatial-specific respiration rates were multiplied by the relative surface area that it represented within a site.

Monthly average WT, WFPS, soil, air temperature, Rs and Rh were calculated from 9 replicate plots per site. Monthly tree leaf litter fall rates were calculated from 27 replicates at the intact site, and 36 replicates for both degraded sites. We calculated a weighted average per hectare and litter fall rates were multiplied by a proportion that accounted for the varying stem densities in each measurement area (Table 5.1). The proportion was set at 1 in the intact site, and the proportion of stems relative to the intact site was calculated for the degraded sites. Larger-size litter was scaled similarly using 3 plots per sites and linearly extrapolating between bi-monthly measurements. The proportion for scaling *M. flexuosa* litter was based on the, respective palm stem densities (see detailed methods and calculations in SI2).

5.2.7 C balance

The peat net C balance in Mg C ha^{-1} yr^{-1} was calculated using equation 2.2 from the 2013 supplement to the 2006 IPCC guidelines for national greenhouse gas inventories for wetlands, as (Drösler et al., 2013):

$$\text{Peat } C_{balance} = LF + RM - R_h - DOC \qquad \text{eq. 1}$$

Where, LF is the average annual litterfall rates during years 2 and 3, RM is the average annual root mortality rate, R_h is the average annual heterotrophic respiration rates across years 2 and 3, and DOC is dissolved organic carbon. Year 1 is not used for the C balance, since respiration measurements were not concurrently done at all sites during that year. We used as default DOC flux the result by Moore et al. (2013), from an undrained Indonesian peatland. Root mortality rates were measured by Grandez Rios (n.d.), at the three sites from March to December 2017. Although there was no interannual variation assess for the DOC flux and root mortality, it is a best-estimate.

Table 5.1 – Relative proportions of hummocks with live and cut palms and surrounding hollows used for upscaling location-specific total soil respiration (R_s) and heterotrophic (R_h) respiration to the site scale proportions they represent, and for scaling litter fall rates to reflect actual stem densities per site.

Site	**R_s or R_h**				**Litter**	
	Live Palm		Cut Palm		Trees	*M. flexuosa*
	hummock	*hollow*	*hummock*	*hollow*		
Intact (I)	0.15	0.85	0.00	0.00	1.0	1.0
Moderately degraded (mD)	0.08	0.79	0.01	0.12	0.9	1.0
Heavily degraded (hD)	0.02	0.59	0.02	0.38	0.4	0.2

5.2.8 Statistics

Statistical analysis was performed using the software IBM SPSS Statistics for Windows 25.0 (IBM Corp. 2017) and statistical significance was set at 5%. Normality of residuals was tested using the Shapiro Wilk test, and visual interpretation of Q-Q plots. Environmental variables and respiration rates at hummocks and hollows, with cut and live palms were compared for each year with a Mann-Whitney U test, and the Kruskal-Wallis test with pair-wise comparisons was used for comparisons between years and sites. The comparison between hummock areas between sites was done with an ANOVA. The comparisons between sites should be used with care due to the lack of site replicates.

Regression models between environmental variables and respiration rates were done with the entire dataset. Data was not split into years, nor was it separated between spatial location or degradation status. The regressions were based on average values calculated for intervals every 10 cm WT, 10% WFPS and 1°C soil temperature. The responses of respiration to WT and WFPS were modelled using exponential, cubic and quadratic polynomial functions. The R^2 values were used to estimate the best fit model and analysis of residuals was used to assess bias. An exponential equation was used to calculate the relationship between temperature and soil respiration, for which the parameter in the exponent was then used to calculate the Q_{10} value.

5.3 Results

5.3.1 Site properties

The density of live *M. flexuosa* palms and trees was lower at the highly degraded site (Figure 5.2a) and the proportion of cut or dead *M. flexuosa* palms increased from 3% in the I site to 19 and 46% in the mD and hD sites, respectively. For trees 3, 9 and 7% of the stem were harvested in the I, mD and hD sites, respectively.

Hummocks supporting cut palms were on average 36, 34 and 25% smaller in surface area than hummocks supporting standing live palms at the I, mD and hD, respectively (Figure 5.2b). The relative proportion of hummocks with live palms reduced considerably with increasing degradation, and vice versa for hummocks with standing cut palms.

Detailed soil properties by microtopography along the degradation gradient are presented in Table S1 (supplementary information). Hummocks had a 12% higher CEC than hollows and a 10% higher C/N ratio than hollows at the I site ($p < 0.05$ for both). Soil C content ($P = 0.01$), C/N ratio ($p < 0.01$), and P content ($p < 0.01$) across microtopographies were lower at the hD site than elsewhere.

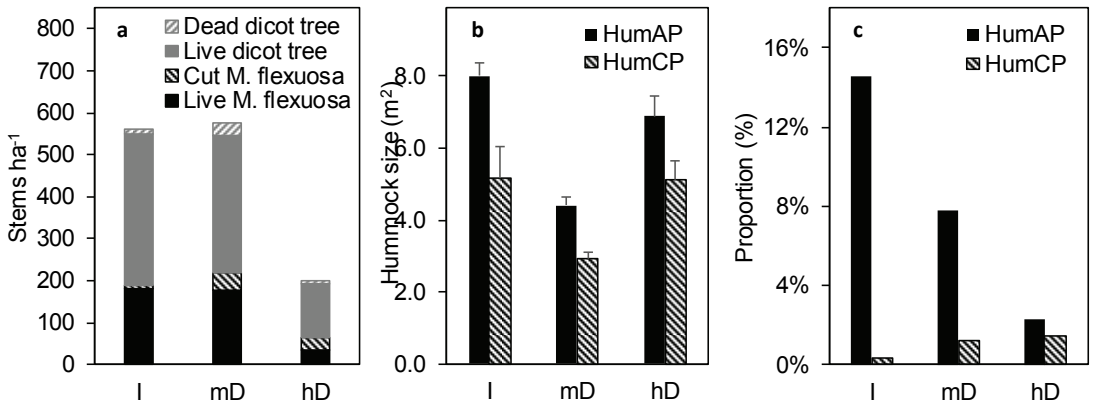

Figure 5.2 – Density of live (AP) and cut (CP) *M. flexuosa* palms and live and dead trees (a); average hummock area of AP and CP (b); and relative proportion of hummocks with AP and CP at the intact (I), moderately degraded (mD), and heavily degraded (hD) sites. In (c) the remaining proportions correspond to area represented by hollows (85%, 91% and 96%, respectively). Error bars represent one standard error, sample sizes are the number of *M. flexuosa* stems ha^{-1} from (a).

Table 5.2 – Average water table depth (WT), water-filled pore space (WFPS), air (T_{air}) and soil (T_{soil}) temperature per year at the intact (I), moderately degraded (mD), and heavily degraded (hD) sites. WT depths are expressed in cm relative to the soil surface with negative values indicating levels below the soil surface. Standard errors are given after the average, and the sample size is in the brackets.

		WT (cm)				**WFPS (%)**				**T_{air} (°C)**		**T_{soil} (°C)**	
Site	**Yr#**	*hummock*		*hollow*		*hummock*		*hollow*					
I	1	−2.0 ±2.5 (167)	Aa	10.6 ±3.1 (165)	Bab	72.1 ±2.2 (108)	b	69.6 ±1.6 (107)	b	29.9 ±0.1 (378)	a	25.3 ±0.1 (405)	a
	2	−11.3 ±1.1 (194)	Aab	−1.6 ±1.3 (194)	Ba	78.6 ±1.2 (187)	Aa	73.2±0.8 (187)	Ba	29.6 ±0.1 (582)	a	24.9 ±0.0 (582)	b
	3	−14.4 ±1.1 (214)	Ab	−5.7 ±0.9 (214)	Bb	79.7 ±0.9 (214)	Aa	70.7 ±0.7 (214)	Bab	29.1 ±0.1 (641)	b	24.2 ±0.0 (641)	c
	Avg	−9.2 ±3.0 (3)	Ac	1.1 ±3.5 (3)	Bab	76.8±2.7 (3)	Ab	71.2 ±2.0 (3)	Bb	29.5c ±0.1 (3)	c	24.8 ±0.1 (3)	
mD	1	5.3 ±1.9 (276)	A	10.8 ±2.2 (275)	B	91.2±1.2 (174)	Ac	87.3 ±1.1 (173)	Bb	31.0 ±0.1 (429)	a	25.9 ±0.1 (489)	a
	2	−2.9 ±0.6 (414)	A	1.3 ±0.5 (414)	B	98.5±0.7 (413)	Aa	92.0 ±0.7 (414)	Ba	30.6 ±0.1 (830)	b	24.9 ±0.0 (830)	b
	3	−0.7 ±0.8 (432)	A	1.8 ±0.7 (432)	B	95.1 ±0.7 (432)	Ab	90.6±0.6 (432)	BaB	29.9 ±0.1 (864)	c	24.1 ±0.0 (864)	c
	Avg	0.6 ±2.2 (3)	Aa	4.6 ±2.4 (3)	Ba	94.9 ±1.6 (3)	Aa	90.0 ±1.4 (3)	Ba	30.5 ±0.1 (3)	b	25.0 ±0.1 (3)	
hD	1	−8.6* ±1.0 (218)	A	−1.9* ±0.8 (211)	B	69.8±2.7 (175)	Aa	75.9 ±2.6 (162)	B	32.5 ±0.1 (434)	a	25.4 ±0.1 (440)	a
	2	−6.7 ±0.6 (431)	A	−2.2 ±0.5 (432)	B	66.3±0.9 (415)	Aa	72.9 ±0.8 (414)	B	31.5 ±0.1 (863)	b	25.0 ±0.0 (863)	b
	3	−6.2 ±0.7 (432)	A	−1.1 ±0.6 (432)	B	68.6 ±0.7 (421)	Ab	70.5 ±0.7 (420)	B	31.8 ±0.1 (821)	ab	24.4 ±0.0 (821)	c
	Avg	−7.2 ±1.3 (3)	Ab	−1.7 ±1.1 (3)	Bb	68.2±2.9 (3)	Ac	73.1 ±2.8 (3)	Bb	31.9 ±0.2 (3)	a	24.9 ±0.1 (3)	

# Years are split up as follows: 1 = Apr15-Mar16, 2 = Apr16-Mar17, 3 = Apr17-Mar18
NA = not available
* not data collected during flooding event
Lowercase letters indicate significant differences between years within a site and microtopography, and between sites within a microtopography for the 3-years annual averages. Uppercase letters indicate significant differences between microtopographies (hummocks and hollows).

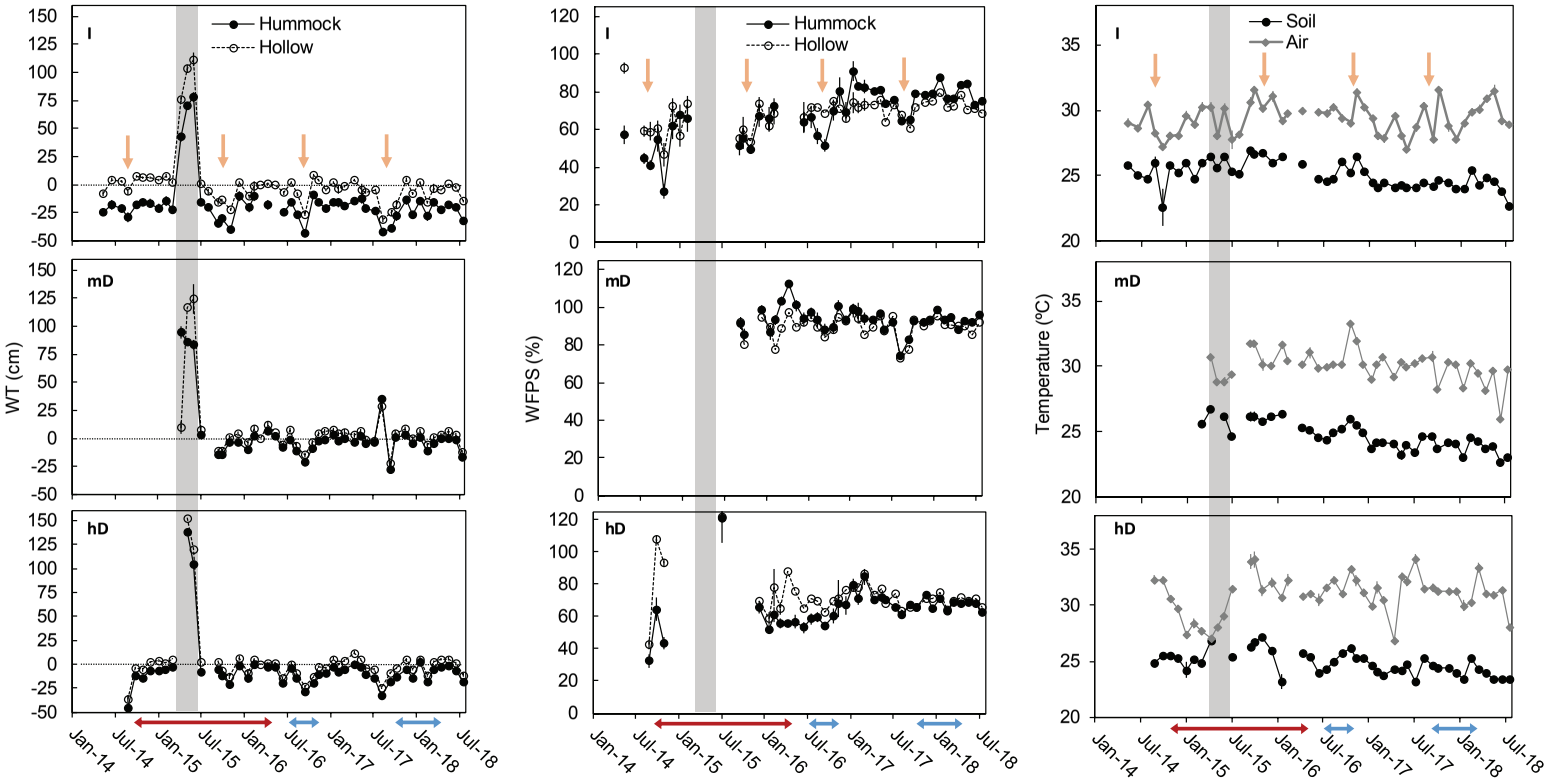

Figure 5.4 – Monthly average water table level (WT), soil water-filled pore space (WFPS) , soil and air temperature measured at the intact (I), moderately degraded (mD), and heavily degraded (hD) sites in Iquitos, Peru between April 2014 and July 2018. Average WT and WFPS are disaggregated by spatial position (hummock, hollow). Soil and air temperatures were similar among microtopography's, therefore the average of both microtopography's is presented. *El Niño* and *La Niña* episodes are indicated by red and blue arrows, respectively. The shaded area shows the flooding event during *El Niño*. Orange arrows indicate the annual cycle with lowest WT and WFPS or highest soil and air temperature values (Supplementary Figure 2 and 4). Positive WT values denote water levels above surface levels, negative values the opposite. Error bars represent one standard error (n_{intact} = 27, n_{mD} = n_{hD} = 36 for WT and WFPS, 54 and 72 for air and soil temperature).

5.3.2 Spatio-temporal variations of environmental factors

The average annual precipitation rate was 2882 ±119 mm between April 2014 and April 2018. The average monthly precipitation was 240 ± 18 mm, but the period between December and March was slightly wetter ($p = 0.04$, 312 ± 31 mm month^{-1}) and covered 54% of the annual precipitation. Our study included one *El Niño* event, and two weak *La Niña* events. The average monthly precipitation was 270 mm month^{-1} during the two *El Niño* years, with heavy rainfall in March and April 2015 (Figure 5.3), totaling almost 1,000 mm. During this period, the water table was exceptionally high and exceeded >1 m above the soil surface (Figure 5.4).

Average monthly WT at hummocks and hollows ranged between -30 ± 2 cm and 94 ± 3 cm during the entire experiment; however, 86% of the WT values were between -20 and +20 cm (Figure 5.4 and Table 5.2). A yearly cycle was observed with lowest WT levels in August and September ($p < 0.01$, Supplementary Figure S2), and higher WT levels for the other months. The average monthly rainfall displays a positive linear relationship with the average monthly WT levels, and WT with WFPS (Supplementary Figure S2 and S3).

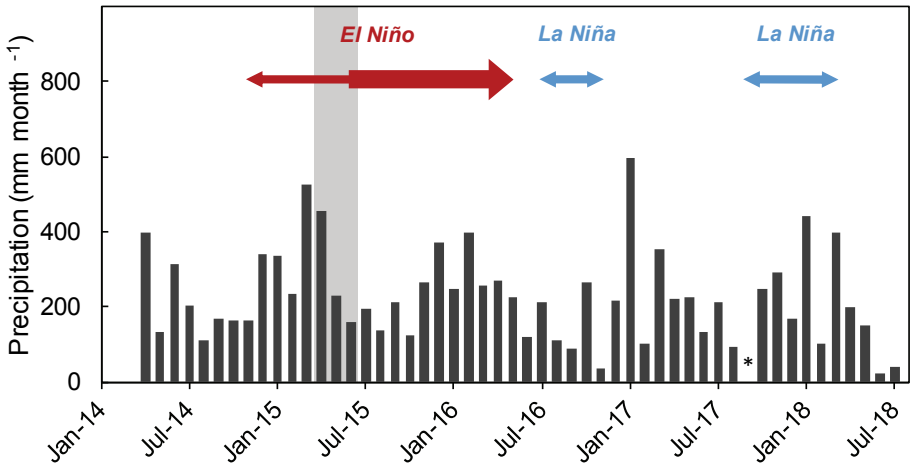

Figure 5.3 – Monthly precipitation at Quistococha between April 2014 and July 2018. The red and blue arrows illustrate the occurrence of Southern Oscillation-episodes. The *El Nino* event was qualified as very strong from June 2015 onwards (NOAA, 2018), marked by the thick red arrow. The asterisk indicates missing data for January 2018. Annual precipitation (April-March) totalled at 3101, 3060, 2606 and 2762 mm for the first to the fourth year of measurement, respectively.

The overall average WFPS was 79.0 % ± 0.3, and monthly averages were between 32% and 100% (Figure 5.4 and Table 5.2). Year to year variations in general were small and only the first year appeared to be drier. The WFPS varied significantly between hummocks and hollows ($p < 0.01$), although the average difference was only 5.1% across all measurements. Differences between sites were much larger (≥25%); the soils at the mD sites were significantly wetter than the soils at the I and hD sites ($p < 0.01$).

Monthly average air temperature ranged between 28.2 and 32.7 °C, and soil temperatures between 22.4 and 26.6 °C (Figure 5.4 and Table 5.2). Air temperature clearly increased with increased level of degradation ($p < 0.01$), while soil temperatures did not.

5.3.3 Spatio-temporal variation of carbon fluxes

Leaf litterfall ranged between 2.3 and 36.2 kg C ha^{-1} d^{-1}. Litterfall was not measured during the flooding event (April to June 2015, Figure 5.5). However, when the water levels went back to normal as from July 2015, a large portion of the vegetation shed their leaves and leaf litterfall during this year (year 1, Apr 2015 – Mar 2016) was about twice the litterfall rates in other years ($p < 0.01$ at all sites, Table 5.3). Measurements of palm leaf and tree branch fall started after the flooding event and exhibited similar rates across years (Table 5.3). The average rate of *M. flexuosa* leaf and tree branch fall across years and sites amounted to 1.0 and 2.3 kg C ha^{-1} d^{-1}, respectively. Two *M. flexuosa* palms were harvested within the plots at the hD site during the experiment (Figure 5.5).

We used stem density for scaling litterfall measurements to the hectares (Table 5.1). The reduced stem density at the hD site led to significantly lower litter inputs than at the mD and I sites (Table 5.3).

Monthly average total soil respiration (R_s) and heterotrophic soil respiration (R_h) ranged between 3.3 – 226.8, and 9.9 – 161.1 Mg C ha^{-1} d^{-1}, respectively. The flooding event caused strong intra-annual variations in both R_s and R_h rates with fluxes close to zero between April and June 2015 (Figure 5.6). As water levels lowered around July 2015, R_s and R_h increased to levels similar to those before the flooding. However, after the WT gradually approached its yearly low point in September 2015, we observed a strong peak in R_s and R_h rates in both hummocks

and hollows that were nearly twice the rates measured before the flooding. The combination of low fluxes during the flooding and the spikes of R_h and R_s after the flooding, led to annual fluxes similar to those in other years. R_h and R_s at hummocks and hollows between years did not display any consistent trend (Table 5.4).

Hummocks had higher average R_s and R_h rates than hollows in all sites for all years combined, except for R_h in the hD (Table 5.4). The higher R_s rates on the hummocks were disproportionally larger compared to R_h in hummocks, which

Table 5.3 – Annual litterfall rates for tree leaves and branches, and *M. flexuosa* leaves and trunks at the Intact (I), moderately degraded (mD), and heavily degraded (hD) sites.

Site	Year[#]	Leaves		Branches	M. flex. leaves	M. flex. trunks	Site-scale litter[§]	
I	1	5.69 ±0.40 (187)	a	NA	NA	NA	NA	
	2	3.48 ±0.23 (311)	b	0.60 ±0.14 (18)	0.37 ±0.16 (18)	0.00 ±0.00 (18)	4.45 ±0.21 (365)	a
	3	2.38 ±0.15 (324)	c	1.16 ±0.43 (18)	0.36 ±0.18 (18)	0.00 ±0.00 (18)	3.90 ±0.14 (378)	b
	Average	3.85 ±0.48 (3)		0.88 ±0.46 (2)	0.37 ±0.24 (2)	0.00 ±0.00 (2)	5.10 ±0.58 (2)	A
mD	1	8.44 ±0.30 (180)	a	NA	NA	NA	NA	
	2	4.03 ±0.16 (432)	b	0.85 ±0.29 (18)	0.66 ±0.26 (18)	0.00 ±0.00 (18)	5.05 ±0.15 (486)	a
	3	2.73 ±0.11 (432)	c	1.02 ±0.19 (18)	0.08 ±0.04 (18)	0.00 ±0.00 (18)	3.47 ±0.10 (486)	b
	Average	5.07 ±0.36 (3)		0.93 ±0.35 (2)	0.37 ±0.26 (2)	0.00 ±0.00 (2)	5.79 ±0.48 (2)	A
hD	1	8.12 ±0.34 (150)	a	NA	NA	NA	NA	
	2	4.17 ±0.20 (384)	b	1.04 ±0.27 (18)	0.75 ±0.33 (18)	0.09 ±0.09 (18)	2.01 ±0.18 (438)	a
	3	3.73 ±0.13 (432)	b	0.53 ±0.11 (18)	0.11 ±0.05 (18)	0.09 ±0.07 (18)	1.56 ±0.12 (486)	b
	Average	5.34 ±0.42 (3)		0.79 ±0.29 (2)	0.43 ±0.33 (2)	0.09 ±0.11 (2)	2.28 ±0.51 (2)	B

All rates are in Mg C ha^{-1} yr^{-1}. Differences between years within site are indicated by lowercase letters, and uppercase letters indicate differences between sites.

[#] Years are split up as follows: 1 = Apr15-Mar16, 2 = Apr16-Mar17, 3 = Apr17-Mar18

[§] Site-scale litter and branch fall litter is calculated by using proportions from Table 5.1

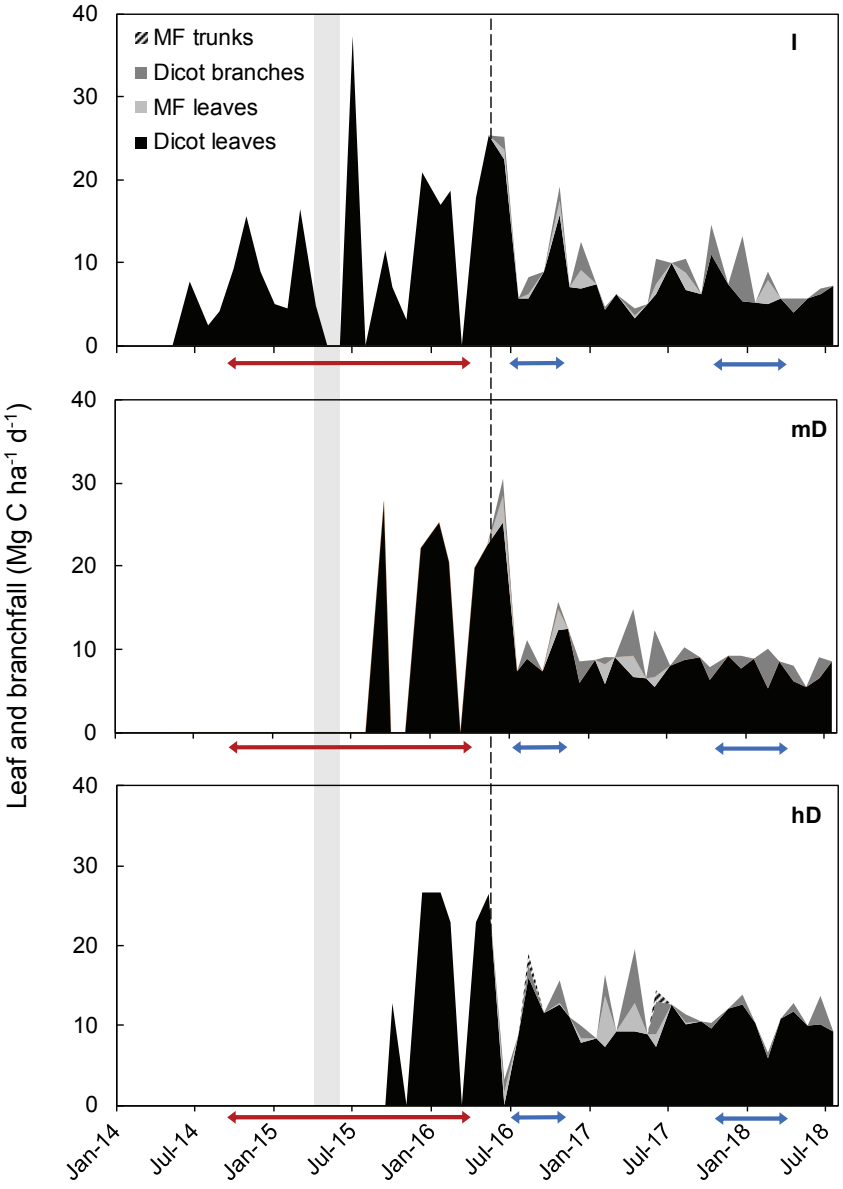

Figure 5.5 – Monthly average trunk, branch and leaf fall from *M. flexuosa* (MF) palms and trees at the Intact (I), moderately degraded (mD), and heavily degraded (hD) sites. The dashed line indicates the start of the measurement of *M. flexuosa* trunk and leaf and tree branch fall. The shaded area indicates the flooding during the *El Niño* event. *El Niño* and *La Niña* episodes are indicated by red and blue arrows, respectively.

indicates a relative higher contribution of root respiration (R_s- R_h) on the hummocks. R_h contributed on average 44%, 92% and 64% to R_s on the hummocks in the I, mD and hD sites, respectively. In hollows this was 67% at the intact site, while at the degraded sites root respiration in hollows was insignificant (i.e. R_h = 100% of Rs).

Respiration close to and far from trees were not significantly different and almost exactly the same (Table 5.4), and impacts of degradation were assumed to be less prominent as was observed for *M. Flexuosa* palm and the subsequent impact on the microtopography (Figure 5.2). Therefore, respiration rates around trees were assumed to equal hollow fluxes. Including tree-specific respiration rates did not lead to meaningful significant differences at the site-scale (see discussion paragraph 5.4.3).

Hummocks with cut palms had, respectively, a 28% and 26% lower R_s and R_h than hummocks with live palms at the mD site ($p < 0.01$) and hD site ($p = 0.04$) (Table 5.4). In the hollows, R_s was less affected by palm harvesting and remained at similar rates, while for R_h a small reduction was visible at the hD site (20%, $p < 0.01$). At the intact site R_s around trees was similar close to and far from stems with a rate on average 73% the R_s rate in hollows around *M. flexuosa* palms.

Site-scale annual R_s and R_h rates are presented in Table 5.4. Across years, R_s varied between sites ($p < 0.01$), where I > hD > mD. R_h was largest at the hD site across years ($p < 0.01$). Year-to-year variation in site-scale R_s and R_h was mostly related to respiration rate variations in hollows, since these represented > 85% of the soil surface at all sites (Figure 5.2, Table 5.1).

Across sites, R_h and R_s increased exponentially with decreasing WT level (Figure 5.7). Total soil respiration doubled for every ~50 cm decrease in WT, and R_h doubled for every ~70 cm decrease in WT. The WFPS showed a near-significant quadratic relationship with R_h (Figure 5.7, $R^2 = 0.74$, $p = 0.06$), whenever the WT was below soil level (WT ≤ 0 cm). The optimum R_h was observed at a WFPS of 57%. R_s displayed a linear decrease with increased WFPS, when the WT was below ground surface. Both total and heterotrophic respiration responded exponentially to soil temperature. The range of soil temperatures was on average between 21°C and 29°C, and the corresponding Q_{10} values among all sites were 1.7 for R_s and R_h, respectively.

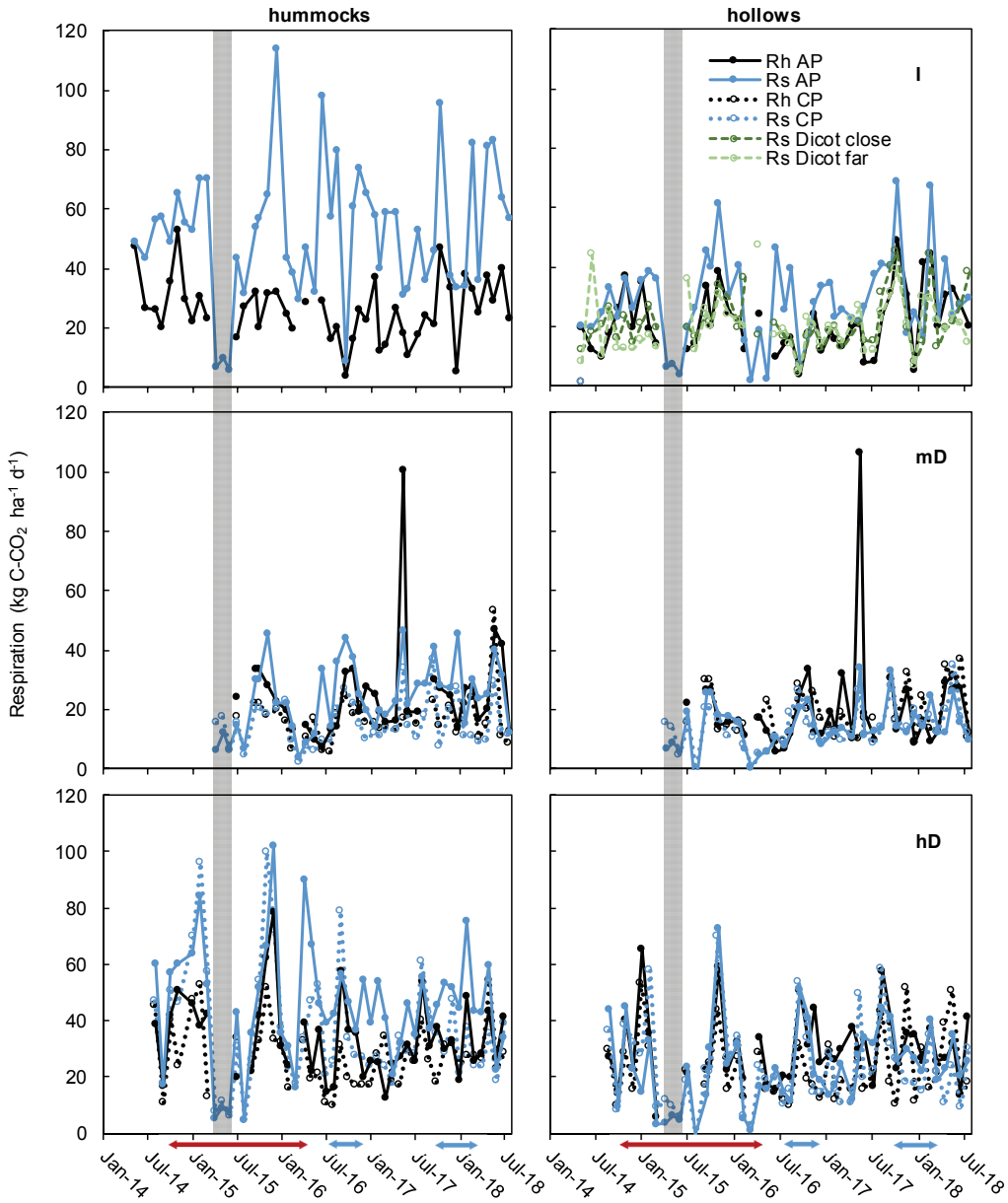

Figure 5.6 – Average monthly total soil respiration (R_s) and heterotrophic soil respiration (R_h) from hummocks and hollows with live *M. flexuosa* palms (AP) and cut *M. flexuosa* palms (CP) at the intact (I), moderately degraded (mD), and heavily degraded (hD) sites. R_s close to and far from trees was also measured at the intact site. Each monthly point is the average of nine measurements, standard errors are omitted for clarity purposes. The shaded area indicates the flooding event during *El Niño*.

Table 5.4 – Annual soil respiration (R_s) and heterotrophic respiration (R_h) from hummocks and hollows with live palms and cut palms at the Intact (I), moderately degraded (mD), and heavily degraded (hD) sites. Standard errors are given after the average, and the sample size is within the brackets.

	Year*	**Live palm**								**Tree**			
		R_s				R_h				R_s			
		hummock		*hollow*		*hummock*		*hollow*		*close*		*far*	
I	1	15.2 ±1.2 (108)	A	9.1 ±0.9 (107)	Bab	9.4 ±0.7 (65)	a	8.6 ±0.7 (61)	a	8.9 ±0.8 (59)	a	8.3 ±0.6 (51)	a
	2	20.7 ±1.5 (108)	A	9.2 ±0.7 (108)	Bb	7.4 ±0.9 (96)	b	5.4 ±0.6 (94)	b	5.8 ±0.4 (94)	b	6.7 ±0.7 (95)	b
	3	17.6 ±1.2 (108)	A	12.4 ±0.9 (108)	Ba	9.0 ±0.8 (105)	ab	9.2 ±1.0 (105)	a	8.7 ±0.8 (107)	a	8.4 ±0.7 (105)	ab
	Avg	17.8 ±2.3 (3)	Aa	10.2 ±1.5 (3)	Ba	8.6 ±1.4 (3)	Ab	7.7 ±1.3 (3)	Bb	7.8 ±1.2 (3)		7.8 ±1.2 (3)	
mD	1	6.6 ±0.9 (107)	Ab	4.6 ±0.6 (100)	Bb	9.2 ±0.8 (60)	a	7.0 ±0.6 (59)	a				
	2	8.6 ±0.7 (108)	Aa	4.5 ±0.3 (108)	Bb	7.3 ±0.7 (99)	b	6.2 ±0.7 (102)	b				
	3	10.9 ±1.0 (108)	Aa	6.5 ±0.6 (108)	Ba	10.7 ±2.4 (98)	Aab	8.7 ±2.3 (98)	Bab				
	Avg	8.7 ±1.5 (3)	Ac	5.2 ±0.9 (3)	Bb	9.1 ±2.7 (3)	Ab	7.3 ±2.5 (3)	Bb				
hD	1	12.9 ±1.3 (103)	Ab	6.9 ±0.9 (103)	Bc	15.6 ±2.6 (54)	a	11.4 ±1.1 (49)					
	2	18.7 ±1.3 (108)	Aa	8.2 ±0.7 (108)	Bb	10.4 ±0.9 (105)	b	10.5 ±0.8 (106)					
	3	16.5 ±1.0 (108)	Aa	11.0 ±0.7 (106)	Ba	12.0 ±0.7 (102)	a	12.0 ±0.9 (102)					
	Avg	16.0 ±2.1 (3)	Ab	8.7 ±1.3 (3)	Ba	12.7 ±2.9 (3)	a	11.3 ±1.6 (3)	a				

continued

Cut palm								Weighted average per site#			
R_s *hummock*		R_s *hollow*		R_h *hummock*		R_h *hollow*		R_s		R_h	
								10.0 ±1.2		8.7 ±0.2	
								10.9 ±1.5		5.7 ±0.1	
								13.2 ±1.2		9.2 ±0.2	
								11.4 ±2.3	a	7.9b ±0.3	b
5.3 ±0.4 (105)		4.3 ±0.4 (105)	b	6.4 ±0.6 (62)		6.9 ±0.7 (60)		4.7 ±0.5		7.1 ±0.5	
4.9 ±0.4 (108)		4.4 ±0.4 (108)	ab	5.5 ±0.5 (101)		6.2 ±0.6 (102)		4.8 ±0.2		6.3 ±0.5	
6.5 ±0.6 (108)		5.9 ±0.5 (108)	a	6.3 ±0.6 (99)		6.4 ±0.6 (99)		6.8 ±0.5		8.6 ±1.8	
5.6b ±0.9 (3)	b	4.9 ±0.7 (3)	b	6.1 ±0.9 (3)	b	6.5 ±1.1 (3)	b	5.4 ±0.7	c	7.3b ±2.0	b
12.1 ±1.2 (106)	A	7.0 ±0.8 (105)	Bb	12.3 ±1.0 (56)	Aa	9.1 ±0.7 (54)	Ba	7.3 ±0.6		10.8 ±0.7	
12.8 ±1.3 (108)	A	7.9 ±0.7 (108)	Bab	7.8 ±0.7 (104)	c	6.7 ±0.5 (106)	b	8.5 ±0.5		9.1 ±0.5	
12.4 ±0.8 (108)	A	10.0 ±0.9 (106)	Aa	9.8 ±0.7 (102)	Ab	8.7 ±0.7 (102)	Bab	10.9 ±0.5		10.9 ±0.6	
12.4 ±1.9 (3)	Aa	8.3 ±1.4 (3)	Ba	10.0 ±1.4 (3)	Aa	8.2 ±1.1 (3)	Ba	8.9 ±0.9	b	10.3a ±1.0	a

R_h and R_s are in Mg C ha^{-1} yr^{-1}. Lowercase letters indicate significant differences between years within a site and microtopography, and between sites within a microtopography for the 3-years annual averages. Uppercase letters indicate significant differences between microtopographies (hummocks and hollows). NA = not available.

* Years are split up as follows: 1 = Apr15-Mar16, 2 = Apr16-Mar17, 3 = Apr17-Mar18.

Site-scale fluxes are calculated using equation 1 – 3 (Supplemental information 2) and proportions from Table 5.1.

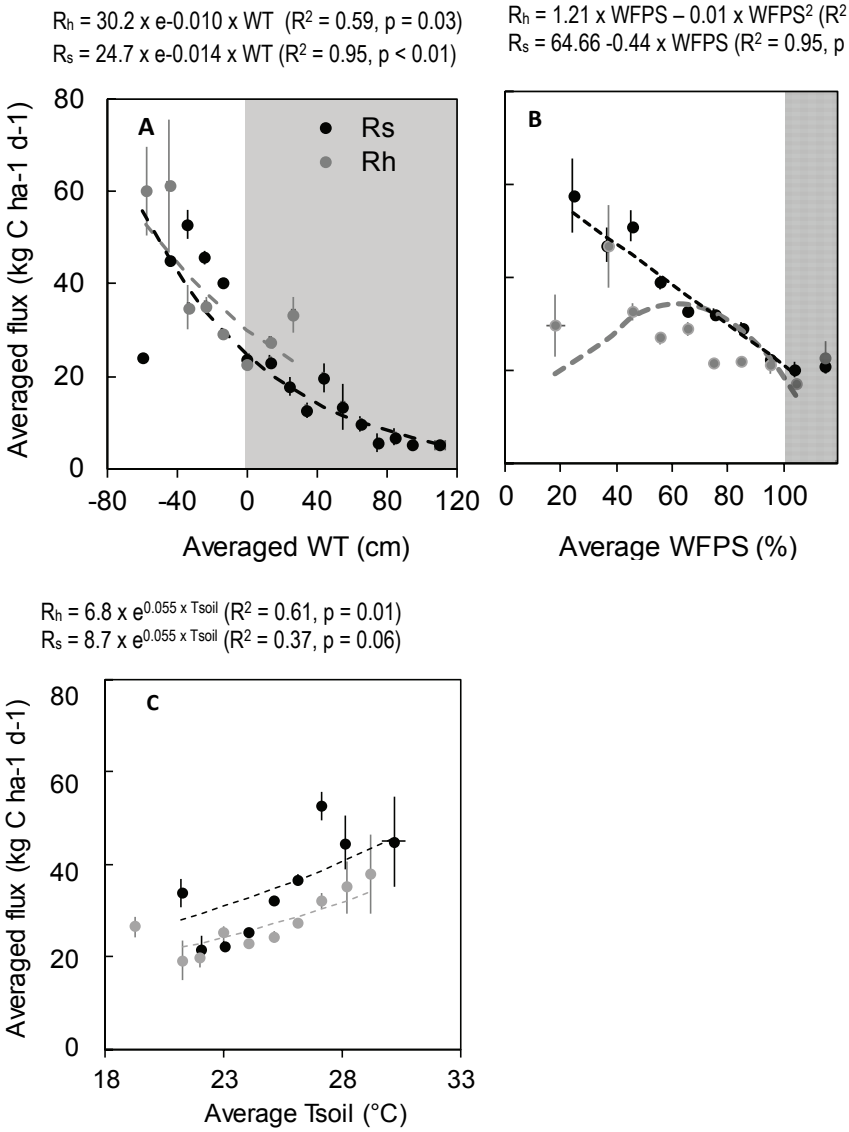

Figure 5.7 – Regressions between water table (WT), water-filled pore space (WFPS), soil temperature (T_{soil}) and average monthly total soil respiration (R_s) and heterotrophic soil respiration (R_h). Averages are calculated per intervals of 10 cm WT, 10% WFPS, and 1°C T_{soil}. Grey shading indicates flooded conditions. WFPS >104% (corresponding to WT above ground surface) were discarded from the regression.

5.4 Discussion

Recurrent and selective harvesting of female fruit-baring *M. flexuosa* palms turned the soil of the peat swamp forest (PSF) from a C neutral state at the I site (-0.1 ± 1.5) and at the mD site (-0.2 ± 2.2), into a net C source of -7.1 ± 1.4 Mg C ha^{-1} yr^{-1} at the hD site (Table 5.5). Results further indicate that harvesting of palms affects hummocks and hollows differently, and that the water table and water-filled pore space are important predictors of total and heterotrophic respiration.

5.4.1 Spatial and temporal variation of environmental factors and their relationship with respiration rates

Soil microtopography in PSFs is highly variable and consists of hummocks and hollows. Typically, hummocks have lower WFPS and higher root content than hollows, resulting in distinct respiration rates and spatial variability (Comeau et al., 2016; Hergoualc'h, Hendry, et al., 2017; Jauhiainen et al., 2005). Our results confirm these distinct characteristics, and indicated that hummocks were significantly drier and had higher total and heterotrophic respiration rates than hollows did (Table 5.2 and Table 5.4). This spatial variability of environmental factors and respiration rates can interact with temporal variability. For example, hummocks are slightly higher than hollows, and are therefore less sensitive to small water table fluctuations (Hirano, Jauhiainen, Inoue, & Takahashi, 2009; Swails et al., 2019). In our study site this was illustrated by the relationship

Table 5.5 – Soil net carbon balances at the intact (I), moderately degraded (mD) and heavily degraded (hD) sites in Iquitos, Peru. The balance is calculated by subtracting the inputs and outputs, negative values equal a carbon source. Litter and R_h rates are the averages from this study, root mortality rates are from Grandez-Rios (n.d.), and dissolved organic carbon (DOC) from Moore et al. (2013).

	Inputs		**Outputs**		**Balance**
	Mg C ha^{-1} yr^{-1}		*Mg C ha^{-1} yr^{-1}*		*Mg C ha^{-1} yr^{-1}*
	Litter	Root mortality	R_h	DOC	
I	5.1a ±0.71	3.4 ±1.3	7.9a ±0.3	0.6 ±0.0	-0.1a ±1.5
mD	5.8a ±0.57	2.0 ±0.8	7.3a ±2.0	0.6 ±0.0	-0.2a ±2.2
hD	2.3b ±0.62	1.5 ±0.7	10.3b ±1.0	0.6 ±0.0	-7.1b ±1.4

between R_h, R_s and WFPS that explained the higher total respiration rate measured at the hummocks, since hummocks more often reach values close to the optimum WFPS (Table 5.2). This is in line with studies from Indonesia that report higher total respiration rates from dry hummocks than wetter hollows (Jauhiainen, Takahashi, Heikkinen, Martikainen, & Vasander, 2005; Swails et al., 2019). The elevated heterotrophic respiration at hummocks in our study site could be due to higher decomposition rates, caused by, for example, more root exudates or a root-induced priming effect (Bengtson, Barker, & Grayston, 2012; Fu & Cheng, 2004).

Next to a spatial variability of WFPS and water table following the microtopography, we observed a seasonal cycle, with lower water tables and WFPS around August as compared to other months. In general, our study site was relatively wet; water table depths observed in Southeast Asia peatlands tend to be lower than -50 cm in the dry period (Jauhiainen et al., 2005; Lawson et al., 2015; Swails et al., 2019), whereas in our study location the water table rarely went below -25 cm at hollows. Whenever the WT did go below the surface level, heterotrophic respiration followed a bell-shaped relationship with WFPS (Figure 5.7b). The optimum at 60% WFPS was in line with values observed for incubated soils from the same sites (van Lent et al., 2019), and peat soils under palm cultivation in Indonesia (Husen, Salma, & Agus, 2014). Below this level the microbial activity is limited by water availability, and above it, oxygen deficiency hampers microbial respiration (Moyano, Manzoni, & Chenu, 2013).

Whenever WT was above the soil, and WFPS was 100%, total and heterotrophic respiration rates of ~10-20 kg C ha^{-1} d^{-1} were still observed. In waterlogged conditions oxygen for respiration is still available via diffusion trough the water column (Blagodatsky & Smith, 2012), and through aerating roots that have been described for *M. flexuosa* palms in the same site (van Lent et al., 2019). Such aerating roots are known to transport oxygen into the soil for a variety of plant functions, such as respiration (Colmer & Voesenek, 2009; Haase & Rätsch, 2010). When the water table further increased, surpassing these aerating roots, respiration rates further decreased towards zero (Figure 5.7).

Both R_s and R_h responded exponentially to changes in soil temperature despite a narrow range of temperatures between 19.2 and 30.2°C. The Q_{10} values of 1.7 for R_s

and R_h are slightly lower than the Q_{10} reported for Southeast Asia of 2.3 – 3.0 using field data (Hirano et al., 2009), and 2.3 using data from laboratory incubations (Brady, 1997). Air temperatures were much more variable than soil temperatures, which is explained by the general wet soil conditions that prevented a rapid warming of the soils. We further expect a low diurnal variation of soil respiration in our sites, because the average differences between soil temperature at the last measurement (6 pm) and first measurement of the next day (7 am) were only ~1.6°C (Supplementary Figure S5). Most of the soil temperature variation was observed between months (Supplementary Figure S4).

5.4.2 Inter-annual variation ENSO effects and the C dynamics

Our study included the very strong 2015-2016 *El Niño* Southern Oscillation event, during which we observed a peak in precipitation rates and an extreme flooding event (Figure 5.3). Contrary to our finding, *El Nino* events commonly result in a precipitation deficiency for the Iquitos region (Marengo, 1998), and previous flooding events of in 1998 and 2012 occurred during wetter-than-normal *La Niña* events (Espinoza et al., 2013; Kelly et al., 2014; Roucoux et al., 2013). Possibly, the 2015 flood was a combined effect of exceptional precipitation and an inflow from the nearby Itaya river, one of the tributaries of the Amazon River. This was also mentioned by Roucoux et al. (2013) for the 2012 flooding event, and reflects the minerotrophic status of the peat (Ca/Mg ratio > 6 in all sites, Supplementary Table S1). Water levels in the Amazon river represent a vast catchment area, and could have risen due to wetter-than-normal rainfall patterns along the west coast of tropical South America during *El Niño* episodes (Seneviratne et al., 2012). This could explain the high water table at our sites during the flooding event, and the lack of correlation between *El Niño*-induced droughts and the incidence of peat fires in the Peruvian Amazon (Lilleskov et al., 2018). The relationships between droughts and peat fires is much stronger for Indonesian PSFs, which are typically ombrotrophic bogs – les influenced by rivers – and, therefore, more sensitive to local precipitation anomalies as was shown by Swails et al. (2019) for the same 2015 *El Niño* event.

Irrespective of the cause of the flooding event, it provided an interesting case for studying the C dynamics of the peatland before and after such conditions. Soil

respiration and heterotrophic respiration were close to zero for three months, as was expected from the relationship between the water table and respiration rates outlined above. After the flooding event, leaf litterfall peaked during the subsequent months (Figure 5.5), due to an increased leaf senescence from understorey vegetation. Flooding is known to cause leaf senescence in various woody plant species, among other responses such as formation of adventitious roots or alterations in root and stem morphology (Kozlowski, 1997). Although wetland species are adapted to wet conditions, possibly the long duration of anoxic conditions during the flooding event led to prolonged stomatal closure and the production of phytotoxic compounds, leading to increased leaf senescence (Kozlowski, 1997; Pezeshki, 2001).

Since leaf litter decomposition (k = 0.84-1.17 years^{-1}) was twice the rate of root decomposition in our sites (k = 0.35-0.55 years^{-1}) (Supplementary Information 3 and Supplementary Figure S8), the C input from leaf litter contributes more to heterotrophic respiration than C from root litter. Thus, the increased litter fall following the flooding event provided an easy-decomposable C input, and likely caused the peak in heterotrophic and total soil respiration at nearly twice the rate measured before the flooding (Figure 5.6).

5.4.3 Site-scale total and heterotrophic respiration

Site-scale R_s at the intact site (11.4 ± 2.3 Mg C ha^{-1} yr^{-1}, Table 5.4) is in line with the 12.9 ± 2.1 Mg C ha^{-1} yr^{-1} average for PSFs of Southeast Asia (Hergoualc'h & Verchot, 2014), and more recent results from Indonesian primary and secondary PSFs of 12.3 ± 0.8 Mg C ha^{-1} yr^{-1} in (Swails et al., 2019), or 14.2 ± 1.1 Mg C ha^{-1} yr^{-1} (Saragi-Sasmito, Murdiyarso, June, & Sasmito, 2018). The moderately degraded site had a R_s that was 47 – 61% lower than in the other sites. The relationship between R_s and WFPS (Figure 5.7), combined with the average *in situ* WFPS per site (Table 5.2), would explain a ~30% lower R_s at the mD site compared to the other sites. This indicates that WFPS is an important factor for site-scale differences, but that a part of the variation could be explained to other factors such as forest degradation (see paragraph 5.4.4).

Site-scale R_s rates did not include a distinction between areas around trees and palms, as those areas were assumed to respire at similar rates as the hollows

around palms. Indeed, during the first year the inclusion of respiration rates measured around trees did not impact site-scale fluxes at the intact site (<2% lower, *data not shown*). During the second and third year this difference was larger (9%), but remained within the standard error of the site-scale R_s flux. In degraded sites, this bias is even less important since the density of trees reduced with increased levels of degradation (Figure 5.2a). Accurately including the area represented by trees and including an effect of tree harvesting on site-scale respiration rates would have required an experimental setup with measurements around trees in all sites, including trenches for heterotrophic respiration rates. However, as outlined above, these effects are likely overshadowed on the site-scale by effects of *M. flexuosa* harvesting and subsequent changes in hummock number and size (Figure 5.2b and c).

Heterotrophic respiration at the I and mD site (7.9 and 7.3 Mg C ha^{-1} yr^{-1}, respectively) were in line with common values for forested peatlands (Hergoualc'h & Verchot, 2014). However, even though our sites were not drained or affected by fire, the heterotrophic respiration at the heavily degraded site (10.3 ± 1.0 Mg C ha^{-1} yr^{-1}) was more similar to heterotrophic respiration rates in drained and burnt peatlands in Southeast Asia (9.5 ± 1.1 Mg C ha^{-1} yr^{-1}).

Separating R_h from R_s is crucial for calculating the C balance of the peat. We applied the trenching method for excluding root respiration from total respiration, which assumes that the remaining fraction measured inside trenches represents the heterotrophic respiration. Although this was the most appropriate method for obtaining plot-scale measurements in a palm-dominated ecosystem, it involved a major soil disturbance at the onset of the experiment such as induced root decomposition and altering the soil moisture (Subke et al., 2006). On the other hand, the exclusion of roots reduces root exudates that would otherwise provide labile C for soil microbes and contribute to heterotrophic respiration rates.

At hummocks the contribution of R_h to R_s in hummocks was 44% at the intact site, and at the degraded sites it varied between 64 – 92% (Table 5.4). However, at hollows several times R_h was larger than nearby measured R_s, resulting in a R_h /R_s ratio larger 1 (see Supplementary Figure S6). Spatial variability could explain this, for example whenever fluxes are very low and the ratio is affected by small

absolute respiration rate changes. However, we made sure to not consequently overestimate R_h rates as discuss below.

Root growth back in to trenched zones was not observed and would have resulted in a steady increase of respiration rates inside trenches over time, as measured fluxes would include root respiration. In addition, there was no significant effect of time since trenching on the observed R_h /R_s ratios, whenever the first 90 days were excluded. Likely the enhanced decomposition was dominated by the temporal and spatial variation of the respiration rates. A root decomposition experiment indicated that 50% of the fine root biomass of *M. flexuosa* and dicot roots is left after 443 and 612 days (Grandez Rios, n.d.). Although this omits the decomposition of coarse roots, it indicates the very gradual decomposition of roots inside trenches. Such low decomposition rates are in line with Chimner & Ewel (2005), and indicate the importance of roots over aboveground litter for the peat accumulation in tropical systems. Additional analyses showed that there was a strong link between the water table and R_h /R_s ratios (Supplementary Figure S7). At flooded conditions, especially in hollows, the R_h /R_s ratio was >1. Correcting monthly measured respiration rates for spatial soil moisture variations between trenched plots non-trenched, did not improve the results. However, whenever the water table was below the surface, the R_h/R_s was 48%, 74% and 78% in hummocks and 57%, 91%, 98% in hollows at the I, mD and hD sites, respectively. For the intact site this was close to average of 53% presented by Hergoualc'h & Verchot (2014), but for the degraded sites were similar to observation made in oil palm plantations on peat. There, root respiration decreases with distance from the palm, and measurements far from palms represents heterotrophic respiration rates (Dariah, Marwanto, & Agus, 2014; Matysek, Evers, Samuel, & Sjogersten, 2018), although others indicate this would overestimate the heterotrophic respiration rate by up to 21% (Hergoualc'h, Hendry, et al., 2017). While oil palm plantations commonly do not have undergrowth and we measure in natural systems, our results indicate that heterotrophic and not root respiration is much more important in hollows.

Since the site-scale R_h fluxes are >85% based on fluxes in hollows (Table 5.1), the measurements of R_h inside trenches are of great importance for the presented site-scale carbon balance. If we multiply average site-scale total

respiration with the R_h/R_s ratio for WT < 0 cm, we get R_h rates of 6.6, 5.3 and 8.9 Mg C ha^{-1} yr^{-1}. This would change the overall C balance of the I and mD site to net sinks of C (1.3 and 1.8), and the hD site to a smaller source (-5.7). Therefore, if corrected for the R_h/R_s ratio, the main conclusion of our study remains that heavily degradation turns these PSFs into a significant C source of 7.0 Mg C ha^{-1} yr^{-1} relative to the intact site for the corrected and non-corrected C-balances, respectively.

5.4.4 Effect of forest degradation on the peat carbon balance

Forest degradation alters the species composition and structure of palm swamp forests (Bhomia et al., 2019; Hergoualc'h, Gutiérrez-Vélez, Menton, & Verchot, 2017). Recurrent harvesting resulted in a lower density of palms and trees in degraded sites (Figure 5.2). The heavily degraded site had 81% less *M. flexuosa* palms compared to the intact site, which was similar as other location in the Pastaza-Marañón basin (89%) (Hergoualc'h, Gutiérrez-Vélez, et al., 2017). These lower palm and tree densities reduced the input of C from litterfall and roots at the site-level (Table 5.5). However, for a wide range of sites throughout the Peruvian Amazon there was no clear link between forest degradation and belowground C stocks (Bhomia et al., 2019), which typically contain 70-90% of the total ecosystem C stock.

Nevertheless, ultimately peat formation is a very gradual process, and per definition is the result of more C input from its vegetation than C output through heterotrophic respiration, dissolved organic matter and physical removals. The negative C balances at the heavily degraded site is mostly caused by a reduction of C inputs (45%), instead of increased C outputs (28%). This trend between sites is illustrated by trends we observed at the micro-scale within sites. Hummocks with standing palms had higher R_h rates than hummocks supporting the stump of harvested *M. flexuosa* palms. This is likely explained by the continued fresh C input from root mortality and leaf litter that drives R_h at hummocks with standing palms, while these inputs are lacking at the hummocks with cut palms. There, the observed R_h likely originates from decomposing older organic matter such as dead roots and leaf litter that remained after palm-harvesting. Possibly, directly after palm-harvesting, respiration rates could spike similarly as we observed after

the flood-induced leaf senescence in our site (Figure 5.5), or the 90-days increased root decomposition after trenching is performed (Supplementary Figure S1), and as has been shown in an Indonesian PSF to last even longer (Hergoualc'h, Hendry, et al., 2017). Over the long run, the increased R_h (C output) at hummocks with cut palms will settle at lower levels, and combined with the lack of fresh litter input will result in a net loss of C in these areas. Indeed, we observed a loss of carbon from these hummocks that were on average 32% smaller than their live-palm counterparts (Figure 5.2c).

Overall, our results show that anthropogenic forest degradation on natural peatlands could lead to a peat soil that turns into a significant carbon source. As recurrent harvesting is on-going, and has been a common practice for many decades (Virapongse et al., 2017), a measurable reduction in soil C stocks following recurrent *M. flexuosa* harvesting within decades could be expected. This highlights the importance to study and measure the effects of land use on the carbon balance in tropical peat swamp forests, even if its land use does not entail drainage or burning.

5.4.5 Regional and global impact of *M. flexuosa* harvesting

Many *M. flexuosa* palm stands in the Pastaza-Marañón basin are male-dominated due to recurrent selective harvesting of female palms for their fruit (Horn et al., 2012; Kahn, 1988), which eventually reduces recruitment of *M. flexuosa* seedlings and a decrease in population (Holm, 2007). Thus, even in situations where an apparent intact *M. flexuosa* dominated PSF is observed, disturbed seedling recruitment could result in an indirect and additional decrease of *M. flexuosa* stem densities over the long term. If such shifts in vegetation resemble the heavily degraded site, it would turn peat soils into a significant C source.

Unfortunately, an exact assessment of degraded *M. flexuosa*-dominated peat swamp area is unavailable to date. Horn et al. (2018) documented the widespread extent of *M. flexuoasa* harvesting throughout the Peruvian Amazon, with around 1,000 MT of fruits shipped from various points in the Pastaza-Marañón basin, and indicates that harvesting of *M. flexuosa* palms is spread troughout the Peruvian Amazon. The exploratory study by Hergoualc'h, Gutiérrez-Vélez, et al. (2017) estimated for a 351,324-ha area within the Pastaza-Marañón basin that 31% was

classified as heavily degraded, and 42% as moderately degraded. The moderately degraded site in our study, however, had a similar stem density compared to the intact site (3% reduction), and was not comparable to the classification as medium degraded used in Hergoualc'h, Gutiérrez-Vélez, et al. (2017). Combining this estimated heavily degraded area with our net C fluxes from the heavily degraded site, would entail a net annual emission of 7.8 Tg C yr^{-1} for the entire Pastaza-Marañón basin (3,560,000 ha).

Other countries where *M. flexuosa* palms grow include Colombia and Brazil. There, leaves are used for local construction work and, moreover, the oil from fruits is commercialized for the international cosmetics market (Virapongse et al., 2017). Exact quantification of the magnitude of these markets, and the extent to which fruits are harvested from *M. flexuosa* stands on peat remains unknown. However, the estimated peatland area in the Brazilian and Colombian Amazon total at 387,200 km^2 (Gumbricht et al., 2017), and would argue for a further study and quantification of forest degradation on peat throughout the Amazon.

In the context of global warming, the hydrological cycle in the Amazon intensified during the past decades, and – for example – led to an increase in extreme floods and droughts (Gloor et al., 2015). If such prolonged and severe flooding events continue to occur it could be expected that peat swamp forests near rivers undergo similar disturbances as we observed. Vegetation development and succession during the last centuries in the Quistococha peatland was highly dynamic, and is affected by rapid changes in fluvial influence, such as the frequency and duration of flooding that can change the vegetation composition (Roucoux et al., 2013). The increase in extreme flooding events might contribute to shifts in vegetation, especially if such trends are combined with anthropogenic forest degradation. Subsequently, our results indicate that such shifts could lead to a situation with lower C input than C output into the soil, and causing the PSF to change into a significant C source (hD site, Table 5.5).

In order to prevent major C emissions from Amazonian peatlands dominated by *M. flexuosa*, its conservation and sustainable management should therefore be aimed at maintaining palm stem densities and promote sustainable harvesting practices such as climbing instead of felling. This would not only maintain a sustainable population growth with sufficient recruitment of new seedlings, it

would also protect the C stored in the peat under these *M. flexuosa* stands. Ultimately, this would conserve the sustainable livelihood for many communities living in the Amazon and provide an important global C sink.

5.5 Acknowledgements

This research was made possible through support to CIFOR by the United States Agency for International Development (Grant number: AID-BFS-G-11-00002) as part of the CGIAR research programs on Forests, Trees and Agroforestry and Climate Change, Agriculture and Food Security (CCAFS). We would like to extend our gratitude towards our partners at the Instituto de Investigaciones de la Amazonía Peruana (IIAP) in Iquitos, and we would especially like to thank Dr. Dennis del Castillo Torres and his team for their support. The government of Loreto is greatly acknowledged for providing acces to the Quistococha Park. We would further like to thank Nicole Mitidieri Rivera for her hard work in the field, and above all this research would not have been possible without the support of the inhabitants of the villages San Julian and Las Brisas, a special thanks to Ulises Mozombite Murayari for his endless effort and hard work.

5.6 Appendix

5.6.1 Ratio of heterotrophic soil respiration to total soil respiration following trenching

At the intact and heavily degraded sites, soil heterotrophic respiration spiked in the first 90 days after trenching (Figure S1) likely as the result of freshly excised roots. Results at the moderately degraded site are not displayed, since the site was flooded in the months following trenching and no data could be collected from the tenches. Therefore, heterotrophic soil respiration and total soil respiration rates from the first three months were discarded from annual flux calculations.

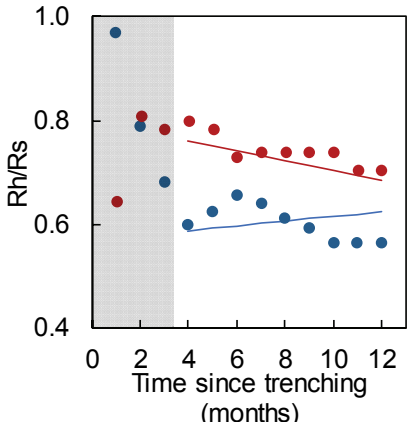

Figure S1 - Monthly average ratio of heterotrophic soil respiration to total soil respiration (Rh/Rs) during the first year after trenching at the intact site (blue circle) and heavily degraded site (red circle). The grey area indicates the first 3 months after trenching which results were discarded from annual computations. The linear regression lines exclude the first three months.

5.6.2 Supplemental Information 2. Inventory of vegetation and microtopography and computation methods for upscaling soil respiration and litterfall

We inventoried the density *of M. flexuosa* palms (stem height > 5 m) and dicot trees (diameter at breast height > 10 cm), and the surface of hummocks with standing live palms and with cut palms in three plots totaling 0.66 ha per site. A stem height of > 5 m for *M. flexuosa* palms was considered because smaller, younger individuals lacked the presence of a hummock. The results of the inventory are presented in Figure 5.2 of the manuscript.

The area of hummocks with standing live or cut palms within each site was calculated as:

$$A_{humAP,\ humCP} = \sum \pi \times r_{humAP,\ humCP}{}^2 - \pi \times r_{palm}{}^2 \qquad \text{eq. 1a}$$

Where $A_{humAP,\ humCP}$ is the area (ha) of hummocks with standing live (AP) or cut palms (CP), $r_{humAP,\ humCP}$ is the radius of the hummock with a standing live or cut palm and r_{palm} the radius at breast height of the standing live palms, or the radius of the stump of a cut palm. The palm radius was subtracted since the area it occupies does not respire.

The remaining soil surface within the site was classified as hollow and its area computed as:

$$A_{holAP} = \left(A_{plot} - A_{humAP} + A_{humCP} \right) \times A_{humAP} \div \left(A_{humAP} + A_{humCP} \right) \qquad \text{eq. 1b}$$

$$A_{holCP} = \left(A_{plot} - A_{humAP} + A_{humCP} \right) \times A_{humCP} \div \left(A_{humAP} + A_{humCP} \right) \qquad \text{eq. 1b}$$

Where A_{hol} is the area characterized as hollows around AP or CP within each site, and A_{plot} is the area (ha) of the plot where densities and areas were sampled. The relative proportion of hummocks with standing live palms (P_{humAP}), hummocks with standing cut palms (P_{humCP}) and their surrounding hollow areas (P_{holAP} and P_{holCP}) at a given site was then calculated as:

$$P_{humAP} = \frac{A_{humAP}}{A_{plot}} \quad \text{eq. 2a}$$

$$P_{humCP} = \frac{A_{humCP}}{A_{plot}} \quad \text{eq. 2b}$$

$$P_{holAP} = \frac{A_{holAP}}{A_{plot}} \quad \text{eq. 2c}$$

$$P_{holCP} = \frac{A_{holCP}}{A_{plot}} \quad \text{eq. 2d}$$

Monthly average R_s and R_h rates were calculated from the nine replicated plots per site (I, mD, hD), palm status (standing live or cut palm) and microtopography (hummock and hollow). At the intact site, monthly average Rs of dicot trees was also computed from nine replicates per microtopography. Annual respiration rates were obtaining by integration of monthly averages applying a linear interpolation between measurement dates, for each year in which measurements overlapped (year 1: from April 2015 to March 2016; year 2: from April 2016 to March 2017; year 3: from April 2017 to March 2018) (see Table 5.4 main manuscript).

Site-scale annual respiration rates were computed by considering the heterogeneity in microtopography (hummocks and hollows) and degradation (live and cut palms) as follows:

$$R_{jk} = P_{humAP,j} \times AF_{humAP,jk} + P_{humCP,j} \times AF_{humCP,jk} + P_{holAP,j} \times AF_{holAP,jk} + P_{holCP,j} \times AF_{holCP,jk} \quad \text{eq. 3}$$

Where R_{jk} is the annual R_s or R_h rate at site j (j = I, mD, hD) and year k. AF is the annual respiration obtained by linear interpolation of monthly fluxes averaged across replicates (n = 9), measured in hummocks (hum) with a standing live (AP) or cut palm (CP), and the surrounding hollows (holAP and holCP, respectively) in site j and year k.

The annual R_s rate measured around dicot trees was not considered in site-scale respiration which aimed at comparing impacts of *M. flexuosa* degradation and effects on hummock and hollow densities. The spatial stratification between hummocks and hollows covered most of the spatial variation at the site level. Respiration close and far to dicot trees were not significantly different and almost

exactly the same (Table 5.4, main manuscript), thus impacts of degradation were assumed to be less prominent as was observed for *M. flexuosa*. The hypothesis was that measurements from hollows around *M. flexuosa* palms would be equal to the measurements around dicot trees, which was true for the first year but thereafter changed. However, annual fluxes with and without including measurements around dicot trees did not substantially change site-scale fluxes, which is discussed in the main manuscript (paragraph 6.2).

Site-scale annual litterfall rates were computed considering the densities of dicot trees and *M. flexuosa* palms. These were calculated relative to the densities measured at the intact site.

Proportion intact site = 1 eq. 4a

Proportion degraded sites =
degraded site stems ha^{-1} / intact site stems ha^{-1} eq. 4b

These proportions were multiplied by the site-scale average litterfall rates, separated for each litterfall category. Categories for dicot tree proportions were dicot leaf litterfall and branch fall; for *M. flexuosa* these were leaves and trunks (see main manuscript paragraph 2.5). Lastly, the total litterfall was the sum of all categories per site per year.

Table S1 – Soil (0–5 cm) properties in hummocks (hum) and hollows (hol) at the intact (I), moderately (mD), and heavily (hD) degraded sites. Averages are given with standard errors. All properties were measured in triplicates, except for bulk density (n = 9).

Site	Spatial position	Bulk density	Ca	K	Mg	Na	CEC	Base Sat.	Ca/Mg	Cu	Mn	Zn	P	%N	%C	C/N
I	Hum	0.093 ±0.006	3911 ±1126	528 ±93	654^{A} ±7	52^{B} ±5	82.4 ±2.3	32 ±6	6.0^{B} ±1.8	0.21 ±0.02	137^{A} ±18	10.0 ±2.3	274 ±20	2.5 ±0.0	45 ±1	17.9^{A} ±0.5
	Hol	0.080^{a} ±0.005	5554^{ab} ±462	269 ±76	321^{B} ±14	89^{A} ±1	68.9 ±6.1	47 ±6	17.5^{A} ±2.2	0.19 ±0.02	24^{Ba} ±3	11.2 ±0.4	176 ±41	2.7 ±0.2	43 ±3	16.3^{B} ±0.4
mD	Hum	0.100 ±0.003	5028 ±1145	492 ±63	444 ±53	66^{B} ±6	77.0 ±5.2	39 ±6	11.5 ±2.3	0.20^{A} ±0.02	238^{A} ±60	9.9^{B} ±1.9	272 ±26	2.4^{B} ±0.1	43 ±1	17.7 ±0.9
	Hol	0.092 $\pm0.002^{a}$	4087^{a} ±298	459 ±74	307 ±25	104^{A} ±11	70.1 ±2.3	35 ±2	13.4 ±1.1	0.12^{B} ±0.01	52^{Bab} ±7	16.8^{A} ±0.9	222 ±63	2.8^{A} ±0.0	46 ±0	16.0 ±0.1
hD	Hum	0.104 ±0.008	6768 ±434	783 ±137	502 ±70	122 ±43	72.0 ±5.9	58 ±7	14.5 ±2.8	0.19 ±0.01	96 ±2	9.0 ±0.7	76 ±21	2.5 ±0.1	35 ±2	14.4 ±0.5
	Hol	0.107^{b} ±0.004	7397^{b} ±92	537 ±126	491 ±61	58 ±5	68.3 ±1.9	63 ±2	15.9 ±2.3	0.20 ±0.02	85^{b} ±6	10.6 ±1.8	67 ±16	2.5 ±0.1	35 ±2	13.9 ±0.2

Uppercase letters indicate a significant difference between hummocks and hollows within a site, small case letters indicate a significant difference between sites within a spatial position. No letters are displayed in the absence of a significant difference.

Bulk density is in g d.w. cm^{-3}, Ca, K, Mg, Na, Cu, Mn, Zn, P are in mg kg^{-1}, Cation exchange capacity (CEC) in cmolc/kg and base saturation, C and N contents in %.

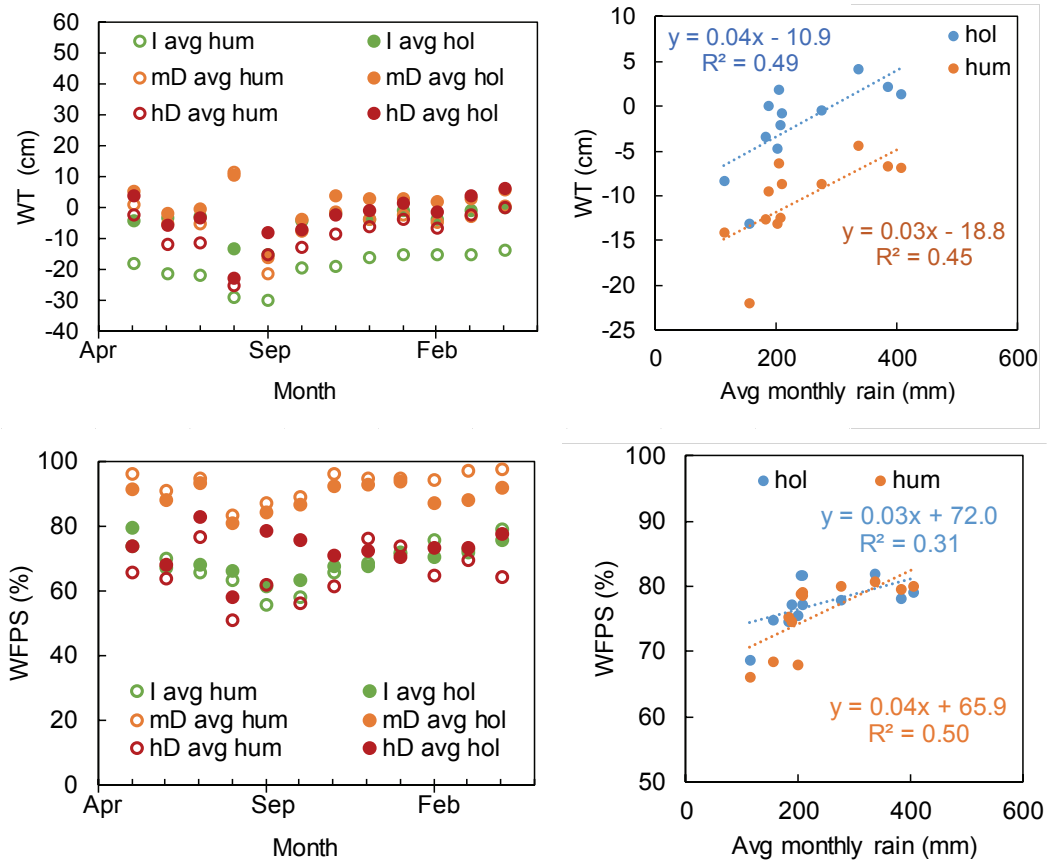

Figure S2 - Average water table (WT), water-filled pore space (WFPS) at the intact (I), moderately (mD) and heavily degraded (hD) sites at hummocks (hum) and hollows (hol). Measurements during the *El Nino* flooding event are excluded in these figures. Overall, August and September have significantly lower WT levels ($p < 0.01$), August has lower WFPS % ($p = 0.02$).

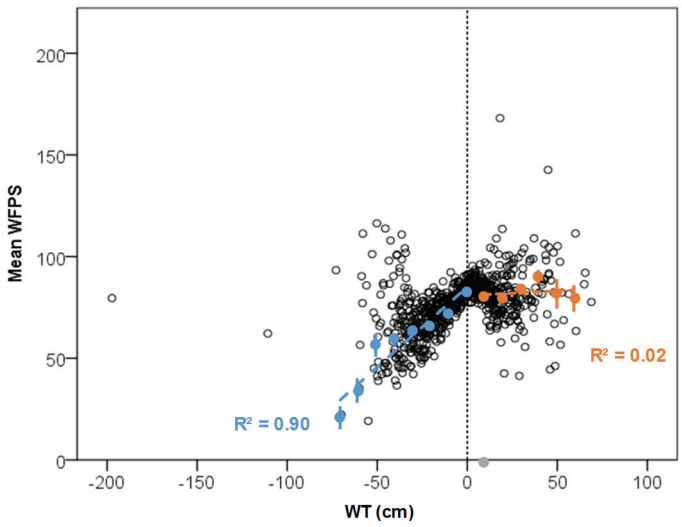

Figure S3 - Mean water-filled pore space (WFPS) and water table (WT) values for all sites (open black circles). Blue and red points indicate average WT and WFPS values, and dashed colored lines are their regression lines. Whenever WT is <0 it correlates well with the WFPS.

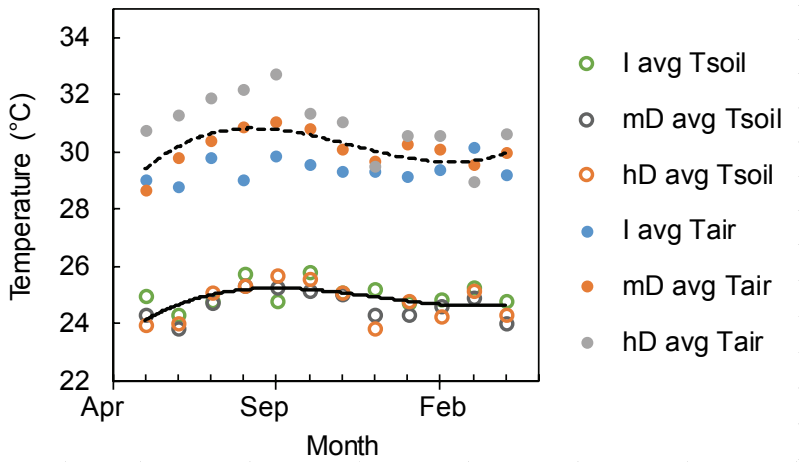

Figure S4 - Average soil (Tsoil) and air (Tair) temperature at the intact (I), moderately (mD) and heavily degraded (hD) sites. Hummocks and hollows did not differ and values presented are the averages. Measurements during the *El Nino* flooding event are excluded in these figures. The air temperature cycle was similar to the yearly water table cycle, but not significant. However, whenever the WT was lower than -40 cm, the air temperature was 1.5 to 3.6 °C higher as compared to months with a WT of -40 cm or higher. The same holds for soil temperatures, but to a smaller degree (0.1 to 1.1 °C).

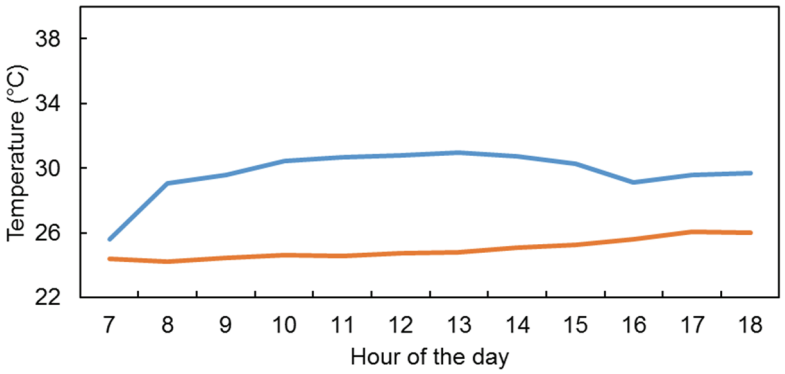

Figure S5 – Average daytime soil (red) and air (blue) temperature variability for all measurements at all sites combined. Averaged soil temperature difference between 18.00 hour and 7.00 hour is 1.6 °C.

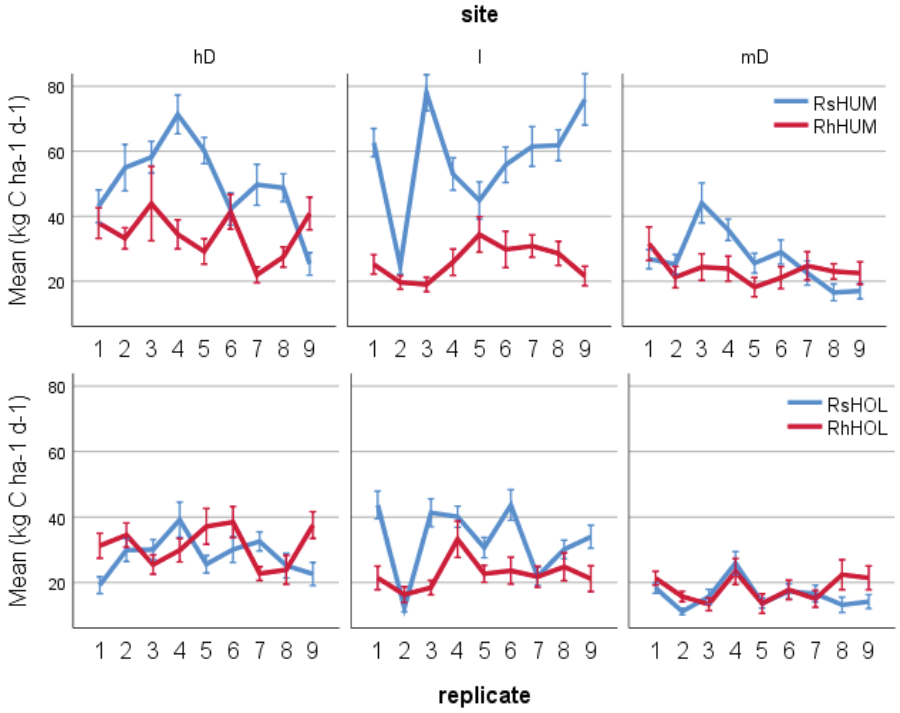

Figure S6 – Average heterotrophic (Rh) and total soil respiration ratio (Rs) at the intact (I), moderately (mD) and heavily degraded (hD) sites for hummocks (hum, top panels) and hollows (hol, lower panels) for each of the 9 replicates per site. Error bars represent one standard error. Several replicates show on average higher Rh rates than Rs rates.

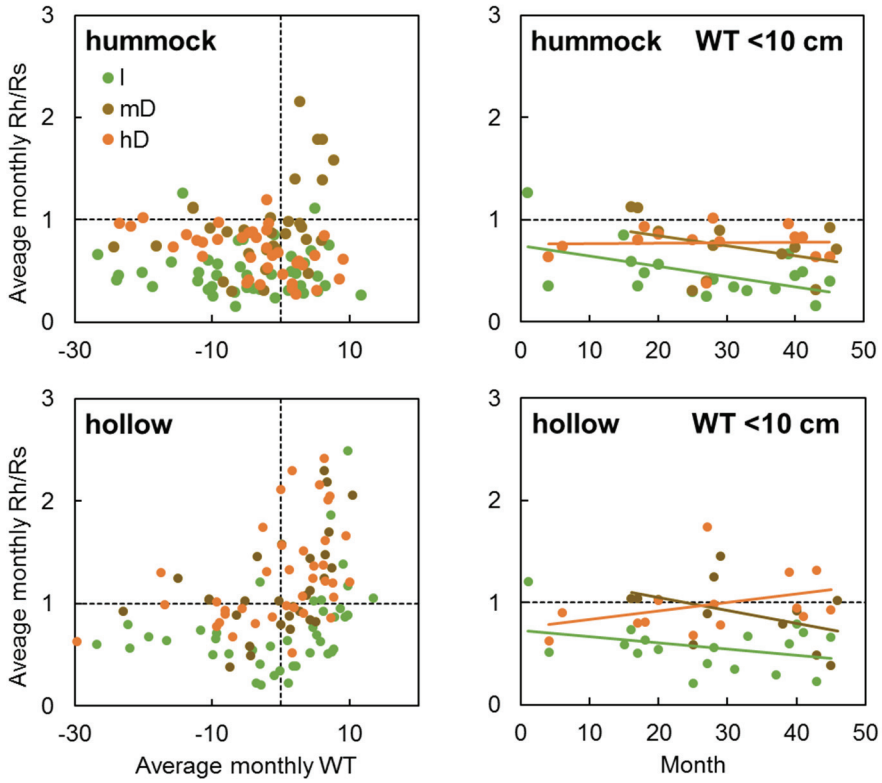

Figure S7 – Link between water table (WT) and the heterotrophic respiration (Rh) to total soil respiration (Rs) ratio in hummocks and hollows at the intact (I), moderately (mD) and heavily degraded (hD) sites. Rh/Rs ratios bigger than 1 were predominantly observed at WT levels larger than zero.

5.6.3 Supplemental Information 3. Litter decomposition experiment

Slow degradation of litter from peat swamps due to poor litter quality provides a potential mechanism for peat accumulation (Cornwell et al., 2008; Zhang et al., 2008). Root litter as opposed to leaf litter is hypothesized to drive peat formation, as the litter is predominantly produced in the anaerobic soil layers (Hoyos-Santillan et al., 2015; Chimner and Ewel, 2005).

The objective of the decomposition experiment was to assess if the decomposition speeds vary along the degradation gradient. This would indicate if the forest degradation for example exerts an effect decomposition speeds, either through litter quality differences (e.g. species composition and C/N changes) or environmental factors (e.g. WT or WFPS).

A litterbag experiment was performed with leaf litter collected at each site. Litter consisted of freshly fallen litter from the forest floor. Homogenized samples with intact leaves (3 g dry weight) were placed in fiberglass mesh bags (15 x 15 cm, 750 µm), with aluminum tags. Per section 27 bags were placed on top of the soil litter in each site (in total 243). During every timestep triplicates of litterbags were collected per section, gently rinsed in the Quistococha research laboratory, checked for new root growth inside the bags and then dried at 60°C to constant mass. Dry weights were used to calculate the decomposition decay constant (k) from linear regression of the percentage of initial mass remaining over time ($\mathrm{Ln}(X_n/X_0) = -kt$). And data was fitted to the exponential decay model ($X_n = X_0 \times e^{-kt}$) (Olson, 1963).

Results show that decomposition rates were 0.99 ±0.05, 1.17 ±0.05, and 0.84 ±0.05 years^{-1} in the I, mD and hD sites, respectively (Figure S8). These values are comparable values ranging from 0.33 to 1.49 years^{-1} in other tropical ecosystems (Hoyos-Santillan et al., 2015). Decomposition rates for roots from the same sites are around twice as low and vary between 0.35 and 0.55 years^{-1} (Grandez Rios, n.d.). This indicates that roots play a more important role in the C balance of the peat soils, whereas litter produced aboveground is relatively quickly decomposed.

Differences between sites were significant, where hD > I > mD. As the degradation gradient is not reflected in this order, it would appear that average water table at the sites would better explain the differences in decomposition (Figure S8).

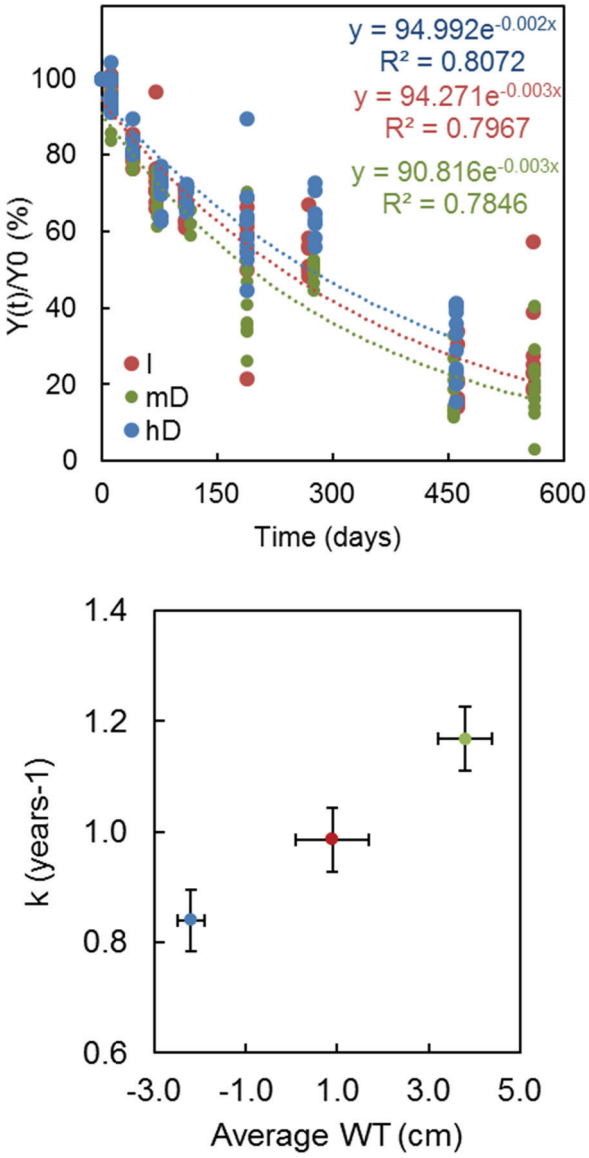

Figure S8 – Percentage of initial mass over time (left pane) and average decomposition speed (*k*) and water table (WT) (right pane) at the intact (I), moderately degraded (mD), and heavily degraded (hD) sites.

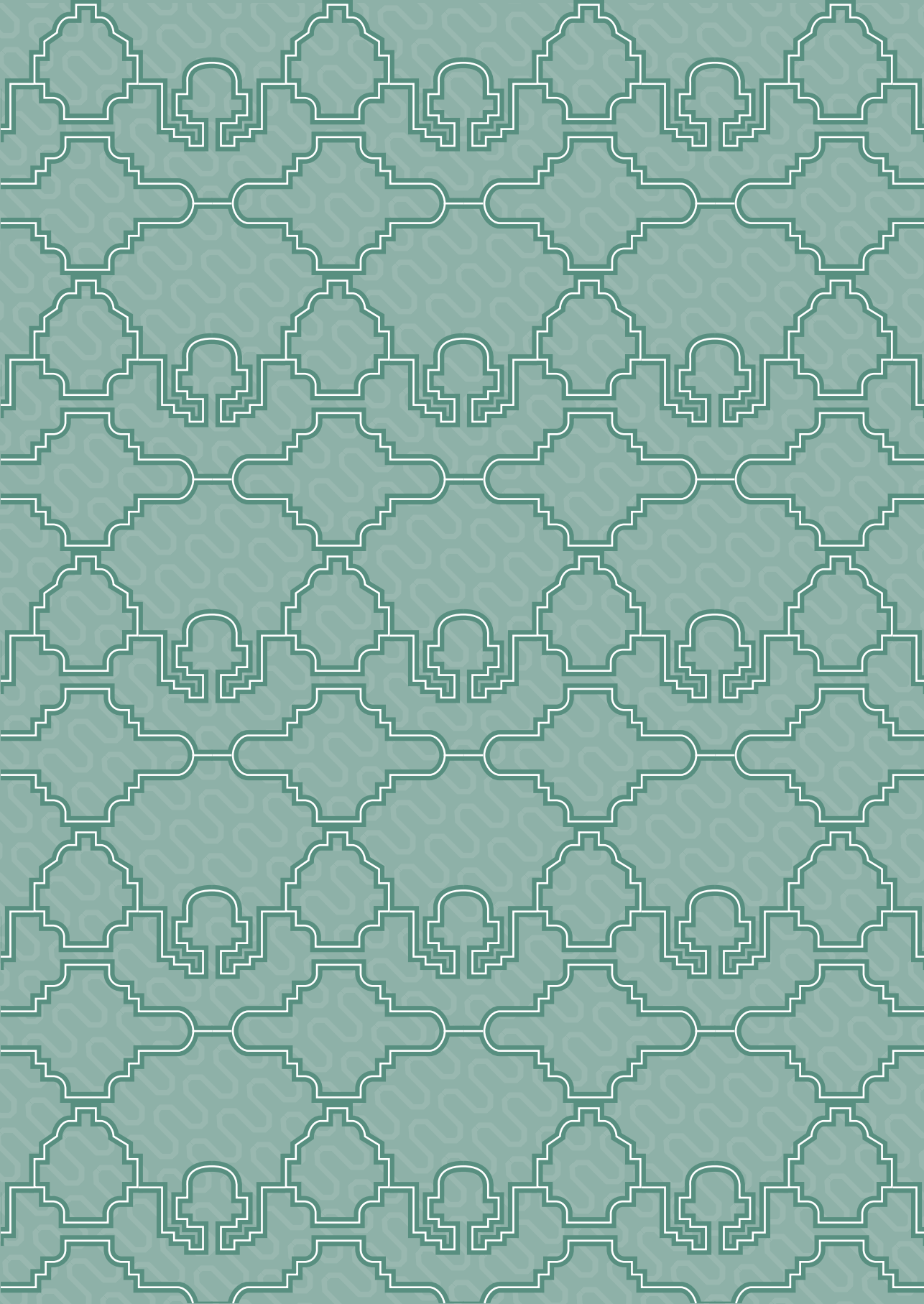

6

General discussion

6 General discussion

The overall goal of my thesis was to increase the mechanistic understanding of the effects of forest conversions on GHG emissions in the tropics, and to contribute to the derivation of robust emission factors for land-use change in the tropics. I aimed to systematically review all studies on N_2O and NO emissions from land use and land-use change in the tropics; to improve current emission factors for land use and land-use change in the tropics; and to examine CO_2, N_2O and CH_4 emissions from a region-specific land use not studied to date: forest degradation in tropical peatlands of the Amazon. For this unique land-use change category, I investigated the effects of forest degradation on ecosystem C-stocks and the soil C balance in a four-year field experiment.

In this chapter I will give a brief summary of the main findings of my thesis research (paragraph 6.1), followed by a general discussion of the main findings and the hypotheses that were outlined in the introduction (paragraph 6.2, 6.3 and 6.4). Subsequently, the main limitations of my research are discussed, as well as some suggestions for future research (paragraph 6.5).

6.1 Summary of main findings

Chapter 2 presents a meta-analysis of reported N_2O and NO emissions from forest conversions in the global tropics. The aim was to provide an updated overview of N_2O and NO emission rates, and determine trends in fluxes after forest conversion. The main finding was that undisturbed tropical forests emit 2.0 kg N_2O-N ha^{-1} yr^{-1} on average, and that emission rates significantly increased after conversion to cropland. Nitrogen (N) input from fertilization was the most important proxy for N_2O emissions at a rate of 1.9% of the N input, which was higher than the 1% IPCC Tier 1 default value (IPCC, 2006). Moreover, time since conversion was an important factor for both unfertilized and fertilized LUCs during the first 10 years after conversion. Few studies have measured emissions from land following the conversion of forest to crop land used to grow important world crops such as soy and oil palm, and very few studies have been conducted in Africa. Tropical wetlands have been exclusively studied in Southeast Asia, while there are also extensive tropical wetlands in South America and Africa. Based on these findings,

I focused my experimental thesis research further on land uses on tropical wetlands in South America.

South America harbours one of the largest areas of tropical peatlands worldwide, with large stretches of shallow peat previously unaccounted for in the Amazon basin (Gumbricht et al., 2017; Draper et al., 2014; Lahteenoja et al, 2011). Experimental data on effects of land use and land-use change on GHG emissions in these peat swamp forests (PSFs) are almost totally absent in the literature. Therefore, I focused on GHG emissions from PSF degradation in the Amazon basin. Most studies on PSF are related to conversion and drainage activities, while in the Amazon the common land use on peat is harvesting of female *M. flexuosa* palms for their fruits. This unique, but widely applied type of forest degradation on peat occurs in relatively remote natural stands throughout the Amazon. Contrary to PSFs in Southeasts Asia, these systems are not drained, nor fertilized.

Chapter 3 explored potential effects of palm harvesting on C losses. Total ecosystem C stocks, floristic composition and degradation status were measured in three regions and twelve sites throughout the Pastza-Marañón river basin in the Peruvian Amazon. Total ecosystem C stocks ranged from 200 to 1600 Mg C ha^{-1} with peat depths up to 2.8 m. These C stocks are immense in comparison to typical tropical rainforests, which have C stocks ranging between 130 and 240 Mg C ha^{-1}, but are relatively small in comparison to common values of 1000 up to 7500 Mg C ha^{-1} stored in Southeast Asian peat deposits of up to 12 m deep (Warren et al., 2017).

Degradation status in the Peruvian PSFs ranged from low to high levels of disturbance with no significant difference between regions. This indicated that degradation is not regional, but occurred throughout the Pastza-Marañón river basin – parts of which are inside a national reserve. Degradation status correlated negatively with palm vegetation C stock, but not with soil C stocks. Thus, C-stock differences between sites could not be used to estimate C losses from the soil following palm-harvesting.

Chapters 4 and 5 present the results of a detailed gain-loss experiment to further study the C balance of peat soils following PSF degradation at three sites. In Chapter 4, factors were studied that drive GHG fluxes, and that were hypothesized to be affected by degradation. These were (1) water table

fluctuations and WFPS% as a proxy for soil aeration, (2) microtopography of the soil surface area in terms of hummock and hollows, (3) soil organic matter quality derived from litter input, and (4) presence of aerating roots that emit CH_4. Microtopography and soil organic matter quality (factors 2 and 3) were found to be the most important factors explaining effects of forest degradation on soil GHG fluxes in PSFs.

Chapter 5 presents the effects of palm-harvesting on the soil C balance. Palm-harvesting affected the microtopography and reduced the number and size of hummocks. Heavily degraded sites had a larger part of their soil surface area classified as hollows. In addition, heterotrophic respiration at hollows increased following degradation, resulting in a larger C output from degraded soils. Water table and WFPS% fluctuations appeared not to affect these trends; these fluctuations mostly affected seasonal respiration fluctuations. I concluded that larger heterotrophic respiration rates in hollows are related to changes in litter quality and quantity. *In vitro* incubated soils from the degraded sites consistently produced more carbon dioxide (CO_2) than soils from less disturbed palm swamp sites (Chapter 4). This was confirmed by *in situ* measurements during ~4 years, with significantly higher heterotrophic respiration rates at the highly degraded site than at the intact site (Chapter 5).

Lower palm and dicot tree stem densities at the heavily degraded site resulted in lower leaf- and wood fall rates. The combined effects of more C output via heterotrophic respiration and less input via litter turned the soil at the heavily degraded PSF into a net C source of -7.1 Mg C ha^{-1} yr^{-1}, while undisturbed sites remained at -0.1 Mg ha^{-1} yr^{-1}. Therefore, forest degradation in PSF causes significant soil C losses – even without drainage or fertilization practices.

6.2 The effect of forest conversions on GHG emissions in the tropics

Land use change can be defined as 'the change of a land cover between two points in time'. Underlying causes of land-use change (LUC) are complex, and an interacting combination of political, economic and social factors (Lambin et al., 2001, 2003), that are often regional-specific and multi-stakeholder-dependent. Hence, mitigating GHG from LUC requires understanding of the processes and controlling factors of GHG emissions for a wide variety of LUC trajectories. The

focus of this thesis is on N_2O and NO emissions from the global tropics, and forest degradation on tropical peat.

6.2.1 Nitrous and nitric oxide emissions from forest conversions in the global tropics

While C stock changes are commonly used to estimate CO_2 emissions, non-CO_2 greenhouse gases are typically estimated by land use and management specific emission factors (IPCC, 2006). In line with **hypothesis 1** (see paragraph 1.5), Chapter 2 indicates that forest conversion to cropland significantly increased N_2O emissions, irrespective of the region or type of crops, and that water-filled pore space (WFPS) and N availability were useful proxies for N_2O and NO emission. In addition, I observed that these emissions are driven by soil cultivation-induced soil organic nitrogen mineralization during the first years, and by N inputs from fertilizers and animal manure.

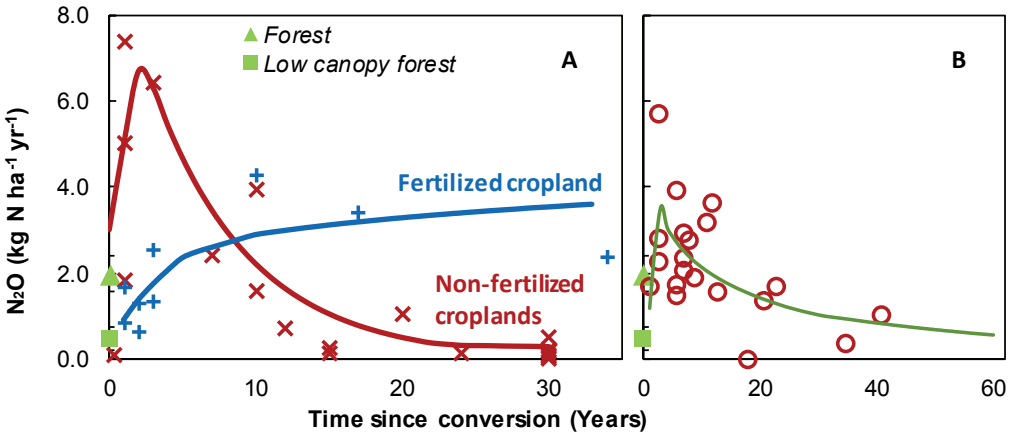

Figure 6.1 – Effect of time since conversion on N_2O fluxes in (a) croplands and (b) unfertilized pastures. Average N_2O flux and 95% confidence intervals are given for upland forests (triangle) and low canopy forests (square). Lines represent a conceptual trend for non-fertilized (red) and fertilized (blue) cases, respectively (adjusted from chapter 2). Average fertilization rate at fertilized croplands is 56 kg N ha^{-1} yr^{-1}.

Emissions of N_2O tended to increase during the first five to ten years after conversion, mainly because of net soil organic N mineralization. After this phase, they tended to decrease in 20 to 30 years to average levels of non-fertilized croplands and pastures (Figure 6.1, adjusted from Chapter 2). Recently, McDaniel et al. (2019) added several new studies to my dataset and confirmed the conceptual line in Figure 6.1 with an exponential decay function that stabilizes at 40 years after conversion at similar levels as the previous land use. The peak during the first years after forest conversion in non-fertilized systems can be explained by use of heavy machinery associated with clear-felling, and soil preparation (e.g. tillage, compaction, drainage in wetland). This temporal variability in emissions indicates that the first ten years following LUC are crucial for GHG budget calculations.

The 'Hole-in-the-Pipe' (HIP) model proposed by Firestone & Davidson (1989) provides an intuitive explanation of how N availability and soil aeration interact and drive N_2O and NO emissions. In most soils, an increase in available N enhances nitrification and denitrification rates which increases the amounts of N_2O and NO produced as a by-product (Davidson et al., 2000; Baggs & Philippot, 2010).

N availability is used in many studies to investigating the percentage of N_2O emitted for every kg of N fertilizer added to the system for tropical and non-tropical ecosystems (e.g. Albanito et al. 2017; Butterbach-Bahl et al., 2013; Cayuela et al. 2017; Liu et al. 2017; Stehfest and Bouwman, 2006). These studies, and those presented in Chapter 2, were used for the Tier 1 approach in the 2019 refinement to the 2006 IPPC guidelines (IPCC, 2019). Although the percentage remained at an average of 1%, a major improvement was made by reducing the uncertainty range by 66% for direct N_2O emissions from managed soils.

In addition, for the Tier 1 approach, a climatic differentiation was made between wet and dry climates, and between situations with synthetic N inputs and those without. Synthetic fertilizer added to managed soils in the wet tropics leads on average to 1.6% N_2O emissions, whereas this is on average 0.6% for other N inputs such as organic amendments, animal manures, crop residues and mineralised N from soil organic matter decomposition. Next to N-content of crop residues, its carbon-to-nitrogen ratio (C/N ratio) may be used as an indicator of N

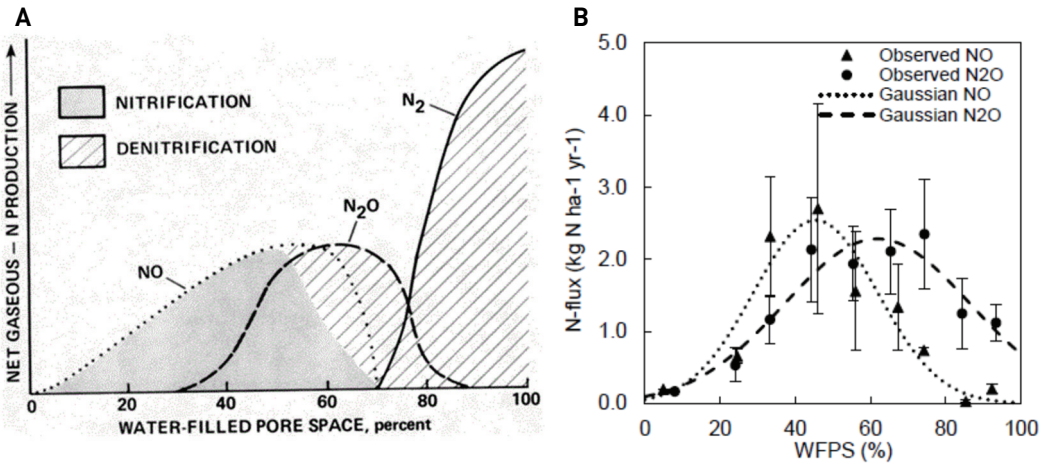

Figure 6.2 – The proposed relative contribution of NO, N_2O and N_2 to the net gaseous N production in the soil at varying WFPS% by Davidson (1991) (a), and in situ measured, annually-averaged N_2O and NO emissions at different WFPS% (Chapter 2) (b).

in an ecosystem (Davidson et al, 2000). Low C/N-ratio litter often results in high net N mineralization rates during decomposition, that subsequently can be converted to nitrate via nitrification processes and/or denitrified to N_2O, NO or N_2. High C/N-ratio litter commonly has lower N mineralization rates and causes relatively low N_2O emissions in the process of organic matter mineralization.

The results from Chapter 2 are in line with the differentiation between wet and dry climates added in the 2019 refinements. Climate is a key determinant of WFPS, and annually averaged WFPS is a useful proxy for total annual N_2O and NO production. Chapter 2 showed that NO an N_2O productions followed a Gaussian type relationship with WFPS. This type of relationship was earlier hypothesized by Davidson (1991) (Figure 6.2a), demonstrated in case studies (Davidson et al., 2000; Davidson and Verchot, 2000; Veldkamp et al., 1998) and used in modelling (Parton et al., 2001; Parton et al., 1993; Potter et al., 1996). For the wide range of soils considered in the dataset of Chapter 2, the optimum WFPS for NO production was at 45%, and for N_2O at 61% (Figure 6.2b). Nitric oxide emission mainly occurs when the WFPS is below field capacity, whereas N_2O is emitted at higher WFPS, exceeding field capacity. This is reflected in the 2019 IPCC guidelines as N_2O emission factors for managed lands that are 0.5% for dry climates and 0.6% and

1.6% for wet climates; the latter two are for synthetic fertilizer and other N inputs, respectively.

6.2.2 Carbon dioxide emissions from degradation of tropical peat swamp forests

The forest transition curve model (van Noordwijk and Sunderland, 2014) provides a useful framework for illustrating the likely effects of LUC on carbon stock changes. Stock changes are associated with CO_2 losses or gains between two phases. Avoiding low tree-cover phases are an option to minimize net CO_2-C losses, for example through transforming degraded forest into agroforests and thereby avoiding intensive annual cropping systems. Forests on mineral soils typically harbour 140-197 Mg C ha^{-1} aboveground, throughout the tropics (Sullivan et al., 2017). For PSFs in the Peruvian Amazon this was between 46 and 123 Mg C ha^{-1}. However, in PSF the majority of C was belowground in the Peruvian Amazon; on average 666 Mg C ha^{-1}, which was between 70 and 90% of the total C stock (Chapter 3). These numbers are in line with other studies in the Peruvian Amazon (Draper et al., 2014, Lähteenoja et al., 2012). Values for Southeast Asian PSFs are within the same order of magnitude, but more than 12 m deep ombrotrophic peat soils can have C-stocks of >75000 Mg C ha^{-1} (Warren et al., 2017).

Since the majority of C is belowground in PSFs, I extended the original forest transition curve with soil C stocks, specifically for anthropogenic-induced forest transitions in PSFs (Figure 6.3). The hypothesis was that the vegetation and soil C stock can alter following natural succession or disturbances, as well through the selective harvesting of *M. flexuosa* palms and logging for timber in natural PSFs ("forest degradation") (**hypothesis 2,** see paragraph 1.5).

I found that soil C stock varied strongly between sites and regions. However, forest degradation did not correlate with total or soil C stocks (Chapter 3). The in-depths study of the peat C balance showed that severely degrading the forest on peat resulted in a negative C balance of -7 Mg C ha^{-1} yr^{-1} (a net source CO_2-C to the atmosphere, Chapter 5). The uncertainty of soil C stocks within all twelve sites (SD) was highly variable and is on average 160 Mg C ha^{-1} yr^{-1} (Chapter 3). It would take more than 22 years of heavy forest degradation to surpass this uncertainty (160/7). The lack of correlation between soil C stock and forest degradation either

indicates that forest degradation was practiced at lower intensities, or that it was practiced in recent times. In both cases, effects of anthropogenic forest disturbances on C stocks are smaller than the variability in soil C stocks that are due to, for example, regional differences in peat accumulation rates. Regional differences in peat accumulation can be affected by meandering rivers that can cause burial or erosion of peat deposits (Neller et al., 1992; Morozova and Smith, 2003).

The effect of palm harvesting and logging in PSFs on the total C stock is initially small (phase 2, Figure 6.3), but the effect becomes substantial if many palms or trees are harvested. This is illustrated in phase 3 in Figure 6.3, when the vegetation C stocks declines sharply. If harvesting results in palm density

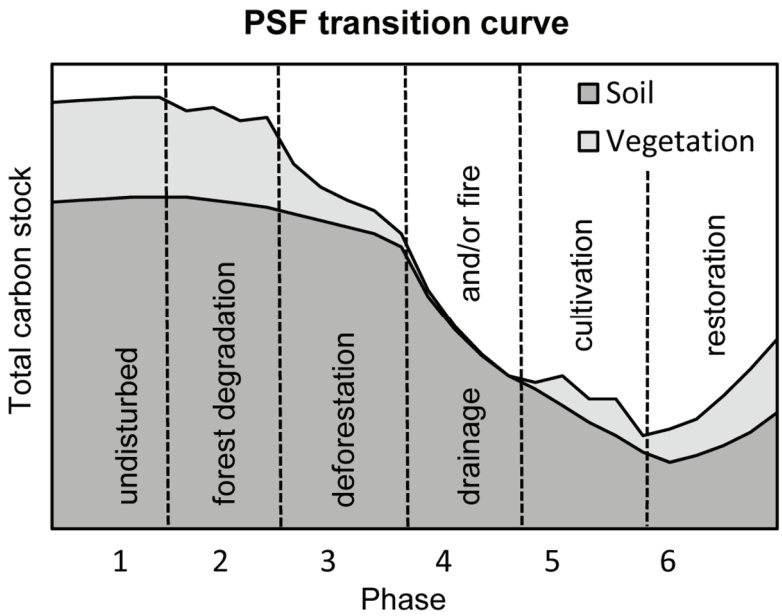

Figure 6.3 – Conceptual forest transition curve for peat swamp forest (PSF) carbon stocks, modified after the forest transition curve (van Noordwijk and Sunderland, 2014). Phases 1 to 3 are based on Chapter 3 and 5, phases 4 to 6 are added and have been derived from literature (discussed below). Note that time elapsed per phase can vary strongly (not indicated in figure), phases are indicated purely for comparisons between phases and their relative C stocks.

reductions of >80% compared to the natural situations, the PSF becomes a net source of C, as illustrated by the C balance of -7 Mg C ha^{-1} yr^{-1} for a degraded site near the city of Iquitos in Peru (Chapter 5).

Although soil C losses are observed during harvesting and forest degradation (phases 2 and 3), drainage and fire causes larger soil C stock losses (phases 4 and 5). It has been estimated that 63 to 98 % of the C lost due to uncontrolled fires in undisturbed, drained and logged or cultivated peat swamps is from the soil (Hergoualc'h and Verchot, 2011). Widespread fires following the 1997 El Niño event caused a loss of 0.19-0.23 Gt C from the peat, while the vegetation contributed 'only' 0.05 Gt from the same 2.5-million-hectare study area in Kalimantan, Indonesia (Page et al., 2002). Degradation of *M. flexuosa*-dominated PSFs in the Amazon are in phases 2 or 3. Phases 4, 5 and 6 have not been observed (yet). These phases are observed in Southeast Asia, and commonly involve drainage, burning, and conversions to plantations (e.g. oil palm or *Acacia*). Peat soils under palm oil cultivation remain a C source throughout the plantation life span (Hergoulac'h and Verchot, 2011).

The importance of sustainable PSF management follows from the PSF transition curve, as it illustrates the magnitude of C that can be lost from these C-rich ecosystems. The extensive PSF conversions observed in Southeast Asia are a cautionary tale for the Amazon. A two-country comparison by Lilleskov et al. (2019) concluded that Indonesian PSFs are under much greater anthropogenic pressure than the Peruvian counterparts. Peruvian PSFs have lower population and road densities; the peatlands are more isolated. In addition, large ombrotrophic dome formations in Indonesia allow for easy drainage and the distinct dry seasons favours burning practices. In Peru, seasonality is less pronounced and fires are not so strongly related to *El Niño* related drought-event as in Asia (Lilleskov et al., 2019). Yet, the Peruvian PSF areas may benefit from governmental policies that recognize their importance and unique features and protect their existence.

Indonesia's government has established the Peatlands Restoration Agency (BRG) recently, in order to reduce peat deforestation and promote peat restoration (Forest news, 2016). The goal is to restore peatlands through active rewetting and revegetation of 2 million ha between 2016 and 2020. Such restoration efforts

ultimately aim to restore the C sequestration capacity as illustrated by the last phase of the PSF transition curve (phase 6, Figure 6.3). This can be done either with endemic vegetation or with paludiculture crops (e.g. Sago, Açai, *M. flexuosa*). However, such shifts in land management require incentivising a complex multi-stakeholder transition (Hergoulac'h et al., 2017).

For the Amazon, the challenge is not to follow all the phases in PSF forest transition curve, but to protect/conserve PSFs or to incentivise its sustainable use (see paragraph 6.3). This would not only prevent CO_2 emissions occurring during phases 4 and 5, but also circumvent complex land policy and governance reforms and technical difficulties of restoration methods (Dohon, Aziz & Dargusch, 2018; Noordwijk et al., 2014).

6.3 How does land use change in natural tropical peatland affect changes in GHG fluxes?

Anthropogenic land-use change may involve major transformations of the soil-plant-atmosphere continuum (Vitousek et al., 1997; Houghton, 2010). As a result of land clearing fires, ploughing and soil cultivation, drainage, fertilization, and crop production, the soil system is highly altered. Soil properties such as bulk density, porosity, moisture, temperature, mineral N content and pH are often affected by LUC (Oertel et al., 2016). Essentially, these alterations of the soil system and its management cause increased GHG emissions after LUC. In this paragraph I focus on mechanisms that explain changes in GHG emissions following forest conversion on natural tropical peatlands.

Land-use change of tropical peatlands commonly involves drainage, which causes increased mineralization of soil organic matter, since oxygen availability increases. The water table has therefore been proposed as an easy-to-use proxy for GHG emission estimates from PSFs conversions to croplands (Hooijer et al., 2010), but water table as a proxy is less suitable for intact or degraded, but non-drained, peat forests. Other proxies such as soil mineral N content may provide more robust relationships with GHG emissions whenever land uses do not require drainage (Hergoualc'h & Verchot, 2014).

Interestingly, the most common land use on tropical peat in the Peruvian Amazon does not involve active drainage. There, degradation is defined as recurrent cutting of palms for fruit harvesting (forest degradation), which can significantly affect the C balance if harvesting occurs at high intensity (Chapter 5). A direct link between this type of forest degradation and water table is absent, as fruit-harvesting occurs in natural stands. Accurately modelling and predicting long-term changes in the soil carbon pool, as well as exchanges of CO_2, N_2O and CH_4 with the atmosphere, thus requires additional information about controlling factors.

Figure 6.4 illustrates four factors that were studied in Chapters 4 and 5: soil moisture indices, presence of aerating roots, litter quality, and microtopography. These factors were hypothesized to be affected by forest degradation and in turn may explain observed changes in GHG production in degraded PSFs as compared to intact ones (**hypothesis 3**, see paragraph 1.5).

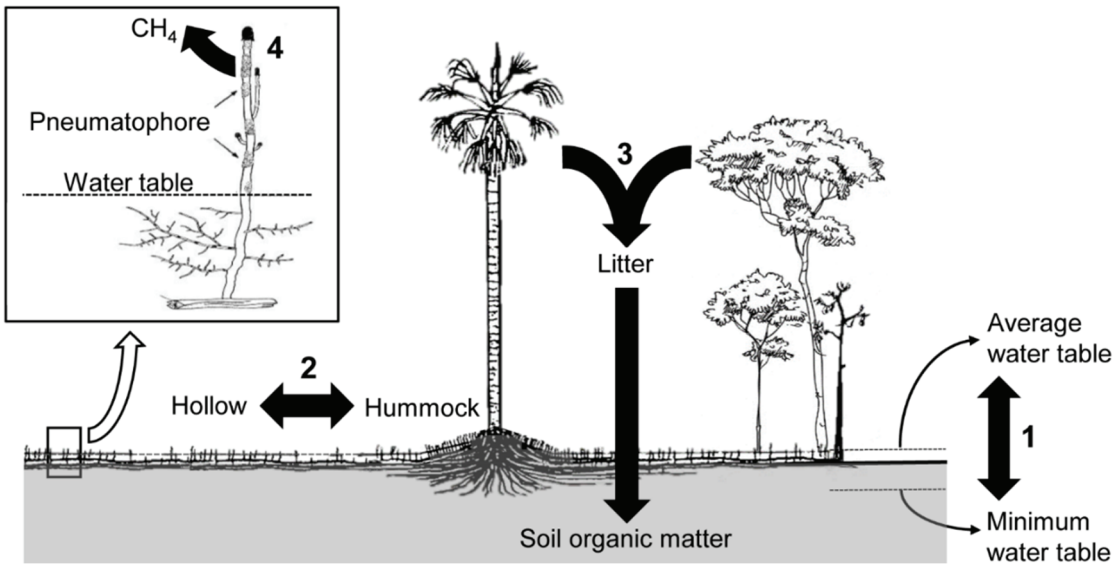

Figure 6.4 – Studied factors that control GHG emissions and can change following palm swamp forest degradation: (1) water table fluctuations and WFPS% as a proxy for soil aeration, (2) microtopography of the soil surface area in terms of hummock and hollows, (3) soil organic matter quality derived from litter input, and (4) aerating roots (pneumatophores) that emit CH_4 from soil.

The first factor considered is soil aeration, commonly estimated by water-filled pore space (WFPS) and water table (WT) (e.g. Husen, Salma, & Agus, 2014; Verchot et al. 2000; Del Grosso et al. 2000; Davidson et al. 2000). The *in vitro* soil incubation experiment presented in Chapter 4 shows that, whenever the WT is below the surface level, heterotrophic respiration followed a bell-shaped relationship with WFPS. This is in line with incubated peat soils under palm cultivation in Indonesia (Husen, Salma, & Agus, 2014). Below the optimal WFPS the microbial activity is limited by water shortage, and above the optimal WFPS, water saturation and oxygen deficiency hamper microbial respiration (Moyano, Manzoni, & Chenu, 2013). *In situ* experiments presented in Chapter 5 revealed that whenever the water table is below the surface, soil respiration also displayed a bell-shaped relationship with WFPS. At high water table levels, the soil respiration diminished towards zero, while CH_4 production went up (Dezzeo et al., *submitted*). This indicates that there was sufficient substrate (organic matter) and that CO_2 production was likely limited by oxygen deficiency. Although these relationships are useful for a mechanistic understanding of GHG fluxes in PSFs, forest degradation did not significantly affect soil moisture indices. In contrast, observed variations were mostly related to seasonality and interannual variations such as El Niño/La Niña events (Chapter 5). I did observe that a flooding event caused a major leaf-shedding event, which can affect litter quality and eventually contribute to forest disturbance/succession and subsequent effects, as discussed in paragraph 0.

The irregular soil microtopography is the second factor considered. The forest floor in PSFs is made up of hummocks supporting palms and hollows surrounding hummocks. Hummocks have lower WFPS and higher root densities than hollows, resulting in distinct differences in respiration rates and hence spatial variability (Comeau et al., 2016; Hergoualc'h, Hendry, et al., 2017; Jauhiainen et al., 2005). Chapter 5 indicates that root and heterotrophic respiration rates were indeed higher at hummocks, and hummocks were less sensitive to WT variations than hollows. However, the peat surface area consisted of ~85% hollows in the undisturbed site, and increased towards 97% in degraded sites due to a reduction in hummocks size and number (Chapter 5). This is a higher percentage than the 65-80% reported for intact PSFs in Southeast Asia (Jauhiainen et al., 2005), and

indicates that respiration rates measured at hollows and their dynamics following forest degradation are more important than rates measured at hummocks.

Hollows at sites with severe forest degradation had higher heterotrophic respiration rates than hollows at intact sites. The higher rates at hollows at degraded sites can be explained by the third factor considered in Chapter 4: litter quality. Under natural conditions, the portion of SOM that is decomposed and emitted as carbon dioxide (CO_2) or methane (CH_4) is usually outweighed by the continuous input of fresh litter and roots (Jauhiainen et al. 2005; Hergoualc'h and Verchot, 2011; Hoyos-Santillan et al. 2015). This results in a net buildup of soil organic matter, or peat formation. Chapter 4 indicated that even though all soils had similar levels of cations and a similar minerotrophic state (Ca/Mg ratio), the soil at the heavily degraded site had a higher degree of humification (lower C/N ratio) but a lower extractable P content (Table 4.1). Litter quality determines the soil organic matter input, and the hypothesis was that changes in vegetation structure and composition had altered these and could explain the observed differences in peat humification. Indeed, the heavily degraded site had more pioneer species and herbaceous vegetation (Chapter 3), which resulted in a lower litter C/N ratio (Table 4.1). This trend is indicative of forest regeneration, which is characterized by more easily decomposable litter instead of harder-to-decompose woody debris (Gehring et al., 2005; Guariguata and Ostertat, 2001). This was further reflected in an increase of dicot leaf litter and a decrease of branch fall with increased levels of degradation (Table 5.3). The altered litter and soil properties in the heavily degraded site led to more easily decomposable soil organic matter and resulted in higher heterotrophic respiration rates *in vitro* (Chapter 4) and *in situ* (Chapter 5). The lower extractable soil P content (Mehlich3) at the heavily degraded site suggests that leaching of dissolved (inorganic and organic) phosphate and uptake by plants has been larger than the mineralization of organic P.

The fourth factor considered is the presence of aerating roots. In waterlogged conditions, oxygen may be still available in the soil via diffusion through the water column and via aerating roots (Blagodatsky & Smith, 2012). Plants may adapt to anoxic conditions (Bruhn et al. 2012) by producing adventitious roots, lenticels and enlarged aerenchymous tissues that enable oxygen transport (Haase and Rätsch,

2010). De Granville (1969) first described the presence of such tissues in the aerating pneumatophores of *M. flexuosa* palms. Chapter 4 indicates that these pneumatophores also conduct CH_4 produced in anoxic soil layers to the atmosphere. Conductance pathways for CH_4 are well-described for rice (see e.g. Minoda & Kimura, 1994), as well as for tree stem lenticels in temperate and tropical forested wetlands (Gauci et al., 2010; Pangala et al. 2013). Amazonian peatlands that harbor *M. flexuosa* palms also directly emit CH_4 produced in anoxic soil layers through pneumatophores, avoiding potential oxidation in upper aerobic soil layers, and consequently cause significant CH_4 emissions even when the water table is below soil surface. Forest degradation could result in reduced aerating root densities, since most roots were observed in the intact site that had the highest *M. flexuosa* stem density. However, the rooting system of a single *M. flexuosa* palm can reach up to 40 m horizontally (Manzi et al., 2009), and pole forests with few *M. flexuosa* palms display similar numbers of pneumatophores (Del Aguila Pasquel, 2017), indicating a non-linear relationship between reduced *M. flexuosa* stem density and pneumatophore densities. Evidently, the impact of palm-harvesting on CH_4-conductance via pneumatophores requires more research.

From the results presented in Chapters 4 and 5 I concluded that the change in vegetation composition and structure is the most important proxy for net C mineralization. A combination of altering soil and litter C/N ratios and changes in the soil microtopography in degraded PSFs, that are not drained, nor fertilized, were the dominant factors (factors 2 and 3, Figure 6.4).

6.4 The effects of changes in vegetation composition and structure on peat accumulation and carbon balance

A key question in the degradation of peat swamp forest is the distinction between anthropogenic disturbances and natural succession / natural disturbances. Changes in the vegetation composition can be a result of natural succession and anthropogenic disturbances, such as the selective harvesting of female fruit-baring *M. flexuosa* palms (see paragraph 1.2). The hypothesis was that severe anthropogenic forest degradation in peat swamp forest causes the peat to switch to a net carbon source to the atmosphere (**hypothesis 4**, see paragraph 1.5).

Results presented in Chapter 3 indicate that sites with deep peat deposits had typical pole forest species (*Pachira brevipes, Oxandra mediocris* and *Platycarpum loretensis*), and the Ca/Mg ratio was indicative of switching from a minerotrophic to an ombrotrophic status (Avispa and Chanchari sites, see Figure 3.4). On the other hand, sites with low *M. flexuosa* densities co-occurred with species representative of seasonally flooded forest in some cases (e.g. *Euterpe precatoria* and *Hura crepitans*), suggesting that these sites were recently developed palm swamps (Pobre Cocha and Shiringal sites). Pollen data and sedimentary evidence confirms that the role of flooding in vegetation transition and succession, and the changes observed during early phases of peat initiation, were a result of autogenic succession and fluvial influence (Roucoux et al., 2013; Kelly et al., 2017).

Anthropogenic disturbances cause some distinct changes in vegetation structure and composition (Hergoualc'h, Gutiérrez-Vélez, et al., 2017). In Chapter 3, a combination of these distinct changes was used to assign degradation classes to each site. The first factor was the *M. flexuosa* population height distribution. The most common practice of harvesting *M. flexuosa* fruits involves cutting down fruit bearing female trees, which causes a localized reduction in the abundance of mature trees and overdominance of younger trees (Hergoualc'h, Gutiérrez-Vélez, et al., 2017; Parodi and Freitas, 1990; Delgado et al., 2007; Manzi and Coomes, 2009). The second factor is based on the presence of *M. flexuosa* seedlings. The selective removal of fruiting trees reduces the viable seed source in a given forest stand, and unavailability of seeds hinders natural regeneration and recruitment of new *M. flexuosa* palms (Horn et al., 2012). The last factor is the quantity of tree trunks on the forest floor. In anthropogenically disturbed sites, typically only fruits and

palm weevils are collected and the trunk and other parts are left behind, causing a disproportionally large fraction of trunks and debris on the forest floor.

Although there was a substantial variation in C stocks between the studied regions and sites, the degradation factors as outlined above did not significantly explain observed variations in total C stocks, nor in soil C stocks (see paragraph 6.3 and Chapter 3). The degradation factors were only correlated to the *M. flexuosa* vegetation C stock, which represented on average 5% of the total ecosystem C stock. However, specific species were indicative for the nature of the transition occurring in the peat swamp forest. In a heavily degraded site (San Julian, Itaya region), dominance of the pioneer species *Cecropia membranacea* is indicative of disturbance (Kelly et al., 2020; Roucoux et al., 2013), which can be due to palm harvesting. The degradation score was highest at San Julian, and the vegetation C stock was only 46 ± 13 Mg C ha^{-1}, which was the lowest of all 12 sampled sites (range: 123 – 46 Mg C ha^{-1}). Nevertheless, the lack of a significant correlation between the degradation score and soil C stocks among all sites made it impossible to relate degradation intensity differences to *soil* C losses between sites.

The presence of a carbon-rich peat soil does not necessarily reflect the C sequestration potential of its current vegetation cover. Seedling recruitment, dispersal and mortality rates span between years to decades and provide a delay between the past suitability of a habitat for species to establish, and the current state ('extinction debt', Tilman et al., 1994; Figueiredo et al., 2019). Peat soil C stocks are built up over millennia, and pollen records taken near my sites in the Itaya region indicated that conditions were favourable for peat formation during the last 2400-1900 years under different vegetation types and hydrological regimes (Roucoux et al, 2013; Kelly et al., 2020). However, the pollen records also showed that *M. flexuosa* may not have been occupying areas where peat was accumulated, but they were present on nearby river sand deposits and on clay substrate (Kellly et al., 2020). So, for the onset of peat formation, they are not an essential species and as the peat had built up, *M. flexuosa* palms moved in later in the succession, forming the typical *M. flexuosa*-dominated palm swamps as seen today (Chapter 3; Kelly et al., 2017).

At the intact site, *M. flexuosa* represented 67% of the basal area and 31% of the stem density (Chapters 3 and 5). The palm produced 15% of the C input at the site scale. Most of which originated from root mortality (11%) instead of leaf litter production (5%). Other species (e.g. *Arecaceae*, *Poaceae*, *Cyperaceae*) combined produced three times as much root litter (32%), and ten times more leaf litter (53%). The *M. flexuosa* palms as a single species accounted for more than a quarter (11/[32+11]) of the root C input in these PSFs. This finding explains why harvesting of *M. flexuosa* palms can have large consequences for the peat swamp C balance, as further discussed below.

Carbon dating of the full peat profile at the undisturbed site by Kelly et al. (2020) revealed a long-term average peat accumulation rate between 1.06 and 1.15 mm per year, or 0.44 to 0.48 Mg C ha^{-1} yr^{-1} (assuming *in-situ*-measured peat bulk density of 0.09 and a 46% C content, Chapter 3). Southeast Asian peatlands have slightly higher long-term median accumulation rates of ~1.3 mm yr^{-1} (Page, Wűst & Banks, 2010). These tropical peatlands have greater accumulation rates than boreal and subarctic peatlands that accumulate at rates of 0.2 to 0.8 mm yr^{-1} (Gorham, 1991). At the intact site, I measured a C balance of -0.1 ±1.5 Mg C ha^{-1} yr^{-1}, which suggesting that peat accumulation and C sequestration rates are currently reducing. Kelly et al. (2017) observed a reduction in peat accumulation between 1300 and 400 cal yr BP in a site 30 km south from ours, at the same time that Mauritia pollen were observed. They proposed that decomposition had increased due to hydrological changes and natural lowering of the water table as the Amazon river moved away laterally, and as peat was building up. My observation and that of Kelly et al. (2017) both indicate that peat accumulation might have slowed down in recent times. Therefore, the question remains if the current vegetation cover at undisturbed sites sustains peat accumulation.

Quantification of the net peat accumulation required an in-dept study of the peat C balance at varying levels of forest degradation. Figure 6.5 presents a summary overview of the results of a four-year monitoring experiment for the undisturbed and heavily degraded sites in Iquitos, Peru (Chapter 5). At the undisturbed site, the overall C input originated for 58% from litter and 42% from roots. Roots are an important C source for peat accumulation (Chimner and Ewel, 2005), especially when sites have nearly constant high-water levels, which

maintain anaerobic soil conditions and hamper root decomposition. Average water table levels were close to the soil surface at the undisturbed site and roots decomposed at around half the speed of leaf litter (Chapter 5). The average heterotrophic respiration rate was close to the sum of root and litter input (Figure 6.5). So, likely at times some 'older' organic matter decomposes as well; which could be explained by priming effects (Bengtson, Barker, & Grayston, 2012; Fu & Cheng, 2004). Thus, I synthesize that the CO_2 from heterotrophic respiration originated mostly from fresh leaf litter on the forest floor and from soil organic matter in upper peat layers, instead of roots and organic matter in deeper layers of the soil. The combined effect was a net C balance of -0.1 ±1.5 Mg C ha^{-1} yr^{-1} at the intact site. The C balance of the peat soil seasonally switches between a C sink and source, because the soil water table varied seasonally. Natural or climate-change induced changes of the water table level can, therefore, easily turn the peat in this site into a net source of C.

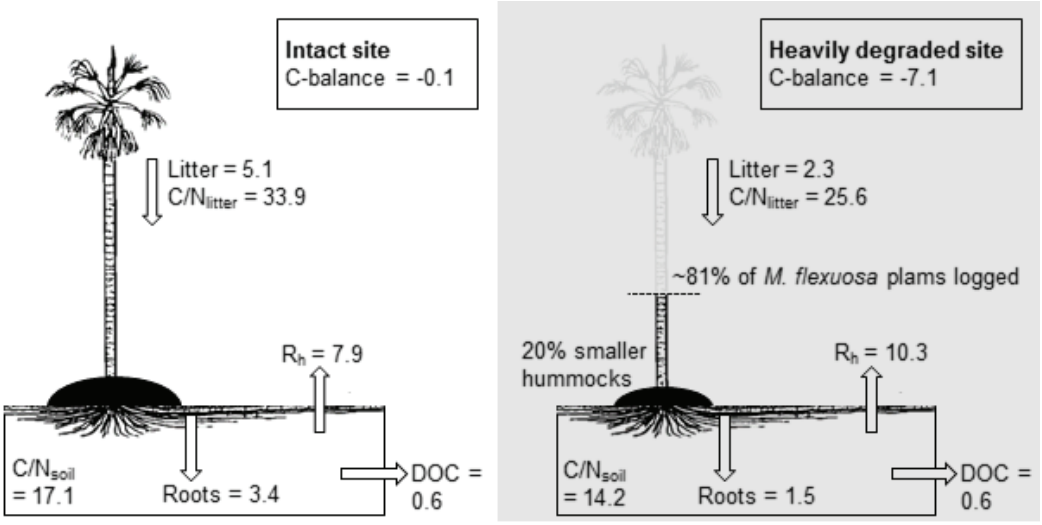

Figure 6.5 – Summary overview of the C-balance of the intact (left figure) and heavily degraded sites (figure on the right) in Iquitos, north-western Peruvian Amazon. The overall input-output C balances are presented in the boxes at the top of the figures. Based on data from Chapters 4 and 5. Al numbers are in Mg C ha^{-1} yr^{-1}, except C/N ratios that are unitless.

While in undisturbed situations the C balance remains close to zero, selective harvesting of *M. flexuosa* palms turned the peat soil into a net C source (Figure 6.5). Degraded sites had less litter input, and increased heterotrophic respiration rates. The litter quantity had changed due to an 81% reduction in *M. flexuosa* palms compared to the intact site. Such reductions were in line with other heavily degraded palm swamps in the Pastaza-Marañón basin (89%) (Hergoualc'h, Gutiérrez-Vélez, et al., 2017). In addition, leaf litter quality altered due to an increase in pioneer vegetation that had produced more easily-decomposable litter and led to higher heterotrophic respiration rates (paragraph 6.3). Reduced input and increased output resulted in a negative C balance at the heavily degraded site of 7.1 Mg C ha^{-1} yr^{-1}. Thus, severe selective harvesting of *M. flexuosa* palms can alter the vegetation composition and structure, such that the underlying peat soils turn into net C sources – even when the peat is not actively drained.

6.5 Conclusions, outlook and future research

The aim of this thesis was to increase the understanding of the factors that control GHG emissions from degrading PSF, and to contribute to improving the GHG emission reporting in the AFOLU sector by investigating the effects of land use and land-use change on GHG emissions in the tropics. Default emission factors are often based on few studies and on short-term measurements, sometimes from other climatic zones or different continents. Further, certain types of land use and land-use change may require even more specific emission factors.

6.5.1 Global N_2O emissions from land use and land-use change in the tropics

The body of research on LUC and N_2O and NO emissions has steadily increased over the past decades, but still gaps remain for Africa and for wetland forest (notably on peat), degraded forest, and for important world crops such as oil palm plantations and soy fields on recently deforested land. The meta-analysis (Chapter 2) helped to improve estimations of current average N_2O emissions per land use in the IPCC guidelines (Tier 1, IPCC 2019), and it may help to improve statistical models that predict N_2O emissions (Tier 2) from land use and land-use change practices. The meta-analysis showed that fertilization N input after land-

use change increases both N_2O and NO fluxes; however, changes in endogenous levels of soil nitrogen availability, together with possible changes in WFPS, were also key factors impacting the changes in N_2O and NO fluxes. These variables should therefore systematically be measured and reported. In addition, studies considering a LUC transition pathway should include in their design all intermediate land use stages (e.g. degraded forest) susceptible to modify N cycling, since these affect N_2O and NO emissions.

6.5.2 Peat swamp forest degradation

This thesis presents the first emission factor for forest degradation in natural peat swamp forests of the Amazon, which is a land use unaccounted for in GHG accounting schemes up to date. When >80% of *M. flexuosa* palms were harvested (the heavily degraded site), 7.1 Mg C was emitted per hectare and year. This is a significant annual C loss, in comparison to land-clearing fires that result in C losses from peat soils of 4.5 to 7.1 Mg C ha^{-1} and for drained peat soils with oil palm that emit on average 9.8 Mg C ha^{-1} yr^{-1} (Hergoulac'h and Verchot, 2011).

First reports on concerns of over-harvesting *M. flexuosa* palms are from the 1980s (Padoch, 1988), and fruit harvesting has increased dramatically in the 30 years thereafter (Horn et al., 2018). At a global level, the C loss from heavily degraded sites represents a significant C source up to 7.8 Tg C yr^{-1} for the entire Pastaza-Marañón basin in the Peruvian Amazon (Chapter 5). Considering the fact that sustainable climbing practices exist for harvesting fruits of *M. flexuosa* palms (Horn et al., 2012), and are currently practiced at small scale (Virapongse et al., 2017), there is a substantial CO_2 emission reduction potential by preventing destructive palm harvesting throughout the Amazon. However, several key questions and directions for future research remain:

1. I took great care to minimize this impact of the trenching experiment (see Chapter 5 and Subke et al., 2006), by excluding the first measurements and by ensuring that no roots were growing back in to the trenched zones. However, water table significantly affected the ratio of heterotrophic to total soil respiration. During high water table levels, fluxes are small and very sensitive to small changes and anomalies. Exclusion of measurements at high water

levels still resulted in heterotrophic respiration that represented 57% to 98% of the total soil respiration at hollows (Chapter 5). Experiments further addressing the effect of water table on heterotrophic to autotrophic respiration rates at varying distances from palms would help to better understand these observations.

2. Another interesting point is to disentangle heterotrophic respiration into its sources: decomposition of root biomass, leaf biomass and/or soil organic matter. Roots decomposed much slower than leaves (Chapter 5), but their relative contribution to *in situ* measured heterotrophic respiration rates remains unknow. A leaf litter fall exclusion experiment in trenched and non-trenched plots would help to estimate old soil organic matter decomposition relative to fresh root and litter decomposition. This allows to better understand the vegetation feedback on peat accumulation rates, which is affected differently by palm-harvesting or natural succession and disturbances (see paragraph 6.4).

3. Anthropogenic and natural disturbance, as well as natural succession all affect the vegetation composition and structure. Disentangling these effects from each other is crucial for correctly addressing anthropogenic GHG emissions from these PSFs. C-stock spatial variability is many times larger than effects of anthropogenic forest degradation; the SD-equivalent of average soil C stocks resembles around 22 years of heavy forest degradation. Peat formation and accumulation is not exclusive to *M. flexuosa*-dominated PSFs (Kelly et al, 2020). It moved in at a later stage in the peat swamp succession, and is expected to reduce in number again as the PSF transitions into C-dense pole forests with more dicot trees (Kelly et al, 2017; Draper et al., 2014). Perhaps, some locations where many *M. flexuosa* palms are harvested would otherwise transition into C-dense pole forests. An experiment in a degraded site that combines an analysis of pollen records with an assessment of palm height distribution anomalies, recruitment rates and remaining trunks (see Chapters 3), would explain if the current vegetation

composition differs from what would be expected from the natural succession (see paragraph 6.4).

4. Accurately upscaling my results would benefit from soil and land cover maps. The intensity of harvesting should ideally be included in such maps, since the intensity of forest degradation had different effects on the peat C balance (Chapter 5). It should be further assessed what harvesting intensity are typical, and at what time interval sites are commonly harvested. A model combining the number of palms harvested within those intervals and the quantity of C emitted from sites after harvesting would enables an exact calculation of C mitigation potential if palms are not harvested but climbed for fruit collection. Such an assessment could incentivize a switch from harvesting to climbing *M. flexuosa* palms for fruit collection and would argue for the conservation of areas under threat of deforestation and/or with high C stocks.

Many PSFs are currently outside of protected reserves, and there is evidence of forest degradation inside current protected areas (Chapter 3, but also see Horn et al., 2018). Ultimately, the goal should be to prevent the trajectory of peat drainage and conversions seen in Southeast Asia (Lilleskov et al., 2018), and as I describe the PSF transition curve (see discussion 6.2.2). Non-destructive fruit extraction could be done by climbing palms and cultivation of *M. flexuosa* in agroforestry systems (Horn et al., 2018). Payment for GHG mitigation efforts could provide an additional incentive, in combination with prolonged income from fruits collected in sustainably managed palm swamp forests throughout the Amazon.

7 References

Albanito, F., Lebender, U., Cornulier, T., Sapkota, T. B., Brentrup, F., Stirling, C., & Hillier, J. (2017). Direct Nitrous Oxide Emission s From Tropical And Sub-Tropical Agricultural Systems-A Review And Modelling Of Emission Factors. Scientific reports, 7(1), 1-12.

Anderson, I. C. and Poth, M. A. (1989). Semiannual losses of nitrogen as NO and N_2O from unburned and burned chaparral, Global Biogeochem. Cycles, 3(2), 121. doi:10.1029/GB003i002p00121

Asner, G.P., Knapp, D.E., Martin, R.E., Tupayachi, R., Anderson, C.B., Mascaro, J., Sinca, F., Chadwick, K.D., Sousan, S., Higgins, M. (2014). The high-resolution carbon geography of Peru. Carnegie Airborne Observatory and the ministry of environment of Perú.

Baccini, A., Goetz, S. J., Walker, W. S., Laporte, N. T., Sun, M., Sulla-Menashe, D., Hackler, J., Beck, P. S. A., Dubayah, R., Friedl, M. A., Samanta, S. and Houghton, R. A. (2012). Estimated carbon dioxide emissions from tropical deforestation improved by carbon-density maps, Nature Climate Change, 2, 182–185. doi:10.1038/nclimate1354

Baggs, E. M. and Philippot, L. (2010). Microbial terrestrial pathways to nitrous oxide. Nitrous Oxide and Climate Change, Earthscan Ltd, London, UK, 4-35, 247.

Bailey H.H. (1951). Peat formation in the tropics and subtropics. Proceeding of the Soil Science Society of America, 283-284.

Bateman, E. J. and Baggs, E. M. (2005). Contributions of nitrification and denitrification to N_2O emissions from soils at different water-filled pore space, Biology and Fertilility of Soils, 41, 379–388. doi:10.1007/s00374-005-0858-3

Baumert, K., Herzog, T. and Pershing, J. (2005). Navigating the Numbers - Greenhouse Gas Data and International Climate Policy, World Resources Institute (WRI), Washington D.C., USA.

Bengtson, P., Barker, J., and Grayston, S. J. (2012). Evidence of a strong coupling between root exudation, C and N availability, and stimulated SOM decomposition caused by rhizosphere priming effects. Ecology and Evolution, 2(8), 1843–1852. doi:10.1002/ece3.311

Bernal, C., Christophoul, F., Darrozes, J., Soula, J.-C., Baby, P., Burgos, J. (2011). Late Glacial and Holocene avulsions of the Rio Pastaza Megafan (Ecuador–Peru): frequency and controlling factors. International Journal of Earth Sciences 100:1759-1782.

Bhomia, R. K., van Lent, J., Rios, J. M. G., Hergoualc'h, K., Coronado, E. N. H., and Murdiyarso, D. (2019). Impacts of Mauritia flexuosa degradation on the carbon stocks of freshwater peatlands in the Pastaza-Marañón river basin of the Peruvian Amazon. Mitigation and Adaptation Strategies for Global Change, 24(4), 645–668. doi:10.1007/s11027-018-9809-9

Blagodatsky, S., and Smith, P. (2012). Soil physics meets soil biology: Towards better mechanistic prediction of greenhouse gas emissions from soil. Soil Biology and Biochemistry, 47, 78–92. doi:10.1016/j.soilbio.2011.12.015

Borenstein, M., Hedges, L. V., Higgins, J. P. T. and Rothstein, H. R. (2009). Introduction to Meta-Analysis, statistics in practice series, John Wiley and Sons, Ltd., Cambridge (UK).

Bradshaw C.J., Sodhi, N.S., Brook, B.W. (2008). Tropical turmoil: a biodiversity tragedy in progress. Front Ecol Environ 7:79-87.

Brady, M. A. (1997). Organic matter dynamics of coastal peat deposits in Sumatra.donesia. The University of British Columbia.

Brown, J.K. (1974). Handbook for Inventorying Downed Woody Material. General Technical Report GTR-INT-16. Service UF (ed.), Missoula.

Bruhn, D., Møller, I.M., Mikkelsen, T.N., Ambus, P. (2012). Terrestrial plant methane production and emission. Physiol Plant 144:201–209. doi: 10.1111/j.1399-3054.2011.01551.x

Butterbach-Bahl, K., Baggs, E. M., Dannenmann, M., Kiese, R., Zechmeister-Boltenstern, S. (2013). Nitrous oxide emissions from soils: how well do we understand the processes and their controls? Philosophical Transactions of the Royal Society B: Biological Sciences, 368:20130122. doi: 10.1098/rstb.2013.0122

Carmichael, M.J., Bernhardt, E.S., Bräuer, S.L., Smith, W.K. (2014). The role of vegetation in methane flux to the atmosphere: should vegetation be included as a distinct category in the global methane budget? In: Biogeochemistry 119, 1–24. doi: 10.1007/s10533-014-9974-1

Cayuela, M. L., Aguilera, E., Sanz-Cobena, A., Adams, D. C., Abalos, D., Barton, L., ... & Smith, P. (2017). Direct nitrous oxide emissions in Mediterranean climate cropping systems: Emission factors based on a meta-analysis of available measurement data. Agriculture, Ecosystems & Environment, 238, 25-35.

Chameides, W. L., Fehsenfeld, F., Rodgers, M. O., Cardelino, C., Martinez, J., Parrish, D., Lonneman, W., Lawson, D. R., Rasmussen, R. A., Zimmerman, P., Greenberg, J., Mlddleton, P. and Wang, T. (1992). Ozone precursor relationships in the ambient atmosphere, Journal of Geophysical Research: Atmospheres, 97, 6037-6055. doi:10.1029/91JD03014

Chen, S. and Huang, Y. (2009). Soil respiration and N 2 O emission in croplands under different ploughing practices: a case study in south-east China. Aust. J. Soil Res., 47, 198. doi:10.1071/SR07225

Chimner, R. A., and Ewel, K. C. (2005). A tropical freshwater wetland: II. Production, decomposition, and peat formation. Wetlands Ecology and Management, 13(6), 671–684. doi:10.1007/s11273-005-0965-9

CAIT Climate Data Explorer (2019). Country Greenhouse Gas Emissions. World Resources Institute, Washington, DC. Available online at: http://cait.wri.org

Collier, S. M., Ruark, M. D., Oates, L. G., Jokela, W. E., Dell, C. J. (2014). Measurement of Greenhouse Gas Flux from Agricultural Soils Using Static Chambers. Journal of Visualized Experiments, 90, e52110–e52110. doi: 10.3791/52110

Colmer, T. D., and Voesenek, L. A. C. J. (2009). Flooding tolerance: suites of plant traits in variable environments. Functional Plant Biology, 36(8), 665. doi:10.1071/FP09144

Comeau, L.-P., Hergoualc'h, K., Hartill, J., Smith, J., Verchot, L. V., Peak, D., and Salim, A. M. (2016). How do the heterotrophic and the total soil respiration of an oil palm plantation on peat respond to nitrogen fertilizer application? Geoderma, 268, 41–51. doi:10.1016/j.geoderma.2016.01.016

Crutzen, P. J. (1970). The influence of nitrogen oxides on the atmospheric ozone content, Q. J. R. Meteorol. Soc., 96, 320–325. doi:10.1002/qj.49709640815.

Curtis JT, McIntosh RP (1951). An Upland Forest Continuum in the Prairie-Forest Border Region of Wisconsin. Ecology 32:476-496.

Dalal, R. C. and Allen, D. E. (2008). Greenhouse gas fluxes from natural ecosystems. Australian Journal of Botany, 56, 369–407. doi:10.1071/bt07128

Dargie, G.C., Lewis, S.L., Lawson, I.T., Mitchard, E.T., Page, S.E., Bocko, Y.E., Ifo, S.A. (2017). Age, extent and carbon storage of the central Congo Basin peatland complex. Nature 542:86-90.

Dariah, A., Marwanto, S., and Agus, F. (2014). Root- and peat-based CO_2 emissions from oil palm plantations. Mitigation and Adaptation Strategies for Global Change, 19(12), 831–843. doi:10.1007/s11027-013-9515-6

Davidson, E.A., Belk, E., Boone, R.D. (1998). Soil water content and temperature as independent or confounded factors controlling soil respiration in a temperate mixed hardwood forest. Global Change Biology 4:217–227. doi: 10.1046/j.1365-2486.1998.00128.x

Davidson, E. A., Keller, M., Erickson, H. E., Verchot, L. V., Veldkamp, E. (2000). Testing a Conceptual Model of Soil Emissions of Nitrous and Nitric Oxides. Bioscience 50:667. doi: 10.1641/0006-3568(2000)050[0667:TACMOS]2.0.CO;2

Davidson, E. A., De Abreu Sá, T. D., Reis Carvalho, C. J., De Oliveira Figueiredo, R., Kato, M. d. S. A., Kato, O. R. and Ishida, F. Y. (2008). An integrated greenhouse gas assessment of an alternative to slash-and-burn agriculture in eastern Amazonia, Global Change Biology, 14, 998–1007. doi:10.1111/j.1365-2486.2008.01542.x

Davidson, E. A. and Kingerlee, W. (1997). A global inventory of nitric oxide emissions from soils, Nutrient cycling in agroecosystems, 48, 37–50. doi:10.1023/A:1009738715891

Davidson, E. A. and Verchot, L. V. (2000). Testing the hole in the pipe model of nitric and nitrous oxide emission from soils using the TRAGNET database, Global Biogeochem. Cycles, 14(4), 1035–1042.

Davidson, E. A., Keller, M., Erickson, H. E., Verchot, L. V. and Veldkamp, E. (2000). Testing a Conceptual Model of Soil Emissions of Nitrous and Nitric Oxides, Bioscience, 50(8), 667. doi:10.1641/0006-3568(2000)050[0667:TACMOS]2.0.CO;2

Davidson, E. A., Vitousek, P. M., Dunkin, K., Garcia-Mendez, G. and Maass, J. M. (1993). Processes regulating soil emissions of NO and N_2O in a seasonally dry tropical forest, Ecology, 74(1), 130–139

Davidson, E. A., Vitousek, P. M., Matson, P. A., Riley, R., García-Méndez, G. and Maass, J. M. (1991). Soil emissions of nitric oxide in a seasonally dry tropical forest of México, Journal of Geophysical Research, 96, 15439. doi:10.1029/91JD01476

Davidson, E.A. (1991). Fluxes of nitrous oxide and nitric oxide from terrestrial ecosystems. Rogers, J.E., Whitman W.B. (Eds.): Microbial Production and Consumption of Greenhouse Gases: Methane, Nitrogen Oxides and Halomethanes. American Society for Microbiology, Washington (DC), 219-235.

De Granville J-J. (1969). Aperçu sur la structure des Pneumatophores de 2 espèces des sols hydromorphes: Mauritia flexuosa L. et Euterpe oleracea Mart. (Palmae) - généralisation au système respiratoire racinaire d'autres palmiers. Dissertation, Centre Orstom de Cayenne.

De Pauw, E., Nachtergaele, F. O., and Antoine, J. (1996). A provisional world climatic resource inventory based on the length-of-growing-period concept. Batjes, N. H., Kauffman, J. H., Spaargaren, O. C. (eds.), National Soil Reference Collections and Databases (NASREC), Wageningen, ISRIC, 30–43.

DeFries, R. S., Rudel, T., Uriarte, M. and Hansen, M. (2010). Deforestation driven by urban population growth and agricultural trade in the twenty-first century, Nature Geoscience, 3(3), 178–181. doi:10.1038/ngeo756

del Aguila-Pasquel, J. (2017). Methane fluxes and porewater dissolved organic carbon dynamics from different peatlands types in the pastaza-marañon basin of the peruvian amazon, Master's Thesis, Michigan Technological University, 2017.

del Aguila-Pasquel, J., Doughty, C. E., Metcalfe, D. B., Silva-Espejo, J. E., Girardin, C. A., Chung Gutierrez, J. A., ... Malhi, Y. (2014). The seasonal cycle of productivity, metabolism and carbon dynamics in a wet aseasonal forest in north-west Amazonia (Iquitos, Peru). Plant Ecol Divers 7:71–83. doi: 10.1080/17550874.2013.798365

Del Grosso, S. J., Parton, W. J., Mosier, A. R., Ojima, D. S., Kulmala, A. E., Phongpan, S. (2000). General model for N_2O and N2 gas emissions from soils due to dentrification. Global Biogeochem Cycles 14:1045–1060. doi: 10.1029/1999GB001225

Del Grosso, S.J., Parton, W.J., Mosier, A.R., Hartman, M., Brenner, J., Ojima, D.S., Schimel, D. (2001). Simulated interaction of carbon dynamics and nitrogen trace gas fluxes using the

DAYCENT model. In Shaffer M.J., Ma L., Hansen, S. (eds), Modeling carbon and nitrogen dynamics for soil management, Lewis Publishers, Boca Raton, Florida, USA, 303-332.

Del Grosso, S.J., Parton, W.J., Mosier, A.R., Walsh, M.K., Ojima, D.S. and Thornton, P.E. (2006). DAYCENT national-scale simulations of nitrous oxide emissions from cropped soils in the United States., Journal of Environmental Quality, 35, 1451–1460. doi:10.2134/jeq2005.0160

Delgado, C., Couturier, G., Mejia, K. (2007) Mauritia flexuosa (Arecaceae: Calamoideae), an Amazonian palm with cultivation purposes in Peru. Fruits 62:157-169.

Dobbie, K. E., McTaggart, I. P. and Smith, K. A. (1999). Nitrous oxide emissions from intensive agricultural systems: Variations between crops and seasons, key driving variables, and mean emission factors, J. Geophys. Res., 104, 26891. doi:10.1029/1999JD900378

Dohong, A., Aziz, A. A., & Dargusch, P. (2018). A review of techniques for effective tropical peatland restoration. Wetlands, 38(2), 275-292.

Dommain, R., Couwenberg, J., Joosten, H. (2011). Development and carbon sequestration of tropical peat domes in south-east Asia: links to post-glacial sea-level changes and Holocene climate variability. Quaternary Science Reviews, 30:999–1010. doi: 10.1016/j.quascirev.2011.01.018

Draper, F.C., Honorio Coronado, E.N., Roucoux, K.H., Lawson, I.T., Pitman N.C., Fine P.V., Phillips, O.L., Torres Montenegro, L.A., Valderrama Sandoval, E., Mesones, I., García-Villacorta, R., Arévalo, F.R.R., Baker, T.R. (2018). Peatland forests are the least diverse tree communities documented in Amazonia, but contribute to high regional beta-diversity. Ecography, 41(8), 1256-1269.

Draper, F. C., Roucoux, K. H., Lawson, I. T., Mitchard, E. T. A., Honorio Coronado, E. N., Lähteenoja, O., Montenegro LT, Sandoval EV, Baker, T. R. (2014). The distribution and amount of carbon in the largest peatland complex in Amazonia. Environmental Research Letters, 9(12), 124017. doi:10.1088/1748-9326/9/12/124017

Driessen, P., Rochimah, L. (1976). The physical properties of lowland peats from Kalimantan Indonesia. Peat and Podzolic Soils and their Potential for Agriculture in Indonesia, 56-73. Soil Research Institute, Bogor Indonesia.

Drösler, M., Verchot, L.V., Freibauer, A., Pan, G., Evans, C.D., Bourbonniere, R.A., Alm, J.P., Page, S., Agus, F., Hergoualc'h, K., Couwenberg, J., Jauhiainen, J., Sabiham, S., Wang, C., Srivastava, N., Borgeau-Chavez, L., Hooijer, A., Minkkinen, K., French, N., Strand, T., Sirin, A., Mickler, R., Tansey, K., Larkin, N. (2014). Chapter 2 Drained inland organic soils. In: Hiraishi, T., Krug, T., Tanabe, K., Srivastava, N., Jamsranjav, B., Fukuda, M., Troxler, T. (Eds.): 2013 Supplement to the 2006 guidelines for national greenhouse gas inventories: Wetlands. IPCC, Switzerland.

Duxbury, J. M., Bouldin, D. R., Terry, R. E. and Tate, R. L. (1982). Emissions of nitrous oxide from soils, Nature, 298, 462–464. doi:10.1038/298462a0

Emilio, T., Quesada, C.A., Costa, F.R., Magnusson, W.E., Schietti, J., Feldpausch, T.R., Brienen, R.J., Baker, T.R., Chave, J., Álvarez, E. (2014). Soil physical conditions limit palm and tree basal area in Amazonian forests. Plant Ecology & Diversity, 7:215-229.

Endress, B. A., Horn, C. M., and Gilmore, M. P. (2013). Mauritia flexuosa palm swamps: Composition, structure and implications for conservation and management. Forest Ecology and Management, 302, 346–353. doi:10.1016/j.foreco.2013.03.051

Erickson, H., Davidson, E. A., Keller, M. and Url, S. (2002). Former Land-Use and Tree Species Affect Nitrogen Oxide Emissions from a Tropical Dry Forest, Oecologia, 130, 297–308. doi:10.1007/S004420100801

Erickson, H., Keller, M. and Davidson (2001). Nitrogen Oxide Fluxes and Nitrogen Cycling during Postagricultural Succession and Forest Fertilization in the Humid Tropics, Ecosystems, 4(1), 67–84. doi:10.1007/s100210000060

Espinoza, J. C., Ronchail, J., Frappart, F., Lavado, W., Santini, W., and Guyot, J. L. (2013). The major floods in the Amazonas river and tributaries (Western Amazon Basin) during the 1970–2012 period: a focus on the 2012 flood. Journal of Hydrometeorology, 14(3), 1000–1008. doi:10.1175/jhm-d-12-0100.1

FAO (2009). FAO's Director-General on How to Feed the World in 2050. Population and Development Review, 35(4), 837–839. doi: 10.1111/j.1728-4457.2009.00312.x

FAO (2010). Global forest resources assessment 2010: main report, Rome, Italy.

Farquharson, R. and Baldock, J. (2008). Concepts in modelling N_2O emissions from land use, Plant Soil, 309, 147–167. doi:10.1007/s11104-007-9485-0

Feldpausch, T.R., Rondon, M.A., Fernandes, E.C.M., Riha, S. J., Wandelli, E. (2004). Carbon and nutrient accumulation in secondary forests regenerating on pastures in Central Amazonia. Ecological applications, 14:164–176. doi: 10.1890/01-6015

Figueiredo, L., Krauss, J., Steffan-Dewenter, I., & Sarmento Cabral, J. (2019). Understanding extinction debts: spatio–temporal scales, mechanisms and a roadmap for future research. Ecography, 42(12), 1973-1990.

Firestone M.K., and Davidson, E. A. (1989). Microbial basis of NO and N_2O production and consumption in soil. In: Andrea, M.O., Schimel, D.S. (Eds.) Exchange of trace gases between terrestrial ecosystems and the atmosphere, Wiley, Toronto, 7–21.

Forest news (2016, 1 December). Nazir Foead: 'The keyword for us is cooperation', https://forestsnews.cifor.org/47040/nazir-foead-the-keyword-for-us-is-cooperation?fnl=

Freitas Alvarado, L., Otárola Acevedo, E., del Castillo Torres, D., Linares Bensimón, C., Martínez Dávila, P., and Malca Salas, G. A. (2006). Instituto de Investigaciones de la Amazonía Peruana - IIAP. Iquitos.

Frolking, S., Roulet, N. T., Moore, T. R., Richard, P. J., Lavoie, M., Muller, S. D. (2001). Modeling Northern Peatland Decomposition and Peat Accumulation. Ecosystems 4:479–498. doi: 10.1007/s10021-001-0105-1

Frolking, S., Roulet, N. T., Tuittila, E. S., Bubier, J. L., Quillet, A., Talbot, J., Richard, P. J. H. (2010). A new model of Holocene peatland net primary production, decomposition, water balance, and peat accumulation. Earth System Dynamics. 1:1–21. doi: 10.5194/esd-1-1-2010

Fu, S., and Cheng, W. (2004). Defoliation affects rhizosphere respiration and rhizosphere priming effect on decomposition of soil organic matter under a sunflower species: Helianthus annuus. Plant and Soil, 263, 345–352. doi:10.1023/b

Furukawa, Y., Inubushi, K., Ali, M., Itang, A. M., Tsuruta, H. (2005). Effect of changing groundwater levels caused by land-use changes on greenhouse gas fluxes from tropical peat lands, Nutrient Cycling in Agroecosystems, 71, 81–91. doi:10.1007/s10705-004-5286-5

Garcia-Montiel, D. C., Steudler, P. A., Piccolo, M. C., Melillo, J. M., Neill, C. and Cerri, C. C. (2001). Controls on soil nitrogen oxygen emissions from forest and pastures in the Brazilian Amazon, Global Biogeochemical Cycles, 15, 1021–1030. doi:10.1029/2000GB001349

Gauci, V., Gowing, D. J., Hornibrook, E. R., Davis, J. M., Dise, N. B. (2010). Woody stem methane emission in mature wetland alder trees. Atmos Environ 44:2157–2160. doi: 10.1016/j.atmosenv.2010.02.034

Gaveau, D. L., Salim, M. A., Hergoualc'h, K., Locatelli, B., Sloan, S., Wooster, M., ... Verchot, L. (2015). Major atmospheric emissions from peat fires in Southeast Asia during non-drought years: evidence from the 2013 Sumatran fires. Scientific Reports, 4, 6112. doi:10.1038/srep06112

Gehring, C., Denich, M., Vlek, P.L.G. (2005). Resilience of secondary forest regrowth after slash-and-burn agriculture in central Amazonia. J Trop Ecol 21:519–527. doi: 10.1017/S0266467405002543

Gelfand, I., Feig, G., Meixner, F. X. and Yakir, D. (2009). Afforestation of semi-arid shrubland reduces biogenic NO emission from soil, Soil Biology and Biochemistry, 41(7), 1561–1570. doi:10.1016/j.soilbio.2009.04.018

Gibbs, H. K., Ruesch, A. S., Achard, F., Clayton, M. K., Holmgren, P., Ramankutty, N. and Foley, J. A. (2010). Tropical forests were the primary sources of new agricultural land in the 1980s and 1990s., Proceedings of the National Academy of Sciences, 107(38) 16732–16737. doi:10.1073/pnas.0910275107

Gloor, M., Barichivich, J., Ziv, G., Brienen, R., Schöngart, J., Peylin, P., Barcante Ladvocat Cintra, B., Feldpausch, T., Phillips, O., Baker, J. (2015). Recent Amazon climate as background for possible ongoing Special Section: Global Biogeochemical Cycles, 29(9), 1384–1399. https://doi.org/10.1002/2014GB005080

Goodman, R.C., Phillips, O.L., del Castillo Torres D., Freitas, L., Cortese, S.T., Monteagudo, A., Baker, T.R. (2013). Amazon palm biomass and allometry. Forest Ecology and Management, 310, 994-1004.

Gorham, E. (1991). Northern peatlands: role in the carbon cycle and probable responses to climatic warming. Ecological applications, 1(2), 182-195.

Grandez Rios, J. (n.d.). Dinamica de raices finas en los bosques de aguajales sobre turba. Universidad Nacional de la Amazonía Peruana.

Guariguata, M.R., Ostertag, R. (2001). Neotropical secondary forest succession: changes in structural and functional characteristics. Forest Ecology and Management, 148:185–206. doi: 10.1016/S0378-1127(00)00535-1

Gumbricht, T., Roman-Cuesta, R. M., Verchot, L., Herold, M., Wittmann, F., Householder, E., Herold, N., Murdiyarso, D. (2017). An expert system model for mapping tropical wetlands and peatlands reveals South America as the largest contributor. Global Change Biology, 23(9), 3581–3599. doi:10.1111/gcb.13689

Gurevitch, J. and Hedges, L. V (1999). Statistical Issues in Ecological Meta-Analyses, Ecology, 80(4), 1142–1149.

Haase, K., and Rätsch, G. (2010). The Morphology and Anatomy of Tree Roots and Their Aeration Strategies, In: Junk, W. J., Piedade, M. T. F., Wittmann, F., Schöngart, J., and Parolin, P. (Eds.) Amazonian floorplain forests: ecophysiology, biodiversity and sustainable management, Ecological Studies 210, Springer, Dordrecht, The Netherlands. doi:10.1007/978-90-481-8725-6

Hadi, A., Inubushi, K., Furukawa, Y., Purnomo, E., Rasmadi, M. and Tsuruta, H. (2005). Greenhouse gas emissions from tropical peatlands of Kalimantan, Indonesia, Nutrient Cycling in Agroecosystems, 71(1), 73-80. doi:10.1007/s10705-004-0380-2

Harmon, M.E., Sexton, J. (1996). Guidelines for measurements of woody detritus in forest ecosystems. US LTER Network Office Seattle (WA).

Harris, N. L., Brown, S., Hagen, S. C., Saatchi, S. S., Petrova, S., Salas, W., Hansen, M. C., Potapov, P. V. and Lotsch, A. (2012). Baseline Map of Carbon Emissions from Deforestation in Tropical Regions, Science, 336(6088), 1573-1576. doi:10.1126/science.1217962

Hedges, L. V. and Olkin, I. (1985). Statistical methods for meta-analysis, Academic Press, London, UK.

Heinen, M. (2006). Simplified denitrification models: Overview and properties, Geoderma, 133, 444–463. doi:10.1016/j.geoderma.2005.06.010

Hergoualc'h, K., Carmenta, R., Atmadja, S., Martius, C., Murdiyarso, D., & Purnomo, H. (2018). Managing peatlands in Indonesia: challenges and opportunities for local and global communities. CIFOR Infobrief, 205.

Hergoualc'h, K., Gutiérrez-Vélez, V.H., Menton, M., Verchot, L.V. (2017). Characterizing degradation of palm swamp peatlands from space and on the ground: An exploratory study in the Peruvian Amazon. Forest Ecology and Management, 393, 63–73. doi: 10.1016/j.foreco.2017.03.016

Hergoualc'h, K., Hendry, D. T., Murdiyarso, D., & Verchot, L. V. (2017). Total and heterotrophic soil respiration in a swamp forest and oil palm plantations on peat in Central Kalimantan, Indonesia. Biogeochemistry, 135(3), 203-220. doi:10.1007/s10533-017-0363-4

Hergoualc'h, K., Verchot, L.V. (2011). Stocks and fluxes of carbon associated with land use change in Southeast Asian tropical peatlands: A review. Global Biogeochem Cycles, 25 (2). doi: 10.1029/2009GB003718

Hergoualc'h, K., and Verchot, L. V. (2014). Greenhouse gas emission factors for land use and land-use change in Southeast Asian peatlands. Mitigation and Adaptation Strategies for Global Change, 19(6), 789–807. doi:10.1007/s11027-013-9511-x

Higgins, J. P. T. and Green, S. (2011). Cochrane Handbook for Systematic Reviews of Interventions Version 5.1.0 [updated March 2011], available from www.cochrane-handbook.org last access: 8 August 2015.

Hillel, D. (1980). Fundamentals of soil physics., Academic Press, London, UK.

Hirano, T., Jauhiainen, J., Inoue, T., and Takahashi, H. (2009). Controls on the carbon balance of tropical peatlands. Ecosystems, 12, 873–887. doi:10.1007/s10021-008-9209-1

Holm, J. A. (2007). Population dynamics of the Amazonian palm Mauritia flexuosa model development and simulation analysis. University of Florida.

Hooijer A., Page, S., Canadell, J., Silvius, M., Kwadijk, J., Wösten, H., Jauhiainen, J. (2010). Current and future CO_2 emissions from drained peatlands in Southeast Asia, Biogeosciences, 7, 1505–1514. doi.org/10.5194/bg-7-1505-2010, 2010

Horn, C. M., Gilmore, M. P., and Endress, B. A. (2012). Ecological and socio-economic factors influencing aguaje (Mauritia flexuosa) resource management in two indigenous communities in the Peruvian Amazon. Forest Ecology and Management, 267, 93–103. doi:10.1016/j.foreco.2011.11.040

Horn, C. M., Vargas Paredes, V. H., Gilmore, M. P., and Endress, B. A. (2018). Spatio-temporal patterns of Mauritia flexuosa fruit extraction in the Peruvian Amazon: Implications for conservation and sustainability. Applied Geography, 97, 98–108. doi:10.1016/J.APGEOG.2018.05.004

Hosonuma, N., Herold, M., De Sy, V., De Fries, R. S., Brockhaus, M., Verchot, L., Angelsen, A. and Romijn, E. (2012). An assessment of deforestation and forest degradation drivers in developing countries, Environmental Research Letters, 7(4), 044009. doi:10.1088/1748-9326/7/4/044009

Houghton, R. A. (2003). Revised estimates of the annual net flux of carbon to the atmosphere from changes in land use and land management 1850-2000, Tellus B: Chemical and Physical Meteorology, 55(2), 378-390. doi:10.1034/j.1600-0889.2003.01450.x

Houghton, R. A. (2005). Aboveground forest biomass and the global carbon balance, Global Change Biology, 11, 945–958. doi:10.1111/j.1365-2486.2005.00955.x

Houghton, R. A. (2010). How well do we know the flux of CO_2 from land-use change? Tellus B: Chemical and Physical Meteorology, 62(5), 337-351.

Householder, J.E., John, P.J., Mathias, W.T., Susan, P., Outi, L. (2012). Peatlands of the Madre de Dios River of Peru: Distribution, Geomorphology, and Habitat Diversity. Wetlands, 32(2), 359-368.

Howard, D.M., Howard, P.J.A. (1993). Relationships between CO_2 evolution, moisture content and temperature for a range of soil types. Soil Biology and Biochemistry, 25, 1537-1537. doi: 10.1016/0038-0717(93)90008-Y

Hoyos-Santillan, J., Lomax, B. H., Large, D., Turner, B. L., Boom, A., Lopez, O. R., Sjögersten, S. (2015). Getting to the root of the problem: litter decomposition and peat formation in lowland Neotropical peatlands. Biogeochemistry, 126(1-2), 115-129. doi: 10.1007/s10533-015-0147-7

Hribljan, J.A., Suarez, E., Bourgeau-Chavez, L., Endres, S., Lilleskov, E.A., Chimbolema, S., Wayson, C., Serocki, E., Chimner, R.A. (2017). Multidate, multisensor remote sensing reveals high density of carbon-rich mountain peatlands in the páramo of Ecuador. Global Change Biology 23:5412-5425.

Hribljan, J.A., Suárez, E., Heckman, K.A., Lilleskov, E.A., Chimner, R.A. (2016). Peatland carbon stocks and accumulation rates in the Ecuadorian páramo. Wetlands ecology and management, 24(2), 113-127.

Husen, E., Salma, S., and Agus, F. (2014). Peat emission control by groundwater management and soil amendments: evidence from laboratory experiments. Mitigation and Adaptation Strategies for Global Change, 19(6), 821–829. doi:10.1007/s11027-013-9526-3

Ishizuka, S., Iswandi, A., Nakajima, Y., Yonemura, S., Sudo, S., Tsuruta, H., Murdiyarso, D. (2005). The variation of greenhouse gas emissions from soils of various land-use/cover types in Jambi province, Indonesia. Nutrient Cycling in Agroecosystems, 71, 17-32.

IPCC (2006). 2006 IPCC Guidelines for National Greenhouse Gas Inventories, Prepared by the National Greenhouse Gas Inventories Programme, Eggleston H. S., Buendia L., Miwa K., Ngara, T. and Tanabe, K. (eds.), IGES, Japan.

IPCC (2014). Climate Change 2014: Mitigation of Climate Change. Contribution of Working Group III to the Fifth Assessment Report of the Intergovernmental Panel on Climate Change, Edenhofer, O., R. Pichs-Madruga, Y. Sokona, E. Farahani, S. Kadner, K. Seyboth, A. Adler, I. Baum, S. Brunner, P. Eickemeier, B. Kriemann, J. Savolainen, S. Schlömer, C. von

Stechow, T. Zwickel and J.C. Minx (eds.), Cambridge University Press, Cambridge, United Kingdom and New York, NY, USA.

IPCC (2019). N_2O emissions from managed soils, and CO_2 emissions from lime and urea application, In: 2019 Refinement to the 2006 IPCC Guidelines for National Greenhouse Gas Inventories, Calvo Buendia, E., Tanabe, K., Kranjc, A., Baasansuren, J., Fukuda, M., Ngarize S., Osako, A., Pyrozhenko, Y., Shermanau, P. and Federici, S. (eds), IPCC, Switzerland.

Jauhiainen, J., Hooijer, A., Page, S.E. (2012). Carbon dioxide emissions from an Acacia plantation on peatland in Sumatra Indonesia. Biogeosciences 9:617–630. doi: 10.5194/bg-9-617-2012

Jauhiainen, J., Silvennoinen, H., Könönen, M., Limin, S., Vasander, H. (2016). Management driven changes in carbon mineralization dynamics of tropical peat. Biogeochemistry 129:115–132. doi: 10.1007/s10533-016-0222-8

Jauhiainen, J., Silvennoinen, H., Hämäläinen, R., Kusin, K., Limin, S., Raison, R. J. and Vasander, H. (2012). Nitrous oxide fluxes from tropical peat with different disturbance history and management, Biogeosciences, 9(4), 1337–1350. doi:10.5194/bg-9-1337-2012

Jauhiainen, J., Takahashi, H., Heikkinen, J. E. P., Martikainen, P. J., and Vasander, H. (2005). Carbon fluxes from a tropical peat swamp forest floor. Global Change Biology, 11, 1788–1797. doi:10.1111/j.1365-2486.2005.01031.x

Jordan, S., Velty, S., Zeitz, J. (2007). The influence of degree of peat decomposition on phosphorus binding forms in fens. Mires and Peat 2:7.

Kahn, F. (1988). Ecology of Economically Important Palms in Peruvian Amazonia. Advances in Economic Botany, 6, 42–49.

Kahn, F. (1991). Palms as key swamp forest resources in Amazonia. Forest Ecololgy Management, 38:133-142.

Kahn, F., Mejia, K. (1990). Palm communities in wetland forest ecosystems of Peruvian Amazonia. Forest Ecolology and Management, 33:169-179.

Kahn, F., Mejia, K., de Castro, A. (1988). Species richness and density of palms in terra firme forests of Amazonia. Biotropica:266-269.

Kalliola, R., Salo, J., Puhakka, M., Rajasilta, M., Häme, T., Neller, R.J., Räsänen, M.E., Danjoy Arias, W.A. (1992). Upper amazon channel migration. Naturwissenschaften 79:75-79.

Kauffman, J.B., Arifanti, V.B., Basuki, I., Kurnianto, S., Novita, N., Murdiyarso, D., Donato, D.C., Warren, M.W. (2016). Protocols for the measurement, monitoring, and reporting of structure, biomass, carbon stocks and greenhouse gas emissions in tropical peat swamp forests. Working paper 221, CIFOR, Bogor, Indonesia.

Kauffman, J.B., Donato, D. (2012). Protocols for the measurement, monitoring and reporting of structure, biomass and carbon stocks in mangrove forests. Center for International Forestry Research Center (CIFOR). Working paper 86, CIFOR, Bogor, Indonesia.

Keller, M. and Reiners, W. A. (1994). Soil-atmosphere exchange of nitrous oxide, nitric oxide, and methane under secondary succession of pasture to forest in the Atlantic lowlands of Costa Rica, Global Biogeochemical Cycles, 8, 399-409. doi:10.1029/94GB01660

Keller, M., Varner, R., Dias, J. D., Silva, H., Crill, P., de Oliveira Jr, R. C. and Asner, G. P. (2005). Soil–atmosphere exchange of nitrous oxide, nitric oxide, methane, and carbon dioxide in logged and undisturbed forest in the Tapajós National Forest, Brazil, Earth Interact., 9(23), 1–28.

Keller, M., Veldkamp, E., Weitz, A. M. and Reiners, W. A. (1993). Effect of pasture age on soil trace-gas emissions from a deforested area of Costa Rica, Nature, 365, 244–246. doi:10.1038/365244a0

Palaeoclimatology, Palaeoecology 468:129-141.

Kelly, T. J., Baird, A. J., Roucoux, K. H., Baker, T. R., Honorio Coronado, E. N., Ríos, M., and Lawson, I. T. (2014). The high hydraulic conductivity of three wooded tropical peat swamps in northeast Peru: Measurements and implications for hydrological function. Hydrological Processes, 28, 3373–3387. doi:10.1002/hyp.9884

Kelly, T.J., Lawson, I.T., Roucoux, K.H., Baker, T.R., Jones, T.D., Sanderson, N.K. (2017). The vegetation history of an Amazonian domed peatland. Palaeogeography,

Kelly, T. J., Lawson, I. T., Roucoux, K. H., Baker, T. R., & Coronado, E. N. H. (2020). Patterns and drivers of development in a west Amazonian peatland during the late Holocene. Quaternary Science Reviews, 230, 106168.

Kim, D.-G., Giltrap, D. and Hernandez-Ramirez, G. (2013a). Background nitrous oxide emissions in agricultural and natural lands: a meta-analysis, Plant Soil, 373, 17–30. doi:10.1007/s11104-013-1762-5

Kim, D.-G., Giltrap, D. and Hernandez-Ramirez, G. (2013b). Erratum to: Background nitrous oxide emissions in agricultural and natural lands: a meta-analysis, Plant Soil, 373(1-2), 1007–1008. doi:10.1007/s11104-013-1883-x

Kluber, H.D., Conrad, R. (1998a). Inhibitory effects of nitrate, nitrite, NO and N_2O on methanogenesis by Methanosarcina barkeri and Methanobacterium bryantii. FEMS Microbiology Ecology, 25, 331-339. doi: 10.1111/j.1574-6941.1998.tb00484.x

Kluber, H.D., Conrad, R. (1998b). Effects of nitrate, nitrite, NO and N_2O on methanogenesis and other redox processes in anoxic rice field soil. FEMS Microbiology Ecology, 25, 301–318. doi: 10.1111/j.1574-6941.1998.tb00482.x

Könönen, M., Jauhiainen, J., Laiho, R., Kusin, K., Vasander, H. (2015). Physical and chemical properties of tropical peat under stabilised land uses. Mires and Peat 16:8.

Koricheva, J., Gurevitch, J. and Mengersen, K. (2013). Handbook of meta-analysis in ecology and evolution, Princeton University Press, Princeton, USA.

Kozlowski, T. T. (1997). Responses of woody plants to flooding and salinity. Tree Physiology, 17(7), 490–490. doi:10.1093/treephys/17.7.490

Kreuzwieser, J., Buchholz, J., Rennenberg, H. (2003). Emission of Methane and Nitrous Oxide by Australian Mangrove Ecosystems. Plant Biology, 5(04), 423-431. doi: 10.1055/s-2003-42712

Kurnianto, S., Warren, M., Talbot, J., Kauffman, B., Murdiyarso, D., Frolking, S. (2015). Carbon accumulation of tropical peatlands over millennia: a modeling approach. Global Change Biology 21, 431-444.

Lähteenoja, O., Flores, B., Nelson, B. (2013). Tropical peat accumulation in Central Amazonia. Wetlands 33, 495-503.

Lähteenoja, O., Page, S. (2011). High diversity of tropical peatland ecosystem types in the Pastaza-Marañón basin, Peruvian Amazonia. Journal of Geophysical Research: Biogeosciences 116.

Lähteenoja, O., Reátegui, Y.R., Räsänen, M., Torres, D.D.C., Oinonen, M., Page, S. (2012). The large Amazonian peatland carbon sink in the subsiding Pastaza-Marañón foreland basin, Peru. Global Change Biology 18, 164-178.

Lähteenoja, O., Ruokolainen, K., Schulman, L., Alvarez, J. (2009a). Amazonian floodplains harbour minerotrophic and ombrotrophic peatlands. Catena, 79, 140-145. 10.1016/J.CATENA.2009.06.006

Lähteenoja, O., Ruokolainen, K., Schulman, L., Oinonen, M. (2009b) Amazonian peatlands: An ignored C sink and potential source. Global Change Biology, 15, 2311–2320. doi: 10.1111/j.1365-2486.2009.01920.x

Lambin, E. F., Geist, H. J. and Lepers, E. (2003). Dynamics of Land-Use and Land-Cover Change in Tropical Regions, Annual review of environment and resources, 28(1), 205-241. doi:10.1146/annurev.energy.28.050302.105459

Lambin, E. F., Turner, B. L., Geist, H. J., Agbola, S. B., Angelsen, A., Bruce, J. W., Coomes, O. T., Dirzo, R., Fischer, G., Folke, C., George, P. S., Homewood, K., Imbernon, J., Leemans, R., Li, X., Moran, E. F., Mortimore, M., Ramakrishnan, P. S., Richards, J. F., Skånes, H., Steffen, W., Stone, G. D., Svedin, U., Veldkamp, T. a., Vogel, C. and Xu, J. (2001). The causes of land-use and land-cover change: Moving beyond the myths, Global environmental change, 11(4), 261-269. doi:10.1016/S0959-3780(01)00007-3

Lawson, I.T., Jones, T.D., Kelly, T.J., Coronado, E.N.H., Roucoux, K.H. (2014). The geochemistry of Amazonian peats. Wetlands 34:905-915.

Lawson, I. T., Kelly, T. J., Aplin, P., Boom, A., Dargie, G., Draper, F. C. H., ... Wheeler, J. (2015). Improving estimates of tropical peatland area, carbon storage, and greenhouse gas fluxes. Wetlands ecology and management, 23(3), 327-346. doi:10.1007/s11273-014-9402-2

Lilleskov, E., McCullough, K., Hergoualc'h, K., del Castillo Torres, D., Chimner, R., Murdiyarso, D., ... Wayson, C. (2019). Is Indonesian peatland loss a cautionary tale for Peru? A two-country comparison of the magnitude and causes of tropical peatland degradation. Mitigation and Adaptation Strategies for Global Change, 24, 591-623. doi:10.1007/s11027-018-9790-3

Limpens, J., Berendse, F., Blodau, C., Canadell, J., Freeman, C., Holden, J., Roulet, N., Rydin, H., Schaepman-Strub, G. (2008). Peatlands and the carbon cycle: from local processes to global implications–a synthesis. Biogeosciences 5:1475-1491.

Lin, S., Iqbal, J., Hu, R. and Feng, M. (2010). N_2O emissions from different land uses in mid-subtropical China, Agric. Ecosyst. Environ., 136(1-2), 40–48. doi:10.1016/j.agee.2009.11.005

Linn, D. M. and Doran, J. W. (1984). Effect of Water-Filled Pore Space on Carbon Dioxide and Nitrous Oxide Production in Tilled and Nontilled Soils, Soil Science Society of America Journal, 48(6), 1267-1272. doi:10.2136/sssaj1984.03615995004800060013x

Liu, S., Lin, F., Wu, S., Ji, C., Sun, Y., Jin, Y., ... Zou, J. (2017). A meta-analysis of fertilizer-induced soil NO and combined NO+ N2O emissions. Global Change Biology, 23(6), 2520-2532.

Ludwig, J., Meixner, F. X., Vogel, B. and Forstner, J. (2001). Soil-air exchange of nitric oxide: An overview of processes, environmental factors, and modeling studies, Biogeochemistry, 52, 225–257. doi:10.1023/a:1006424330555

Luizao, F., Luizao, R., Matson, P., Livingston, G. and Vitousek, P. (1989). Nitrous oxide flux following tropical land clearing, Global Biogeochem. Cycles, 3(89), 281–285. doi:10.1029/GB003i003p00281

Manzi, M., Coomes, O.T. (2009). Managing Amazonian palms for community use: A case of aguaje palm (*Mauritia flexuosa*) in Peru. Forest Ecology and Management 257, 510-517.

Marengo, J. (1998). Climatología de la zona de Iquitos, Perú. Kalliola, R. and Flores Paitán, S. (Eds.), Geoecología y desarrollo amazónico: estudio integrado en la zona de Iquitos, Perú, 35–57. Annales Universitatis Turkuensis Ser A II 114, University of Turku, Finland.

Mathieu, O., Lévêque, J., Hénault, C., Milloux, M. J., Bizouard, F., Andreux, F. (2006). Emissions and spatial variability of N_2O, N2 and nitrous oxide mole fraction at the field scale, revealed with 15N isotopic techniques. Soil Biology and Biochemistry, 38(5), 941-951. doi: 10.1016/j.soilbio.2005.08.010

Matson, P. A., Billow, C., Hall, S. and Zachariassen, J. (1996). Fertilization practices and soil variations control nitrogen oxide emissions from tropical sugar cane, J. Geophys. Res., 101, 18533. doi:10.1029/96JD01536

Matson, P. A., Vitousek, P. M., Livingston, G. P. and Swanberg, N. A. (1990). Sources of variation in nitrous oxide flux from Amazonian ecosystems, Journal of Geophysical Research: Atmospheres, 95, 16789-16798. doi:10.1029/JD095iD10p16789

Matysek, M., Evers, S., Samuel, M. K., and Sjogersten, S. (2018). High heterotrophic CO_2 emissions from a Malaysian oil palm plantations during dry-season. Wetlands Ecology and Management, 26(3), 415–424. doi:10.1007/s11273-017-9583-6

McDaniel, M. D., Saha, D., Dumont, M. G., Hernández, M., & Adams, M. A. (2019). The Effect of Land-Use Change on Soil CH 4 and N 2 O Fluxes: A Global Meta-Analysis. Ecosystems, 22(6), 1424-1443.

Meixner, F. X., Fickinger, T., Marufu, L., Ser, D., Nathaus, F. J., Makina, E., Mukurumbira, L. and Andreae, M. O. (1997). Preliminary results on nitric oxide emission from a southern African savanna ecosystem, Nutrient Cycling in Agroecosystems, 123–138.

Melillo, J.M., Aber, J.D., Linkins, A.E., Ricca, A., Fry, B., Nadelhoffer, K.J. (1989). Carbon and nitrogen dynamics along the decay continuum: Plant litter to soil organic matter. Plant Soil 115:189-198.

Melillo, J. M., Steudler, P. A., Feigl, B. J., Neill, C., Garcia, D., Piccolo, M. C., Cerri, C. C. and Tian, H. (2001). Nitrous oxide emissions from forests and pastures of various ages in the Brazilian Amazon, Journal of Geophysical Research: Atmospheres, 106, 34179-34188. doi:10.1029/2000JD000036

Melling, L., Hatano, R., Goh, K.J. (2005). Methane fluxes from three ecosystems in tropical peatland of Sarawak, Malaysia. Soil Biology and Biochemistry, 37, 1445–1453. doi: 10.1016/J.SOILBIO.2005.01.001

Mertz, O., Müller, D., Sikor, T., Hett, C., Heinimann, A., ... Sun, Z. (2012). The forgotten D: challenges of addressing forest degradation in complex mosaic landscapes under REDD+, Geografisk Tidsskrift-Danish Journal of Geography, 112, 63-76. doi:10.1080/00167223.2012.709678

MINAM (2010) Mapa del Patrimonio Forestal Nacional. Dirección General de Evaluación, Valoración y Financiamiento del Patrimonio Natura, Ministerio del Ambiente, Lima, Peru.

Minoda, T., and Kimura, M. (1994). Contribution of photosynthesized carbon to the methane emitted from paddy fields. Geophysical Research Letters, 21(18), 2007-2010.

Moore, T.R., Dalva, M. (1997). Methane and carbon dioxide exchange potentials of peat soils in aerobic and anaerobic laboratory conditions. Soil Biology and Biochemistry, 29(8), 1157-1164.

Moore, S., Evans, C. D., Page, S. E., Garnett, M. H., Jones, T. G., Freeman, C., ... Gauci, V. (2013). Deep instability of deforested tropical peatlands revealed by fluvial organic carbon fluxes. Nature, 493(7434), 660–663. doi:10.1038/nature11818

Morozova, G.S., Smith, N.D. (2003). Organic matter deposition in the Saskatchewan River floodplain (Cumberland Marshes, Canada): effects of progradational avulsions. Sedimentary Geology 157:15-29.

Moyano, F. E., Manzoni, S., and Chenu, C. (2013). Responses of soil heterotrophic respiration to moisture availability: An exploration of processes and models. Soil Biology and Biochemistry, 59, 72–85. doi:10.1016/J.SOILBIO.2013.01.002

Murdiyarso, D., Kauffman, J. B., and Verchot, L. V. (2013). Climate change mitigation strategies should include tropical wetlands. Carbon Management, 4, 491–499. doi:10.4155/Cmt.13.46

Myhre, G., Shindell, D., Bréon, F.-M., Collins, W., Fuglestvedt, J., Huang, J., Koch, D., Lamarque, J.-F., Lee, D., Mendoza, B., Nakajima, T., Robock, A., Stephens, G., Takemura, T., Zhang, H. (2013). Anthropogenic and Natural Radiative Forcing. Stocker, T.F., Qin, D., Plattner, G.-K., Tignor, M., Allen, S.K., Boschung, J., Nauels, A., Xia, Y., Bex, V., Midgley, P.M. (Eds.), Climate Change 2013 The Physical Science Basis. Working Group I Contributionto the Fifth Assessment Report of the Intergovernmental Panel on Climate Change. Cambridge University Press, Cambridge, United Kingdom and New York, NY, USA, 2013.

Neill, C., Piccolo, M. C., Steudler, P. a., Melillo, J. M., Feigl, B. J. and Cerri, C. C. (1995). Nitrogen dynamics in soils of forests and active pastures in the western Brazilian Amazon Basin, Soil Biology and Biochemistry, 27(9), 1167-1175. doi:10.1016/0038-0717(95)00036-E

Neill, C., Steudler, P. A., Garcia-Montiel, D. C., Melillo, J. M., Feigl, B. J., Piccolo, M. C. and Cerri, C. C. (2005). Rates and controls of nitrous oxide and nitric oxide emissions following conversion of forest to pasture in Rondônia, Nutrient Cycling in Agroecosystems, 71(1), 1-15. doi:10.1007/s10705-004-0378-9

Neller, R., Salo, J., Rasanen, M. (1992). On the formation of blocked valley lakes by channel avulsion in Upper Amazon foreland basins. Zeitschrift fur Geomorphologie 36, 401-411.

Nilsson, M., Bohlin, E. (1993). Methane and Carbon Dioxide Concentrations in Bogs and Fens--with Special Reference to Methane and carbon dioxide concentrations in bogs and fens - with special reference to the effects of the botanical composition of the peat. Journal of Ecology, 81(4), 615-625.

NOAA (2018). Climate Prediction Center. Retrieved September 28, 2018, from http://origin.cpc.ncep.noaa.gov/products/analysis_monitoring/ensostuff/ONI_v5.php

Oertel, C., Matschullat, J., Zurba, K., Zimmermann, F., & Erasmi, S. (2016). Greenhouse gas emissions from soils—A review. Geochemistry, 76(3), 327-352.

Oktarita, S., Hergoualc'h, K., Anwar, S., and Verchot, L.V. (2017). Substantial N_2O emissions from peat decomposition and N fertilization in an oil palm plantation exacerbated by hotspots. Environmental Research Letters 12(10), 104007.

Pacheco Santos, L.M. (2005). Nutritional and ecological aspects of buriti or aguaje (*Mauritia flexuosa* Linnaeus filius): A carotene-rich palm fruit from Latin America. Ecology of food and nutrition, 44(5), 345-358. doi: 10.1080/03670240500253369

Padoch, C. (1988). Aguaje (*Mauritia flexuosa* L. f.) in the economy of Iquitos, Peru. Advances in Economic Botany, 6, 214-224.

Page, S. E., Siegert, F., Rieley, J. O., Boehm, H. D. V., Jaya, A., & Limin, S. (2002). The amount of carbon released from peat and forest fires in Indonesia during 1997. Nature, 420(6911), 61-65.

Page, S. E., Rieley, J. O., and Banks, C. J. (2011). Global and regional importance of the tropical peatland carbon pool. Global Change Biology, 17(2), 798–818. doi:10.1111/j.1365-2486.2010.02279.x

Page, S. E., Wűst, R. A. J., Weiss, D., Rieley, J. O., Shotyk, W., Limin, S. H. (2004). A record of Late Pleistocene and Holocene carbon accumulation and climate change from an equatorial peat bog (Kalimantan, Indonesia): implications for past, present and future carbon dynamics, Journal of Quaternary Science, 19(7), 625-635. doi: 10.1002/jqs.884

Page, S., Wűst, R., & Banks, C. (2010). Past and present carbon accumulation and loss in Southeast Asian peatlands. Pages News, 18(1), 25-26.

Palace, M., Keller, M., Hurtt, G., Frolking, S. (2012). A review of above ground necromass in tropical forests. Tropical forests. Intech.

Pangala, S.R., Moore, S., Hornibrook, E.R.C., Gauci, V. (2013). Trees are major conduits for methane egress from tropical forested wetlands. New Phytologist, 197(2), 524-531. doi: 10.1111/nph.12031

Parodi, J.L., Freitas, D. (1990) Geographical aspects of forested wetlands in the lower Ucayali, Peruvian Amazonia. Forest Ecology and Management, 33, 157-168.

Parton, W. J., Holland, E. A., Del Grosso, S. J., Hartman, M. D., Martin, R. E., Mosier, A. R., Ojima, D. S. and Schimel, D. S. (2001). Generalized model for NOx and N_2O emissions from soils, J. Geophys. Res., 106, 17403. doi:10.1029/2001JD900101

Parton, W. J., Scurlock, J. M. O., Ojima, D. S., Gilmanov, T. G., Scholes, R. J., Schimel, D. S., ... Kamnalrut, A. (1993). Observations and modeling of biomass and soil organic matter dynamics for the grassland biome worldwide. Global biogeochemical cycles 7(4):785-809.

Pendrill, F., Persson, U. M., Godar, J., Kastner, T., Moran, D., Schmidt, S., & Wood, R. (2019). Agricultural and forestry trade drives large share of tropical deforestation emissions. Global environmental change, 56, 1-10.

Pérez, T., Romero, J., and Sanhueza, E. (2007). Effect of conversion of natural grassland to cropland on nitric oxide emissions from Venezuelan savanna soils. A four-year monitoring study, Nutrient Cycling in Agroecosystems, 77, 101–113.

Pezeshki, S. R. (2001). Wetland plant responses to soil flooding. Environmental and Experimental Botany, 46(3), 299–312. doi:10.1016/S0098-8472(01)00107-1

Phalan, B., Bertzky, M., Butchart, S. H. M., Donald, P. F., Scharlemann, J. P. W., Stattersfield, A. J. and Balmford, A. (2013). Crop Expansion and Conservation Priorities in Tropical Countries, PLoS One, 8, e51759. doi:10.1371/journal.pone.0051759

Pihlatie, M., Ambus, P., Rinne, J., Pilegaard, K., Vesala, T. (2005). Plant-mediated nitrous oxide emissions from beech (Fagus sylvatica) leaves. New Phytol 168:93–98. doi: 10.1111/j.1469-8137.2005.01542.x

Posa, M.R.C., Wijedasa, L.S., Corlett, R.T. (2011). Biodiversity and conservation of tropical peat swamp forests. Bioscience 61:49-57.

Potter, C. S., Matson, P. A., Vitousek, P. M., Davidson, E. A. (1996). Process modeling of controls on nitrogen trace gas emissions from soils worldwide, Journal of Geophysical Research: Atmospheres, 101, 1361-1377. 1361. doi:10.1029/95JD02028

Purbopuspito, J., Veldkamp, E., Brumme, R. and Murdiyarso, D. (2006). Trace gas fluxes and nitrogen cycling along an elevation sequence of tropical montane forests in Central Sulawesi.donesia, Global Biogeochemical Cycles, 20(3). doi:10.1029/2005GB002516

Purvaja, R., Ramesh, R., Frenzel, P. (2004). Plant-mediated methane emission from an Indian mangrove. Global Change Biology 10:1825–1834. doi: 10.1111/j.1365-2486.2004.00834.x

Queiroz, J.S., Silva, F., Ipenza, C., Hernick, C., Batallanos, L., Griswold, D., Rogers, A.E. (2014). Peru Tropical Forest and Biodiversity Assessment. US Foreign Assistance Act, Section 118/119 Report, USAID, United States.

Räsänen, M., Neller, R., Salo, J., Jungner, H. (1992). Recent and ancient fluvial deposition systems in the Amazonian foreland basin, Peru. Geological Magazine 129:293-306.

Räsänen, M.E., Salo, J., Jungnert, H., Pittman, L.R. (1990). Evolution of the western Amazon lowland relief: impact of Andean foreland dynamics. Terra Nova 2:320-332.

Rieley, J., Wüst, R., Jauhiainen, J., Page, S., Wösten, H., Hooijer, A., Siegert, F., Limin, S., Vasander, H., Stahlhut, M. (2008). Tropical peatlands: carbon stores, carbon gas emissions and contribution to climate change processes. In: Peatlands and Climate Change, International Peat Society, Vapaudenkatu, Finland.

Rodríguez, F. (1990). Los suelos de áreas inundables de la Amazonía Peruana: Potencial, limitaciones y estrategias para su investigación. Folia Amazónica IIAP 2:7-25.

Ross, D.S., Ketterings, Q. (2011). Recommended Methods for Determining Soil Cation Exchange Capacity. Sims, J.T., Wolf, A. (eds). Recommended soil testing procedures for the northeastern United States, 3rd edn. Agricultural Experiment Station, University of Delaware, Newark, USA.

Roucoux, K. H., Lawson, I. T., Jones, T. D., Baker, T. R., Coronado, E. N. H., Gosling, W. D., and Lähteenoja, O. (2013). Vegetation development in an Amazonian peatland. Palaeogeography, Palaeoclimatology, Palaeoecology, 374, 242–255. doi:10.1016/j.palaeo.2013.01.023

Roy, R., Conrad, R. (1999). Effect of methanogenic precursors (acetate, hydrogen, propionate) on the suppression of methane production by nitrate in anoxic rice field soil. FEMS Microbiology Ecology, 28(1), 49-61. doi: 10.1111/j.1574-6941.1999.tb00560.x

Ryan, M.G., Law, B.E. (2005). Interpreting, measuring, and modeling soil respiration. Biogeochemistry 73:3–27.

Saragi-Sasmito, M. F., Murdiyarso, D., June, T., and Sasmito, S. D. (2018). Carbon stocks, emissions, and aboveground productivity in restored secondary tropical peat swamp forests. Mitigation and Adaptation Strategies for Global Change, 1–13. doi:10.1007/s11027-018-9793-0

Schlesinger, W.H., Bernhardt, E.S. (2013). The Global Carbon Cycle. Schlesinger, W.H., Bernhardt, E.S. (eds). Biogeochemistry: an analysis of global change, 3rd edn. Academic Press, Waltham, USA, 419–444.

Seneviratne, S. I., Nicholls, N., Easterling, D., Goodess, C. M., Kanae, S., Kossin, J., ... Zhang, X. (2012). Changes in climate extremes and their impacts on the natural physical environment. Managing the Risks of Extreme Events and Disasters to Advance Climate Change Adaptation. In: C. B. Field, V. Barros, T. F. Stocker, D. Qin, D. J. Dokken, K. L. Ebi, ... P. M. Midgley (Eds.), Managing the Risks of Extreme Events and Disasters to Advance Climate Change Adaptation, A Special Report of Working Groups I and II of the Intergovernmental Panel on Climate Change (IPCC). Cambridge University Press, Cambridge, UK. doi:10.2134/jeq2008.0015br

Sierra, C.A., del Valle, J.I., Orrego, S.A., Moreno, F.H., Harmon, M.E., Zapata, M., Colorado, G.J., Herrera, M.A., Lara, W., Restrepo, D.E., Berrouet, L.M., Loaiza, L.M., Benjumea, J.F. (2007). Total carbon stocks in a tropical forest landscape of the Porce region, Colombia. Forest Ecology and Management, 243(2-3), 299-309.

Simard, R. (1993). Ammonium acetate-extractable elements. Soil sampling and methods of analysis:39-42.

Skiba, U. and Smith, K. A. (2000). The control of nitrous oxide emissions from agricultural and natural soils, Chemosphere-Global Change Science, 2(3-4), 379-386. doi:10.1016/S1465-9972(00)00016-7

Skiba, U., Jones, S., Dragosits, U., Drewer, J., Fowler, D., Rees, R. M., Pappa, V. A., Cardenas, L., Chadwick, D., Yamulki, S. and Manning, A. J. (2012). UK emissions of the greenhouse gas nitrous oxide, Philosophical Transactions of the Royal Society B: Biological Sciences, 367(1593), 1175-1185. doi:10.1098/rstb.2011.0356

Smith, K. A., Ball, T., Conen, F., Dobbie, K. E., Massheder, J., Rey, A. (2003). Exchange of greenhousegases between soil and atmosphere: interactions of soil physical factors and biological processes. European journal of soil science, 54(4), 779-791. doi: 10.1046/j.1365-2389.2003.00567.x

Smith, N.D., Cross, T.A., Dufficy, J.P., Clough, S.R. (1989). Anatomy of an avulsion. Sedimentology 36:1-23.

Stehfest, E. and Bouwman, L. (2006). N_2O and NO emission from agricultural fields and soils under natural vegetation: Summarizing available measurement data and modeling of global annual emissions, Nutrient Cycling in Agroecosystems, 74(3), 207-228. doi:10.1007/s10705-006-9000-7

Stern, N. (2008). The economics of climate change, American Economic Review, 98:2, 1-37.

Steudler, P., Melillo, J. M., Bowden, R. and Castro, M. (1991). The effects of natural and human disturbances on soil nitrogen dynamics and trace gas fluxes in a Puerto Rican wet forest, Biotropica, 23, 356–363.

Streck, C. and Parker, C. (2012). Financing REDD. Analysing REDD, edited by A. Angelsen, M. Brockhaus, and L. V. Verchot, 111–127, Center for International Forestry Research, Bogor, Indonesia.

Subke, J. A. Inglima, I., and Cotrufo, M. F. (2006). Trends and methodological impacts in soil CO_2 efflux partitioning: A metaanalytical review. Global Change Biology, 12, 921–943. doi:10.1111/j.1365-2486.2006.01117.x

Sullivan, M. J., Talbot, J., Lewis, S. L., Phillips, O. L., Qie, L., Begne, S. K., ... & Miles, L. (2017). Diversity and carbon storage across the tropical forest biome. Scientific Reports, 7(1), 1-12.

Swails, E., Jaye, D., Verchot, L., Hergoualc'h, K., Schirrmann, M., Borchard, N., ... Lawrence, D. (2017). Will CO_2 Emissions from Drained Tropical Peatlands Decline Over Time? Links Between Soil Organic Matter Quality, Nutrients, and C Mineralization Rates. Ecosystems. doi: 10.1007/s10021-017-0190-4

Swails, E., Hertanti, D., Hergoualc'h, K., Verchot, L., and Lawrence, D. (2019). The response of soil respiration to climatic drivers in undrained forest and drained oil palm plantations in an Indonesian peatland. Biogeochemistry, 142(1), 37–51. doi:10.1007/s10533-018-0519-x

Takakai, F., Morishita, T., Hashidoko, Y., Darung, U., Kuramochi, K., Dohong, S., Limin, S. H. and Hatano, R. (2006). Effects of agricultural land-use change and forest fire on N_2O emission from tropical peatlands, Central Kalimantan Indonesia, Soil Science & Plant Nutrition, 52(5), 662-674. doi:10.1111/j.1747-0765.2006.00084.x

Teh, Y. A., Wayne, M., Berrio, J. C., Boom, A., Page, S. E. (2017). Seasonal variability in methane and nitrous oxide fluxes from tropical peatlands in the western Amazon basin. Biogeosciences 14:3669–3683. doi: 10.5194/bg-14-3669-2017

Teh, Y.A., Silver, W.L., Conrad, M.E. (2005). Oxygen effects on methane production and oxidation in humid tropical forest soils. Global Change Biology 11:1283–1297. doi: 10.1111/j.1365-2486.2005.00983.x

Terborgh, J., Andresen, E. (1998). The composition of Amazonian forests: patterns at local and regional scales. Journal of Tropical Ecology 14:645-664.

Terry, R., Tate, R. and Duxbury, J. (1981). Nitrous oxide emissions from drained, cultivated organic soils of South Florida, Journal of the Air Pollution Control Association, 31(11), 1173-1176. doi:10.1080/00022470.1981.10465342

Tfaily, M. M., Cooper, W. T., Kostka, J. E., Chanton, P. R., Schadt, C. W., Hanson, P. J., ... Chanton, J. P. (2014). Organic matter transformation in the peat column at Marcell Experimental Forest: Humification and vertical stratification, Journal of Geophysical Research: Biogeosciences, 119(4), 661-675. doi: 10.1002/2013JG002492

Thompson, I.D., Guariguata, M.R., Okabe, K., Bahamondez, C., Nasi, R., Heymell, V., Sabogal, C. (2013). An operational framework for defining and monitoring forest degradation. Ecology and Society 18:20.

Tilman, D., May, R. M., Lehman, C. L., & Nowak, M. A. (1994). Habitat destruction and the extinction debt. Nature, 371(6492), 65-66.

Updegraff, K., Pastor, J., Bridgham, S.D., Johnston, C.A. (1995). Environmental and Substrate Controls over Carbon and Nitrogen Mineralization in Northern Wetlands. Ecological applications, 5(1), 151-163. doi: 10.2307/1942060

Van Lent, J., Hergoualc'h, K., Verchot, L. (2015). Reviews and syntheses: Soil N_2O and NO emissions from land use and land-use change in the tropics and subtropics: a meta-analysis. Biogeosciences, 12, 7299–7313. doi: 10.5194/bg-12-7299-2015

Van Lent, J., Hergoualc'h, K., Verchot, L., Oenema, O., and van Groenigen, J. W. (2019). Greenhouse gas emissions along a peat swamp forest degradation gradient in the Peruvian Amazon: soil moisture and palm roots effects. Mitigation and Adaptation Strategies for Global Change, 24(4), 625–643. doi:10.1007/s11027-018-9796-x

Van Noordwijk, M., Martikainen, P., Bottner, P., Cuevas, E., Rouland, C., Dhillion, S. S. (1998). Global change and root function. Global Change Biology 4:759–772. doi: 10.1046/j.1365-2486.1998.00192.x

Van Noordwijk, M., Matthews, R., Agus, F., Farmer, J., Verchot, L., Hergoualc'h, K., ... & Dewi, S. (2014). Mud, muddle and models in the knowledge value-chain to action on tropical peatland conservation. Mitigation and Adaptation Strategies for Global Change, 19(6), 887-905.

Van Noordwijk, M., and Sunderland, T.C.H. (2014) Productive landscapes: what role for forests, trees and agroforestry?, ETFRN News 56.

Veldkamp, E. and Keller, M. (1997). Nitrogen oxide emissions from a banana plantation in the humid tropics, Journal of Geophysical Research: Atmospheres, 102, 15889-15898. doi:10.1029/97JD00767

Veldkamp, E., Davidson, E., Erickson, H., Keller, M. and Weitz, A. (1999). Soil nitrogen cycling and nitrogen oxide emissions along a pasture chronosequence in the humid tropics of

Costa Rica, Soil Biology and Biochemistry, 31(3), 387-394. doi:10.1016/S0038-0717(98)00141-2

Veldkamp, E., Keller, M. and Nuñez, M. (1998). Effect of pasture management on N_2O and NO emissions from soils in the humid tropics of Costa Rica, Global Biogeochemical Cycles, 12(1), 71. doi:10.1029/97GB02730

Veldkamp, E., Purbopuspito, J., Corre, M. D., Brumme, R. and Murdiyarso, D. (2008). Land use change effects on trace gas fluxes in the forest margins of Central Sulawesi, Indonesia, Journal of Geophysical Research, 113, G02003. doi:10.1029/2007JG000522

Verchot, L. V., Davidson, E. A., Cattânio, J. H., Ackerman, I.L. (2000). Land-Use Change and Biogeochemical Controls of Methane Fluxes in Soils of Eastern Amazonia. Ecosystems 3:41–56. doi: 10.1007/s100210000009

Verchot, L. V., Davidson, E. A., Cattânio, J. H., Ackerman, I. L., Erickson, H. E. and Keller, M. (1999). Land use change and biogeochemical controls of nitrogen oxide emissions from soils in eastern Amazonia. Global Biogeochemical Cycles, 13(1), 31-46. doi:10.1029/1998GB900019

Verchot, L. V., Hutabarat, L., Hairiah, K. and van Noordwijk, M. (2006). Nitrogen availability and soil N_2O emissions following conversion of forests to coffee in southern Sumatra, Global biogeochemical cycles, 20(4), GB4008. doi:10.1029/2005GB002469

Virapongse, A., Endress, B. A., Gilmore, M. P., Horn, C., and Romulo, C. (2017). Ecology, livelihoods, and management of the Mauritia flexuosa palm in South America. Global Ecology and Conservation, 10, 70–92. doi:10.1016/j.gecco.2016.12.005

Vitousek, P. M., Aber, J. D., Howarth, R. W., Likens, G. E., Matson, P. A., Schindler, D. W., ... & Tilman, D. G. (1997). Human alteration of the global nitrogen cycle: sources and consequences. Ecological applications, 7(3), 737-750.

Wang, M. C. and Bushman, B. J. (1998). Using the normal quantile plot to explore meta-analytic data sets. Psychological Methods, 3(1), 46–54. doi:10.1037/1082-989X.3.1.46

Warren, M., Hergoualc'h, K., Kauffman, J. B., Murdiyarso, D., & Kolka, R. (2017). An appraisal of Indonesia's immense peat carbon stock using national peatland maps: uncertainties and potential losses from conversion. Carbon balance and management, 12(1), 12.

Werner, C., Butterbach-Bahl, K., Haas, E., Hickler, T., Kiese, R. (2007). A global inventory of N_2O emissions from tropical rainforest soils using a detailed biogechemical model, Global Biochemical Cycles, 21, GB3010. doi:10.1029/2006GB002909

Werner, C., Zheng, X., Tang, J., Xie, B., Liu, C., Kiese, R., Butterbachy-Bahl, K. (2006). N_2O, CH_4 and CO_2 emissions from seasonal tropical rainforests and a rubber plantation in Southwest China, Plant Soil, 289, 335-353

Wick, B., Veldkamp, E., de Mello, W. Z., Keller, M. and Crill, P. (2005). Nitrous oxide fluxes and nitrogen cycling along a pasture chronosequence in Central Amazonia, Brazil, Biogeosciences, 2, 175-187. doi:10.5194/bgd-2-499-2005

Xiong, Z., Xie, Y., Xing, G., Zhu, Z. and Butenhoff, C. (2006). Measurements of nitrous oxide emissions from vegetable production in China, Atmospheric Environment, 40(12), 2225-2234. doi:10.1016/j.atmosenv.2005.12.008

Xu, J., Morris, P. J., Liu, J., and Holden, J. (2018). PEATMAP: Refining estimates of global peatland distribution based on a meta-analysis. CATENA, 160, 134–140. doi:10.1016/J.CATENA.2017.09.010

Yashiro, Y., Kadir, W. R., Okuda, T. and Koizumi, H. (2008). The effects of logging on soil greenhouse gas (CO_2, CH_4, N_2O) flux in a tropical rain forest, Peninsular Malaysia, Agricultural and Forest Meteorology, 148(5), 799-806. doi:10.1016/j.agrformet.2008.01.010

Yule, C.M., Gomez, L.N. (2009) Leaf litter decomposition in a tropical peat swamp forest in Peninsular Malaysia. Wetlands Ecology and Management, 17(3), 231-241.

Zambrana, N.Y.P., Byg, A., Svenning. J.-C., Moraes, M., Grandez, C., Balslev, H. (2007) Diversity of palm uses in the western Amazon. Biodiversity and Conservation, 16(10), 2771-2787.

Ziadi, N., Sen Tran T. (2007). Mehlich 3-extractable elements. Carter, M., Gregorich, E. (eds). Soil sampling and methods of analysis, 2nd edition. Taylor and Francis Group, Boca Raton, USA, 81–88.

8 Summary

Forest conversion and degradation are important contributors to worldwide anthropogenic greenhouse gas (GHG) emissions. In the tropics, GHG emissions from such land uses and land-use changes in general comprises a large share of the national GHG emissions. IPCC Tier 1 guidelines are typically used for estimating the national annual GHG emissions, but these guidelines are not always correctly applicable to a tropical context. This can lead to situations where GHG estimates are based on measurements from other climatic zones and/or different continents. Another source of low accuracy in GHG emission estimation is when emission factors for specific tropical land use practices are missing and are not included in national GHG emission budgets. In this thesis I focus on both of these problems by increasing the mechanistic understanding of the effects of forest conversions on GHG emissions in the tropics, and to contribute to the derivation of robust emission factors for land-use change in the tropics.

In **Chapter 1** the objectives are explained. The first objective is to systematically review all studies on N_2O and NO emissions from land use and land-use change in the tropics, and to improve current emission factors for land use and land-use change in the tropics. The second objective is to examine CO_2, N_2O and CH_4 emissions from a region-specific land use not studied to date: forest degradation in tropical peatlands of the Amazon. For this unique land-use change category, I investigate the effects of forest degradation on ecosystem C-stocks and the soil C balance in a four-year field experiment. These two objectives are addressed in following four chapters.

Chapter 2 presents a meta-analysis of reported N_2O and NO emissions from forest conversions in the global tropics. The aim was to provide an updated overview of N_2O and NO emission rates, and determine trends in fluxes after forest conversion. The main finding was that undisturbed tropical forests emit 2.0 kg N_2O-N ha^{-1} yr^{-1} on average, and that emission rates significantly increased after conversion to cropland. Nitrogen (N) input from fertilization was the most important proxy for N_2O emissions at a rate of 1.9% of the N input, which was higher than the 1% IPCC Tier 1 default value (IPCC, 2006). Moreover, time since conversion was an important factor for both unfertilized and fertilized LUCs during the first 10 years after conversion. Few studies have measured emissions

from land following the conversion of forest to crop land used to grow important world crops such as soy and oil palm, and very few studies have been conducted in Africa. Tropical wetlands have been exclusively studied in Southeast Asia, while there are also extensive tropical wetlands in South America and Africa. Based on these findings, I focused my experimental thesis research further on land uses on tropical wetlands in South America.

South America harbours one of the largest areas of tropical peatlands worldwide, with large stretches of shallow peat previously unaccounted for in the Amazon basin (Gumbricht et al., 2017; Draper et al., 2014; Lahteenoja et al, 2011). Experimental data on effects of land use and land-use change on GHG emissions in these peat swamp forests (PSFs) are almost totally absent in the literature. Therefore, I focused on GHG emissions from PSF degradation in the Amazon basin. Most studies on PSF are related to conversion and drainage activities, while in the Amazon the common land use on peat is harvesting of female *M. flexuosa* palms for their fruits. This unique, but widely applied type of forest degradation on peat occurs in relatively remote natural stands throughout the Amazon. Contrary to PSFs in Southeasts Asia, these systems are not drained, nor fertilized.

Chapter 3 explored potential effects of palm harvesting on C losses. Total ecosystem C stocks, floristic composition and degradation status were measured in three regions and twelve sites throughout the Pastza-Marañón river basin in the Peruvian Amazon. Total ecosystem C stocks ranged from 200 to 1600 Mg C ha^{-1} with peat depths up to 2.8 m. These C stocks are immense in comparison to typical tropical rainforests, which have C stocks ranging between 130 and 240 Mg C ha^{-1}, but are relatively small in comparison to common values of 1000 up to 7500 Mg C ha^{-1} stored in Southeast Asian peat deposits of up to 12 m deep (Warren et al., 2017).

Degradation status in the Peruvian PSFs ranged from low to high levels of disturbance with no significant difference between regions. This indicated that degradation is not regional, but occurred throughout the Pastza-Marañón river basin – parts of which are inside a national reserve. Degradation status correlated negatively with palm vegetation C stock, but not with soil C stocks. Thus, C-stock differences between sites could not be used to estimate C losses from the soil following palm-harvesting.

Chapters 4 and 5 present the results of a detailed gain-loss experiment to further study the C balance of peat soils following PSF degradation at three sites. In **Chapter 4**, factors were studied that drive GHG fluxes, and that were hypothesized to be affected by degradation. These were (1) water table fluctuations and WFPS% as a proxy for soil aeration, (2) microtopography of the soil surface area in terms of hummock and hollows, (3) soil organic matter quality derived from litter input, and (4) presence of aerating roots that emit CH_4. Microtopography and soil organic matter quality (factors 2 and 3) were found to be the most important factors explaining effects of forest degradation on soil GHG fluxes in PSFs.

Chapter 5 presents the effects of palm-harvesting on the soil C balance. Palm-harvesting affected the microtopography and reduced the number and size of hummocks. Heavily degraded sites had a larger part of their soil surface area classified as hollows. In addition, heterotrophic respiration at hollows increased following degradation, resulting in a larger C output from degraded soils. Water table and WFPS% fluctuations appeared not to affect these trends; these fluctuations mostly affected seasonal respiration fluctuations. I concluded that larger heterotrophic respiration rates in hollows are related to changes in litter quality and quantity. *In vitro* incubated soils from the degraded sites consistently produced more carbon dioxide (CO_2) than soils from less disturbed palm swamp sites (Chapter 4). This was confirmed by *in situ* measurements during ~4 years, with significantly higher heterotrophic respiration rates at the highly degraded site than at the intact site (Chapter 5).

Lower palm and dicot tree stem densities at the heavily degraded site resulted in lower leaf- and wood fall rates. The combined effects of more C output via heterotrophic respiration and less input via litter turned the soil at the heavily degraded PSF into a net C source of -7.1 Mg C ha^{-1} yr^{-1}, while undisturbed sites remained at -0.1 Mg ha^{-1} yr^{-1}. Therefore, forest degradation in PSF causes significant soil C losses – even without drainage or fertilization practices.

In **Chapter 6**, the general discussion, I conclude that there is a substantial CO_2 emission reduction potential by preventing destructive palm harvesting throughout the Amazon. First reports on concerns of over-harvesting *M. flexuosa* palms in the Peruvian Amazon are from the 1980s, and fruit harvesting has

increased dramatically in the 30 years thereafter (Horn et al., 2018; Padoch, 1988). I show that C loss from forest degradation on peat is estimated to represents a significant C source up to 7.8 Tg C yr^{-1} for the entire Pastaza-Marañón basin. Ultimately, the goal should be to prevent the trajectory of peat drainage and conversions seen in Southeast Asia. Non-destructive fruit extraction could be done by climbing palms and cultivation of *M. flexuosa* in agroforestry systems. Payment for GHG mitigation efforts could provide an additional incentive, in combination with prolonged income from fruits collected in sustainably managed palm swamp forests throughout the Amazon.

9 Resumen

La conversión y degradación de los bosques contribuyen de manera importante a las emisiones antropogénicas de gases de efecto invernadero (GEI) en todo el mundo. En los trópicos, las emisiones de GEI por el uso del suelo y los cambios de uso del suelo en general comprenden una gran parte de las emisiones nacionales de GEI. Las pautas del Nivel 1 del IPCC se utilizan normalmente para estimar las emisiones anuales de GEI a nivel nacional, pero estas pautas no siempre se aplican correctamente a un contexto tropical. Esto puede conducir a situaciones en las que las estimaciones de GEI se basan en mediciones de otras zonas climáticas y / o continentes diferentes. Otra fuente de baja precisión en la estimación de emisiones de GEI es cuando faltan factores de emisión para prácticas específicas de uso del suelo tropical y no se incluyen en los presupuestos nacionales de emisiones de GEI. En esta tesis me centro en ambos problemas aumentando la comprensión mecanicista de los efectos de las conversiones de bosques en las emisiones de GEI en los trópicos y contribuyendo a la derivación de factores de emisión robustos para el cambio de uso del suelo en los trópicos.

En el **Capítulo 1** se explican los objetivos. El primer objetivo es revisar sistemáticamente todos los estudios sobre las emisiones de N_2O y NO del uso del suelo y el cambio de uso del suelo en los trópicos, así como, mejorar los factores de emisión actuales para el uso del suelo y el cambio de uso del suelo. El segundo objetivo es examinar las emisiones de CO_2, N_2O y CH_4 de una región con uso del suelo no estudiado hasta la fecha: la degradación de los bosques en las turberas tropicales de la Amazonía. En esta categoría única de cambio de uso del suelo, investigue los efectos de la degradación forestal en los reservorios del Carbono (C) del ecosistema y el balance de C en el suelo a lo largo de un experimento de campo de cuatro años de duración. Estos dos objetivos se tratan en los siguientes cuatro capítulos.

Capítulo 2 presenta un meta-análisis de las emisiones de N_2O y NO asociadas a las conversiones forestales y reportadas para la región tropical. El objetivo fue proporcionar una visión general actualizada de las tasas de emisión de N_2O y NO, y determinar las tendencias en los flujos después de la conversión forestal por perturbación antrópica. El principal hallazgo fue que los bosques tropicales no

perturbados emiten en promedio 2.0 kg de N_2O-N ha^{-1} $año^{-1}$, y que las tasas de emisión aumentaron significativamente después de la conversión a campos de cultivo. La incorporación de nitrógeno (N) al suelo debido a la fertilización fue el indicador más importante para las emisiones de N_2O con una tasa del 1.9% de la incorporación de N, que fue superior al valor del 1% determinado por el *Tier* 1 del IPCC (IPCC, 2006). Además, el tiempo transcurrido desde la conversión fue un factor importante para los CUS no fertilizados y fertilizados durante los primeros 10 años después de la conversión. Pocos estudios han medido las emisiones en suelos después de la conversión de bosques a campos de cultivo que producen cultivos de importancia mundial como la soya y la palma aceitera, y muy pocos estudios se han llevado a cabo en África. Los humedales tropicales han sido exclusivamente estudiados en el sudeste asiático, mientras que también hay extensos humedales tropicales en América del Sur y África. En base a estos hallazgos, la parte experimental de mi investigación se enfocó en los usos del suelo de los humedales tropicales en América del Sur.

América del Sur alberga una de las áreas más grandes de turberas tropicales en todo el mundo, con grandes extensiones de turba poco profunda que no fueron registradas previamente en la cuenca Amazónica (Gumbricht et al., 2017; Draper et al., 2014; Lahteenoja et al, 2011). Datos experimentales sobre los efectos del uso del suelo y el cambio del uso del suelo sobre las emisiones de GEI en estos bosques pantanosos de turberas (PSF) son casi ausentes en la literatura. Por lo tanto, me enfoqué en las emisiones de GEI provenientes de la degradación de los PSF en la cuenca Amazónica. La mayoría de los estudios sobre PSF están relacionados con actividades como conversión y drenaje, mientras que en la Amazonía es común que el uso del suelo de la turba sea la tala de palmeras femeninas de *M. flexuosa* para la cosecha de sus frutos. Este tipo único, pero ampliamente aplicado, de degradación forestal en la turba se produce en rodales naturales relativamente remotos en todo la Amazonía. A diferencia de los PSF en el sudeste asiático, estos sistemas no se drenan ni se fertilizan.

El **Capítulo 3** exploró los efectos potenciales de la tala de palmeras en las pérdidas C. Los reservorios totales de C del ecosistema, la composición florística y el estado de degradación se midieron en tres regiones y doce sitios a lo largo de la cuenca Pastaza-Marañón en la Amazonía peruana. Los reservorios totales de C

del ecosistema variaron de 200 a 1600 Mg C ha^{-1} con profundidades de turba de hasta 2.8 m. Estos reservorios de C son inmensos en comparación con los valores típicos de los bosques lluviosos tropicales, que tienen reservorios de C que oscilan entre 130 y 240 Mg C ha^{-1}, pero son relativamente pequeños en comparación con los valores de 1000 hasta 7500 Mg C ha^{-1} comúnmente registrados en depósitos de turba del sudeste asiático, que alcanzan hasta los 12 m de profundidad (Warren et al., 2017).

El estado de degradación en los PSF peruanas varió desde niveles bajos a altos de perturbación sin mostrar diferencias significativas entre las regiones. Esto indicó que la degradación no es regional, sino que ocurrió en toda la cuenca de los ríos Pastaza-Marañón – que incluye partes ubicadas dentro de una reserva nacional. El estado de degradación se correlacionó negativamente con el reservorio de C de la vegetación de palmeras, pero no con el reservorio de C del suelo. Por lo tanto, las diferencias del reservorio de C entre sitios no podrían ser usadas para estimar las pérdidas de C en el suelo después de la tala de palmeras.

Los capítulos 4 y 5 presentan los resultados de un experimento detallado de pérdida y ganancia para estudiar el balance de C de los suelos de turba después de la degradación del PSF en tres sitios. En el **Capítulo 4**, se estudiaron los factores que impulsan los flujos de GEI, y se hipotetizaron que se verían afectados por la degradación. Estos factores fueron (1) fluctuaciones de la capa freática y % de WFPS como indicador para la aireación del suelo, (2) microtopografía de la superficie del suelo en términos de montículos y huecos – superficies elevadas y planas respectivamente, (3) calidad de la materia orgánica del suelo derivada de la hojarasca, y (4) presencia de neumatóforos que emiten CH_4. Se encontró que la microtopografía y la calidad de la materia orgánica del suelo (factores 2 y 3) son los factores más importantes que explican los efectos de la degradación de los bosques en los flujos de GEI del suelo en los PSF.

Capítulo 5 presenta los efectos de la tala de palmeras en el balance de C en el suelo. La cosecha de las palmeras afectó la microtopografía y redujo el número y el tamaño de los montículos. En los sitios muy degradados una gran parte de la superficie de suelo estuvo clasificada como huecos. Además, la respiración heterotrófica en los huecos aumentó después de la degradación, lo que resultó en una mayor emisión de C de los suelos degradados. Las fluctuaciones de la capa

freática y el % de WFPS parecieron no afectar estas tendencias; sino que afectaron principalmente las fluctuaciones estacionales de la respiración. Llegué a la conclusión de que las tasas de respiración heterotrófica más grandes en huecos están relacionadas con cambios en la calidad y cantidad de la hojarasca. Los suelos de los sitios degradados incubados *in vitro* produjeron consistentemente más dióxido de carbono (CO_2) que los suelos de los pantanos de palmeras menos perturbados (Capítulo 4). Esto fue confirmado por mediciones *in situ* realizadas durante ~ 4 años, con tasas de respiración heterotrófica significativamente más altas en el sitio altamente degradado que en el sitio intacto (Capítulo 5).

Las densidades más bajas de los tallos de las palmeras y dicotiledóneas en el sitio degradado resultaron en tasas más bajas de caída de hojas secas y madera muerta. Los efectos combinados de mayor emisión de C a través de la respiración heterotrófica y menor incorporación de C a través de la hojarasca convirtieron al suelo del PSF altamente degradado en una fuente de C neta de -7.1 Mg C ha^{-1} $año^{-1}$, mientras que los sitios no perturbados permanecieron en -0.1 Mg ha^{-1} $año^{-1}$. Por lo tanto, la degradación forestal en PSF causa pérdidas significativas de C en el suelo, incluso sin prácticas de drenaje o fertilización.

En el **Capítulo 6**, la discusión general, concluyo que existe un potencial sustancial de reducción de emisiones de CO_2 al evitar la cosecha destructiva de frutos de palmeras en toda la Amazonía. Los primeros reportes alertando sobre la sobreexplotación de palmeras de *M. flexuosa* en la Amazonía Peruana datan de la década de 1980, y la cosecha de frutos ha aumentado dramáticamente en los 30 años posteriores (Horn et al., 2018; Padoch, 1988). Yo muestro que la pérdida de C por la degradación forestal en la turba representa una fuente de C significativa de hasta 7.8 Tg C $año^{-1}$ para toda la cuenca Pastaza-Marañón. A la larga, el objetivo debería ser evitar que en la cuenca Pastaza-Marañón ocurran actividades como el drenaje de turba y las conversiones observadas en el sudeste asiático. La cosecha no destructiva del fruto podría hacerse trepando palmeras y cultivando *M. flexuosa* en sistemas agroforestales. El pago por los esfuerzos de mitigación de GEI podría proporcionar un incentivo adicional, en combinación con el ingreso económico constante por la cosecha sostenible de frutos de los bosques pantanosos de palmeras manejados en todo la Amazonía.

10 Samenvatting

Boskap en bosdegradatie zijn een belangrijke oorzaak van door mensen geproduceerde broeikasgasemissies. In tropische regio's beslaan dergelijke emissies vaak een belangrijk deel van de nationale uitstoot. Voor het schatten van die uitstoot worden vaak algemene Tier 1 IPCC-richtlijnen gebruikt, maar deze zijn veelal niet gebaseerd op de tropische context. Dit betekent dat de emissiefactoren uit andere klimatologische regio's of continenten gebruikt worden. Daarnaast zijn er specifieke vormen van tropisch landgebruik waarvoor geen emissiefactoren bestaan, waardoor mogelijke broeikasgasemissies die hierbij vrijkomen niet meegenomen worden in berekeningen van nationale broeikasgasuitstoot. Mijn proefschrift heeft daarom als overkoepelend doel meer inzicht te verkrijgen in de vorming van broeikasgassen die vrijkomen bij het omzetten van tropisch bos naar een ander landgebruik.

In **Hoofdstuk 1** wordt dit doel verder uitgewerkt. De eerste stap is een overzicht verkrijgen van alle studies over N_2O en NO-emissies die vrijkomen bij landgebruikverandering in de tropen en vervolgens daarmee bestaande IPCC emissiefactoren te verbeteren. Als tweede stap heb ik broeikasgasemissies bestudeerd die vrijkomen bij bosdegradatie op tropische veengronden in het Amazoneregenwoud. Deze degradatie is een vorm van regionaal landgebruik dat tot op heden nog niet bestudeerd is. Gedurende een vierjarig experiment heb ik het effect van bosdegradatie op de koolstofbalans en de koolstofopslagcapaciteit onderzocht in dit unieke gebied. Deze twee stappen van mijn onderzoek zijn uitgewerkt in de volgende hoofstukken.

Hoofdstuk 2 presenteert een meta-analyse van alle gepubliceerde studies die zijn gedaan in de tropen over N_2O- en NO-emissies die vrijkomen bij het omzetten van bos naar ander landgebruik. Het doel was om ten eerste huidige emissiefactoren te verbeteren aan de hand van deze meest recente literatuur en ten tweede te beschrijven hoe de broeikasgasproductie ontwikkelt in de jaren na boskap. Het belangrijkste resultaat is dat ongerepte tropische bossen gemiddeld 2.0 kg N_2O-N ha^{-1} yr^{-1} uitstoten en dat vooral de omzetting naar landbouw de N_2O-emissies significant en substantieel vergroten. Stikstofbemesting blijkt de beste indicatie voor N_2O in tropische regio's: gemiddeld 1.9% van de toegediende stikstof wordt uitgestoten als N_2O. Dit percentage is beduidend hoger dan de 1% uit de

(toentertijd) meest recente IPCC-richtlijnen (IPCC, 2006). Ongeacht het gebruik van stikstofbemesting, blijkt dat de 10 jaar direct na ontbossing gekarakteriseerd wordt door verhoging van N_2O-emissies. Verder laat de meta-analyse zien dat er weinig studies gedaan zijn in Afrika en ontbreekt het aan onderzoek naar belangrijke gewassen als soja en palmolie. Kap van tropisch veenbos is daarnaast een categorie die buitengewoon weinig aandacht heeft gekregen buiten Zuidoost-Azië, hoewel er in recente literatuur bijvoorbeeld grote veengebieden zijn beschreven in zowel Afrika als Zuid-Amerika. Het resterende deel van mijn onderzoek heb ik daarom gericht op landgebruikverandering in veengebieden van Zuid-Amerika en op de effecten die dit heeft op de productie van broeikasgasemissies.

Het Amazonewoud in Zuid-Amerika huisvest een van de grootste tropische veengebieden in de wereld. Dit zijn veelal ondiepe veengronden, maar ze bevatten toch enorme hoeveelheden koolstof door de grote oppervlakte die ze volgens recente schattingen beslaan (Gumbricht et al., 2017; Draper et a., 2014; Lahteenoja et al, 2011). Hoewel deze gebieden beschreven zijn, zijn er nauwelijks studies naar broeikasgasemissies en hoe die kunnen veranderen ten gevolge van degradatie. De meeste studies over Zuidoost-Aziatische veengebieden beschrijven de gevolgen van drainage en boskap, terwijl in het Amazonewoud degradatie in veengebied vooral komt door het oogsten van de *Mauritia flexuosa* palm en zijn vruchten in onaangetaste bossen. Deze unieke, maar lokaal veel voorkomende vorm van landgebruik wordt in grote delen van de Peruaanse Amazone toegepast in relatief afgelegen, ongerepte veengebieden die niet actief gedraineerd, noch bemest worden.

Hoofdstuk 3 beschrijft de mogelijke effecten van *M. flexuosa*-oogst op de koolstofopslag van een veenecosysteem. In drie regio's en twaalf studielocaties van het Pastaza-Marañón stroomgebied, binnen de Peruaanse Amazone, zijn drie zaken gemeten: de totale ecosysteemkoolstofopslag, de botanische samenstelling en het niveau van degradatie. De totale koolstofopslag in het ecosysteem varieerde van 200 tot 1600 Mg C ha^{-1}, waarbij veendieptes tot 2,8 meter zijn gemeten. Deze koolstofopslag is enorm in vergelijking met tropische regenwouden op minerale bodems, waarbij een koolstofopslag gemeten wordt tussen de 130 en 240 Mg C ha^{-1}. In vergelijking met de veengebieden in Zuidoost-

Azië, met een koolstofopslag van 1000 tot 7500 Mg C ha^{-1}, is het echter aan de lage kant, ook omdat hier veendieptes van twaalf meter worden gerapporteerd (Warren et al., 2017). In elk van de drie regio's zijn locaties aangetroffen met lage tot hoge degradatie-intensiteit. Dit geeft aan dat het oogsten van palmen in alle regio's gebeurt – ook in delen die binnen een nationaal reservaat vallen. Een hoge degradatie-intensiteit correleerde negatief met de koolstofopslag in de vegetatie, maar niet met de koolstofopslag in de bodem. Hierdoor konden verschillen tussen studielocaties niet gebruikt worden om in te schatten wat bodemkoolstofverliezen zijn als gevolg van bosdegradatie.

Hoofdstuk 4 en 5 gaan dieper in op de koolstofbalans van veenbodems en hoe die varieert bij verschillende intensiteit van palmoogst. In **Hoofdstuk 4** worden factoren onderzocht die kunnen aanzetten tot een grote broeikasgasproductie in veenbodems waar palmen geoogst worden. Deze factoren zijn: variaties in bodemvochtigheid en het grondwaterpeil als maatstaf voor zuurstofbeschikbaarheid (factor 1), micro-topografische verschillen in de bodem in de vorm van hoogtes en laagtes (factor 2), de kwaliteit van het bodemorganisch materiaal en bladstrooisel (factor 3), en de aanwezigheid van luchtwortels die methaan kunnen uitstoten (factor 4). Verschillen in micro-topografie en bodemorganisch materiaal (factor 2 en 3) bleken de belangrijkste factoren voor broeikasgasproductie als gevolg van bosdegradatie op tropisch veen.

Hoofdstuk 5 beschrijft vervolgens het effect van de palmoogst op de bodemkoolstofbalans. Het oogsten van palmbomen zorgt ervoor dat de hoogtes rondom palmbomen in formaat en oppervlakte afnemen; de zwaar gedegradeerde studielocaties hebben daardoor meer lagergelegen delen. Daarbij komt dat deze lagergelegen delen in zwaar gedegradeerde gebieden een hogere microbiële respiratie hadden, oftewel hogere afbraaksnelheden van het veen, wat zorgt voor een groter koolstofverlies uit de bodem. Het grondwaterpeil en de bodemvochtigheid lijken deze trend niet te beïnvloeden, maar verklaart alleen waargenomen seizoensverschillen door het jaar heen. Een afname van strooiselproductie en een verandering van de strooiselkwaliteit blijken wel een belangrijke rol te hebben bij het koolstofverlies. In zwaar gedegradeerde studielocaties wordt kwalitatief ander strooisel geproduceerd omdat de botanische samenstelling is veranderd door de selectieve palmenkap. Dit leidt tot

een toename van veenafbraak, ofwel de hetrotroof-geproduceerde CO_2. Daarnaast zorgt de bosdegradatie voor minder strooiselproductie, wat leidt tot minder koolstofopname in de bodem. Dit wordt bevestigd door *in vitro*-incubaties van bodems, waarbij bodems van zwaar gedegradeerde sites consistent meer hetrotroof-geproduceerd CO_2 aanmaakten ten opzichte van minder gedegradeerde veengronden (Hoofdstuk 4). Deze trend is ook *in situ* bevestigd, aan de hand van een vierjarig experiment waarbij CO_2-emissies (hetrotroof en autotroof) zijn gemeten in gedegradeerde en niet-gedegradeerde studielocaties (Hoofdstuk 5). De combinatie van deze verminderde strooiselproductie en het koolstofverlies door toename van veenafbraak zorgt voor een negatieve koolstofbalans in de zwaar gedegradeerde studielocatie van -7.1 Mg CO_2-C ha^{-1} yr^{-1} (netto CO_2-C uitstoot), terwijl de niet-gedegradeerde studielocatie geen significante hoeveelheid koolstof verloor (-0.1 Mg CO_2-C ha^{-1} yr^{-1}). Daarom is de conclusie dat intensieve bosdegradatie op tropische veenbodem kan leiden tot significant koolstofverlies, ook wanneer de bodem niet gedraineerd of bemest wordt.

In **Hoofdstuk 6**, tot slot, bediscussieer ik dat er een substantiële reductie van CO_2-uitstoot mogelijk is als de *M. flexuosa* palm in het gehele Pastaza-Marañón stroomgebied niet destructief geoogst zou worden voor zijn vruchten. Ik laat zien dat het koolstofverlies van deze vorm van bosdegradatie op veen kan leiden tot een bron van CO_2-uitstoot van 7.8 Tg C yr^{-1} voor het gehele Pastaza-Marañón stroomgebied. Een dergelijk grote bron van CO_2 is een extra zorg, bovenop de zorgen over de duurzaamheid van palmoogst in de Peruaanse Amazone en de toekomstige beschikbaarheid van voldoende vruchten (Horn et al., 2018; Padoch, 1988). Het ultieme doel voor deze veengebieden zou moeten zijn om verdere degradatie te stoppen en hetzelfde lot van drainage en conversie te voorkomen, zoals te zien in Zuidoost-Azië. Het niet-destructief oogsten van de vruchten, door bijvoorbeeld in de palm te klimmen, of door de palm te cultiveren in een *agroforestry* systeem, kan bijdragen aan het vasthouden van koolstof in de onderliggende bodem, terwijl er wel vruchten geoogst kunnen worden. Een betalingssysteem voor de mitigatie van CO_2-uitstoot kan daarbij mogelijk een extra impuls geven om de vruchten duurzaam te oogsten en dit waardevolle ecosysteem te behouden in het gehele Amazonewoud.

11 Acknowledgements / Dankwoord

First of all, I would like to thank the people at CIFOR in Indonesia and Peru. My time at CIFOR has been amazing, full of encounters with inspiring people. It has brought me many opportunities for which I am very grateful. A special thanks to Kristell and Lou, who first hired me and have tutored me for many years. Thanks for your patience and guidance during all those years.

Further I would like to thank the CIFOR-Lima crew, my stay in Lima would not have been as joyful as it was without you: Manual, Peter, Martha, Ann, Bruno, Ashwin, Jasmin, Matias, Laura and Florie. Monica and Gloria, thanks for all your help with weird requests such as a letter explaining to air attendants that I'm carrying glass vials which are not harmful and are simply filled with air. Marcella and Mariela, I would not know how to have done all this work without your assistance in the lab and the thousands of samples I brought back from the jungle. Thanks for your patience as well, and for treating the gas chromatograph as your kid: trying to understand what it has done and why it's not doing what you've asked. A special thanks to Louis-Pierre who helped me when I was setting up my experiments and for hanging out on Sundays with beer and barbecue.

Rupesh, I thank you for the fruitful collaboration and time we've spend in the field together. It's been really nice to co-author a paper with you and to have had the opportunity to meet several times afterwards. Thanks also for the photo's I've used in this thesis.

I am very grateful to the group of people who have helped me with the field work around Iquitos. A special thanks to Ulises Mozombite Murayari, your commitment to my research project has been endless. Keeping an eye out and basically being my ears and eyes in the field. It was a pleasure to work with you and thank you for the warm welcome in your house. Nicole Mitidieri Rivera, you've helped me a lot when I first arrived in Iquitos – guiding me around and setting up all the experiments. You've proven to work under very challenging conditions and were eager to learn and think along with the experiments. Julio Miguel Grandez Rios, working in swamps is challenging, but we managed to make the best out of it. You're always enthusiastic, making jokes and keeping the group spirit positive. At the same time, you never loose focus and make sure the work is done correctly

and you were always aware of maintaining the scientific quality where it should be.

The people at IIAP, especially Dennis del Castillo and Ricardo Farranay, thank you for the collaboration between IIAP and CIFOR. Your expertise and knowledge abled me to gather a nice group of people and study the fascinating swamps around Iquitos and the entire Peruvian Amazon – your effort is greatly appreciated.

I would also like thank the Regional Government of Loreto for giving access to the Quistococha Park. This collaboration is not only valuable for my study, it has enabled many researches to study this ecosystem and has led to an interdisciplinary body of knowledge about this unique area. I sincerely hope it will continue into the future and that what we learn there can be used throughout the Amazon.

Verder wil ik de mensen van de vakgroep Bodembiologie van Wageningen UR bedanken. Op de eerste plek Jan Willem en Oene, dank voor jullie voortdurende begeleiding, zowel inhoudelijk als bij het hele proces, dat pieken en dalen heeft gekend. Hoewel ik een groot gedeelte van de tijd niet in Wageningen was, vond ik onze afspraken altijd erg motiverend. Oene, in het bijzonder vond ik het erg fijn hoe jij me hielp uit te zoomen en met de helikopterview naar het grotere plaatje te kijken. Jan Willem, ik heb veel van je geleerd, vooral in de laatste fase en het schrijven van de publicaties.

Dan zijn er de vele vrienden in mijn omgeving die ik dankbaar ben. In het bijzonder zijn er een aantal die ik apart wil benoemen.

Osgar, Matthijs en Harmen: Ja hoooorr! Eindelijk, m'n werkstukje is af! Dit is dus dat ding waar ik al die tijd mee bezig was. Dank aan jullie voor de vele vermakelijke en volkomen random avonturen in alle uithoeken van Europa de afgelopen jaren. En natuurlijk voor de leuke avonden tussendoor, waarop ik alle strubbelingen en succesjes rondom dit project kwijt kon – of het in ieder geval even kon vergeten. Hoewel we momenteel allen behoorlijk druk bezet zijn met luiers, hypotheken en andere irrelevante ambities zien we elkaar hopelijk nog vaak (met of zonder jullie vrouwen en kinderen!). Osgar, jij in het bijzonder bedankt voor de hulp bij de PhD. Ik denk dat de metingen die jij verrichtte aan de omtrek van de bomen fenomenaal zijn geweest. Echt indrukwekkend hoe je ondanks de hitte,

een slechte knie, met tienduizend muggen in het moeras tot aan je heupen, zonder enige kennis van de Spaanse taal toch maar mooi baanbrekend onderzoek hebt verricht. Maar even serieus, superleuk dat je hebt kunnen regelen om langs te komen en ook dank voor de morele steun bij zo'n beetje alles wat ik/we hebben meegemaakt de afgelopen jaren. Alleen al hierom fantastisch dat jij me ook nog helpt als paranimf bij m'n spreekbeurt over dit werkstukje.

M'n bestuur, zo blijf ik jullie ook na 14 (omg!) jaar nog steeds noemen. Roy, Marjo, El, Luc en Suz – het is altijd gezellig, druk en chaotisch. Ik heb toch vooral leuke herinneringen aan de regelmatige weekendjes waarop we veel meemaken, delen en wat daarmee een soort reflecterende functie heeft door de jaren heen. Hopelijk gaan we hier nog lang mee door: biooooooo-licious! Suz, een speciaal woordje van dank voor jou voor het mede mogelijk maken van deze PhD en natuurlijk was het superleuk het eerste jaar in Indonesië bij CIFOR samen te hebben meegemaakt. Het is daarom ook een eer en waar genoegen om samen met jou als paranimf het eind van dit avontuur af te sluiten.

Roos, leuk om tegelijk met jou tegelijk in Peru te zijn geweest en via jou ook een mooi deel van Peru te hebben mogen zien anders dan het moeras van m'n onderzoek en de woestijn van Lima. Dank ook voor de nodige import van kaas voor de queso cabezas in Peru.

Dagmar, jij bedankt voor de hulp bij het vormgeven van dit boekje en de website; ik ben erg echt super blij mee!

De collega's van Aeres Hogeschool in Almere. Drie jaar geleden ben ik parttime aan de slag gegaan bij jullie, naast m'n PhD. Vanaf dag 1 een heerlijke werkplek, waar ik met veel plezier kom. In het bijzonder dank aan Linda en Wil voor hun steun, ruimte en vrijheid die ik heb gekregen om deze combinatie te maken en vol te kunnen houden.

De hanggroep van de C. van Maasdijkstraat. Wat moet ik zeggen anders dan: beter een goede buur dan een verre vriend. Bedankt voor de leuke spontane borrels en ook dat jullie ervoor zorgden dat ik in het laatste staartje tijdens de coronamaanden nog iets anders zag dan m'n beeldscherm.

Naast vrienden is familie als ankerpunt onmisbaar. Pap en mam, dank voor jullie steun en onvermoeide interesse in alles wat ik doe. Elke keer stonden jullie weer

klaar bij de gate van Schiphol met een spandoek, ballon of gewoon een hele grote blije glimlach. Ik realiseer het me nu ik zelf vader ben steeds meer, maar die onvoorwaardelijke liefde is erg waardevol. Dank dat jullie mij altijd hebben laten doen wat ik wilde, gesteund in de keuzes die ik maakte – ondanks dat ik van jullie gewoon kapper in Harderwijk had mogen worden. Ik denk dat jullie daarmee precies dat hebben gedaan wat ik nodig had: een constante basis, van waaruit ik zelf (letterlijk) de wereld heb kunnen ontdekken.

Adriaan, Nicole, Jochem, Pieter, Mariëlle en Willem, jullie bedankt voor de steun bij het telkens weer naar het buitenland vertrekken en de gezelligheid en warmte die het altijd extra fijn maakte om weer terug te zijn in Nederland. Ik vind het waardevol hoe we met z'n drietjes als broers en zus de dinertjes hebben en hoop die traditie nog lang vol te houden. Adriaan, het was bijzonder dat jij met Mirjam bent langs geweest in Peru. Terugkijkend is dat een extra bijzondere ervaring om samen gedeeld te hebben.

Jos, Marian, Koenraad, Annie, Lucas en Hugo, het is altijd erg fijn bij jullie te zijn en dank voor de warme ontvangsten, de gezelligheid, de goede gesprekken, het heerlijke eten, gewoon thuis of op vakantie in Taiwan of de Achterhoek. Ook bedankt voor jullie perfecte werkplek waar ik de laatste jaren veel gebruik van heb gemaakt tijdens de werkvakanties.

Als laatste mijn gezinnetje: Florian, Linde en Jojanneke. De tijd dat dit proefschrift tot stand kwam heeft me veel gebracht, maar zonder enige twijfel steken jullie daar met kop en schouders bovenuit. Het is een soort levensvreugde waar geen ervaring of titel tegenop kan. Jojanneke, jij reisde mij overal achterna, hebt je baan opgezegd, je eigen ambities even op pauze gezet en vooral mij gesteund en aangemoedigd in goede en slechte tijden. Ik kan je daar niet genoeg voor bedanken. De keuze om naar het buitenland te gaan was een moeilijke, maar jij maakte het eenvoudig om voor Nederland te kiezen, om op mijn knieën te gaan en om alles te doen en laten voor onze twee prachtige kinderen. We hebben de afgelopen tijd al mogen ervaren hoe het is om niet elk weekend, elke vakantie en de vele avonden 'kwijt' te zijn aan de PhD – het wordt alleen maar leuker, en dat komt omdat ik zo ontzettend blij ben met jullie en zielsveel van jullie hou.

12 PE&RC Training and Education Statement

With the training and education activities listed below the PhD candidate has complied with the requirements set by the C.T. de Wit Graduate School for Production Ecology and Resource Conservation (PE&RC) which comprises of a minimum total of 32 ECTS (= 22 weeks of activities).

Review of literature (6 ECTS)

- Soil N_2O and NO emissions from land use and land-use change in the tropics and subtropics: a meta-analysis

Writing of project proposal (4.5 ECTS)

- The effect of land-use change on greenhouse gas emissions from peatlands of the Peruvian Amazon (2014)

Post-graduate courses (3 ECTS)

- Statistics course linear models; PE&RC (2014)
- Statistics course mixed models; PE&RC (2015)
- Soil ecology; PE&RC (2016)

Laboratory training and working visits (0.3 ECTS)

- Gas chromatograph training; GC company Perkin Elmer & Cientifica Andina (2014)

Invited review of (unpublished) journal manuscript (2 ECTS)

- Eco Egineering: habitat reconstruction; ecotechnology; synthetic ecology; bioengineering; restoration ecology; ecology conservation; ecosystem rehabilitation; stream and river restoration; reclamation ecology; non-renewable resource conservation (2014)
- Geoderma: soil biology, soil greenhouse gas emissions, land-use change and climate change (2017)

Deficiency, refresh, brush-up courses (1.5 ECTS)

- World soils and their assessment, Spring School; ISRIC (2015)

Competence strengthening / skills courses (3.6 ECTS)

- The choice; WGS (2016)
- Scientific writing; WGS (2016)
- Project and time management; WGS (2017)

PE&RC Annual meetings, seminars and the PE&RC weekend (1.2 ECTS)

- PE&RC last years weekend
- Netherlands annual ecology meeting; Lunteren, the Netherlands

Discussion groups / local seminars / other scientific meetings (4.8 ECTS)

- Discussion group at CIFOR; Lima (2014)
- Peat group Iquitos; Peru (2014)
- PE&RC Discussion group: CSA / REDD+; the Netherlands (2015-2017)
- SOQ PhD ring; the Netherlands (2016-2017)

International symposia, workshops and conferences (16.1 ECTS)

- IUFRO Landscape conference; oral presentation; Concepcion, Chile (2012)
- Seventh international symposium on non-CO_2 greenhouse gases; oral presentation; Amsterdam, the Netherlands (2014)
- XX Congreso Latinoamercano de Suelos; poster presentation; Cusco, Peru (2014)
- 5th International Ecosummit ecological sustainability; oral presentation; Montpellier, France (2016)
- Peatlands in the Amzon, workshop Ministerio del Ambiente IIAP & CIFOR; oral presentation; Iquitos, Peru (2016)
- European geosciences union general assembly; poster presentation; Vienna, Austria (2017)
- IUFRO 125th Anniversary congress; oral presentation; Freiburg, Germany (2017)
- Eighth International symposium on non-CO_2 greenhouse gases; oral presentation; Amsterdam, the Netherlands (2019)

13 About the author

Jeffrey van Lent was born on March 26th, 1986 in Harderwijk, The Netherlands. He obtained a bachelor's and master's degree at Utrecht University, specializing in ecology and natural resources management. During his master he did an internship at the UNAM in Mexico and studied sustainable harvesting of a non-timber forest product. His second internship was at the Dutch government and focused on the use of biomass from landscape management for bio-energy production. After obtaining his master's degree he started working at the Centre for International Forestry Research in 2012, where he continued to work on ecology and its application in resources management: greenhouse gas emission from land-use change. After a research assistant position, he started a PhD at CIFOR and Wageningen UR in 2014. Since 2017 he lectures applied biology at Aeres University of Applied Sciences. There, his work focusses on ecology, research methods, climate change and forestry. He supervises students and coordinates applied science student projects in collaboration with partners in- and outside Academia.

Publications	Citations
Van Lent, J, Hergoualc'h, K, & Verchot, LV (2015). Soil N_2O and NO emissions from land use and land-use change in the tropics and subtropics: a meta-analysis. *Biogeosciences,* 12, 7299-7313.	52
Bhomia, RK, van Lent, J, Rios, JMG, Hergoualc'h, K, Coronado, ENH, & Murdiyarso, D (2019). Impacts of *Mauritia flexuosa* degradation on the carbon stocks of freshwater peatlands in the Pastaza-Marañón river basin of the Peruvian Amazon. Mitigation and Adaptation Strategies for Global Change, 24(4), 645-668.	5
van Lent, J, Hergoualc'h, K, Verchot, L, Oenema, O, & van Groenigen, JW (2019). Greenhouse gas emissions along a peat swamp forest degradation gradient in the Peruvian Amazon: soil moisture and palm roots effects. Mitigation and Adaptation Strategies for Global Change, 24(4), 625-643.	5
van Lent, J, Hernández-Barrios, JC, Anten, NPR, Martínez-Ramos, M (2014). Defoliation effects on seed dispersal and seedling recruitment in a tropical rain forest understorey palm. *Journal of Ecology 102 (3),* 709-720	17

This research was conducted under the Sustainable Wetlands Adaptation and Mitigation Program (SWAMP) and CIFOR's Global Comparative Study on REDD+. It was generously supported by the governments of the United States of America (Grant MTO-069018) and Norway (Grant agreement # QZA-12/0882). It was undertaken as part of the CGIAR research program on Forests, Trees and Agroforestry (CRP-FTA) with financial support from the CGIAR Fund Donors.

Financial support from Wageningen University for printing this thesis is gratefully acknowledged.

Cover design by Dagmar van Schaik
Printed by Printenbind.nl on PaperWise paper